STUDIES ON THE MECHANISM OF ACTION OF THE ANTIMICROBIAL S-LINKED GLYCOPEPTIDE SUBLANCIN

BY

CHANTAL VAITIARE GARCIA DE GONZALO

DISSERTATION

Submitted in partial fulfillment of the requirements
for the degree of Doctor of Philosophy in Chemistry
in the Graduate College of the
University of Illinois at Urbana-Champaign, 2015

Urbana, Illinois

Doctoral Committee:

Professor Wilfred A. van der Donk, Chair
Professor Paul J. Hergenrother
Professor Satish K. Nair
Professor Douglas A. Mitchell

ABSTRACT

Infectious diseases are a continuing threat to human health. In particular, the rapid development of bacterial antibiotic resistance not only decreases the effectiveness of known antibiotics, but also increases the need for the ongoing discovery of novel drugs. Since the discovery of penicillin, natural products have become a great source of templates for the development of new antibiotics. Derivatization of known drugs is one approach commonly used to combat rapidly evolving bacterial strains. However, the mechanisms of actions of derivatized drugs are more often than not very similar to the parent compound, making it difficult to develop drugs with new and unique modes of action by generating analogs. Ribosomally synthesized and post-translationally modified peptide (RiPP) natural products are a rapidly expanding class of compounds with antimicrobial activity. Sublancin is one of five members of the glycocin family of RiPPs, and contains an unusual S-linked glycosylation. This unprecedented post-translational modification, as well as its increased stability, when compared to known RiPP antimicrobials, suggests a unique antibacterial mode of action. In an effort to understand the remarkable stability of sublancin, the three-dimensional NMR structure was solved, as described in chapter 2, revealing that hydrophobic interactions as well as hydrogen bonding are responsible for the stable and well-structured peptide.

Unlike better-understood natural products, the molecular target of sublancin is currently unknown. In order to further understand how sublancin exerts its activity against bacteria, a number of sublancin analogues were made. These analogues were prepared either by heterologous expression followed by *in vitro* modification, as well as by solid phase peptide synthesis. The antimicrobial activity of all analogues was then assessed against sensitive bacteria and sublancin-resistant mutant strains.

While sublancin exhibits sub-micromolar activity against Gram-positive bacteria, its molecular target is currently unknown. Chapter 3 describes studies focused on understanding sublancin's mode of action. In chapter 4 we performed super resolution microscopy and determined that sublancin localizes to the cell membrane. Furthermore, the mechanism of action of the *S*-glycosyltransferase SunS, the enzyme responsible for installing an S-linked sugar onto sublancin, was studied in chapter 5, which provided insights into its enzymatic mechanism. The understanding of the biosynthesis of these unique peptides can aid in the bioengineering of other, more potent complex molecules.

.

For my parents
Hernán Garcia De Gonzalo and Lorena M. Coppa

&

il mio amore
Piero Sartori

ACKNOWLEDGEMENTS

I wish to express my sincerest gratitude to my parents Hernán Garcia De Gonzalo and Lorena M. Coppa for all their sacrifices and hard work that allowed me to get where I am. There are no words that can truly describe my appreciation. I want to thank my brothers Ricardo Garcia De Gonzalo and Simon Garcia De Gonzalo for being there when I needed them the most. I would also like to thank all of my family, the Garcia De Gonzalo, the Coppa, and the Sartori for all their support and encouragement throughout these years. I would like to specially thank the one person that was with me every step of the way during this chapter of my life. Piero Sartori, *amore mio*, I do not have words to express how much your support, throughout these years, means to me. Even though we were oceans apart most of the time, you have given me the unimaginable strength to continue forward. I am blessed to have you by my side. Thanks for putting up with me at all hours of the day. I love who I am when I am with you, you are my dearest friend, my deepest love, you are the very best of me.

I am indebted to my advisor, Professor Wilfred van der Donk, whose patience, support, advice, generosity and extremely nice personality allowed me to grow as an individual and researcher. I am especially grateful for not being fired for being an accomplice in many of Spencer's celebration "ideas". I have the utmost respect for Wilfred and for his strength and willingness to ensure the lab's success and each lab member's education. The research described herein would not have been possible without his efforts to provide me with guidance and the freedom to decide how to use the available resources. I would also like to thank Professor Paul Hergenrother, Professor Satish Nair, and Professor Douglas Mitchell for serving on my committee and all their advice, suggestions and collaborations throughout the years.

Many thanks to the incredible facilities at UIUC, especially the Functional Genomics facility, the Flow Cytometry facility, the Metabolomics Center, and the NMR facility. I would like to thank Dr. Dean Olson for his NMR expertise, his daily visits to our bay and for the great times we had during Halloween 2014. I would also like to thank Dr. Lingyang Zhu for all her help solving the NMR structure of sublancin that resulted in a great publication ☺.

Every member of van der land has made these past five years fly by. I sincerely believe that I was very lucky in joining such a great research environment. I would like to start by expressing my appreciation for former and current members for always giving me a reason to smile everyday. I would like to thank Martha Freeland for the great chats we had in the morning during my early years and also Nan Holda for keeping the lab organized. I am thankful for the training and knowledge passed down to me by former members, Dr. Trent Oman, Dr. Ian Gut, Dr. Huan Wang, Dr. Juan Velasquez, Dr. Neha Garg, Dr. Patrick Knerr, Dr. Noah Bindman, Dr. John Hung, Dr. Xiao Yang, and current members, Dr. Mark Walker, Dr. Gabrielle Thibodeaux, Dr. Christopher Thibodeaux, Xiling Zhao, Kenton Hetrick, Lindsay Repka and of course Manuel Ortega. Thanks to all members with whom I have developed great friendships, Manuel A. Ortega, Gabrielle Thibodeaux, Kenton Hetrick, Xiling Zhao, and Mark Walker and many others for their companionship in and outside of lab. Thanks everyone for the endless memories and video footage I was able to capture throughout the years. I will not forget RAL 145-147 music Fridays that drove most of us to the edge of sanity after listening to the same songs over and over again. I am thankful for the great friendships outside of the van der Donk group as well—Briah Trinh, Madeline Lopez Muñoz, Vinayak Agarwal, Jagadesswaran Chandrasekar, Jessie Peh, Ariana Bravo, Maria Alejandra Bautista, Alex Stanton, everyone in SACNAS and Nancy Olson for her kindness, generosity and incredible cooking ☺.

Finally I would like to sincerely thank the Chemistry Department, the chemical biology and organic student offices, the graduate student office, the Ullyott fellowship, the National Institutes of Health, the Howard Hughes Medical Institute, and the Chemical Biology Interface training grant for supporting me throughout these years.

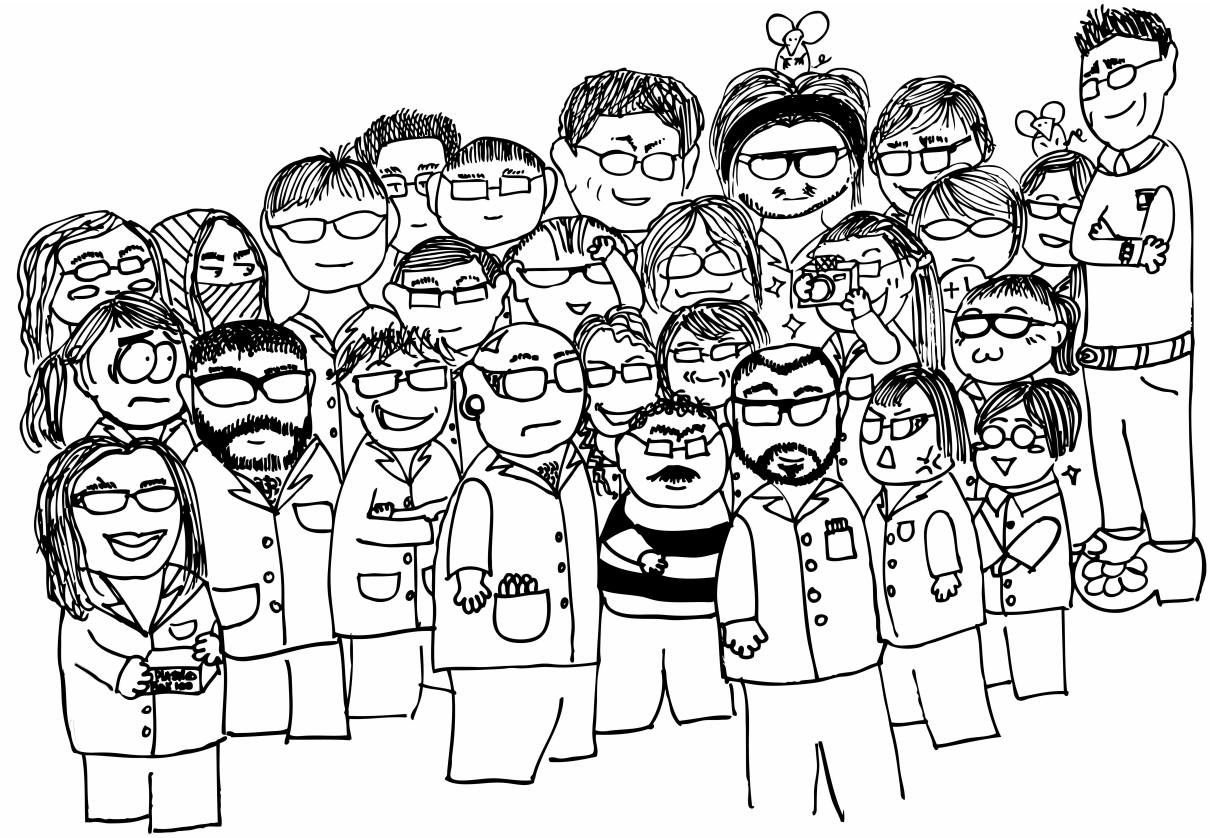

Front row (left to right): Gabrielle T., Chris T., Kenton H., Mark W., Nidhi K., Silvia B., Shubhanip B., Manuel O., Xi Z., Chang H. **Middle row (left to right):** Lindsay R., Subha M., Josh W., Weixin T., Chantal GDG., Xiao Y.,Yi Y., Debapriya D. **Back row (left to right):** Emily U., Linna A., Zhengan Z., Zedu H., Liujie H., Abraham W., Nick L., Ian B. **Tall one on the right:** Wilfred van der Donk

TABLE OF CONTENTS

LIST OF FIGURES

FIGURE **PAGE**

LIST OF TABLES

TABLE **PAGE**

CHAPTER 1. THE GLYCOCIN FAMILY OF RIPP NATURAL PRODUCTS

1.1 INTRODUCTION

The human body harbors close to ten trillion cells and it is home to a hundred trillion bacteria, in other words our human cells are outnumbered 10:1.[1,2] The collection of resident bacteria in the human body is collectively known as the microbiome. The microbiome is essential in maintaining our health and the largest and most diverse population of bacteria is known to reside in our guts.[1-3] These residents help in the digestion of food, in manufacturing nutrients that we are unable to make, and in protecting us by suppressing the growth of pathogens.[1,2] For the most part, the bacteria are our allies, but when bacteria acquire genes that make them resistant to our antibiotics, they can be turned into our enemies. Antimicrobial resistance is a present-day global threat.[4,5] It is estimated that over 700,000 people die each year as a consequence of antibiotic resistant infections across the world, and that by 2050 over 10 million lives will be lost each year.[5]

The discovery of new antibacterial agents that function through novel modes of action would be an important contribution in the struggle against multidrug-resistant infections. The rise in antibiotic resistance is of increasing concern due to the limited number of targets affected by our current pool of antibiotics. There are over two hundred approved antibacterial drugs that target essentially the same bacterial processes, which include protein synthesis, DNA replication, RNA synthesis, folate biosynthesis, and cell wall biosynthesis.[6-8] However, an increasing number of strains have overcome the action of these drugs through selective pressure that caused them to acquire mutations in the original targets rendering them resistant to the drug used to treat them.[9] Such target modifications can bestow resistance to drugs with analogous binding sites, a common scenario.[8] Given our current situation with regards to the emergence of antibiotic

resistance, one solution involves the discovery and development of new antimicrobial drugs that act on previously unexploited targets. Nature has proven to be a rich source of natural product therapeutics. Therefore there may be no better place to discover new pharmaceutically relevant compounds than investigating what nature has already designed and evolved.[10]

A fast-growing class of natural compounds is the ribosomally synthesized and post-translational modified peptide (RiPPs) natural products. RiPPs display remarkable diversity in their structures, bioactivities and organisms that produce them. Their structures include the 20 proteinogenic amino acids, as well as modified amino acids and various decorations to their peptide scaffolds.[11,12] These modifications are important because of their ability to convert a flexible linear peptide into a conformational rigid structure. This rigidity is hypothesized to be important for target binding and increased metabolic stability.[11-13] Importantly, there is a unifying characteristic in that these molecules are biosynthesized in a similar fashion. These compounds are ribosomally synthesized as inactive precursor peptides that comprise an N-terminal leader peptide followed by a C-terminal core peptide that undergoes extensive enzyme-mediated post-translational modifications that convert them into their biologically active forms (Figure 1.1).[10,11]

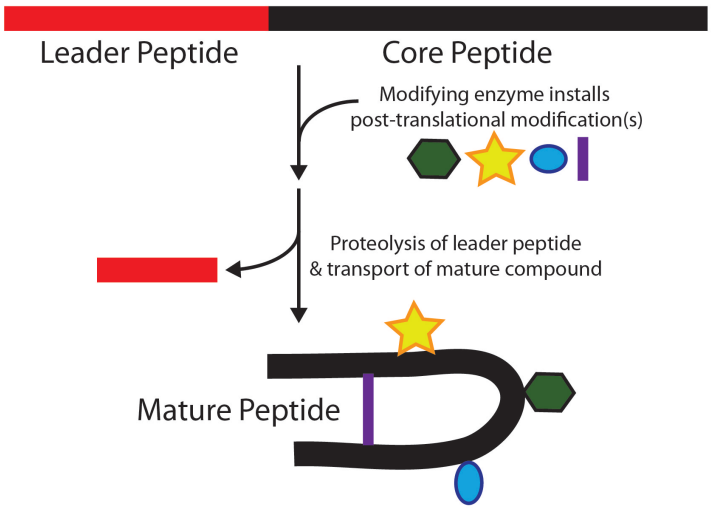

Figure 1.1 General biosynthetic scheme for ribosomally synthesized and post-translationally modified peptide natural products.

1.2 OVERVIEW OF GLYCOCINS

One class of ribosomally synthesized and post-translationally modified peptide natural products are the glycocins.[11] Glycocins are produced by bacteria and have potent antimicrobial activities. They are characterized by the presence of one or multiple sugar moieties in their core peptide and two disulfide bonds that serve to stabilize the structure.[14] To date there are five known members of the glycocin family of natural products, including glycocin F, sublancin 168, plantaricin ASM1 (a.k.a ASM1), thurandacin A and thurandacin B.[14-18]

In 1998, Paik and coworkers reported the discovery of a novel lantibiotic, which they named sublancin 168.[19] The reported structure of sublancin contained a dehydroalanine residue and thioether crosslink, specifically a methyllanthionine moiety that is characteristic of lantibiotics. It was also reported to contain two disulfide bridges, which at the time were unprecedented in lantibiotics (Figure 1.2).[19] Lantibiotics are also part of the RiPP class of natural products and are characterized by the presence of dehydro amino acids dehydroalanine (Dha) and dehydrobutyrine (Dhb) and thioether crosslinks termed lanthionine or methyllanthionine.[20,21]

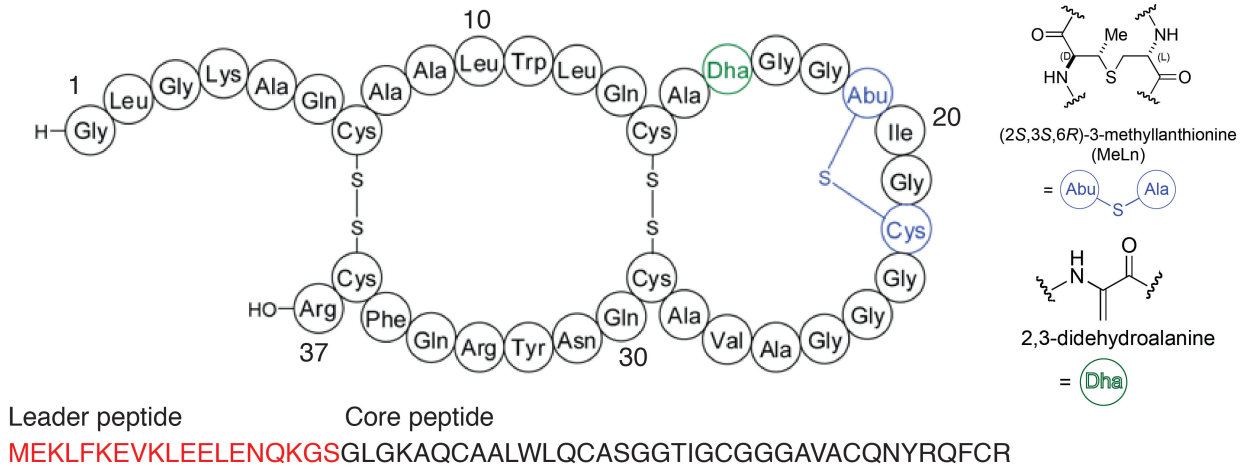

Figure 1.2 Originally proposed structure of sublancin 168.
Figure reproduced from Dr. Trent Oman's thesis.

Sublancin, produced by *Bacillus subtilis* 168 was shown to be extremely stable and displayed antimicrobial activity against a subset of Gram-positive bacteria.[19] In 2011, Dr. Oman, a former graduate student in the van der Donk laboratory, revised the structure of sublancin 168 from a lantibiotic to a novel S-linked glycopeptide.[15] Dr. Oman showed that the precursor peptide was being modified by the glycosyltransferase SunS, which installs a glucose via a β-S-linkage to Cys22 thereby reclassifying it as the first member of the glycocins (Figure 1.3).[15]

The remaining glycocins are also modified by dedicated glycosyltransferases. Glycocin F is secreted by *Lactobacillus plantarum* KW30 and is modified by the glycosyltransferase GccA and contains an N-acetylglucosamine β-O-linked to Ser18, and an N-acetylhexosamine-β-S-linked to its C-terminal Cys43.[16,22] ASM1 was originally discovered in 2010, and it was also believed to be part of the lantibiotic family but was later reclassified after analysis of the biosynthetic gene cluster revealed no lanthipeptide post-translational modifying enzymes.[18] ASM1, secreted by *Lactobacillus plantarum* A-1, is an orthologue of glycocin F differing in five

residues, all of which are located in the flexible C-terminal tail (Figure 1.3).[14,16] Early in 2014 thurandacin A and B were added to the glycocin family after Dr. Huan Wang, a former member of the van der Donk group reconstituted the putative products of a biosynthetic gene cluster from *Bacillus thruingiensis serovar andalousiensis* BGSC 4AW1. Thurandacin A is modified by a glucose moiety at both Ser19 and Cys28, while thurandacin B is modified only at Cys28 (Figure 1.3) by the glycosyltransferase ThuS.[17]

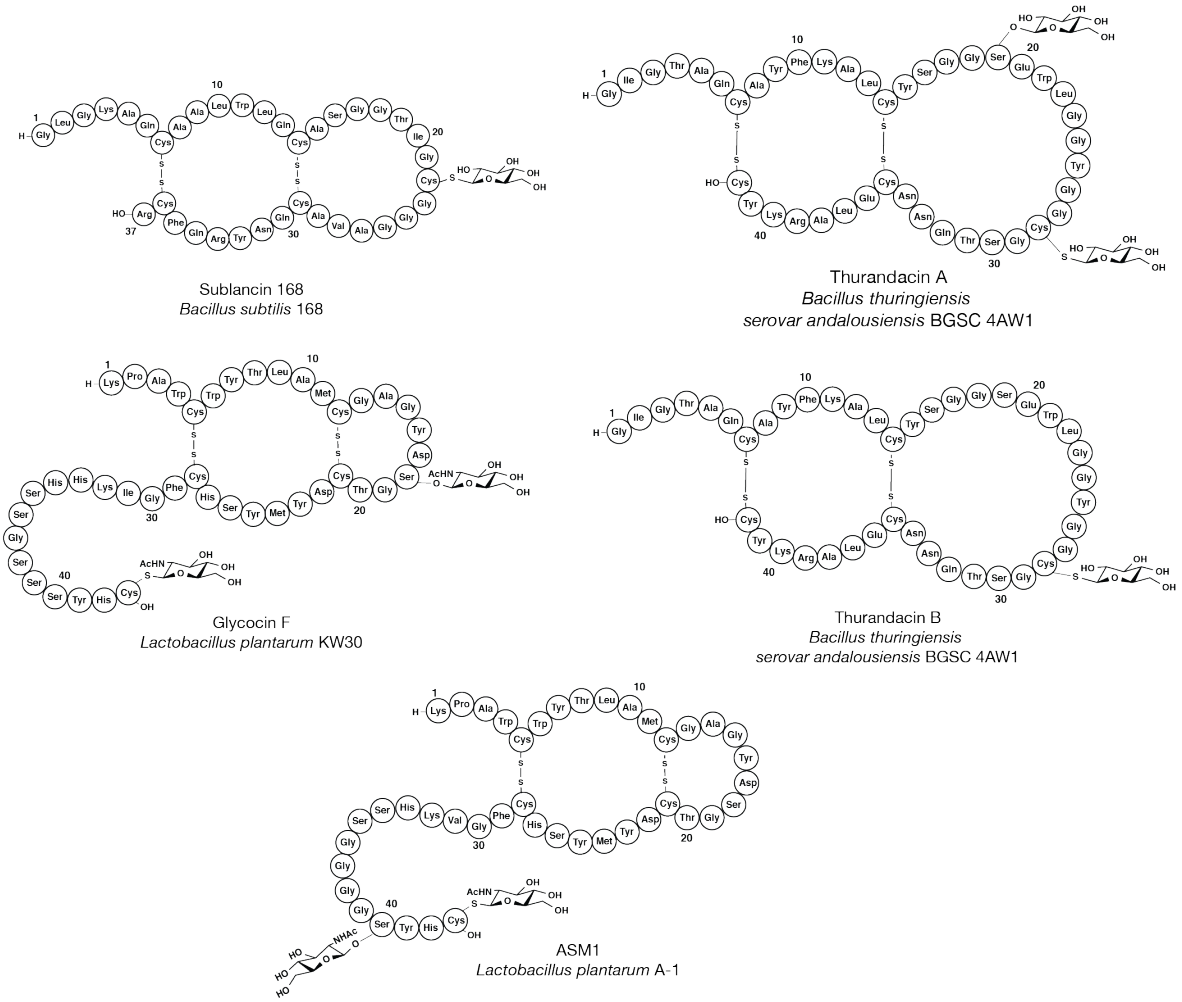

Figure 1.3 Glycocin family of natural products.

Sublancin (top left), glycocin F (middle left) thurandacin A (top right), thurandacin B (middle right), and ASM1 (bottom).

1.3 GLYCOCIN MODE OF ACTION

At present, the mode of action of sublancin and other members of the glycocin family remains elusive. We do know, however, that carbohydrates are abundant biomolecules that can be found appended to lipids, proteins, peptides, and natural products.[23] Glycosylation is an essential post-translational modification in eukaryotic cells where a carbohydrate is typically linked to the oxygen atom of Ser/Thr or the nitrogen atom of Asn.[23] In addition, glycosylation plays important roles in protein folding and secretion, cell-cell signaling, modulation of bioactivity of natural products and proteolytic stability. Glycosylated natural products such as vancomycin, teicoplanin, bleomycin and others, are commonly used as antimicrobial drugs, and today some glycosylated natural products are becoming promising anti-cancer drug candidates.[24-29] Some of the advantages of appending a sugar moiety include decreased toxicity and increased solubility.[30,31] The glycosylations present in the glycocin family of natural products are unusual because (1) bacteria do not typically glycosylate peptides and proteins, and (2) current members contain the only known cysteine S-glycosylations of ribosomally synthesized antimicrobial peptides.[32-34] Conjugation to Cys through an S-linked glycosidic linkage is extremely rare. To date, only a few studies have reported carbohydrates linked to the sulfur atom of Cys.[15,16] The earliest reports of S-linked glycopeptides date back to 1971 and include compounds found in human urine,[35] human erythrocyte membrane[36,37] and white muscle albumin in cod.[38] To determine the S-linkages, these compounds were subjected to dansyl-Edman degradation, acid hydrolysis and derivatization for gas chromatography identification of the sugar. No further extensive characterizations of the glycosylated proteins has been performed.[16]

S-glycosylation to Cys is more stable than the O-glycosylation to Ser, both at low and high pH.[32-34] Sulfur is less electronegative than oxygen and thus has a lower affinity for protons and

less likely to form the conjugate acid intermediate involved in glucoside hydrolysis.[39] This explains why S-linked sugars are more stable against glycosidases.[40] Due to the desirable characteristics of S-linked glycopeptides they have been the subject of several investigations.[41-45]

Since glycosylation is conserved in all reported glycocins to date, it is hypothesized that it must be involved in the mechanism of action of these natural products. Many natural products (ribosomally synthesized or not) with antibacterial activity inhibit the biosynthesis of the peptidoglycan (Figure 1.4).[46] For example, the non-ribosomally synthesized glycopeptide vancomycin acts by binding to the pentapeptide of the peptidoglycan monomers and non-crosslinked polymers thus blocking the formation of the peptide cross-links by transpeptidase enzymes.[47,48] Nisin, a prominent RiPP, acts against bacteria via a dual mechanism of action. It forms pores in the cytoplasmic membrane by using lipid II as a docking molecule[49,50] sequestering lipid II, thus making it unavailable for the biosynthesis of peptidoglycan.[51-53] Given the known membrane disruption potential of these natural products, in chapter 3, we investigated the possibility of sublancin acting upon the cell membrane, and we now know that this is not the case as sublancin was shown to not inhibit lipid II polymerization nor disrupt the membrane potential of the cell.[54] Furthermore, the sugar moieties found on the glycocins has been shown to be essential for activity. Work by Oman et al. have shown that the release of the glucose moiety, via acid-hydrolysis, from sublancin resulted in the loss of activity of the peptide.[15] Work to understand the role of the sugar moiety is still underway.

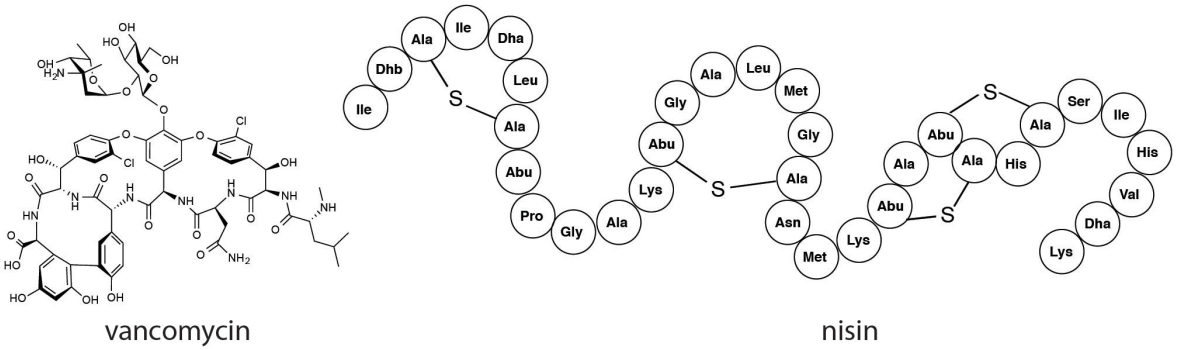

Figure 1.4 Peptidoglycan biosynthesis inhibitors.

Structures of Vancomycin (left) and nisin (right), two well-studied antimicrobial agents that disrupt bacterial peptidoglycan biosynthesis.

Factors affecting the susceptibility of Gram-positive strains to sublancin have been studied by van Dijl and coworkers. The NaCl content of the growth medium has been shown to be a key determinant in the susceptibility of *Bacillus* and *Staphylococcus* strains but it does not affect the stability, activity and production of sublancin.[55] Based on this observation, it was proposed that sublancin affects the mechanosensitive ion channels of the cell. Mechanosensitive ion channels are membrane embedded channels found in archaea and eukaryotes, and are especially widespread among bacteria (Figure 1.5).[56-60] The channels control the efflux of osmoprotectants and osmolytes upon hypo-osmotic shock. When cells experience an abrupt decrease in the osmolarity of their extracellular environment they allow ions and osmolytes to rapidly exit from the cytoplasm in order to maintain adequate turgor pressure. The release of ions protects the cells from lysis due to overpressure caused by an equilibrium driven influx of water. Mechanosensitive ion channels are classified into large, small and mini, and designated as MscL, MscS, and MscM respectively.[56,57] MscL has the largest pore size and opens when the pressure applied is high. The structures of the proteins *Mycobacterium tuberculosis* (TBMscL),[61] *Staphylococcus aureus* (SaMscL),[62] and *Escherichia coli* (EcMscL)[63,64] have been solved by

crystallography or proposed based on structural homology. TBMscL and SaMscL have an overall sequence similarity of 37 and 51 percent compared to EcMscL.[65]

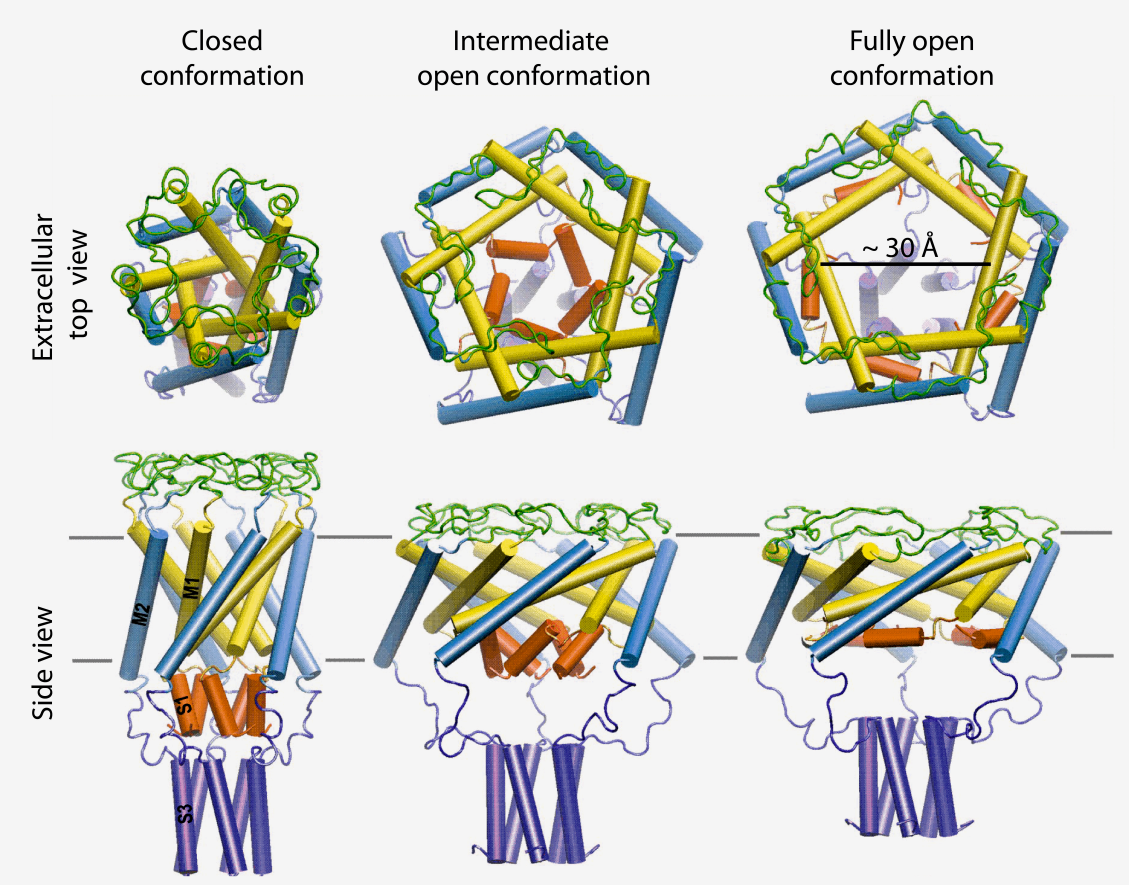

Figure 1.5 Mechanosensitive ion channels structure.

Molecular model of *E. coli* mechanosensitive large ion channel (EcMscL) in the closed-resting (left), intermediate open (middle) and fully open (right) conformations. The channels are multimers of a subunit containing an N-terminal helix S1 (orange), two transmembrane helices TM1 (yellow) and TM2 (blue), a periplasmic loop (green) and cytoplasmic helix S3 (purple). Figure adapted with permission from Mechanosensitive channels: what can we learn from 'simple' model systems?[66]

Van Dijl and coworkers have shown that the susceptibility of *B. subtilis* and *S. aureus* strains to sublancin increases if the bacteria overexpress the MscL channel. When the NaCl concentration in the media was increased from 1% to 5% the bacteria were less sensitive to sublancin at higher salt concentrations.[55] Moreover, the growth of *B. subtilis* and *S. aureus* MscL deletion mutants was hardly inhibited when exposed to sublancin.[55] Whether sublancin takes

advantage of the changes in turgor pressure to block the Msc channels or as means to enter the cells and affect a cytoplasmic target is yet to be determined.

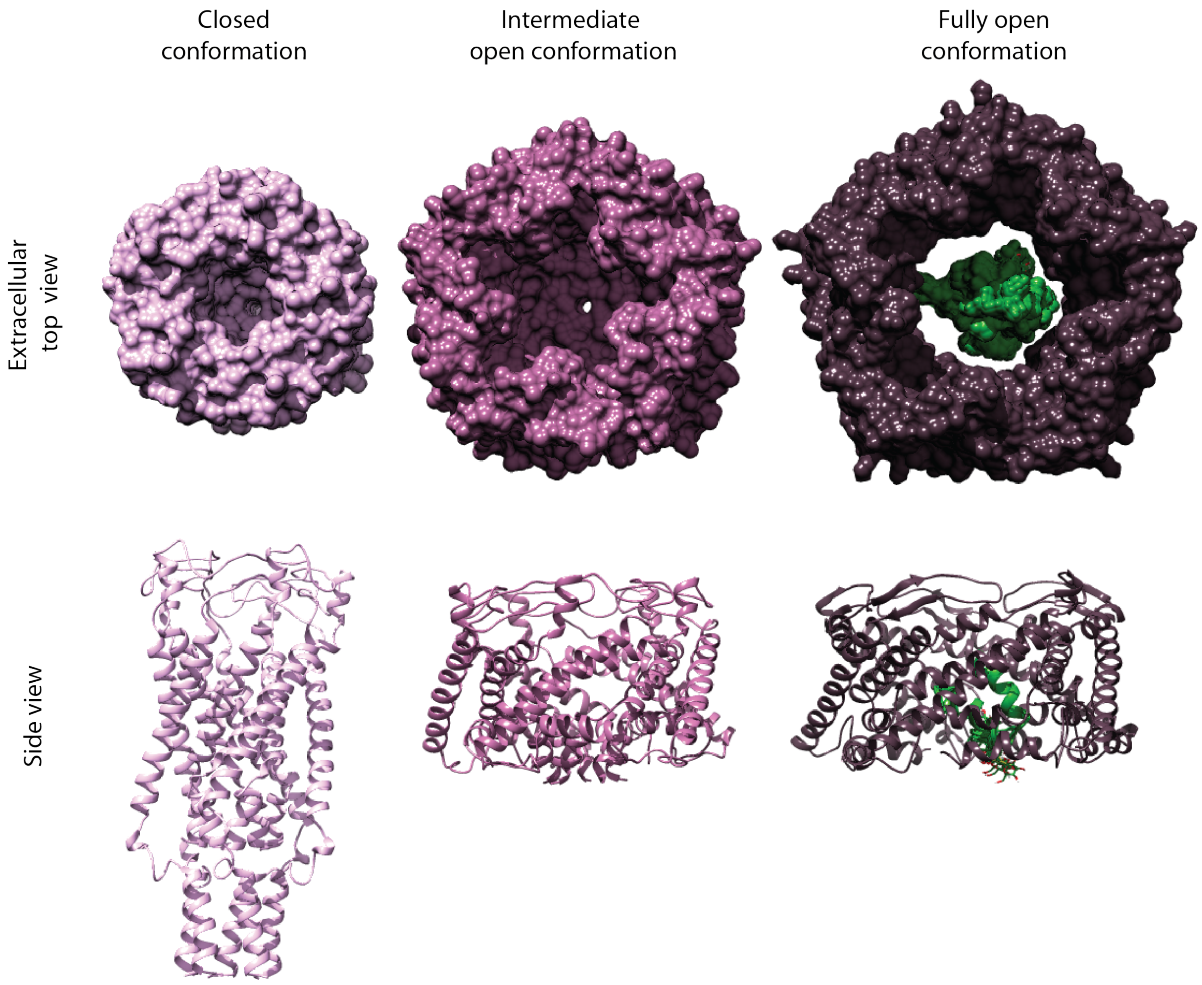

Figure 1.6 Surface models of EcMscL with sublancin.

Surface molecular model of *E. coli* mechanosensitive large ion channel (EcMscL) in the closed-resting conformation (left), intermediate open conformation (middle) and sublancin (green) docked in the channel of the fully open (right) conformations.

More recent studies that were part of my graduate studies, discussed in chapter 3, describe how sublancin exhibits sub-micromolar activity against bacteria and will focus on understanding how it exerts its activity by interaction with the phosphoenolpyruvate:sugar phosphotransferase

system (PTS). The study of S-linked glycopeptides will expand our knowledge of these unique RiPPs, and perhaps elucidate their hypothesized novel modes of actions. Furthermore, elucidation of the mechanism of action of such compounds could help us develop structurally similar and more potent antimicrobial peptides.

1.4 BIOSYNTHESIS

1.4.1 Gene organization

Like other members of the RiPP family of natural products glycocin biosynthetic genes are clustered. At present a universal gene designation has not been established for the glycocin family. So far, each individual glycocin has its own gene designation for identification. For example, the sublancin biosynthetic genes are designated as *sun* and those for glycocin F are designated as *gcc*. For the purpose of this thesis the generic gene designation *glyc* will be used to represent the locus symbol for glycocins in general. Thus far, only a few glycocin gene clusters have been identified via homology, and these studies show similar gene organization for glycocin production.[67-69] In almost all known glycocins and putative glycocins, the biosynthetic gene cluster includes genes encoding for a precursor peptide (*glycA*) and the modification enzymes responsible for glycosylation (*glycS*), a thiol-disulfide oxidoreductase(s) (*glycO*), an immunity gene (*glycI*), and a transporter/protease (*glycT*) responsible for the removal of the leader peptide followed by extracellular transport of the mature glycocin (Figure 1.7). Additional genes, such as those that encode for regulation, may also be found within these clusters or they may be located on closely linked operons.[21] For sublancin these genes are known as *sunA, bdbB* and *bdbA, sunI,* and *sunT* respectively, and are located on a SPβ prophage, a viral genome that was integrated in to the circular DNA chromosome of *B. subtilis* 168.

The order of events for the biosynthetic modifications that occur on the sublancin precursor peptide, SunA, are yet to be determined. Experimental observations (Chapter 6) point towards the glycosyltransferase, SunS, attaching the sugar moiety first, followed by the folding of the peptide by the thio-disulfide oxidoreductases, and leader sequence removal by SunT as the mature peptide, sublancin, is transported out of the cell. Whether some glycocins are capable of undergoing additional post-translational modification aside from the formation of disulfide bridges and O- and/or S-linked glycosylation is yet to be uncovered.

1.4.2 Precursor peptides

The production of mature glycocins begins with the translation of *glycA* genes. These genes encode a precursor peptide (GlycA) that contains an N-terminal leader peptide region that can range anywhere from 19 to 38 amino acids in length and a C-terminal core peptide region that will undergo post-translational modification and ultimately become the mature glycocin. The C-terminal peptide region of known and putative glycocins can vary in length between 37 to 48 amino acids.[15-17] The leader and core amino acid peptide sequences of sublancin, thurandacin A & B, glycocin F and ASM1 contain serine residues, but only some of those located in the core peptide undergo glycosylation. In addition only the core peptides of these five natural products contain Cys, and all of them are involved either in disulfide formation or are post-translationally modified with a sugar moiety (Figure 1.8).

Similar to the lantibiotic family of RiPPs, the glycocins have leader peptides that are typically rich in Lys, Glu and Leu residues, as observed in the JKLX (J = E, K, or S) and KEBXXXELEXXXG motifs (B = V, L, or I), and usually end in a GG or GS motif (Figures 1.8A and 1.9).[10] Analysis of the leader peptides using the protein sequence analysis workbench PSIPRED predicts that the leader peptides form a hydrophilic helical structure (Figure 1.8 B, C).

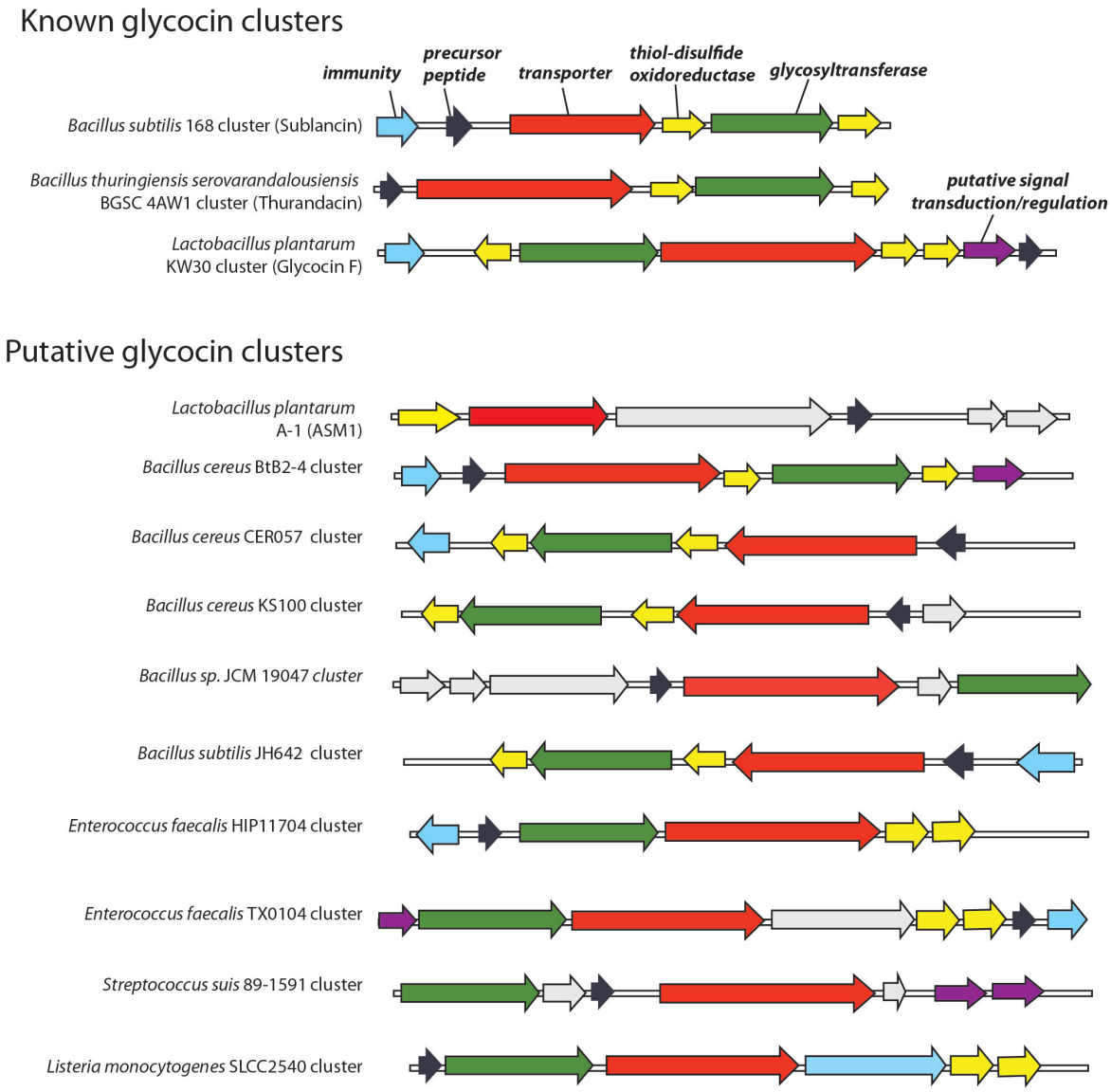

Figure 1.7 Organization of representative glycocin biosynthetic gene clusters.

The biosynthetic gene cluster for the production of known glycocins including sublancin, thurandacin, and glycocin F, and the biosynthetic gene clusters for the production of putative glycocins. The precursor peptide is colored in black, glycosyltransferase in green, thioredoxin oxidoreductases in yellow, transporter in red, immunity protein in blue, putative regulation signals in purple and unknown genes in grey.

Several hypotheses have been proposed to help explain the role(s) of the leader peptides for many classes of RiPPs. Potential roles include acting as a secretion signal. Most RiPPs have little homology to small molecule natural products regularly secreted across the cytoplasmic membrane through either the Sec-pathway or Tat-pathway.[10,12] The Sec-pathway or *Sec*retion route, translocates unfolded proteins while the Tat-pathway or *T*win-*a*rginine translocation pathway, serves to transport folded proteins.

The leader peptide serving as a recognition motif for the modification enzymes is another hypothesis.[70] If the leader peptide is in fact acting as a recognition motif, it could allow for the engineering of natural product analogs with different core topologies.[10,12] Oman et al. investigated the role of the sublancin leader peptide and showed that the leader peptide is important for the efficient glycosylation activity of SunS, but not essential. Incubation of SunS and SunA core peptide resulted in full glycosylation at Cys22 in SunA.[15] Alternatively the leader may assist the modification enzymes in folding or stabilizing the precursor peptide against degradation by behaving like a cis-acting chaperone.[71] It has been additionally proposed that the leader peptide could be inactivating the natural product until it is fully modified and secreted outside the producing organism.[72] Indeed, antimicrobial assays of *in vitro* glycosylated and oxidatively folded precursor SunA peptide, that had the leader peptide still attached, showed loss of bioactivity against sublancin sensitive cells.[70,73]

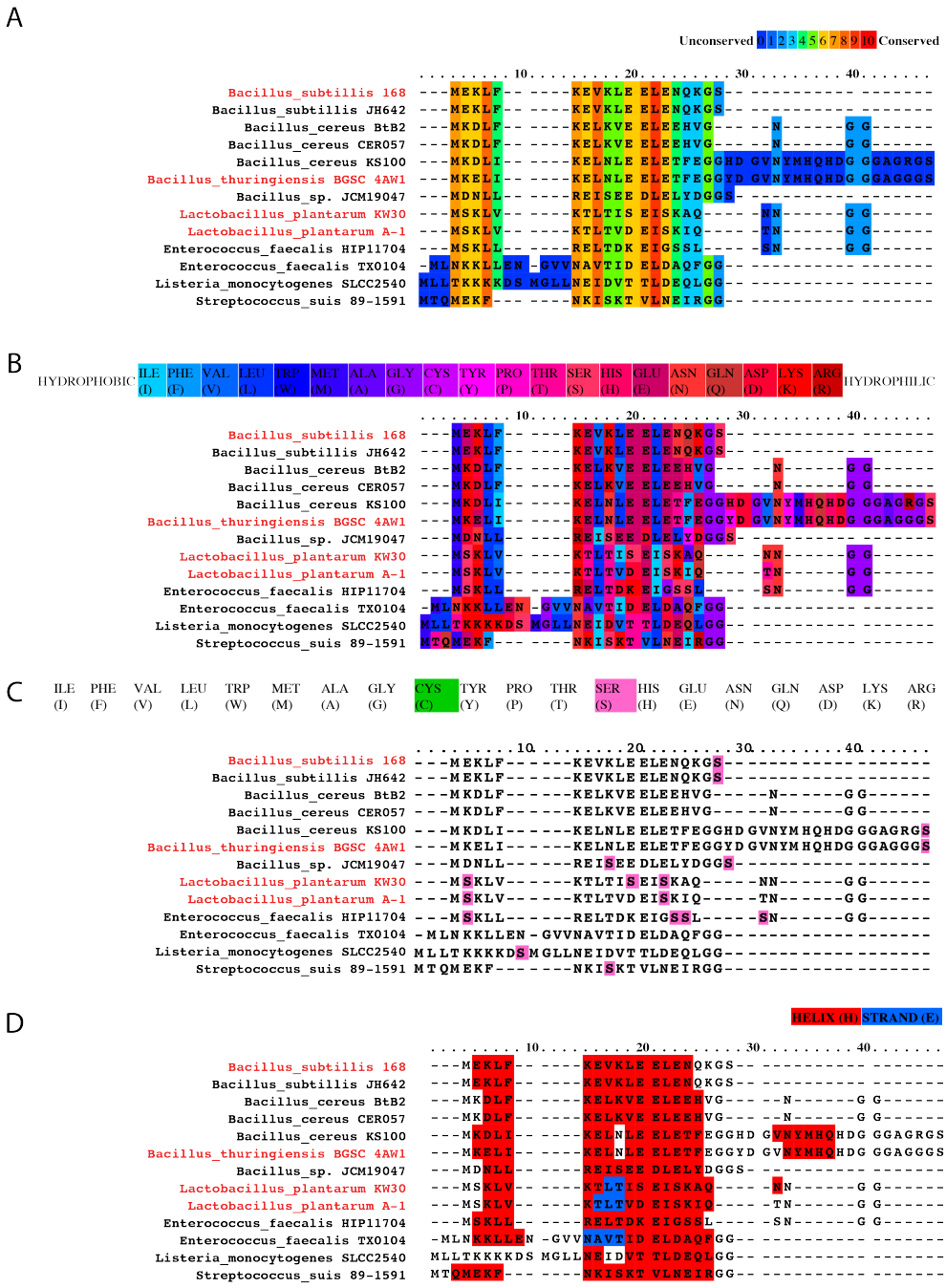

Figure 1.8 Leader sequence conservation among known and putative glycocins.

Sequence alignment as performed by PRALINE of leader peptides of some members of the glycocin family of natural products. (a) Sequence alignment displaying the degree of amino acid conservation, blue indicates low conservation and red indicates high conservation. (b) Sequence alignment displaying the degree of hydrophobicity. (c) Sequence alignment displaying all cysteine residues in green and serine residues in pink. (d) Sequence alignment using the workbench PSIPRED indicating predicted secondary structures, red indicates a predicted helix and blue indicates beta strands.

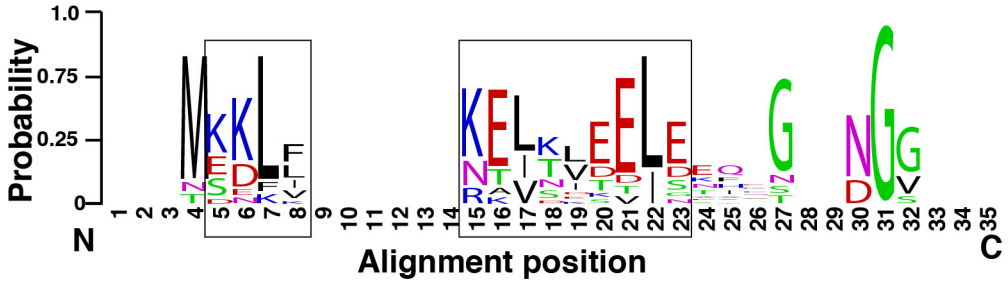

Figure 1.9 Glycocin leader peptide sequence alignment.

Glycocins have leader peptides that are typically rich in Lys, Glu and Leu residues, as observed in the JKLX (J = E, K, or S) and KEBXXXELEXXXG motifs (B = V, L, or I), and usually end in a GG or GS motifs.

The core peptides of the glycocin family have low sequence identity but contain two conserved nested disulfide bridges that help fold the peptide into a hairpin and stabilize the overall structure. Thus far, all known glycocins have a CX_6C-X_n-CX_6C or $(CX_6C)_2$ motif (Figure 1.3). It has been observed, however, that putative glycocins contain either the $(CX_6C)_2$ motif, or a $(CX_{13}C)_2$ motif (Figures 1.10C and 1.11).[14] The $(CX_6C)_2$ motifs had been predicted by PSIPRED to be embedded within helical structures in the core peptide.[74] NMR solution structures of both sublancin and glycocin F have confirmed the predicted helical structures,[75,76] which confer a helix-loop-helix topology to the core peptides (Figure 1.10D). The N-terminal helix (Helix A) is more hydrophobic than the C-terminal helix (Helix B) and the interhelical region contains anywhere between 9 to 14 residues and mainly those with small or no side chains such as glycine (Figure 1.10B). A CX_nC motif is not uncommon in the natural product world. Quite a few unmodified peptide toxins (arthropod toxins, conotoxins, and antifungals) contain the CX_nC-X_m-CX_oC motif within a helix-loop-helix conformation.[77-79] It is important to note that the integrity of the disulfide bridges holding the hairpin structure together is essential for peptide activity.[14,15,70]

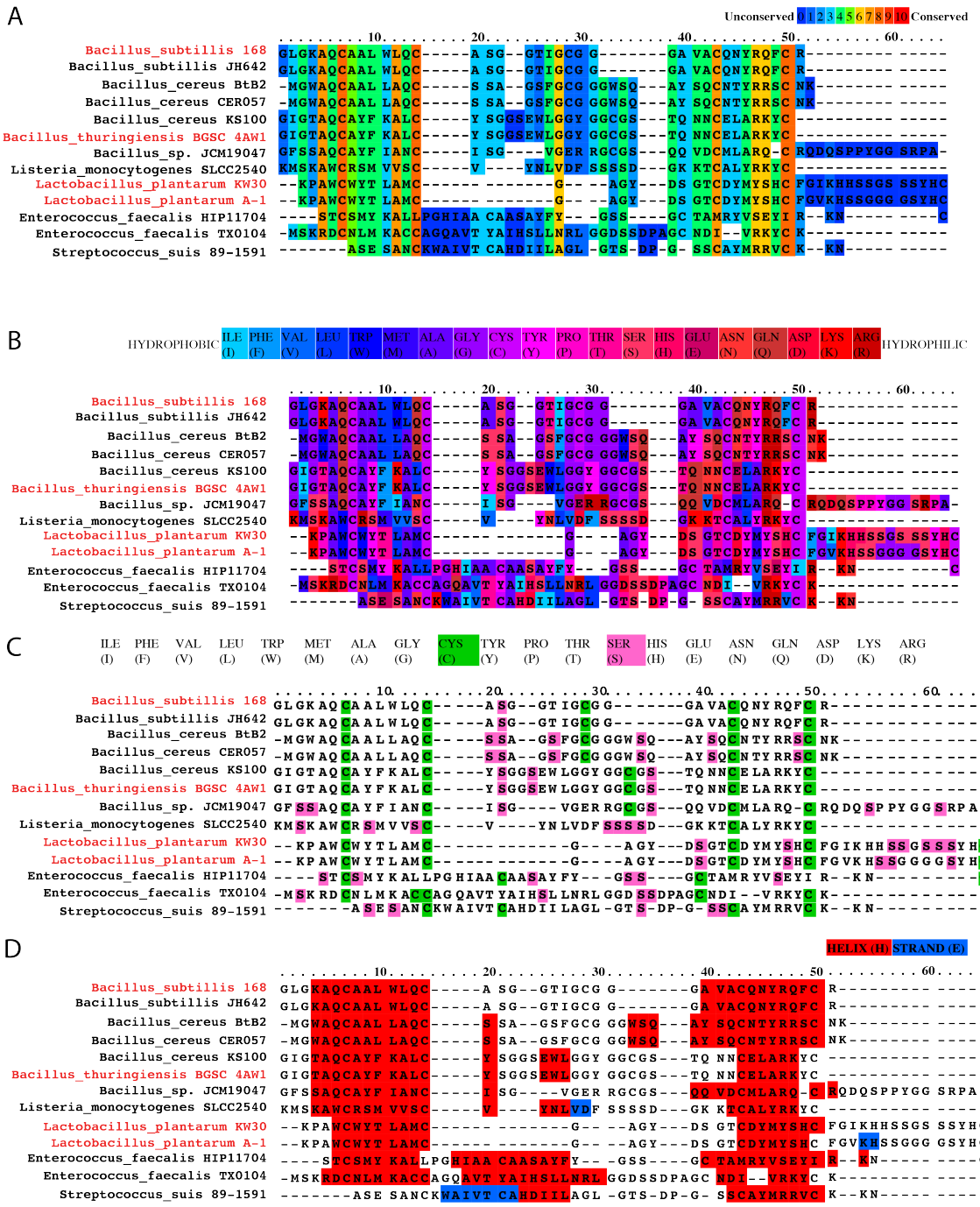

Figure 1.10 Core peptide sequence conservation among glycocins.

Sequence alignment as performed by PRALINE of the core peptides of some members of the glycocin family of natural products. (a) Sequence alignment displaying the degree of amino acid conservation, blue indicates low conservation and red indicates high conservation. (b) Sequence alignment displaying the degree of hydrophobicity. (c) Sequence alignment displaying all cysteine residues in green and serine residues in pink. (d) Sequence alignment using the workbench PSIPRED indicating predicted secondary structures, red indicates a predicted helix and glue indicated beta strands.

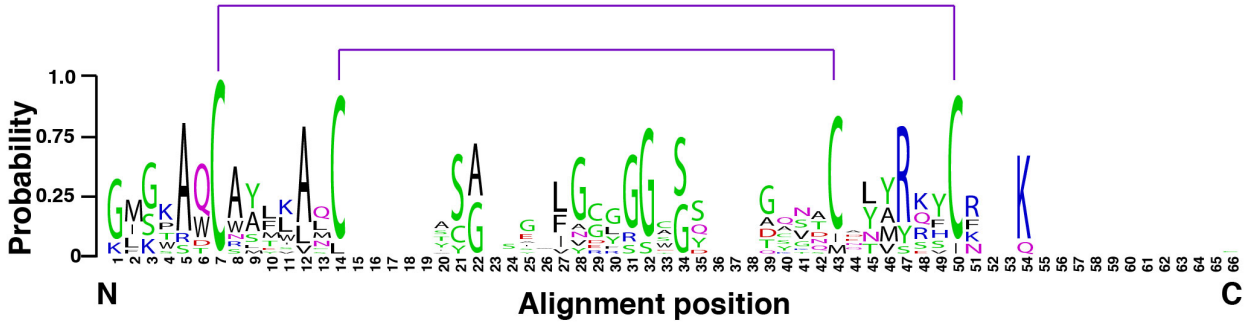

Figure 1.11 Glycocin core peptide sequence alignment.

The $(CX_6C)_2$ motifs as predicted by PSIPRED is embedded within helical structures in the core peptide. Cysteines involved in disulfide bridge formation are shown in green with purple lines indicating corresponding disulfide bond.

1.4.3 Glycocin glycosyltransferases

The formation of the glycosidic linkage to serine or cysteine residues of the core peptides is performed by a glycosyltransferase modifying enzyme (GlycS). It has been speculated that the S-glycosidic linkages may have evolved because of their stability[32] and relative resistance to cleavage by extracellular and cell envelope glycosidases and transglycosylases, similar to the strategy of incomportaing D-amino acids into peptides to decrease the chance of proteolysis.[33,34,80] GlycS proteins are normally medium to small in size with close to 430 amino acids (approximately 50 kDa). The sequence identity within the GlycS protein family is only around 28% (Figure 1.12) and *in silico* analysis of the primary sequence of GlycS proteins reveals overall hydrophilic structures (Figure 1.13). Structural prediction tools (PSIPRED) anticipated a series of helical regions and beta strands (Figure 1.14).[74] In vitro studies of SunS, the glycosyltransferase of the sublancin cluster, demonstrated high regioselectivity. When reduced SunA was incubated with SunS, only Cys22 was glycosylated even though SunA has five available cysteine residues available.[15]

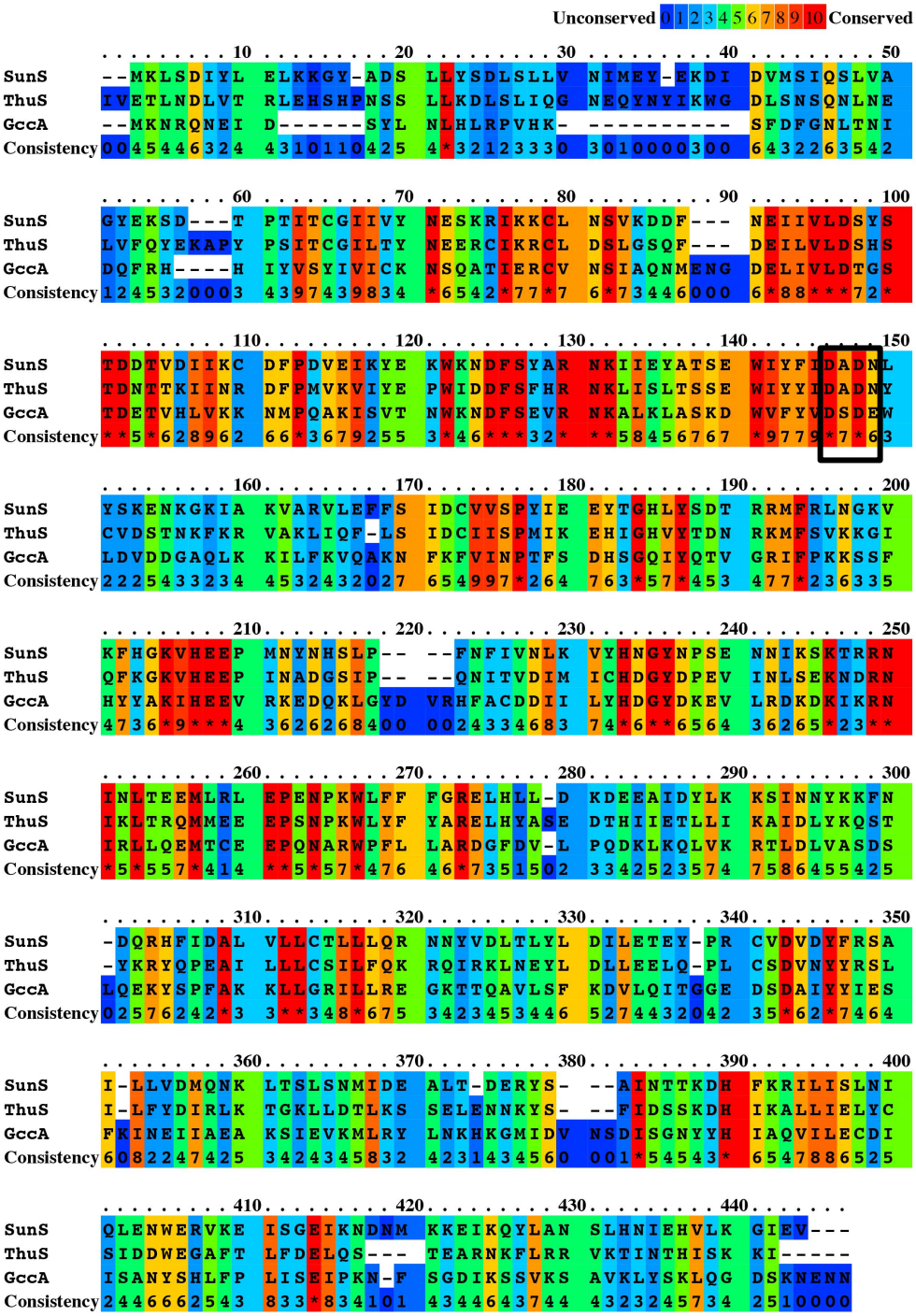

Figure 1.12 Glycocin glycosyltransferase sequence alignment and amino acid conservation.

Sequence alignment of known S-glycosyltransferases associated with glycocins showing their conservation using PRALINE. The scoring scheme works from 0 for the least conserved alignment position up to 10 (designated as an *) for the most conserved alignment position. The black box shows important conserved catalytic residues also known as the DxD motif.

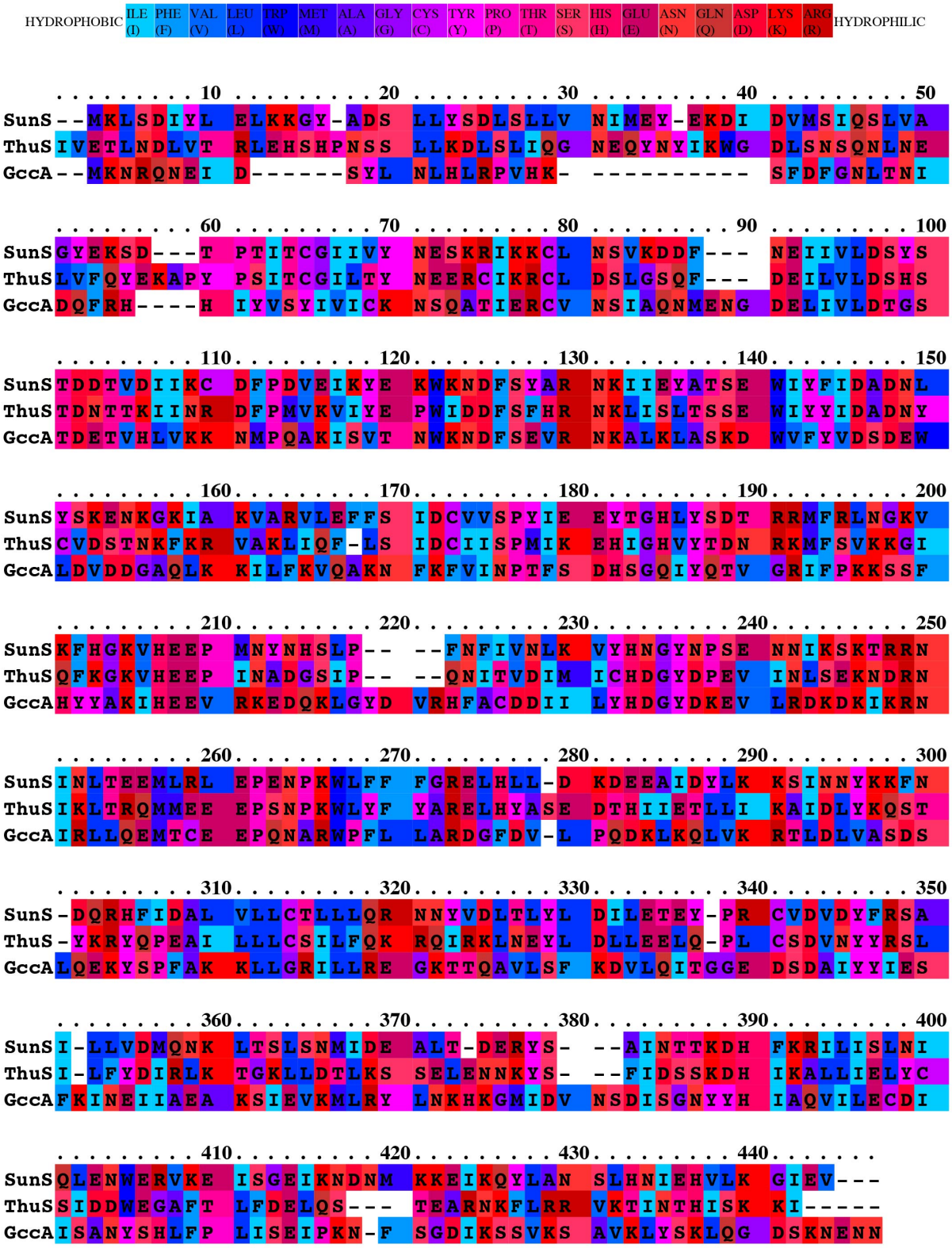

Figure 1.13 Glycocin glycosyltransferase sequence alignment and amino acid hydrophobicity.

Sequence alignment of known S-glycosyltransferases showing their overall hydrophobicity using PRALINE.

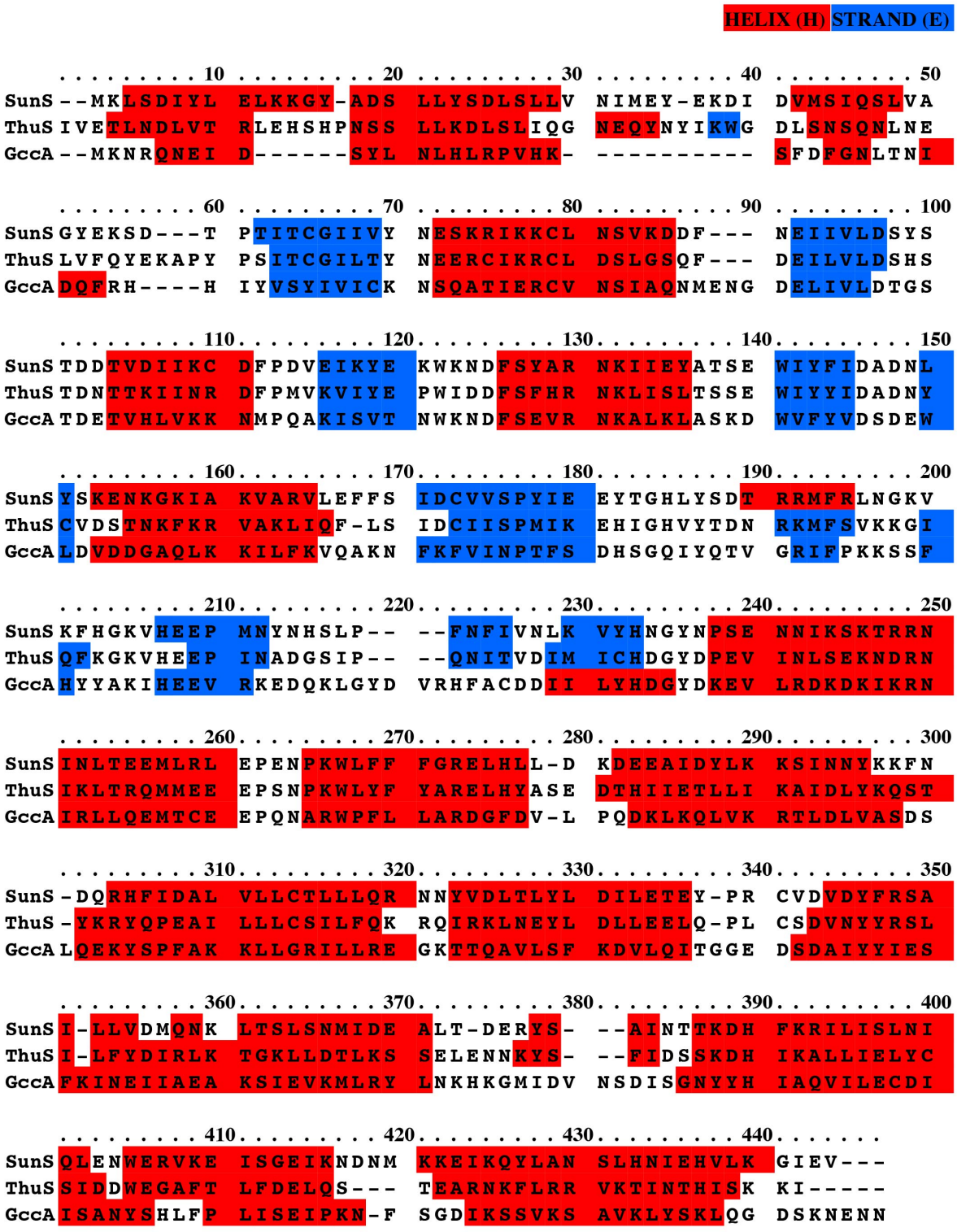

Figure 1.14 Glycocin glycosyltransferase sequence alignment and secondary structure prediction.

Sequence alignment of known S-glycosyltransferases showing their predicted secondary structures using PRALINE. Red indicates a predicted helical structure and blue indicates a beta strands.

Oman et al. performed in vitro experiments, using a SunA substrate with an engineered Factor Xa cleavage site between the leader and core peptides (SunAXa), to study the substrate selectivity of SunS. Surprisingly, SunS is highly substrate tolerant with respect to the nucleotide sugar donor.[15] When SunS is incubated with activated sugar donors including: UDP-N-acetylglucosamine (UDP-GlcNAc), UDP-galactose (UDP-Gal), GDP-mannose (UDP-Man), or UDP-xylose (UDP-Xyl), SunAXa was successfully glycosylated at Cys22 although the reactions with these substrates were less efficient when compared to UDP-glucose (UDP-Glc) (Figure 1.15). The substrate specificity of SunS will be further discussed in chapter 6.

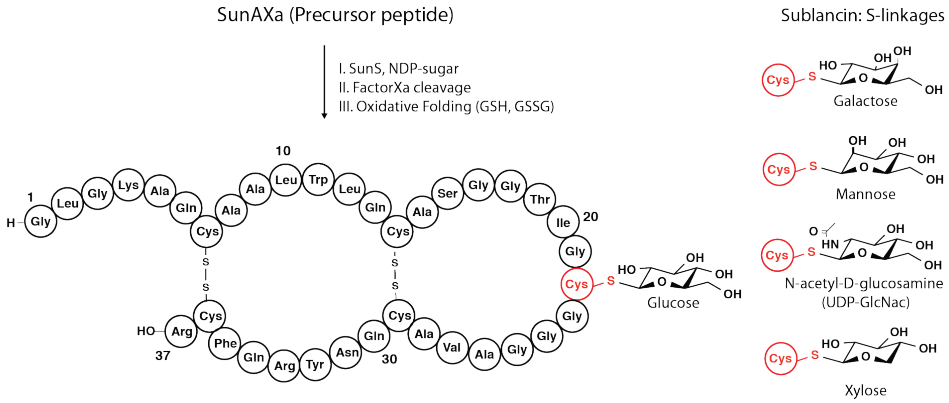

Figure 1.15 Sublancin sugar analogs produced in vitro with the glycosyltransferase SunS.

Due to the observation that three out of four of the cysteines involved in disulfide bond in sublancin are flanked by alanine and glutamine, a few SunA mutants were generated by Dr. Huan Wang to study the whether these residues were involved in SunS substrate recognition (Figure 1.16). The flanking residues of Cys22 were mutated to a series of charged and uncharged residues.[15] Although the mutant SunA peptides were substrates for SunS, Oman et al. and Wang et al. showed that the flanking residues do affect the efficiency of catalysis.[70] These studies opened up the possibility that the overall peptide sequence is responsible for guiding the activity of the glycosyltransferase rather than the flanking residues of the glycosylated amino acid. Wang

et al. further investigated the peptide substrate specificity and selectivity of SunS by generating SunA mutants containing amino acid insertions or deletions that resulted in a "change in register". Both the SunAXaΔIle and SunAXa-S16-G17insAAA (triple Ala insertion mutant between Ser16 and Gly17) mutants were fully glycosylated by SunS at Cys22. Insertions or deletions after the helical region did not have an effect on the selectivity of SunS. In addition, a double glycosylated SunA was observed when the flanking residues of Cys14 were mutated to Gly. But when Thr19 was mutated to Cys two monoglycosylated peptides were detected (i.e. either Cys19 or Cys22 was glycosylated). A truncated SunA mutant expanding residues 5 to 33 with an W11P mutation, SunA(5-33)W11P, was not a substrate for SunS while the SunA(5-33) peptide was. Incorporating a helix breaking residue Pro disrupts Helix A and suggests that SunS recognizes the N-terminal helix of the core peptide to glycosylate Cys22 in the adjacent flexible loop.[70]

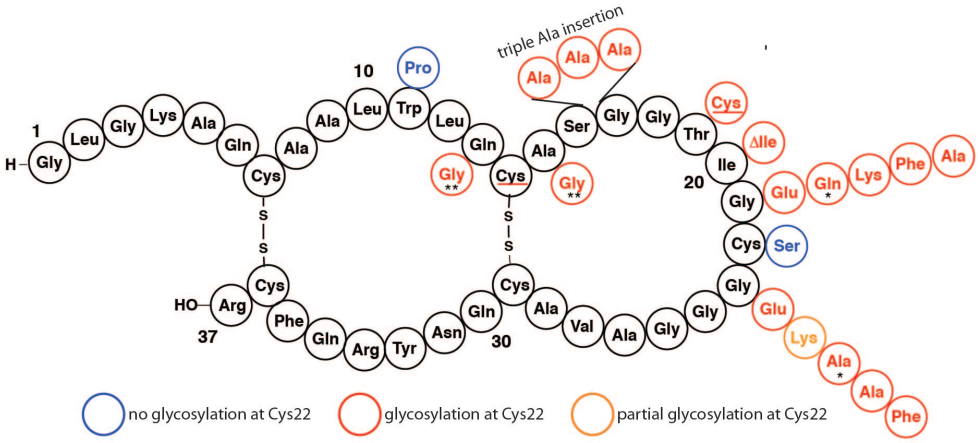

Figure 1.16 Substrate specificity and selectivity of SunS.

SunAXaΔIle and SunAXa-S16-G17insAAA (triple Ala insertion mutant between Ser16 and Gly17) mutants were fully glycosylated by SunS at Cys22. A double glycosylated SunA was observed when the flanking residues of Cys14 were mutated to Gly. When Thr19 was mutated to Cys two monoglycosylated peptides were detected (i.e. either Cys19 or Cys22 was glycosylated). A truncated SunA mutant encompassing residues 5 to 33 with W11P mutation, SunA(5-33)W11P, was not a substrate for SunS while the SunA(5-33) peptide was. Single asterisk = double mutant Gln and Ala, double asterix = double mutant Gly resulting in Cys22 glycosylation and Cys14 glycosylation. When Thr19 was mutated to Cys either Cys19 or Cys22 were glycosylated but not both.

1.4.4 Thiol-disulfide oxidoreductases (TDORs)

The characteristic disulfide bridges of the glycocin family of natural products are installed by thiol-disulfide oxidoreductases (TDORs) and these disulfide bonds are critical for the biological activity of glycocins.[81] Disulfide bonds are found mostly in extracellular proteins and peptides and tend to be highly conserved among protein families.[82] Structurally important disulfide modifications are known to provide natural products with unusually high structural stability thus making them difficult to degrade.[83,84] Once the mature product forms it is difficult to gain access to the disulfides in order to unfold the product due to the formation of hydrophobic cores.[85,86] TDORs involved in sublancin disulfide formation are encoded within the biosynthetic gene cluster. These genes are known as *Bacillus* disulfide bond genes, or bdb.[81,87] *Bacillus subtilis* contains four such *bdb* genes, *bdbA*, *B*, *C* and *D*, The SPβ prophage that contains sublancin's operon, includes *bdbB* and *bdbA* (Figure 1.7). Dorenbos et al. have shown that *bdbB* and *bdbC* are involved in the production of sublancin, but that *bdbA* is not absolutely required for activity of the peptide. *bdbB* however, has a major role in sublancin production and *bdbC* can partly replace *bdbB*.[81]

1.4.5 Proteolysis and export

Quite a few ribosomally synthesized natural product gene clusters code for proteins that are responsible for the enzymatic removal of the leader peptide followed by the extracellular transport of the mature product. The glycocin biosynthetic gene clusters contain the *glycT* gene that encodes the proteolytic GlycT enzyme. As mentioned previously glycocins have leader peptides that usually end in a "double glycine" GG or GS motifs which are known to be cleavage sites for natural product proteases such as those found in the class II lantibiotic biosynthetic

clusters. BLAST sequence analysis of the glycT genes for sublancin (SunT) and glycocin F (GccB) predicts a bifunctional ABC transporter with features including an amino-terminal cytoplasmic peptidase domain and a carboxyl terminal ATP-binding domain (Figure 1.17).[16,88,89] These features would allow the GlycT to cleave after the double glycine moiety and transport the product out of the cell.[90] Dorenbos et al. have shown that SunT is indispensable for sublancin production,[81] and it is believed that the glycocin leader peptide inactivates the mature product while it is still located inside of the cell. In addition, it is thought that the GlycT protein transports the product and cleaves the leader peptide off before it is released to the extracellular environment.[91]

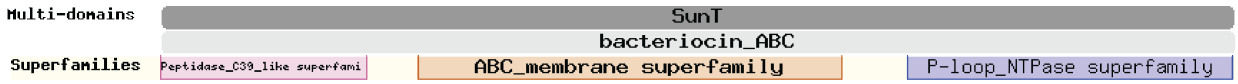

Figure 1.17 Graphical representation of SunT conserved domains.

Pink: Peptidase family C39 mostly contains bacteriocin-processing endopeptidases from bacteria. The cysteine peptidases in family C39 cleave the "double-glycine" leader peptides from the precursors of various bacteriocins. The cleavage is mediated by the transporter as part of the secretion process. Orange: ABC transporter transmembrane region; This family represents a unit of six transmembrane helices. Blue: P-loop containing Nucleoside Triphosphate Hydrolases; Members of the P-loop NTPase domain superfamily are characterized by a conserved nucleotide phosphate-binding motif.

1.4.6 Immunity

Bacteriocin-producing bacteria have several mechanisms to protect themselves against toxic effects of their natural products. One such mechanism is by employing an ABC transporter that can actively pump the toxin out of the cell, thus preventing a toxic level buildup of the bacteriocin inside of the cell.[92,93] Alternatively, the bacteria can produce small immunity proteins that are associated with the cell membrane and can intercept the toxin by binding to it before it can damage the cell. The latter case is seen mainly in the immunity proteins produced by

lantibiotics called LanI.[94-96] Another option is to change the charge of the cell membrane or cell wall thus making the membrane more positively charged and therefore more resistant to cationic bacteriocins.[97,98]

For years it was unclear which gene of the SPβ prophage was responsible for the immunity of *Bacillus subtilis* 168 against sublancin. In 1999 all 187 genes located in the SPβ prophage were screened by Lazarevic et al. for homology to known producer immunity genes, but no homology was determined at the time. It was not until 2009 that Dubois et al. showed that only 1 of the 187 genes is indispensable for immunity of *B. subtilis* 168 against sublancin. The required gene was named *sunI*. SunI is a 105 residue protein (12.1 kDa) that was predicted to be a membrane protein with an N-terminal transmembrane domain and an N_{out}-C_{in} topology with the majority of the protein localized in the cytoplasm. Due to low sequence similarity to other immunity proteins and its unique topology, SunI was classified in a new class of bacteriocin-producer immunity proteins.[89]

1.5 OUTLOOK

The glycocin family of ribosomally synthesized peptide natural products has only recently been established. Their hypothezised novel mechanisms of actions has the potential to offer novel therapeutics and their biosynthetic enzymes have the potential to become novel tools for chemical biology research. Sublancin has bactericidal activity against *Bacillus* strains and methicillin-resistant *Staphylococcus aureus* strains.[99,100] Research to understand one particular member of this family, sublancin, spans over 17 years of work but the mechanism by which glycocins exert their activity is still not fully understood. In order to provide additional insight into the mode of action of sublancin, this thesis describes the nuclear magnetic resonance (NMR) solution structure determination of sublancin (Chapter 2), efforts in elucidating the mechanism of

action of sublancin by studying the Phosphotransferase system (Chapter 3) and through sublancin structural analogs (Chapter 4), localization studies of sublancin by super resolution microscopy (Chapter 5), and mechanistic investigations of the glycosyltransferase SunS responsible for installing a glucose moiety at Cys22 of sublancin (Chapter 6).

1.6 REFERENCES

(1) Wassenaar, T. *Bacteria: The Benign, the Bad, and the Beautiful*; John Wiley & Sons, 2011.

(2) Mullard, A. *Nature* **2008**, *453*, 578. "Microbiology: the inside story".

(3) Tralau, T.; Sowada, J.; Luch, A. *Expert Opin Drug Metab Toxicol* **2014**, *11*, 411. "Insights on the human microbiome and its xenobiotic metabolism: what is known about its effects on human physiology?".

(4) Fair, R. J.; Tor, Y. *Perspect Medicin Chem* **2014**, *6*, 25. "Antibiotics and bacterial resistance in the 21st century".

(5) O'Neill, J. *Antimicrobial Resistance: Tackling a crisis for the health and wealth of nations*, 2014.

(6) Overbye, K. M.; Barrett, J. F. *Drug Discov Today* **2005**, *10*, 45. "Antibiotics: where did we go wrong?".

(7) Lange, R. P.; Locher, H. H.; Wyss, P. C.; Then, R. L. *Curr Pharm Des* **2007**, *13*, 3140. "The targets of currently used antibacterial agents: lessons for drug discovery.".

(8) Silver, L. L. *Clin Microbiol Rev* **2011**, *24*, 71. "Challenges of Antibacterial Discovery".

(9) Rosamond, J.; Allsop, A. *Science* **2000**, *287*, 1973. "Harnessing the power of the genome in the search for new antibiotics".

(10) Oman, T. J.; van der Donk, W. A. *Nat Chem Biol* **2010**, *6*, 9. "Follow the leader: the use of leader peptides to guide natural product biosynthesis".

(11) Arnison, P. G.; Bibb, M. J.; Bierbaum, G.; Bowers, A. A.; Bugni, T. S.; Bulaj, G.; Camarero, J. A.; Campopiano, D. J.; Challis, G. L.; Clardy, J.; Cotter, P. D.; Craik, D. J.; Dawson, M.; Dittmann, E.; Donadio, S.; Dorrestein, P. C.; Entian, K. D.; Fischbach, M. A.; Garavelli, J. S.; Goransson, U.; Gruber, C. W.; Haft, D. H.; Hemscheidt, T. K.; Hertweck, C.; Hill, C.; Horswill, A. R.; Jaspars, M.; Kelly, W. L.; Klinman, J. P.; Kuipers, O. P.; Link, A. J.; Liu, W.; Marahiel, M. A.; Mitchell, D. A.; Moll, G. N.; Moore, B. S.; Muller, R.; Nair, S. K.; Nes, I. F.; Norris, G. E.; Olivera, B. M.; Onaka, H.;

Patchett, M. L.; Piel, J.; Reaney, M. J.; Rebuffat, S.; Ross, R. P.; Sahl, H. G.; Schmidt, E. W.; Selsted, M. E.; Severinov, K.; Shen, B.; Sivonen, K.; Smith, L.; Stein, T.; Sussmuth, R. D.; Tagg, J. R.; Tang, G. L.; Truman, A. W.; Vederas, J. C.; Walsh, C. T.; Walton, J. D.; Wenzel, S. C.; Willey, J. M.; van der Donk, W. A. *Nat Prod Rep* **2013**, *30*, 108. "Ribosomally synthesized and post-translationally modified peptide natural products: overview and recommendations for a universal nomenclature".

(12) Yang, X.; van der Donk, W. A. *Chem Eur J* **2013**, *19*, 7662. "Ribosomally Synthesized and Post-translationally Modified Peptide Natural Products: New Insights Into the Role of Leader and Core Peptides During Biosynthesis".

(13) Dunbar, K. L.; Mitchell, D. A. *ACS Chem Biol* **2013**, *8*, 473. "Revealing Nature's Synthetic Potential Through the Study of Ribosomal Natural Product Biosynthesis".

(14) Norris, G. E.; Patchett, M. L. In *Natural Products Analysis*; John Wiley & Sons, Inc: 2014, p 507.

(15) Oman, T. J.; Boettcher, J. M.; Wang, H.; Okalibe, X. N.; van der Donk, W. A. *Nat Chem Biol* **2011**, *7*, 78. "Sublancin is not a lantibiotic but an S-linked glycopeptide".

(16) Stepper, J.; Shastri, S.; Loo, T. S.; Preston, J. C.; Novak, P.; Man, P.; Moore, C. H.; Havlicek, V.; Patchett, M. L.; Norris, G. E. *FEBS Lett* **2011**, *585*, 645. "Cysteine S-glycosylation, a new post-translational modification found in glycopeptide bacteriocins".

(17) Wang, H.; Oman, T. J.; Zhang, R.; Garcia De Gonzalo, C. V.; Zhang, Q.; van der Donk, W. A. *J Am Chem Soc* **2014**, *136*, 84. "The glycosyltransferase involved in thurandacin biosynthesis catalyzes both O- and S-glycosylation".

(18) Hata, T.; Tanaka, R.; Ohmomo, S. *Int J Food Microbiol* **2010**, *137*, 94. "Isolation and characterization of plantaricin ASM1: a new bacteriocin produced by Lactobacillus plantarum A-1".

(19) Paik, S. H.; Chakicherla, A.; Hansen, J. N. *J Biol Chem* **1998**, *273*, 23134. "Identification and characterization of the structural and transporter genes for, and the chemical and biological properties of, sublancin 168, a novel lantibiotic produced by Bacillus subtilis 168".

(20) Oman, T. J.; van der Donk, W. A. *ACS Chem Biol* **2009**, *4*, 865. "Insights into the mode of action of the two-peptide lantibiotic haloduracin".

(21) Willey, J. M.; van der Donk, W. A. *Annu Rev Microbiol* **2007**, *61*, 477. "Lantibiotics: Peptides of Diverse Structure and Function".

(22) Brimble, M. A.; Edwards, P. J.; Harris, P. W.; Norris, G. E.; Patchett, M. L.; Wright, T. H.; Yang, S. H.; Carley, S. E. *Chemistry* **2015**, *21*, 3556. "Synthesis of the antimicrobial s-linked glycopeptide, glycocin f".

(23) Spiro, R. G. *Glycobiology* **2002**, *12*, 43R. "Protein glycosylation: nature, distribution, enzymatic formation, and disease implications of glycopeptide bonds".

(24) Asano, N. *Cell Mol Life Sci* **2009**, *66*, 1479. "Sugar-mimicking glycosidase inhibitors: bioactivity and application".

(25) Inouye S; Tsuruoka T; T., N. *J Antibiot* **1966**, *19*, 288. "The structure of nojirimycin, a piperidinose sugar antibiotic.".

(26) Asano, N. *Glycobiology* **2003**, *13*, 93R. "Glycosidase inhibitors: update and perspectives on practical use".

(27) Kajimoto, T.; Node, M. *Curr Top Med Chem* **2009**, *9*, 13. "Inhibitors against glycosidases as medicines".

(28) Schoner, W.; Scheiner-Bobis, G. *Am J Cardiovasc Drugs* **2007**, *7*, 173. "Endogenous and exogenous cardiac glycosides and their mechanisms of action".

(29) Newman, R. A.; Yang, P.; Pawlus, A. D.; Block, K. I. *Mol Interv* **2008**, *8*, 36. "Cardiac glycosides as novel cancer therapeutic agents".

(30) Saleem, M.; Nazir, M.; Ali, M. S.; Hussain, H.; Lee, Y. S.; Riaz, N.; Jabbar, A. *Nat Prod Rep* **2010**, *27*, 238. "Antimicrobial natural products: an update on future antibiotic drug candidates".

(31) Neuhof, T.; Schmieder, P.; Seibold, M.; Preussel, K.; von Dohren, H. *Bioorg Med Chem Lett* **2006**, *16*, 4220. "Hassallidin B--second antifungal member of the Hassallidin family".

(32) Baran, E.; Drabarek, S. *Pol J Chem* **1978**, *52*, 941. "Studies on Synthesis of S-Glycosidic Bond Between Cysteine and Glucose or Galactose".

(33) Jahn, M.; Marles, J.; Warren, R. A.; Withers, S. G. *Angew Chem Int Ed Engl* **2003**, *42*, 352. "Thioglycoligases: mutant glycosidases for thioglycoside synthesis".

(34) Driguez, H. *Chembiochem* **2001**, *2*, 311. "Thiooligosaccharides as tools for structural biology".

(35) Lote, C. J.; Weiss, J. B. *FEBS Lett* **1971**, *16*, 81. "Identification of digalactosylcysteine in a glycopeptide isolated from urine by a new preparative technique".

(36) Lote, C. J.; Weiss, J. B. *Biochem J* **1971**, *123*, 25P. "Identification in urine of a low-molecular-weight highly polar glycopeptide containing cysteinyl-galactose".

(37) Weiss, J. B.; Lote, C. J.; Bobinski, H. *Nat New Biol* **1971**, *234*, 25. "New low molecular weight glycopeptide containing triglucosylcysteine in human erythrocyte membrane".

(38) Elsayed, S.; Bennich, H. *Scand J Immun* **1975**, *4*, 203. "The Primary Structure of Allergen M from Cod".

(39) Specker, D.; Wittmann, V. In *Glycopeptides and Glycoproteins*; Wittmann, V., Ed.; Springer Berlin Heidelberg: 2007; Vol. 267, p 65.

(40) Thayer, D. A.; Yu, H. N.; Galan, M. C.; Wong, C.-H. *Angew. Chem. Int. Ed.* **2005**, *44*, 4596. "A General Strategy toward S-Linked Glycopeptides".

(41) Cohen, S. B.; Halcomb, R. L. *J Am Chem Soc* **2002**, *124*, 2534. "Application of serine- and threonine-derived cyclic sulfamidates for the preparation of S-linked glycosyl amino acids in solution- and solid-phase peptide synthesis".

(42) Galonic, D. P.; Van Der Donk, W. A.; Gin, D. Y. *Chemistry* **2003**, *9*, 5997. "Oligosaccharide-peptide ligation of glycosyl thiolates with dehydropeptides: synthesis of S-linked mucin-related glycopeptide conjugates".

(43) Galonic, D. P.; van der Donk, W. A.; Gin, D. Y. *J Am Chem Soc* **2004**, *126*, 12712. "Site-selective conjugation of thiols with aziridine-2-carboxylic acid-containing peptides".

(44) Galonic, D. P.; Ide, N. D.; van der Donk, W. A.; Gin, D. Y. *J Am Chem Soc* **2005**, *127*, 7359. "Aziridine-2-carboxylic acid-containing peptides: application to solution- and solid-phase convergent site-selective peptide modification".

(45) Hili, R.; Rai, V.; Yudin, A. K. *J Am Chem Soc* **2010**, *132*, 2889. "Macrocyclization of linear peptides enabled by amphoteric molecules".

(46) Breukink, E.; de Kruijff, B. *Nat Rev Drug Discov* **2006**, *5*, 321. "Lipid II as a target for antibiotics".

(47) Hammes, W. P.; Neuhaus, F. C. *Antimicrob Agents Chemother* **1974**, *6*, 722. "On the mechanism of action of vancomycin: inhibition of peptidoglycan synthesis in Gaffkya homari".

(48) Nagarajan, R. *Glycopeptide antibiotics*; Marcel Dekker: New York, 1994; Vol. 63.

(49) Hsu, S. T.; Breukink, E.; Tischenko, E.; Lutters, M. A.; de Kruijff, B.; Kaptein, R.; Bonvin, A. M.; van Nuland, N. A. *Nat Struct Mol Biol* **2004**, *11*, 963. "The nisin-lipid II complex reveals a pyrophosphate cage that provides a blueprint for novel antibiotics".

(50) Brotz, H.; Josten, M.; Wiedemann, I.; Schneider, U.; Gotz, F.; Bierbaum, G.; Sahl, H. G. *Mol Microbiol* **1998**, *30*, 317. "Role of lipid-bound peptidoglycan precursors in the formation of pores by nisin, epidermin and other lantibiotics".

(51) Breukink, E.; Wiedemann, I.; van Kraaij, C.; Kuipers, O. P.; Sahl, H. G.; de Kruijff, B. *Science* **1999**, *286*, 2361. "Use of the cell wall precursor lipid II by a pore-forming peptide antibiotic".

(52) Hasper, H. E.; Kramer, N. E.; Smith, J. L.; Hillman, J. D.; Zachariah, C.; Kuipers, O. P.; de Kruijff, B.; Breukink, E. *Science* **2006**, *313*, 1636. "An alternative bactericidal mechanism of action for lantibiotic peptides that target lipid II".

(53) Wiedemann, I.; Breukink, E.; van Kraaij, C.; Kuipers, O. P.; Bierbaum, G.; de Kruijff, B.; Sahl, H. G. *J Biol Chem* **2001**, *276*, 1772. "Specific binding of nisin to the peptidoglycan precursor lipid II combines pore formation and inhibition of cell wall biosynthesis for potent antibiotic activity".

(54) Oman, T. J.; Lupoli, T. J.; Wang, T. S.; Kahne, D.; Walker, S.; van der Donk, W. A. *J Am Chem Soc* **2011**, *133*, 17544. "Haloduracin alpha Binds the Peptidoglycan Precursor Lipid II with 2:1 Stoichiometry".

(55) Kouwen, T. R.; Trip, E. N.; Denham, E. L.; Sibbald, M. J.; Dubois, J. Y.; van Dijl, J. M. *Antimicrob Agents Chemother* **2009**, *53*, 4702. "The large mechanosensitive channel MscL determines bacterial susceptibility to the bacteriocin sublancin 168".

(56) Blount, P.; Sukharev, S. I.; Moe, P. C.; Martinac, B.; Kung, C. *Methods Enzymol* **1999**, *294*, 458. "Mechanosensitive channels of bacteria".

(57) Martinac, B. *Cell Physiol Biochem* **2001**, *11*, 61. "Mechanosensitive channels in prokaryotes".

(58) Pivetti, C. D.; Yen, M. R.; Miller, S.; Busch, W.; Tseng, Y. H.; Booth, I. R.; Saier, M. H., Jr. *Microbiol Mol Biol Rev* **2003**, *67*, 66. "Two families of mechanosensitive channel proteins".

(59) Blount, P.; Sukharev, S. I.; Moe, P.; Kung, C. *Biol Bull* **1997**, *192*, 126. "Mechanosensitive channels of E. coli: a genetic and molecular dissection".

(60) Sukharev, S. I.; Blount, P.; Martinac, B.; Kung, C. *Annu Rev Physiol* **1997**, *59*, 633. "Mechanosensitive channels of Escherichia coli: the MscL gene, protein, and activities".

(61) Chang, G.; Spencer, R. H.; Lee, A. T.; Barclay, M. T.; Rees, D. C. *Science* **1998**, *282*, 2220. "Structure of the MscL homolog from Mycobacterium tuberculosis: a gated mechanosensitive ion channel".

(62) Liu, Z.; Gandhi, C. S.; Rees, D. C. *Nature* **2009**, *461*, 120. "Structure of a tetrameric MscL in an expanded intermediate state".

(63) Iscla, I.; Levin, G.; Wray, R.; Reynolds, R.; Blount, P. *Biophys J* **2004**, *87*, 3172. "Defining the physical gate of a mechanosensitive channel, MscL, by engineering metal-binding sites".

(64) Levin, G.; Blount, P. *Biophys J* **2004**, *86*, 2862. "Cysteine scanning of MscL transmembrane domains reveals residues critical for mechanosensitive channel gating".

(65) Yoshimura, K.; Sokabe, M. *J R Soc Interface* **2010**, *7 Suppl 3*, S307. "Mechanosensitivity of ion channels based on protein-lipid interactions".

(66) Sukharev, S.; Anishkin, A. *Trends Neurosci* **2004**, *27*, 345. "Mechanosensitive channels: what can we learn from 'simple' model systems?".

(67) Sahl, H.-G.; Jack, R. W.; Bierbaum, G. *Eur J Biochem* **1995**, *230*, 827. "Biosynthesis and Biological Activities of Lantibiotics with Unique Post-Translational Modifications".

(68) Siezen, R. J.; Kuipers, O. P.; de Vos, W. M. *Antonie van Leeuwenhoek* **1996**, *69*, 171. "Comparison of lantibiotic gene clusters and encoded proteins".

(69) Chatterjee, C.; Paul, M.; Xie, L.; van der Donk, W. A. *Chem Rev* **2005**, *105*, 633. "Biosynthesis and Mode of Action of Lantibiotics".

(70) Wang, H.; van der Donk, W. A. *J Am Chem Soc* **2011**, *133*, 16394. "Substrate selectivity of the sublancin S-glycosyltransferase".

(71) Braun, P.; Tommassen, J. *Trends Microbiol.* **1998**, *6*, 6. "Function of bacterial propeptides".

(72) Xie, L.; Miller, L. M.; Chatterjee, C.; Averin, O.; Kelleher, N. L.; van der Donk, W. A. *Science* **2004**, *303*, 679. "Lacticin 481: in vitro reconstitution of lantibiotic synthetase activity".

(73) Oman, T. J. PhD Thesis, University of Illinois at Urbana-Champaign, 2011.

(74) Jones, D. T. *J Mol Biol* **1999**, *292*, 195. "Protein secondary structure prediction based on position-specific scoring matrices".

(75) Garcia De Gonzalo, C. V.; Zhu, L.; Oman, T. J.; van der Donk, W. A. *ACS Chem Biol* **2014**, *9*, 796. "NMR structure of the S-linked glycopeptide sublancin 168".

(76) Venugopal, H.; Edwards, P. J.; Schwalbe, M.; Claridge, J. K.; Libich, D. S.; Stepper, J.; Loo, T.; Patchett, M. L.; Norris, G. E.; Pascal, S. M. *Biochemistry* **2011**, *50*, 2748. "Structural, dynamic, and chemical characterization of a novel S-glycosylated bacteriocin".

(77) Chagot, B.; Pimentel, C.; Dai, L.; Pil, J.; Tytgat, J.; Nakajima, T.; Corzo, G.; Darbon, H.; Ferrat, G. *Biochem J* **2005**, *388*, 263. "An unusual fold for potassium channel blockers: NMR structure of three toxins from the scorpion Opisthacanthus madagascariensis".

(78) Saucedo, A. L.; Flores-Solis, D.; Rodriguez de la Vega, R. C.; Ramirez-Cordero, B.; Hernandez-Lopez, R.; Cano-Sanchez, P.; Noriega Navarro, R.; Garcia-Valdes, J.; Coronas-Valderrama, F.; de Roodt, A.; Brieba, L. G.; Domingos Possani, L.; del Rio-Portilla, F. *J Biol Chem* **2012**, *287*, 12321. "New tricks of an old pattern: structural versatility of scorpion toxins with common cysteine spacing".

(79) Srinivasan, K. N.; Sivaraja, V.; Huys, I.; Sasaki, T.; Cheng, B.; Kumar, T. K.; Sato, K.; Tytgat, J.; Yu, C.; San, B. C.; Ranganathan, S.; Bowie, H. J.; Kini, R. M.; Gopalakrishnakone, P. *J Biol Chem* **2002**, *277*, 30040. "kappa-Hefutoxin1, a novel toxin from the scorpion Heterometrus fulvipes with unique structure and function. Importance of the functional diad in potassium channel selectivity".

(80) Zasloff, M. *Nature* **2002**, *415*, 389. "Antimicrobial peptides of multicellular organisms".

(81) Dorenbos, R.; Stein, T.; Kabel, J.; Bruand, C.; Bolhuis, A.; Bron, S.; Quax, W. J.; Van Dijl, J. M. *J Biol Chem* **2002**, *277*, 16682. "Thiol-disulfide oxidoreductases are essential for the production of the lantibiotic sublancin 168".

(82) Thornton, J. M. *J Mol Biol* **1981**, *151*, 261. "Disulphide bridges in globular proteins".

(83) Ahern, T. J.; Klibanov, A. M. *Science* **1985**, *228*, 1280. "The mechanisms of irreversible enzyme inactivation at 100C".

(84) Price-Carter, M.; Hull, M. S.; Goldenberg, D. P. *Biochemistry* **1998**, *37*, 9851. "Roles of individual disulfide bonds in the stability and folding of an omega-conotoxin".

(85) Daly, N. L.; Craik, D. J. *IUBMB Life* **2009**, *61*, 144. "Structural studies of conotoxins".

(86) Westermann, J.-C.; Craik, D. J. In *Comprehensive Natural Products II*; Liu, H.-W., Mander, L., Eds.; Elsevier: Oxford, 2010, p 257.

(87) Ritz, D.; Beckwith, J. *Annu Rev Microbiol* **2001**, *55*, 21. "Roles of thiol-redox pathways in bacteria".

(88) McAuliffe, O.; Ross, R. P.; Hill, C. *FEMS Microbiol Rev* **2001**, *25*, 285. "Lantibiotics: structure, biosynthesis and mode of action".

(89) Dubois, J. Y.; Kouwen, T. R.; Schurich, A. K.; Reis, C. R.; Ensing, H. T.; Trip, E. N.; Zweers, J. C.; van Dijl, J. M. *Antimicrob Agents Chemother* **2009**, *53*, 651. "Immunity to the bacteriocin sublancin 168 Is determined by the SunI (YolF) protein of Bacillus subtilis".

(90) Havarstein, L. S.; Diep, D. B.; Nes, I. F. *Mol Microbiol* **1995**, *16*, 229. "A family of bacteriocin ABC transporters carry out proteolytic processing of their substrates concomitant with export".

(91) Ishii, S.; Yano, T.; Hayashi, H. *J Biol Chem* **2006**, *281*, 4726. "Expression and characterization of the peptidase domain of Streptococcus pneumoniae ComA, a bifunctional ATP-binding cassette transporter involved in quorum sensing pathway".

(92) Peschel, A.; Götz, F. *J Bacteriol* **1996**, *178*, 531. "Analysis of the Staphylococcus epidermidis genes epiF, -E, and -G involved in epidermin immunity".

(93) Rince, A.; Dufour, A.; Uguen, P.; Le Pennec, J. P.; Haras, D. *Appl Environ Microbiol* **1997**, *63*, 4252. "Characterization of the lacticin 481 operon: the Lactococcus lactis genes lctF, lctE, and lctG encode a putative ABC transporter involved in bacteriocin immunity".

(94) Hoffmann, A.; Schneider, T.; Pag, U.; Sahl, H. G. *Appl Environ Microbiol* **2004**, *70*, 3263. "Localization and functional analysis of PepI, the immunity peptide of Pep5-producing Staphylococcus epidermidis strain 5".

(95) Stein, T.; Heinzmann, S.; Dusterhus, S.; Borchert, S.; Entian, K. D. *J Bacteriol* **2005**, *187*, 822. "Expression and functional analysis of the subtilin immunity genes spaIFEG in the subtilin-sensitive host Bacillus subtilis MO1099".

(96) Stein, T.; Heinzmann, S.; Solovieva, I.; Entian, K. D. *J Biol Chem* **2003**, *278*, 89. "Function of Lactococcus lactis nisin immunity genes nisI and nisFEG after coordinated expression in the surrogate host Bacillus subtilis".

(97) Peschel, A.; Collins, L. V. *Peptides* **2001**, *22*, 1651. "Staphylococcal resistance to antimicrobial peptides of mammalian and bacterial origin".

(98) Peschel, A.; Otto, M.; Jack, R. W.; Kalbacher, H.; Jung, G.; Götz, F. *J Biol Chem* **1999**, *274*, 8405. "Inactivation of the dlt operon in Staphylococcus aureus confers sensitivity to defensins, protegrins, and other antimicrobial peptides".

(99) Wang, Q.; Zeng, X.; Wang, S.; Hou, C.; Yang, F.; Ma, X.; Thacker, P.; Qiao, S. *Anat Rec (Hoboken)* **2014**, *297*, 1454. "The bacteriocin sublancin attenuates intestinal injury in young mice infected with Staphylococcus aureus".

(100) Ji, S.; Li, W.; Baloch, A. R.; Wang, M.; Cao, B. *Microb Cell Fact* **2015**, *14*, 17. "Improved production of sublancin via introduction of three characteristic promoters into operon clusters responsible for this novel distinct glycopeptide biosynthesis".

CHAPTER 2. HIGH RESOLUTION NMR STRUCTURE OF THE S-LINKED GLYCOPEPTIDE SUBLANCIN[a, b]

2.1 INTRODUCTION

Glycocins, as discussed in chapter 1, belong to the family of ribosomally synthesized and post-translationally modified peptide (RiPPs) natural products.[1] One such glycocin is sublancin 168, a 37 amino acid peptide produced by *Bacillus subtilis* 168 (Figure 2.1).[2,3] To understand glycocin peptides in more depth and obtain insight into their potential mode of action, it is essential to elucidate their three-dimensional structures at high resolution. Glycocin F (GccF), a 43 amino acid peptide produced by *Lactobacillus plantarum* KW30, was the second peptide to be classified as a member of the glycocin family (Figure 2.1).[4] Pascal and coworkers reported the nuclear magnetic resonance (NMR) structure of GccF, which contains both S- and O-linked *N*-acetyl glucosamine (Figure 2.1).[5] The primary sequences of sublancin 168 and glycocin F display similarities as well as some key differences. Both peptides contain two disulfides and a loop region, but the loop in sublancin is longer than that in glycocin F. Furthermore, the C-terminus of sublancin is shorter by 13 residues, it contains one glycosylation compared to two in GccF, and the S-linked sugar is located in the loop region rather than at the C-terminal residue. Furthermore, the primary sequences of the two peptides are quite different (Figure 2.1). Because of the unknown role(s) of the glycosylations in glycocins, we determined the three-dimensional structure of sublancin 168 to compare it to the structure of GccF.

---

[a] Reproduced in part with permission from: "NMR structure of the S-linked glycopeptide sublancin 168." *ACS Chem. Biol*. **2014**, ***9***, 796-801. Copyright 2014 American Chemical Society.

[b] All NMR experiments and data analysis were performed with the help of Dr. Lingyang Zhu, NMR Laboratory, School of Chemical Sciences, University of Illinois at Urbana−Champaign.

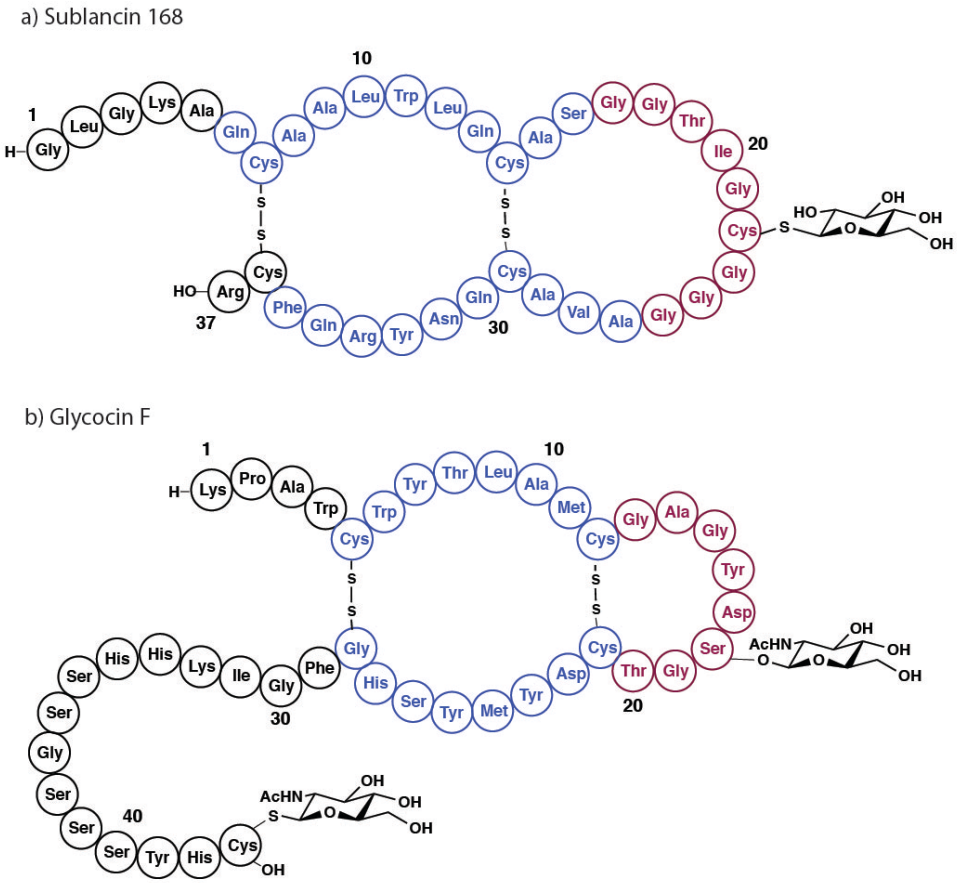

Figure 2.1 Structure of sublancin and glycocin F.

a) Sublancin 168 b) Glycocin F. Helical regions are depicted in blue and loop regions in magenta.

2.2 RESULTS AND DISCUSSION

2.2.1 Structure determination

The ^{1}H-^{15}N HSQC spectrum of sublancin produced 36 amide backbone signals and 10 side chain nitrogen resonances (Figure 2.2). All resonances were assigned (Table 2.3) and the structure of sublancin 168 was solved with 634 structural constraints derived from 3D ^{1}H-^{13}C-^{15}N HNCA, 3D ^{1}H-^{13}C-^{15}N CBCA(CO)NH, 2D ^{1}H-^{15}N HSQC, 2D ^{1}H-^{13}C HSQC (Figure 2.3), 3D ^{15}N HSQC-NOESY, 3D ^{15}N HSQC-TOCSY, 2D ^{1}H-^{1}H TOCSY (Figure 2.4), 2D ^{1}H-^{1}H NOESY (Figure 2.5), 3D ^{15}N HNHA, and DQCOSY experiments.

An ensemble of 15 sublancin structures with the lowest NMR constraint violations and lowest XPLOR energies[6,7] were used for detailed analysis, with the structural statistics given in Table 2.1. All experimental NMR constraints were satisfied in the structures, with all Nuclear Overhauser Effect (NOE) violations below 0.5 Å, J-coupling violations below 1 Hz, and dihedral angle constraints below the 5^{o} violation limit.

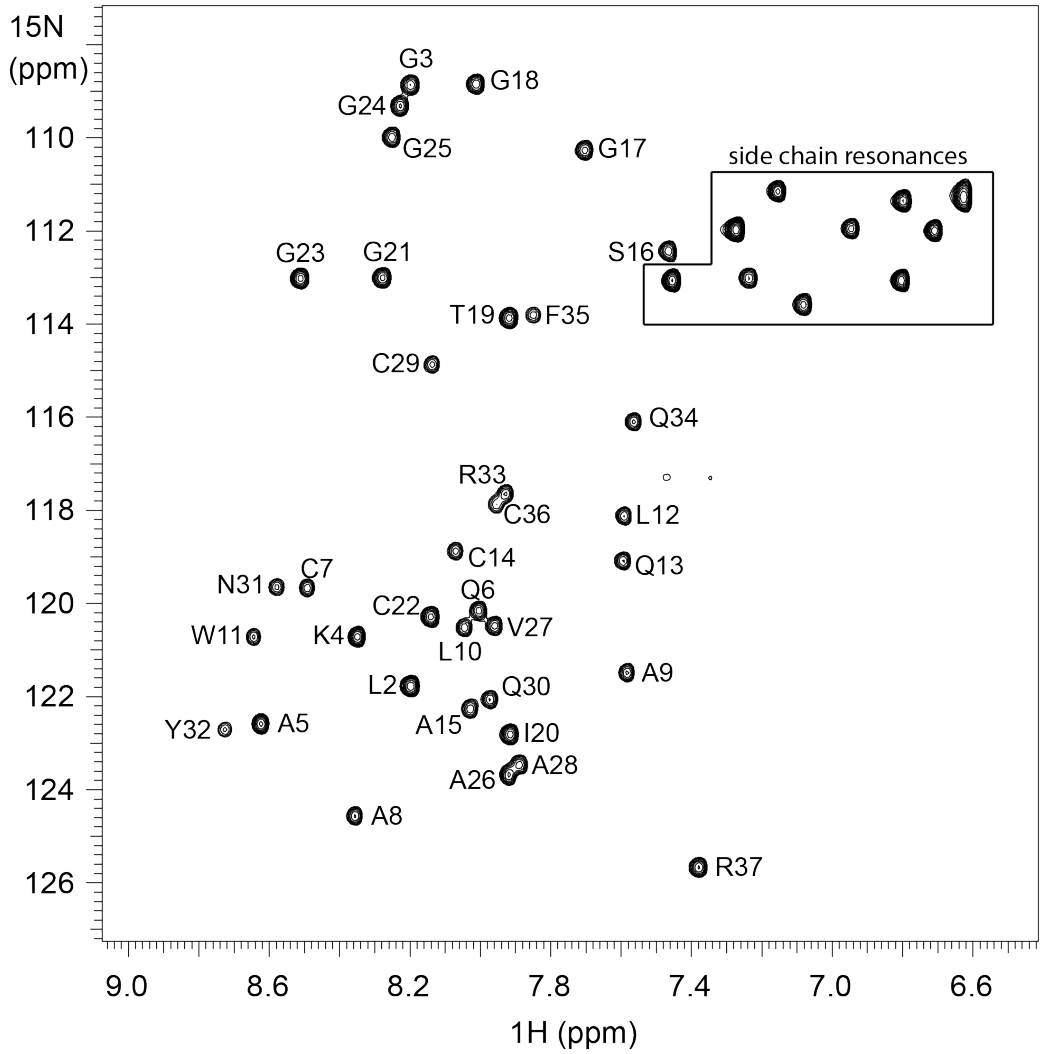

Figure 2.2 ^{1}H-^{15}N HSQC spectrum of sublancin.

The cross peaks correspond to the backbone amide region of ^{1}H-^{15}N correlations in the HSQC spectrum recorded at 25 °C. Specific amino acid assignments are indicated. Side chain nitrogen resonances are located within the boxed region.

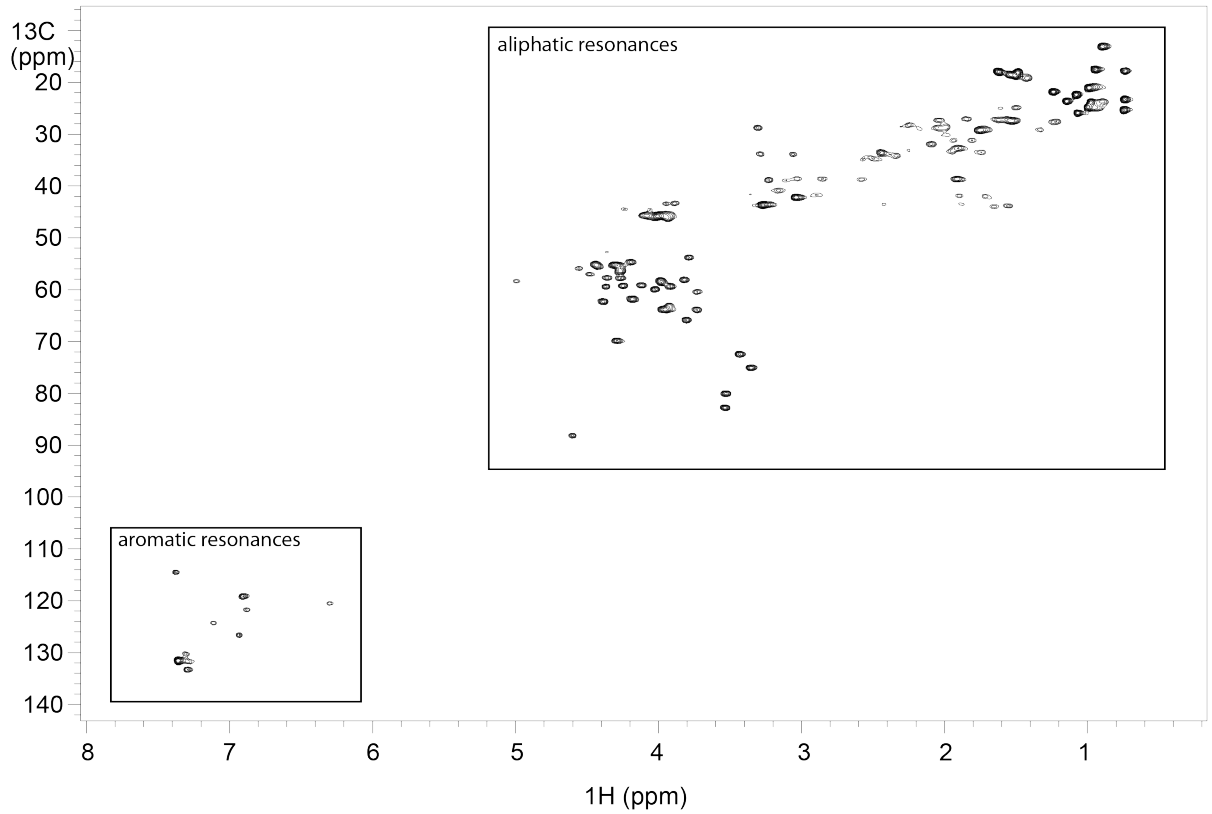

Figure 2.3 ^{1}H-^{13}C HSQC spectrum of sublancin.
The cross peaks correspond to the aromatic and aliphatic carbon region of ^{1}H-^{13}C correlations in the HSQC spectrum recorded at 25 °C.

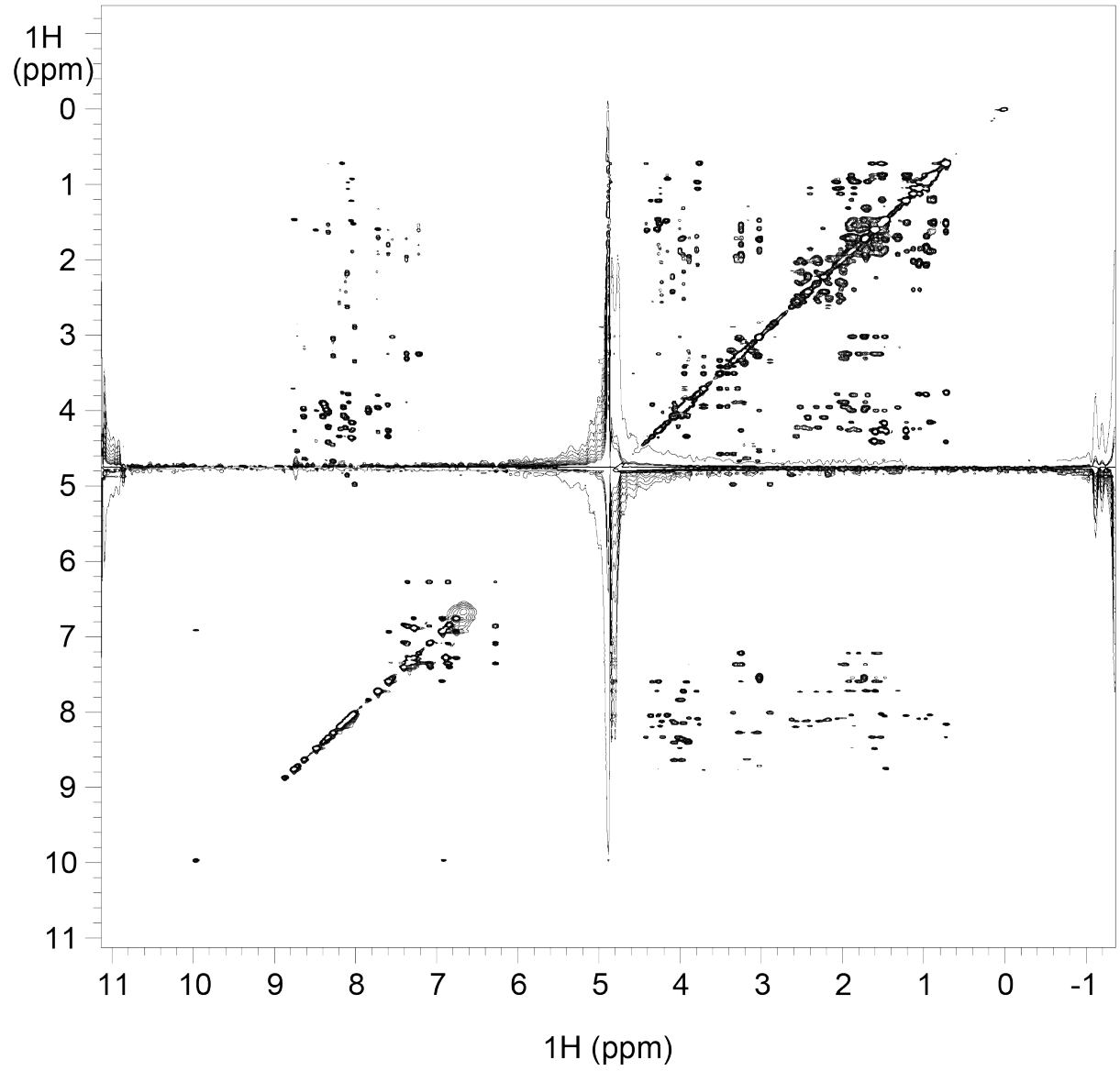

Figure 2.4 ^{1}H-^{1}H TOCSY spectrum of sublancin.
Total correlation spectroscopy spectrum recorded at 80 ms and 25 °C.

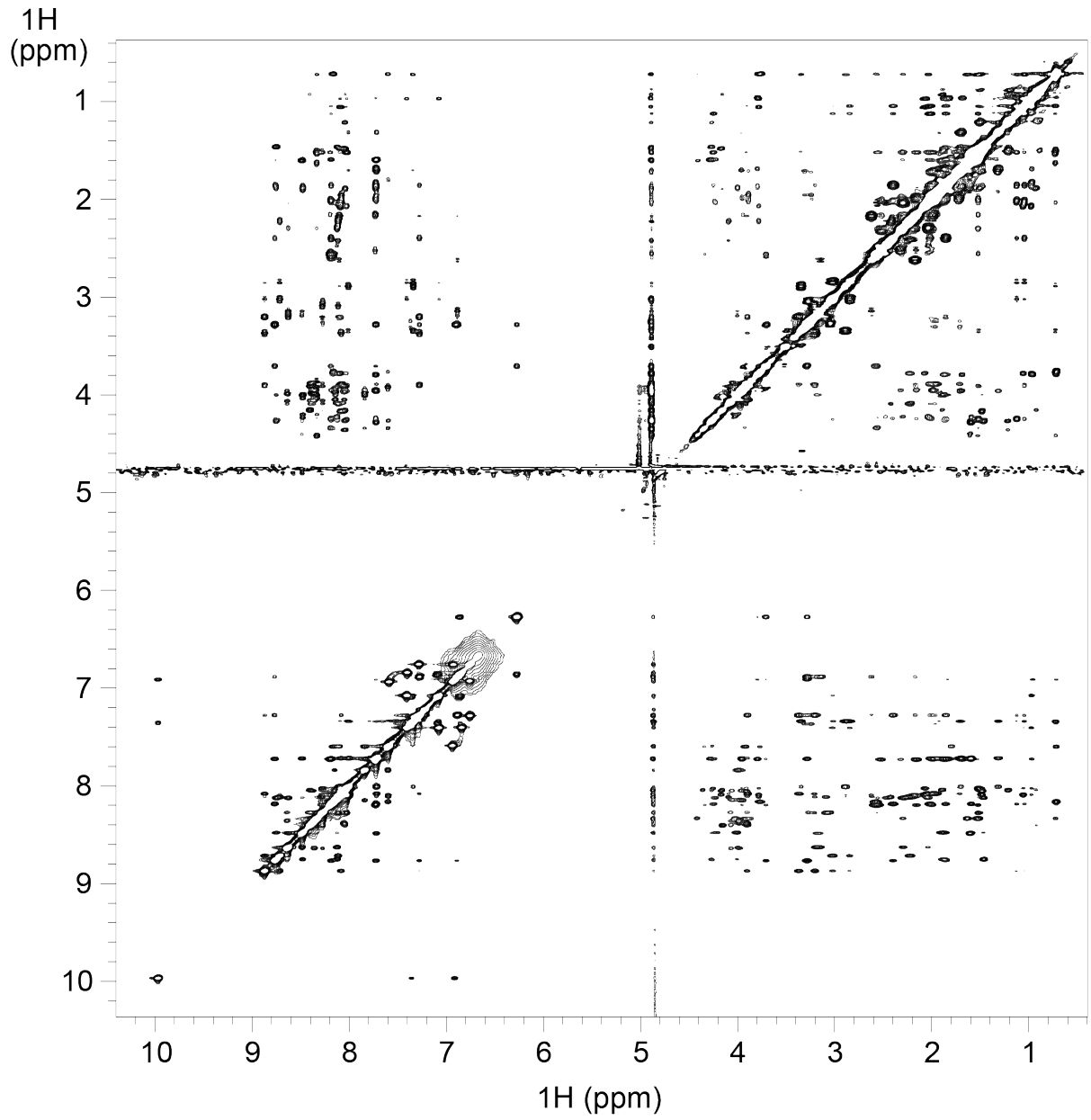

Figure 2.5 ^{1}H-^{1}H NOESY spectrum of sublancin.
Nuclear overhauser effect spectroscopy spectrum recorded at 250 ms and 25 °C.

Table 2.1 Structural statistics for sublancin 168.

Total restraints used	634
Total NOE restraints	531
Intraresidue	184
Sequential (|i – j| = 1)	185
Medium (1 < |i – j| ≤ 4)	100
Long range (|i – j| > 4)	62
Dihedral	
ϕ Angles	23
X_1Angles	16
Disulfide Bridges (Cys7-Cys36, Cys14-Cys29)	2
Hydrogen bonds?	62
r.m.s.d. from experimental distance restraints	
Bonds (Å)	0.006± 0.000
Bond angles (degrees)	0.682± 0.029
Improper torsions (degrees)	0.498± 0.025
Average pairwise r.m.s.d (Å)	
Backbone atoms in helical regions (6-16)	0.38
Backbone atoms in helical regions (26-35)	0.28
All backbone atoms (residues 1-37)	0.65
All heavy atoms in helical regions (6-16)	0.79
All heavy atoms in helical regions (26-35)	1.17
All heavy atoms (residues 1-37)	1.45
Procheck analysis	
Residues in most favorable regions (%)	85.7
Residues in additional allowed regions (%)	0.0
Residues in generously allowed regions (%)	14.3
Residues in disallowed regions (%)	0.0

[a]Helical regions include residues 6-16 and 26-35.

Procheck analysis of an ensemble of 15 conformers shows Cys22 in a generously allowed region of the Ramachandran plot (Figure 2.6). This finding is not uncommon for Cys. Previous studies have shown that Ser followed by Cys are the residues with the highest propensity for location in generously allowed and disallowed regions.[8] Two additional residues, Leu2 and Ala5, are also found in the generously allowed regions (Figure 2.6). The average pairwise root-mean-square deviation (rmsd) for backbone heavy atoms (C′, Cα, N) of all residues (1–37) is 0.79 Å, with smaller values in well-structured regions (Table 2.1).

The restraints that have the greatest weight in a structure calculation are those of medium- and long-range NOEs.[9] The three-dimensional structure of sublancin was obtained from over 160 medium- and long-range restraints, resulting in well-defined α helices as well as loop regions. Overall, an average of more than 17 NMR constraints per residue was used for the structural calculation.

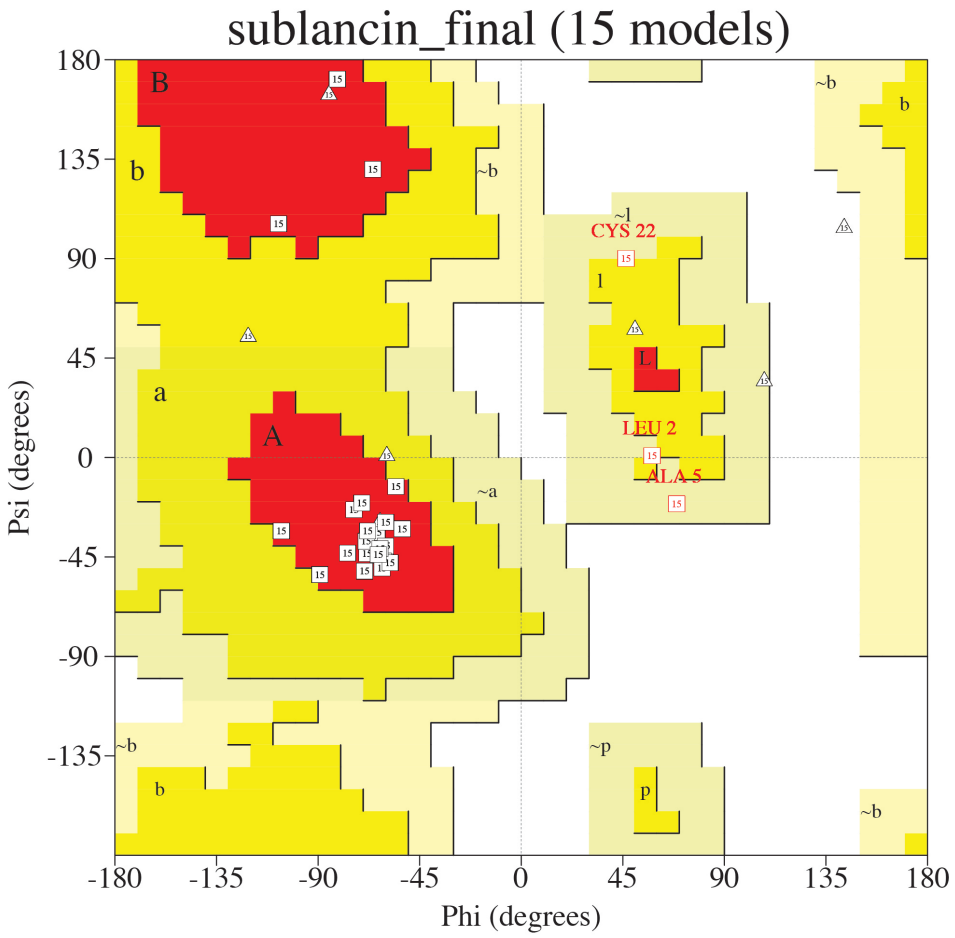

Glycine residues are shown as triangles all other residues as squares

Plot Statistics

89.3% Residues in most favored regions (Regions A, B, L shown in **RED**)
0.0% Residues in additional allowed regions (Regions a, b, l , p shown in YELLOW)
10.7% Residues in generously allowed regions (Regions ~a, ~b, ~l , ~p shown in LIGHT YELLOW)
0.0% Residues in disallowed regions

Figure 2.6 Ramachandran plot.

The quality of the NMR structure composed of 15 conformers was evaluated using PROCHECK.

2.2.2 Description of the structure

The ribbon diagram of a representative structure of sublancin is shown in Figure 2.7a. As predicted by analysis of the primary sequence and on the basis of backbone dihedral angles and characteristic NOEs, the solution structure shows two well-defined alpha helices encompassing residues 6-16 and 26-35. Superposition of the backbone Cα atoms of the 15 lowest energy conformers is shown in Figure 2.7b illustrating the highly ordered structure. Helices A and B are not antiparallel but rather offset from one another at an approximately 25 degree angle. The two helices are connected by an extended loop region. This interhelical loop (residues 17-25) is not flexible, but has a well-defined conformation, with the loop folded on top of both helices (Figure 2.7). In addition, the N-terminal pentapeptide of sublancin is also well defined. The ordered conformation of the interhelix and N-terminal loops is evidenced by 24% of all long range NOEs coming from these regions. The N-terminal amino group is partially solvent accessible, it is inserted between the two helices (Figure 2.7a), and the N-terminal amine is stabilized by cation-π interactions with the aromatic side chain of Phe35 (Figure 2.8).[10,11]

The superposition of the structures shows that the sugar moiety is the least well-defined section of the structure (Figure 2.9), also indicated by the lack of NOE restraints between the glucose unit and the loop region. We did observe an NOE restraint between one of the β protons of Cys22 to the H1 proton of the glucose moiety, that supports the β-linkage of the glucose to the sulfur atom of Cys22 reported previously.[2] No obvious hydrophobic interactions were observed between the hydrophobic face of the glucose and amino acids of the peptide. The structure of the C-terminal portion of sublancin is also well-defined as indicated by the observed medium and long range NOE restraints. In addition, the surface model representation of the structure (Figure 2.10) shows how the sulfur atoms of Cys7, Cys29, and Cys36, involved in disulfide bridges, are

partially solvent exposed. The very compact structure of sublancin (Figure 2.7b, c) provides a possible explanation for the extraordinary high chemical stability of sublancin reported previously.[3]

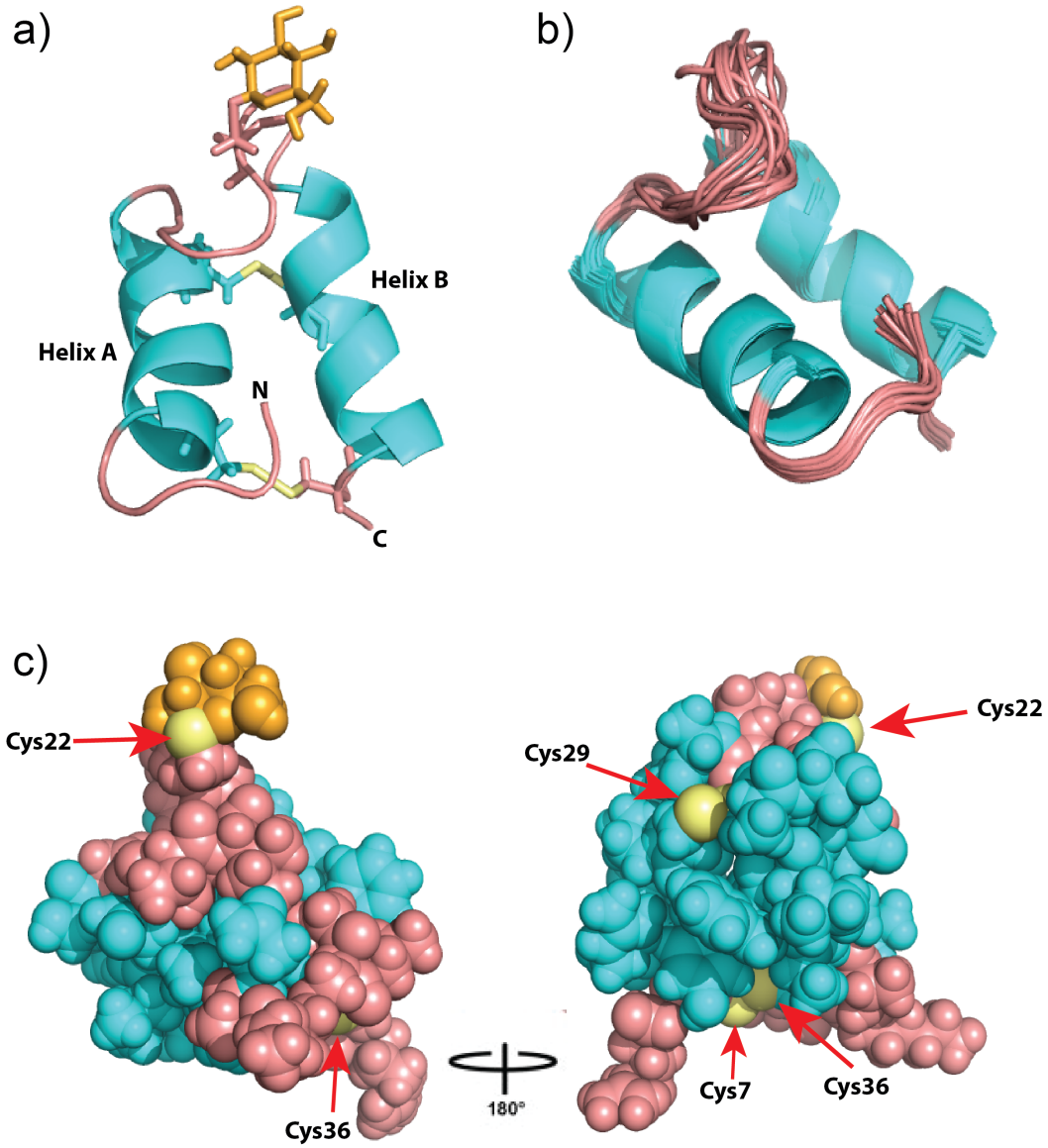

Figure 2.7 Three-dimensional solution structure of sublancin 168.

a) Ribbon diagram of the lowest energy conformer with helices labeled and colored in cyan, the loop regions, with N- and C- termini labeled, are colored pink, and the disulfide bridges in yellow. b) Ensemble of the 15 lowest energy conformers depicting all backbone atoms. c) Ball and stick representation of the lowest energy conformer with the loop regions in pink coming together to seal off one face of the helices. Exposed sulfur atoms are labeled.

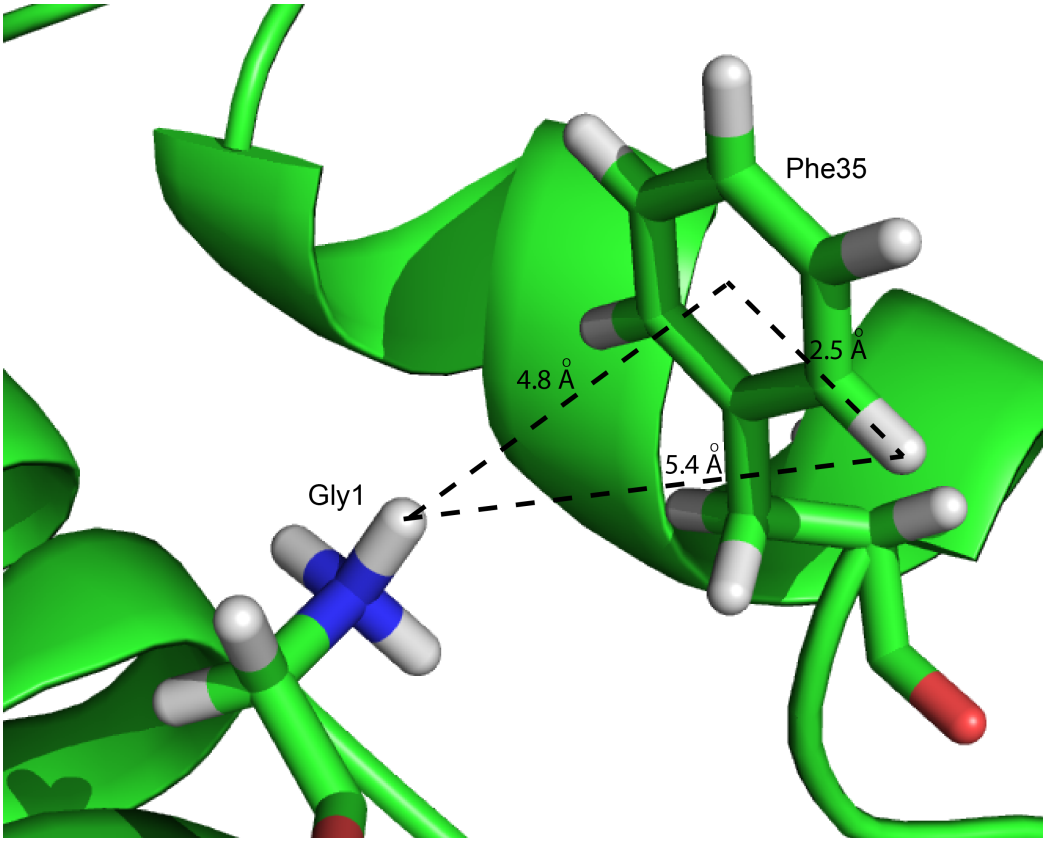

Figure 2.8 Cation-π interaction between Gly1 and Phe35.
The protonated N-terminal amine group of Gly1 displays cation-π interactions with the side chain of Phe35 at a distance of 4.7 Å.

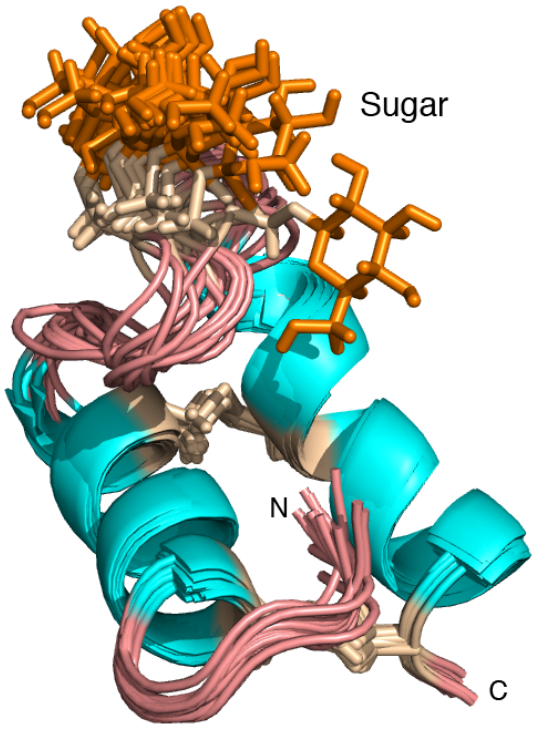

Figure 2.9 Three-dimensional solution structure of sublancin 168.

Ribbon diagram of the final ensemble of 15 conformers. Helices colored in cyan, the loop regions, and N- and C-termini are colored pink, the sugar is colored in orange, and cysteine residues in beige.

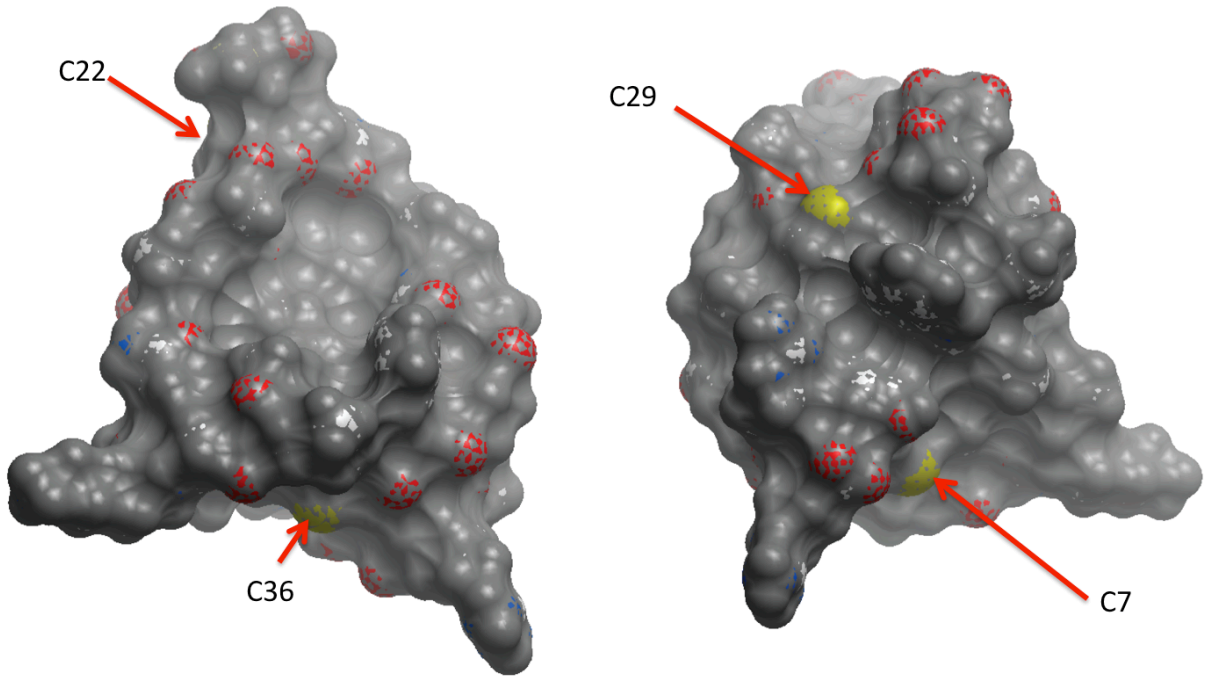

Figure 2.10 Sublancin surface model representation.

The sulfur atoms of Cys7, Cys29, and Cys36, involved in disulfide bridges, are partially solvent exposed. Exposed sulfur atoms are shown in yellow.

2.2.3 Hydrogen bond interactions

The ensemble of the 15 lowest energy conformers calculated without hydrogen bond restraints was analyzed using Chimera software to predict tentative hydrogen bond interactions between residues in the interhelical loop and the helices (Figure 2.11). Hydrogen bond interactions were investigated with a series of deuterium exchange ^{1}H-^{15}N HSQC experiments with a ^{15}N-labeled sublancin sample. Within the first few minutes, we observed protection from exchange of 27 backbone amide protons as well as the side chain protons of Asn31 (Table 2.2).

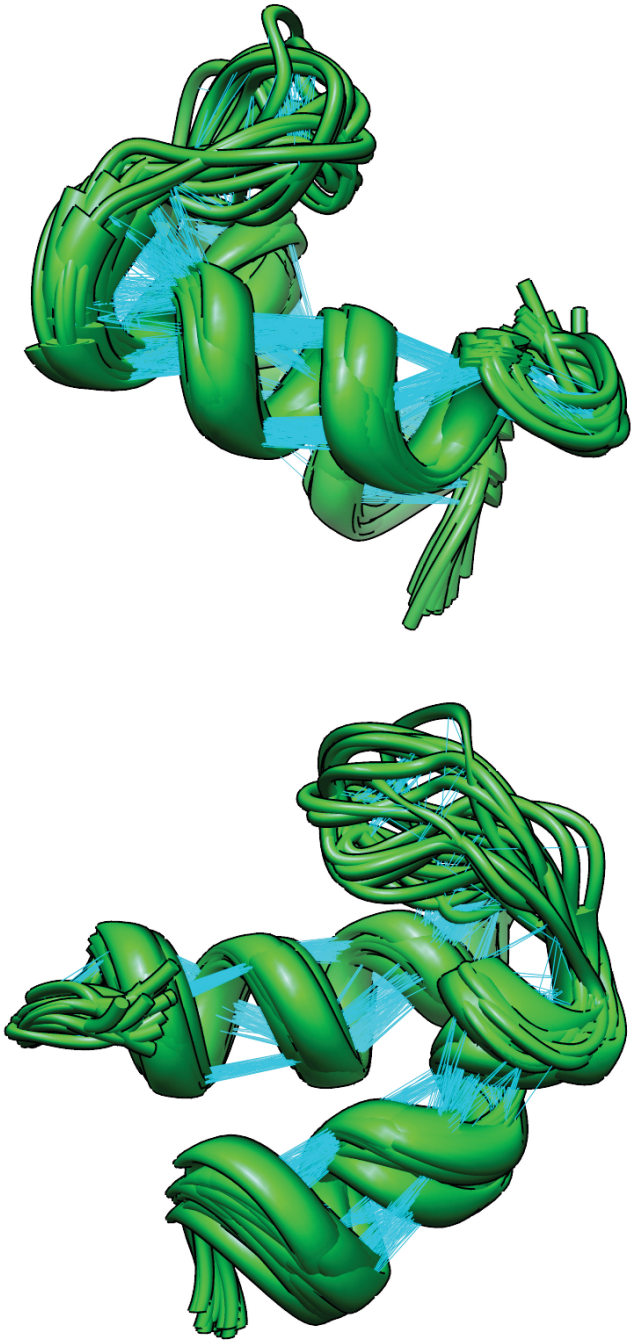

Figure 2.11 Calculated sublancin backbone ribbon diagram without hydrogen bond restraints.

Sublancin backbone ribbon diagram of the 15 lowest energy conformers calculated without hydrogen bond restraints. The figure also displays predicted hydrogen bonds (cyan) obtained using the Chimera software package.

Table 2.2 Hydrogen bond identification by deuterium exchange.

Time	# Signals	HN signals observed
7 min	27	G3, Q6, C7, A8, A9, L10, W11, L12, Q13, C14, A15, S16, G17, G18, I20, A26, V27, A28, C29, Q30, N31, Y32, R33, Q34, F35, C36, R37
14 min	20	C7, A8, A9, L10, W11, L12, Q13, C14, A15, S16, A28, C29, Q30, N31, Y32, R33, Q34, F35, C36, R37
30 min	15	A9, L10, W11, L12, Q13, C14, A15, C29, Q30, N31, Y32, R33, Q34, F35, C36
60 min	12	A9, L10, W11, L12, Q13, C14, A15, Y32, R33, Q34, F35, C36
45 h	8	L10, W11, L12, Q13, C14, Y32, F35, C36

As expected, most of the hydrogen bond donors belonged to residues involved in helix formation, but several hydrogen bond interactions were located in the loop region, including the amide hydrogens of Gly17, Gly18, and Ile20 (Figure 2.12a). On the basis of hydrogen bond distance restrictions, the amide protons from Gly17 and Gly18 interact with the carbonyl oxygen of the side chain of Gln13. In addition, the amide proton of Ile20 hydrogen bonds with the side chain oxygen atom from Thr19. The well-defined turn is reinforced by additional hydrogen bonds between the amide N–H of Ser16, the last residue in helix A, and the side chain carbonyl of Gln13 (Figure 2.12a). The other end of the loop is held in place by hydrogen bonds involving the amide protons of Ala26, Val27, and Ala28, located in helix B, which interact with the carbonyl oxygen atoms of Gly24 and Gly25 (Figure 2.12b). These hydrogen bond interactions located at the beginning and end of the loop offer a plausible explanation as to why the loop is folded on top of the two helices, although the flexibility of the loop seen in Figure 2.7b is also reflected in exchange of most of the protons involved in hydrogen bond interactions of the loop residues by 14 min (Table 2.2). After 45 h, 8 amide protons were still protected from exchange (Table 2.2). Of these, 5 protons are located in helix A (Leu10, Trp11, Leu12, Gln13, Cys14) and 3 in helix B (Tyr32, Phe35, and Cys36).

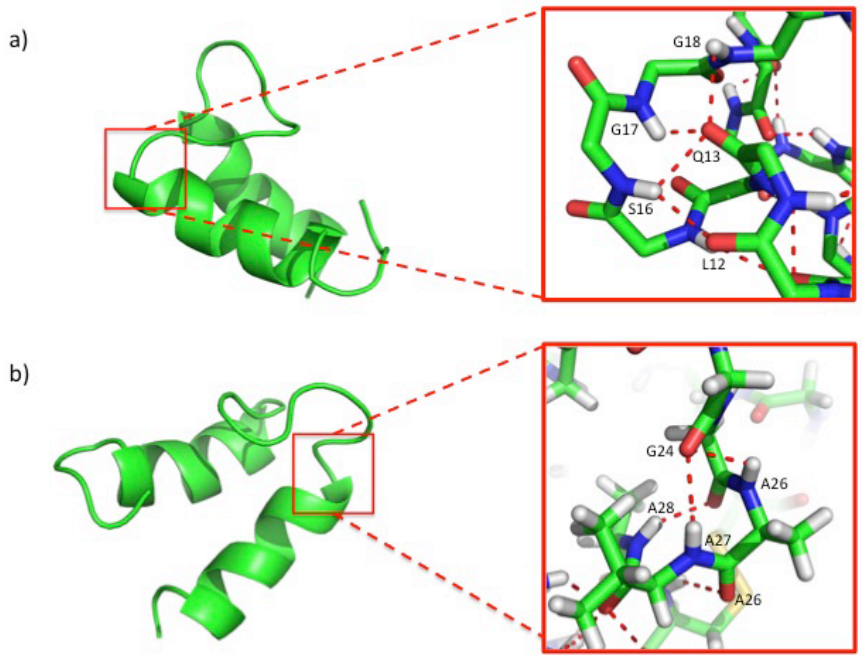

Figure 2.12 Hydrogen bond interactions in the interhelical loop region.

Ribbon diagram showing the hydrogen bonds between residues in the loop and the helices. Hydrogen bond interactions are depicted in red.

2.2.4 Hydrophobic interactions

The compact and well-defined structure of sublancin is also enforced in part by hydrophobic interactions. As shown in Figure 2.13, a hydrophobic core consisting of Leu2, Leu10, Trp11, Ala28, Tyr32, and Phe35 helps maintain the structure, including a hydrophobic interaction between Ile20 in the loop and Leu10 in helix A. Use of the program IsoCleft Finder[12] identified Gly1, Gln6, Leu10, Ile20, Gly21, Gly23, Val27, Ala28, Asn31, and Phe35 as residues involved in creating a small hydrophobic cleft (Figure 2.14) that may be important for target binding.

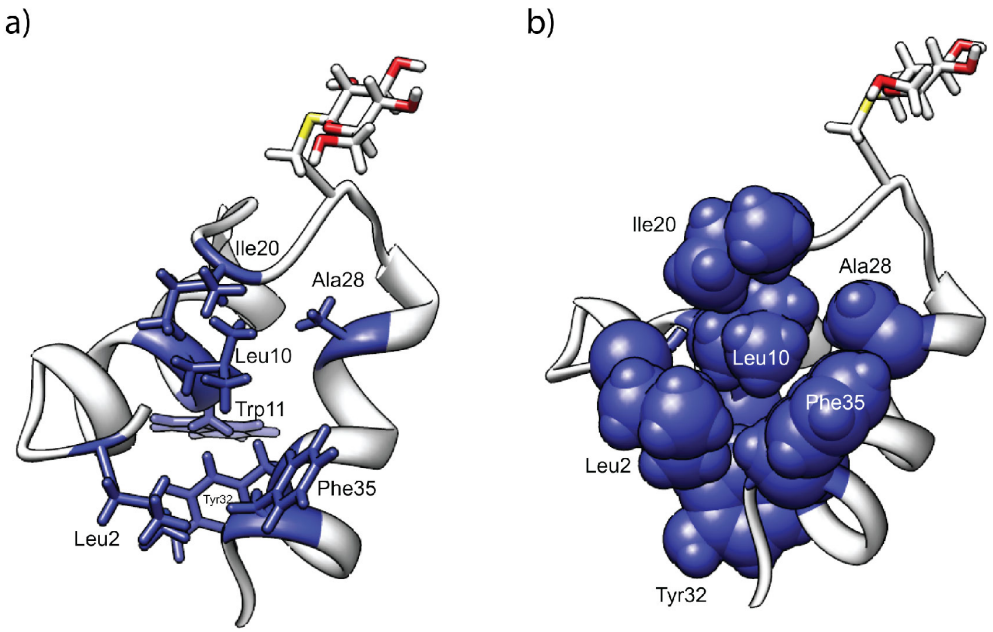

Figure 2.13 Hydrophobic interactions.

Ribbon diagram of sublancin depicting the hydrophobic residues in (a) sticks or (b) spheres.

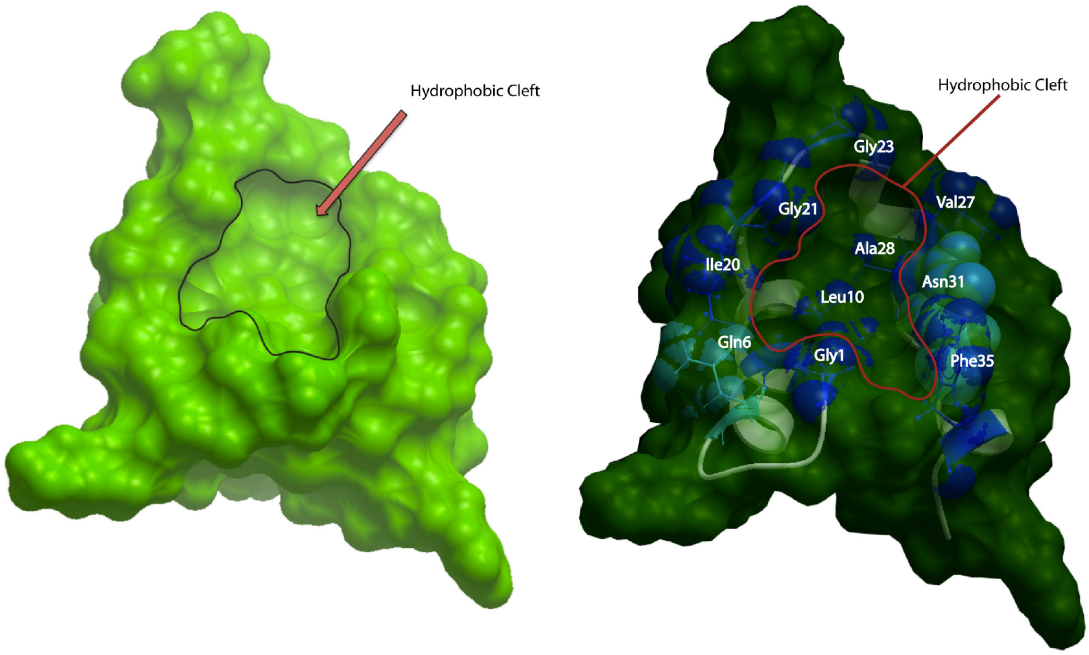

Figure 2.14 Sublancin surface model representation.

A small hydrophobic cleft is formed by Gly1, Gln6, Leu10, Ile20, Gly21, Gly23, Val27, Ala28, Asn31 and Phe35 might be a site for interaction with a target.

2.2.5 Glycocin structural comparison

The three-dimensional structures of GccF and sublancin were superimposed to visualize structural similarities and differences of these two glycocins (Figure 2.15). The orientation of the helices matches very closely, with both structures displaying the 25-degree offset, even though the primary sequences of the amino acids involved in helix formation are vastly different. As expected based on the primary sequences, the helices in sublancin are longer. The location and orientation of the sugar moiety in the interhelix loop is quite different in GccF and sublancin 168 and the N-and C-terminal segments are also oriented quite differently (Figure 2.15). The lack of defined contacts between the glucose and the peptide in the sublancin structure does not provide any evidence for a role of the sugar in folding of the peptide as is often seen for glycopeptides,[13-17] although an interaction with the biosynthetic thiol-disulfide oxidoreductases[18] cannot be ruled out. Biochemical evidence shows that glycosylation takes place before folding (Chapter 6) The conformational flexibility of the sugar does provide a possibly explanation for the ease by which the S-linked glucose in sublancin could be substituted by several other hexoses during biosynthesis as described in previous work.[2] The previous observation that the stereochemistry of the hexose in these analogs was not critical for antimicrobial activity of sublancin 168,[2] combined with the initial observation that the Cys22Ser analog was active (but see chapter 4), and that the glucose in the structure shown here is conformationally flexible suggests that the sugar in sublancin 168 may not be installed for target recognition. These findings are consistent with the previous suggestion that the sugar in sublancin might fulfill a role in self-protection in the producing strain.[19] However, data presented in chapter 3 on the mode of action of sublancin indicate a link to glucose uptake that appears more than coincidental in light of the glucose conjugated to the molecule.

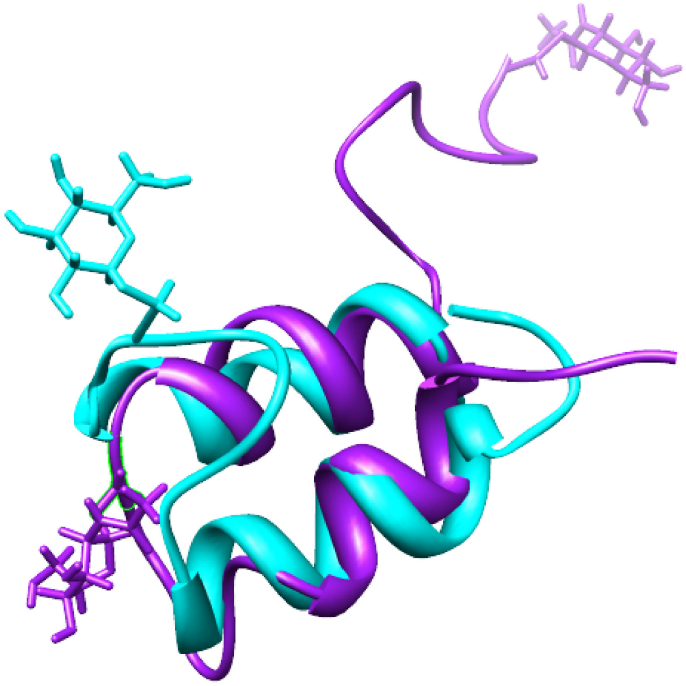

Figure 2.15 Superposition of sublancin 168 and glycocin F.
Sublancin is depicted in cyan and glycocin F in magenta.

2.3 SUMMARY

In summary, the solution structure of sublancin 168, a member of a small group of glycosylated antimicrobial peptides known as glycocins and a 37-amino-acid peptide produced by *Bacillus subtilis* 168, was solved by NMR spectroscopy. Sublancin's structure is highly compact with well-defined N- and C-terminal regions, two nearly antiparallel helices, and a conformationally highly structured interhelix loop that carries the glucose. The two helices span residues 6–16 and 26–35, and the loop region encompasses residues 17–25. The 9-amino-acid loop region contains a β-S-linked glucose moiety attached to Cys22. Hydrophobic interactions as well as hydrogen bonding are responsible for the well-structured loop region. The three-dimensional structure provides an explanation for the previously reported extraordinary high

stability of sublancin 168. Further studies, described in chapter 3, have been performed to better understand the mode of action of the glycocin group of antimicrobial peptides.

2.4 EXPERIMENTAL

2.4.1 Materials, cultures, and conditions

All chemicals and HPLC grade solvents were purchased from Sigma-Aldrich.. Growth media were obtained from Difco Laboratories (Detroit MI),. CHCA (α-cyano-4-hydroxycinnamic acid, MALDI matrix) was obtained from Fluka. Matrix-assisted laser desorption/ionization time-of-flight (MALDI-TOF) mass spectrometry was performed at the Mass Spectrometry Laboratory from the School of Chemical Sciences at UIUC using a Bruker Daltonics UltrafleXtreme MALDI TOFTOF and an Applied Biosystems Voyager-DE STR (Foster City CA) instruments. Salt-containing MS samples were purified via Millipore Zip-Tip_{C18} pipette tips (Billerica MA).

2.4.2 Production of sublancin

Sublancin was isolated from Bacillus subtilis 168 as previously described by Dr. Oman.[2] Briefly, a culture of *B. subtilis* 168 was grown in LB media under aerobic conditions at 37 °C for 12-15 h. The overnight culture was used to inoculate (at 1%) 500 mL volumes of Medium A in 2 L flasks. Medium A consisted of 900 mL of Medium A nutrient broth combined with 100 mL of 10X Medium A salts. Medium A nutrient broth was prepared by dissolving 20 g sucrose, 11.7 g citric acid, 4 g Na_2SO_4, 4.2 g $(NH_4)_2HPO_4$, and 5 g yeast extract in 900 mL of millipore water. The pH was adjusted to 6.8-6.9 using NaOH and the medium was autoclaved. Medium A salts (10X) were prepared by dissolving 7.62 g KCl, 4.18 g $MgCl_2$-6 H_2O, 0.543 g $MnCl_2$-4 H_2O, 0.49 g $FeCl_3$-6 H_2O, and 0.208 g $ZnCl_2$ in 1 L of millipore water followed by sterilization via 0.22

mm filtration. The Medium A cultures were grown under aerobic condition at 37 °C for 28-48 h with vigorous agitation. A color change to pinkish-brown was observed and the pH of cultures had lowered to 6-6.5, the Sublancin production was consistently observed when these events occurred. The cultures were grown an additional 24-48 h after the color change was observed.

Cultures were acidified to pH 2.5 with concentrated phosphoric acid (85% in water) and centrifuged to remove cells and insoluble material. Sublancin was isolated by ammonium sulfate precipitation. Briefly, a 500 mL volume of sublancin-containing culture supernatant was combined with 245 g $(NH_4)_2SO_4$ in a 1 L glass bottle to provide a 75% ammonium sulfate saturation at 4 °C. The precipitation mixture was stirred at 4 °C for 24 h and precipitated sublancin was isolated from the solution by centrifugation. The pelleted peptide was re-solubilized in 50/50 ACN/water with 0.1% TFA and was analyzed by MALDI-TOF MS. A 1 mL aliquot of sample was combined with 1 mL of matrix consisting of saturated a-cyano-4-hydroxy-cinnamic acid matrix in 50% ACN/50% water with 0.1% TFA, and the total volume was spotted onto a MALDI target and dried under ambient conditions prior to analysis. The sublancin containing product were combined, lyophilized to dryness, and stored under N_2 at −80 °C until purification by preparative HPLC.

Preparative HPLC was performed using a Waters Delta 600 instrument equipped with a Phenomenex Jupiter Proteo C12 column (10 mm, 90 Å, 250 mm x 15 mm) equilibrated in 2% B (solvent A = 0.1% TFA in water, solvent B = 0.0866% TFA in 80% ACN/20% water). Dry sublancin material was resuspended in 2% B and was applied to the column. Sublancin was eluted by maintaining the mobile phase at 2% B for 1 min, followed by an increase to 100% B over 45 min with a flow rate of 10.0 mL/min. Under these conditions, sublancin eluted at 21.6 min. All fractions were analyzed by MALDI-TOF MS as described above. Purified sublancin

was lyophilized to dryness and stored under N_2 at −80 °C until further use. Typical yields were 8 mg sublancin per liter of processed Medium A culture.

2.4.3 Production of isotopically labeled sublancin

Cells containing ^{13}C-labeled sublancin were obtained by growing *B. subtilis* 168 on M9 minimal medium containing uniformly ^{13}C-labeled glucose. A culture of *B. subtilis* 168 was grown in LB medium for 15 h with aeration. This culture was used to inoculate a 500 mL volume of minimal media in a 2 L flask. The minimal media contained the following components per 500 mL total volume: 25 mL of 20% ^{13}C-glucose, 100 mL of 5X M9 salts, 5 mL of 4 mg mL^{-1} leucine, 500 µL of 20 mg mL^{-1} $CaCl_2$, 500 µL of 120 mg mL^{-1} $MgSO_4$, 100 µL of 5 mg mL^{-1} D-biotin, 100 µL of 5 mg mL^{-1} thiamine-HCl, 500 µL of 1000X heavy metal stock solution, and 368.3 mL of millipore water to bring the total volume to 500 mL. The 5X M9 salts solution consisted of 64 g Na_2HPO_4 $7H_2O$, 15 g KH_2PO_4, 2.5 g NaCl, 5 g NH_4Cl, and 1 L millipore water. The 1000X heavy metal stock solution was prepared by combining the all components in 1 M HCl, stirring overnight at 25° C, and sterilizing by filtration to remove insoluble material (Table 2.3).

Cells containing ^{15}N-labeled sublancin sample were obtained by growing *B. subtilis* 168 on M9 minimal medium containing glucose. A culture of *B. subtilis* 168 was grown in LB medium for 15 h with aeration. This culture was used to inoculate a 500 mL volume of minimal media in a 2 L flask. The minimal media contained the following components per 500 mL total volume: 25 mL of 20% glucose, 100 mL of 5X M9 salts, 5 mL of 4 mg mL^{-1} leucine, 500 µL of 20 mg mL^{-1} $CaCl_2$, 500 µL of 120 mg mL^{-1} $MgSO_4$, 100 µL of 5 mg mL^{-1} D-biotin, 100 µL of 5 mg mL^{-1} thiamine-HCl, 500 µL of 1000X heavy metal stock solution, and 368.3 mL of millipore water to bring the total volume to 500 mL. The 5X M9 salts solution consisted of 64 g Na_2HPO_4

$7H_2O$, 15 g KH_2PO_4, 2.5 g NaCl, 5 g $^{15}NH_4Cl$, and 1 L millipore water. The 1000X heavy metal stock solution was prepared (Table 2.3).

Cells containing $^{13}C/^{15}N$-labeled sublancin sample were obtained by growing *B. subtilis* 168 on M9 minimal medium containing uniformly ^{13}C-labeled glucose [25]and $^{15}NH_4Cl$. The minimal media contained the following components per 500 mL total volume: 25 mL of 20% ^{13}C-glucose, 100 mL of 5X M9 salts, 5 mL of 4 mg mL^{-1} leucine, 500 µL of 20 mg mL^{-1} $CaCl_2$, 500 µL of 120 mg mL^{-1} $MgSO_4$, 100 µL of 5 mg mL^{-1} D-biotin, 100 µL of 5 mg mL^{-1} thiamine-HCl, 500 µL of 1000X heavy metal stock solution, and 368.3 mL of millipore water to bring the total volume to 500 mL. The 5X M9 salts solution consisted of 64 g Na_2HPO_4 $7H_2O$, 15 g KH_2PO_4, 2.5 g NaCl, 5 g $^{15}NH_4Cl$, and 1 L millipore water. The 1000X heavy metal stock solution was prepared (Table 2.3).

Table 2.3 1000X heavy metal stock solution recipe.

Component	Amount
$MoNa_2SO_4•2H_2O$	500 mg
$CoCl_2$	250 mg
$CuSO_4•5H_2O$	175 mg
$MnSO_4•H_2O$	1 g
$MgSO_4•7H_2O$	8.75 g
$ZnSO_4•7H_2O$	1.25 g
$FeCl_2•4H_2O$	1.25 g
$CaCl_2•2H_2O$	2.5 g
H_3BO_3	1 g
1 M HCl	to 1 L

For the production of the cells containing labeled sublancin a culture of *B. subtilis* 168 was grown in LB medium for 15 h with aeration. This culture was used to inoculate a 500 mL volume of minimal media described above in a 2 L flask and was grown at 37° C with aeration. The production of labeled sublancin was monitored by periodic sampling of the growing culture and analysis via MALDI-TOF mass spectrometry. Briefly, a 1 mL aliquot of *B. subtilis* 168 minimal media culture was acidified to pH 2 with concentrated phosphoric acid (85% in water). The sample was centrifuged to remove cells and the supernatant was $ZipTip_{C18}$ desalted, and analyzed by mass spectrometry. Typically, isolation and purification process was started 24 h after the first detection of labeled product. Labeled sublancin was generally observed within 48-72 h post-inoculation. Isotopically labeled sublancin was purified by preparative HPLC using a Waters Delta 600 instrument equipped with a Phenomenex Jupiter Proteo C12 column (10 μm, 90 Å, 250 mm x 15 mm) equilibrated in 2% B (solvent A = 0.1% TFA in water, solvent B = 0.0866% TFA in 80% ACN/20% water). Dry sublancin material was resuspended in 2% B and was applied to the column. Sublancin was eluted by maintaining the mobile phase at 2% B for 1 min, followed by an increase to 100% B over 45 min with a flow rate of 10.0 mL/min. Under these conditions, sublancin eluted at 21.7 min. All fractions were analyzed by MALDI-TOF MS as described above. Purified sublancin was lyophilized to dryness and stored under N_2 at −80 °C until further use. A natural abundance sublancin sample was prepared during the preparation of the labeled peptides as a control.

2.4.4 Sample preparation

One wild type and three isotopically labeled sublancin samples were prepared for NMR analysis. NMR samples contained 2.5 mM peptide in 90%H_2O/10%D_2O or 100% D_2O. For a sample in 100% D_2O, lyophilized sublancin was dissolved in 100% D_2O (Cambridge Isotope

Laboratories) to exchange amide protons and simplify the NMR spectrum in the down field region. The sample was lyophilized, the procedure was repeated twice, and the final sample was dissolved in D_2O to a final concentration of approximately 2.5 mM. For a sample in 90% H_2O/10% D_2O, lyophilized sublancin was dissolved in 90% H_2O/10% D_2O to a final concentration of approximately 2.5 mM.

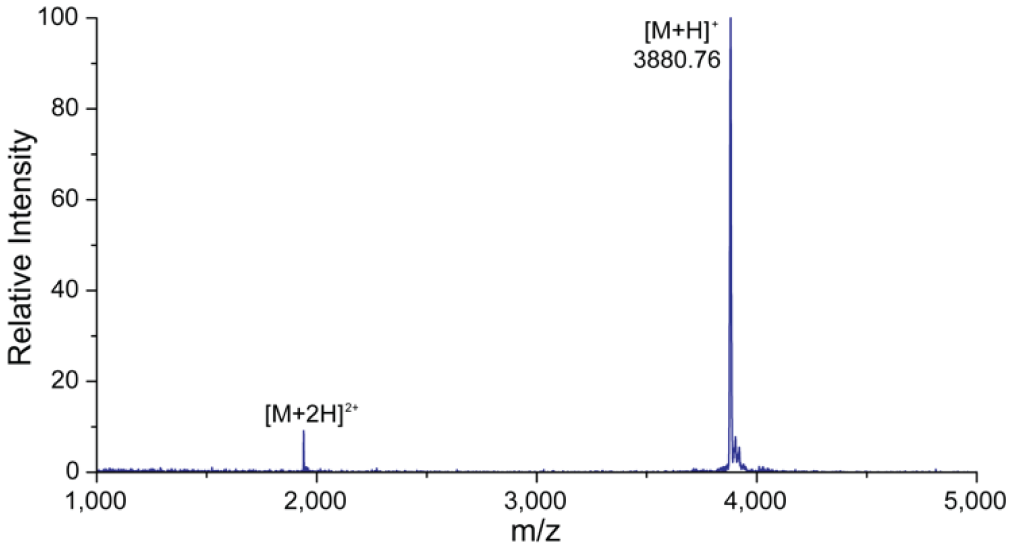

Figure 2.16 Mass spectrum of natural abundance sublancin.

MALDI-TOF mass spectrum of purified natural abundance sublancin that was produced in parallel with the isotopic labeling preparations except using natural abundance culture growth medium. Expected [M+H]: 3876.74, observed: 3880.76

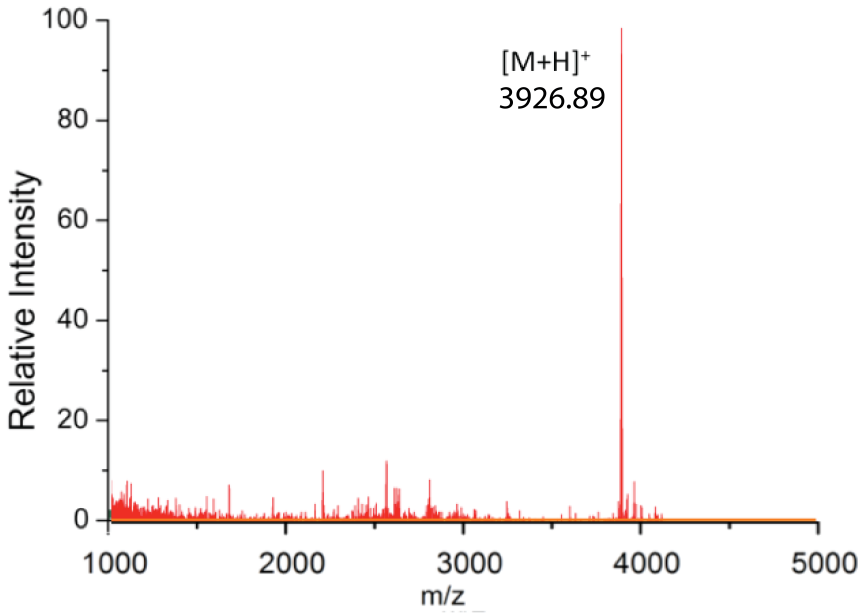

Figure 2.17 Mass spectrum of ^{15}N-labeled sublancin.

MALDI-TOF mass spectrum of purified, uniformly ^{15}N-labeled sublancin. Expected [M+H]: 3926.31, observed: 3926.89.

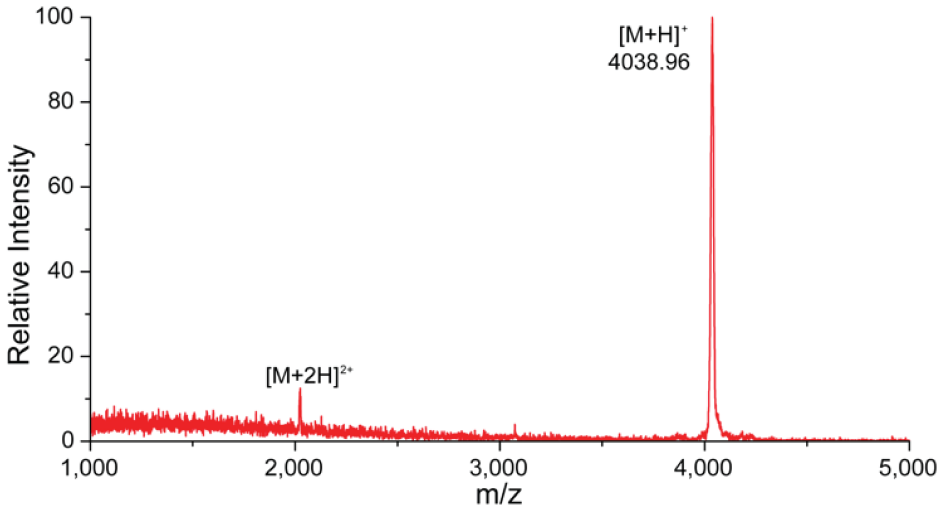

Figure 2.18 Mass spectrum of ^{13}C-labeled sublancin.

MALDI-TOF mass spectrum of purified uniformly ^{13}C-labeled sublancin. Expected [M+H]: 4040.38, observed: 4038.96.

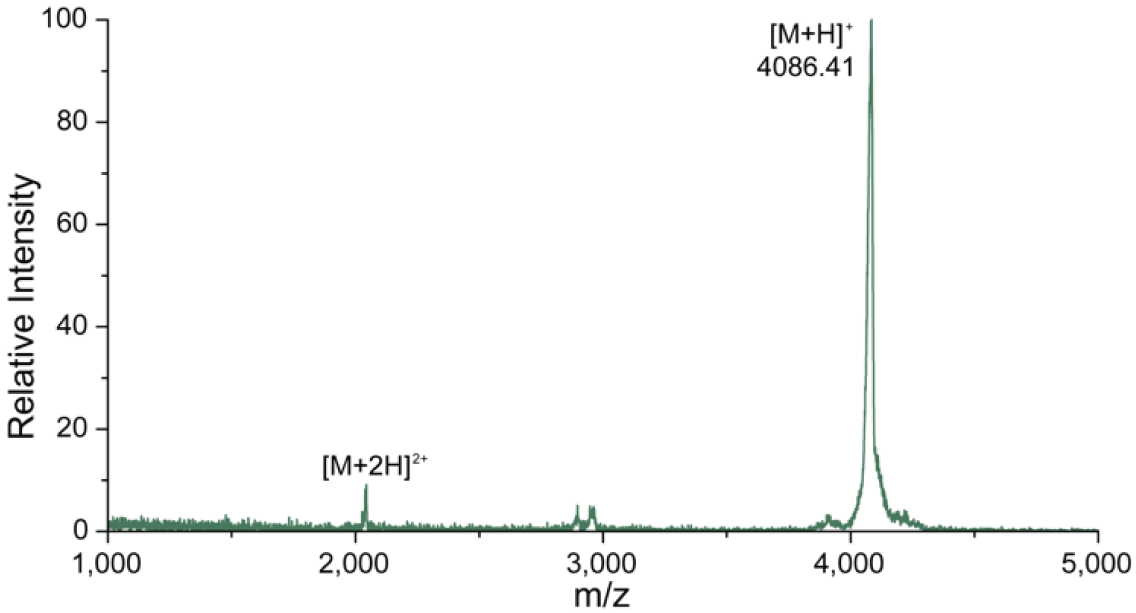

Figure 2.19 Mass spectrum of $^{13}C/^{15}N$-labeled sublancin.

MALDI-TOF mass spectrum of purified uniformly $^{13}C/^{15}N$-labeled sublancin. Expected [M+H]: 4090.38, observed: 4086.41.

2.4.5 NMR spectroscopy

All NMR experiments were performed at 25 ^{o}C on Varian INOVA 500 MHz, 600 MHz and 750 MHz spectrometers equipped with a 5 mm triple resonance (^{1}H-^{13}C-^{15}N) triaxial gradient probe and pulse-shaping capabilities. The VNMRJ 2.1B software with the BioPack suite of pulse sequences was used. The spectra were processed with NMRPipe software,[20] and analyzed by Sparky[21] and VNMRJ (Agilent Technology).

Table 2.4 Sublancin chemical shift assignments.

Residue	CA	CB	HN	N	HA	HB	HG	HD	HE	Other
Gly 1	45.2			108.2	3.93 3.86					
Leu 2	55.0	43.9	8.34	121.1	4.41	1.63	1.514	0.714		
Gly 3	44.5		8.34	108.3	4.20 4.02					
Lys 4	54.9	41.2	8.49	119.4	3.98	1.89	1.585, 1.474	1.722, 1.29	3.03	HZ 7.38
Ala 5	55.3	18.1	8.74	121.7	4.26	1.46				
Gln 6	59.3	28.5	8.14	119.6	4.21	2.29, 2.01	2.555, 2.456			
Cys 7	60.8	40.7	8.62	119.3	4.63	3.17				
Ala 8	55.5	17.7	8.49	124.0	4.40	1.60				
Ala 9	55.3	18.0	7.72	120.9	4.27	1.58				
Leu 10	57.7	43.6	8.18	119.9	4.24	2.39, 2.02	1.85	1.126, 1.041		
Trp 11	60.5	28.1	8.78	120.2	3.70	3.69, 3.28		6.902	9.97, 6.27	HZ 7.35, NE 128.5
Leu 12	58.0	41.8	7.73	117.5	3.80	1.86, 1.68	1.849	0.959		
Gln 13	58.6	29.0	7.73	118.5	3.94	2.15, 1.99	2.517, 2.303		7.59, 6.94	NE 112.5
Cys 14	57.7	38.7	8.21	118.3	4.33	2.56				
Ala 15	54.0	17.7	8.17	121.6	3.76	0.71				
Ser 16	59.4	63.7	7.60	111.8	4.33	3.91				
Gly 17	45.6		7.84	109.7	3.99					
Gly 18	45.8		8.15	108.2	4.05 3.94					
Thr 19	62.3	69.8	8.06	113.3	4.35	4.26	1.221			
Ile 20	61.9	38.3	8.06	122.3	4.14	1.88	1.512, 1.206	0.919		
Gly 21	45.3		8.42	112.4	4.06 3.89					
Cys 22	61.0	33.8	8.28	120.3	4.67	3.27, 3.03				
Gly 23	45.9		8.65	112.7	4.07, 3.95					
Gly 24	45.4		8.37	108.8	3.98					
Gly 25	46.1		8.39	109.4	3.90					
Ala 26	54.8	18.8	8.06	123.1	4.16	1.47				
Val 27	65.8	31.9	8.10	119.9	3.77	2.05	1.07, 0.965			
Ala 28	55.7	18.3	8.03	122.9	4.24	1.51				
Cys 29	56.9	38.8	8.27	114.3	4.45	3.21, 3.08				
Gln 30	59.2	28.2	8.11	121.5	4.08	2.20	2.417		7.41, 6.85	NE 111.5
Asn 31	59.4	38.5	8.72	119.1	4.53	3.00, 2.87		7.417, 7.088		ND 111.4
Tyr 32	62.9	38.6	8.86	122.1	3.89	3.36, 3.20		7.27	6.88	
Arg 33	59.2	30.1	8.06	117.0	3.90	2.03, 1.95	1.707	3.301, 3.229		

Table 2.4 (cont.)										
Gln 34	58.2	29.3	7.70	115.5	3.94	1.68, 1.29	1.822		7.28, 6.76	NE 110.6
Phe 35	58.2	41.4	7.99	113.2	4.98	3.33, 2.87				
Cys 36	55.8	43.1	8.09	117.3	4.85	2.62, 2.16				
Arg 37	57.3		7.52	125.3	4.18	1.89, 1.76	1.60, 1.53			
	H1, C1	**H2, C2**	**H3, C3**	**H4, C4**	**H5, C5**	**H6, C6**				
GLC	4.60, 88.3	3.31, 75.2	3.52, 80.2	3.43, 72.6	3.53, 82.8	3.93, 3.72, 64.0				

2.4.6 Peptide chemical shift assignments

Backbone resonance assignments (^{15}N, ^{13}Ca, and ^{13}Cb) were obtained from 3D ^{1}H-^{13}C-^{15}N HNCA spectra recorded with a spectral width of 14 ppm (2048 points), 36 ppm (32 points) and 36 ppm (32 points) in ^{1}H, ^{13}C, and ^{15}N dimensions, respectively, 3D ^{1}H-^{13}C-^{15}N CBCA(CO)NH spectra were recorded with a spectral width of 14 ppm (2048 points), 96 ppm (32 points), and 36 ppm (32 points) for ^{1}H, ^{13}C and ^{15}N dimensions, respectively and ^{1}H-^{15}N HSQC spectra were recorded with a spectral width of 14 ppm (2048 points) and 36 ppm (256 points) in the ^{1}H and ^{15}N dimensions The proton signals from the amino acid side chains were assigned by analysis of 3D ^{15}N HSQC-NOESY (150 ms NOESY mixing time), and 3D ^{15}N HSQC-TOCSY (80 ms TOCSY mixing time) spectra and two-dimensional ^{1}H-^{1}H TOCSY (80 ms mixing time) and ^{1}H-^{1}H NOESY (200 ms mixing time).

The dihedral angle restrains were obtained based on $^{3}J_{HN}$-H_{α} coupling constants measured in an HNHA experiment using ^{15}N-labeled sublancin and were obtained from the Torsion Angle Likelihood Obtained from Shift and Sequence similarity (TALOS)[20,22] program based on backbone chemical shifts.

2.4.7 Hydrogen bond identification by deuterium exchange

A sample lyophilized from 90%H_2O/10%D_2O was dissolved in 100% D_2O. A series of ^{1}H-^{15}N HSQC spectra with a 7 min duration each were collected. Hydrogen bonding donors were identified within the first 7 min with 27 backbone and 1 side chain NH observed, with 3 three signals belonging to residues located in the loop region (Gly17, Gly18 and Ile20). After the first 30 min, 15 signals were still present, by 60 min 12 signals were present, and by 45 h 8 signals could still be observed (Table 2.2).

2.4.8 Sugar chemical shift assignments

Sugar assignments were obtained by analysis of TOCSY (80 ms mixing time), ^{1}H-^{13}C HSQC, and DQCOSY spectra for identification of neighboring protons.

2.4.9 Structure calculations (XPLOR, Dih, Hbond)

The three-dimensional structure of the peptide was calculated based on both distance and angle restraints by using the simulated annealing protocol in the NIH version of X-PLOR[6,7] 3.1 and the quality of the NMR structures was evaluated using the program PROCHECK.[23-25] Distance restraints were derived from NOE peak heights in the ^{15}N HSQC NOESY with a 150 ms mixing time and from two-dimensional NOESY spectra with a 200 ms mixing time collected on unlabeled material. The distance restraints were grouped by classifying the NOE cross-peak heights into ranges of 2.5, 3.5, 5.0, and 6.0 Å (strong, medium, weak, and very weak, respectively). The peptide backbone restraints extracted from $J_{NH\alpha}$ and TALOS were used as dihedral phi and psi angle restraints. A list of the number of NMR distances and angle restraints used for structural calculations is given in Table 2.1. In total 150 structures were calculated. An ensemble of 15 structures with the lowest total energy was chosen for structural analysis.

2.5 REFERENCES

(1) Arnison, P. G.; Bibb, M. J.; Bierbaum, G.; Bowers, A. A.; Bugni, T. S.; Bulaj, G.; Camarero, J. A.; Campopiano, D. J.; Challis, G. L.; Clardy, J.; Cotter, P. D.; Craik, D. J.; Dawson, M.; Dittmann, E.; Donadio, S.; Dorrestein, P. C.; Entian, K. D.; Fischbach, M. A.; Garavelli, J. S.; Goransson, U.; Gruber, C. W.; Haft, D. H.; Hemscheidt, T. K.; Hertweck, C.; Hill, C.; Horswill, A. R.; Jaspars, M.; Kelly, W. L.; Klinman, J. P.; Kuipers, O. P.; Link, A. J.; Liu, W.; Marahiel, M. A.; Mitchell, D. A.; Moll, G. N.; Moore, B. S.; Muller, R.; Nair, S. K.; Nes, I. F.; Norris, G. E.; Olivera, B. M.; Onaka, H.; Patchett, M. L.; Piel, J.; Reaney, M. J.; Rebuffat, S.; Ross, R. P.; Sahl, H. G.; Schmidt, E. W.; Selsted, M. E.; Severinov, K.; Shen, B.; Sivonen, K.; Smith, L.; Stein, T.; Sussmuth, R. D.; Tagg, J. R.; Tang, G. L.; Truman, A. W.; Vederas, J. C.; Walsh, C. T.; Walton, J. D.; Wenzel, S. C.; Willey, J. M.; van der Donk, W. A. *Nat Prod Rep* **2013**, *30*, 108. "Ribosomally synthesized and post-translationally modified peptide natural products: overview and recommendations for a universal nomenclature".

(2) Oman, T. J.; Boettcher, J. M.; Wang, H.; Okalibe, X. N.; van der Donk, W. A. *Nat Chem Biol* **2011**, *7*, 78. "Sublancin is not a lantibiotic but an S-linked glycopeptide".

(3) Paik, S. H.; Chakicherla, A.; Hansen, J. N. *J Biol Chem* **1998**, *273*, 23134. "Identification and characterization of the structural and transporter genes for, and the chemical and biological properties of, sublancin 168, a novel lantibiotic produced by Bacillus subtilis 168".

(4) Stepper, J.; Shastri, S.; Loo, T. S.; Preston, J. C.; Novak, P.; Man, P.; Moore, C. H.; Havlicek, V.; Patchett, M. L.; Norris, G. E. *FEBS Lett* **2011**, *585*, 645. "Cysteine S-glycosylation, a new post-translational modification found in glycopeptide bacteriocins".

(5) Venugopal, H.; Edwards, P. J.; Schwalbe, M.; Claridge, J. K.; Libich, D. S.; Stepper, J.; Loo, T.; Patchett, M. L.; Norris, G. E.; Pascal, S. M. *Biochemistry* **2011**, *50*, 2748. "Structural, dynamic, and chemical characterization of a novel S-glycosylated bacteriocin".

(6) Schwieters, C. D.; Kuszewski, J. J.; Tjandra, N.; Clore, G. M. *J Magn Reson* **2003**, *160*, 65. "The Xplor-NIH NMR molecular structure determination package".

(7) Schwieters, C. D.; Kuszewski, J. J.; Tjandra, N.; Clore, G. M. *Progr. NMR Spectroscopy* **2006**, *48*, 47. "Using Xplor-NIH for NMR molecular structure determination".

(8) Pal, D.; Chakrabarti, P. *Biopolymers* **2002**, *63*, 195. "On residues in the disallowed region of the Ramachandran map".

(9) Wüthrich, K. *NMR of Proteins and Nucleic Acids*; Wiley-Interscience, 1986.

(10) Dougherty, D. A. *Science* **1996**, *271*, 163. "Cation-π Interactions in Chemistry and Biology: A New View of Benzene, Phe, Tyr, and Trp".

(11) Dougherty, D. A. *Acc Chem Res* **2013**, *46*, 885. "The Cation-π Interaction".

(12) Kurbatova, N.; Chartier, M.; Zylber, M. I.; Najmanovich, R. *F1000Research* **2013**, *2*, 117. "IsoCleft Finder – a web-based tool for the detection and analysis of protein binding-site geometric and chemical similarities".

(13) Wang, C.; Eufemi, M.; Turano, C.; Giartosio, A. *Biochemistry* **1996**, *35*, 7299. "Influence of the carbohydrate moiety on the stability of glycoproteins".

(14) Helenius, A.; Aebi, M. *Annu Rev Biochem* **2004**, *73*, 1019. "Roles of N-linked glycans in the endoplasmic reticulum".

(15) Chen, M. M.; Bartlett, A. I.; Nerenberg, P. S.; Friel, C. T.; Hackenberger, C. P.; Stultz, C. M.; Radford, S. E.; Imperiali, B. *Proc Natl Acad Sci U S A* **2010**, *107*, 22528. "Perturbing the folding energy landscape of the bacterial immunity protein Im7 by site-specific N-linked glycosylation".

(16) Culyba, E. K.; Price, J. L.; Hanson, S. R.; Dhar, A.; Wong, C. H.; Gruebele, M.; Powers, E. T.; Kelly, J. W. *Science* **2011**, *331*, 571. "Protein native-state stabilization by placing aromatic side chains in N-glycosylated reverse turns".

(17) Hanson, S. R.; Culyba, E. K.; Hsu, T. L.; Wong, C. H.; Kelly, J. W.; Powers, E. T. *Proc Natl Acad Sci U S A* **2009**, *106*, 3131. "The core trisaccharide of an N-linked glycoprotein intrinsically accelerates folding and enhances stability".

(18) Dorenbos, R.; Stein, T.; Kabel, J.; Bruand, C.; Bolhuis, A.; Bron, S.; Quax, W. J.; Van Dijl, J. M. *J Biol Chem* **2002**, *277*, 16682. "Thiol-disulfide oxidoreductases are essential for the production of the lantibiotic sublancin 168".

(19) Wang, H.; van der Donk, W. A. *J Am Chem Soc* **2011**, *133*, 16394. "Substrate selectivity of the sublancin S-glycosyltransferase".

(20) Delaglio, F.; Grzesiek, S.; Vuister, G. W.; Zhu, G.; Pfeifer, J.; Bax, A. *J Biomol NMR* **1995**, *6*, 277. "NMRPipe: a multidimensional spectral processing system based on UNIX pipes".

(21) Lee, W.; Westler, W. M.; Bahrami, A.; Eghbalnia, H. R.; Markley, J. L. *Bioinformatics* **2009**, *25*, 2085. "PINE-SPARKY: graphical interface for evaluating automated probabilistic peak assignments in protein NMR spectroscopy".

(22) Cornilescu, G.; Delaglio, F.; Bax, A. *J Biomol NMR* **1999**, *13*, 289. "Protein backbone angle restraints from searching a database for chemical shift and sequence homology".

(23) Raaijmakers, H.; Vix, O.; Toro, I.; Golz, S.; Kemper, B.; Suck, D. *EMBO J.* **1999**, *18*, 1447. "X-ray structure of T4 endonuclease VII: a DNA junction resolvase with a novel fold and unusual domain-swapped dimer architecture".

(24) Laskowski, R. A.; Rullmannn, J. A.; MacArthur, M. W.; Kaptein, R.; Thornton, J. M. *J Biomol NMR* **1996**, *8*, 477. "AQUA and PROCHECK-NMR: programs for checking the quality of protein structures solved by NMR".

(25) Morris, A. L.; MacArthur, M. W.; Hutchinson, E. G.; Thornton, J. M. *Proteins* **1992**, *12*, 345. "Stereochemical quality of protein structure coordinates".

CHAPTER 3. THE PHOSPHOENOLPYRUVATE:SUGAR PHOSPHOTRANSFERASE SYSTEM IS INVOLVED IN SENSITIVITY TO SUBLANCIN[a, b]

3.1 INTRODUCTION

Many bacteriocins are heavily post-translationally processed during their biosynthesis and these modifications are required for activity.[1] As discussed briefly in chapter 1, nisin is the most studied bacteriocin and belongs to the lantibiotic family.[2] The mode of action of nisin involves binding to lipid II, which prevents further cell wall synthesis, followed by formation of pores within the membrane. Leakage of essential metabolites from these cells results in death of the bacteria. Targeting of lipid II by bacteriocins is a common mechanism of action.[3-5] Other mechanisms include the targeting of phosphotransferase systems,[6,7] acting as Trojan horses,[8,9] parasitizing iron-uptake pathways,[10] and causing the collapse of membrane potential together with leakage of ions and/or a decrease in intracellular ATP concentrations.[11] There is much interest in bacteriocins for use in control of bacterial infections and therefore in their mechanisms of action.

Sublancin is capable of killing several species of Gram-positive bacteria, such as *Staphylococcus aureus*, including methicillin resistant *S. aureus* (MRSA).[12] The genes necessary for the synthesis of sublancin are also included in the SPβ prophage region and are expressed from two promoters. The biosynthetic operon is made up of five individual genes, which are responsible for producing active sublancin. The *sunT* gene is responsible for the export of sublancin and cleavage of its leader sequence. Two thiol-disulfide oxidoreductases, encoded by

---

[a] Reproduced in part with permission from: "The Phosphoenolpyruvate:Sugar Phosphotransferase system is involved in sensitivity to the glycosylated bacteriocin sublancin." Antimicrob. Agents Chemother. **2015**, doi:10.1128/AAC.01519-15. Copyright 2015 Antimicrobial Agents and Chemotherapy.
[b] All *B. subtilis* ΔSPβ mutagenesis and knockout studies were performed by the van Dijl research group

bdbA (the only gene of the operon that is dispensable for active sublancin production) and *bdbB*, are responsible for creating the two disulfide bonds of sublancin. These disulfide bonds involve four of the five cysteine residues that are present in the sublancin peptide.[13] The fifth cysteine residue undergoes glucosylation by the glucosyltransferase encoded by the *sunS* gene.[14] The second promoter drives expression of a gene encoding the immunity protein SunI that is also required for the production of active sublancin by protecting the producing organism from sublancin.[15]

Chapter 1 discussed how sublancin is one of five bacteriocins that have so far been described as being S-glycosylated. The mechanisms by which glycosylated bacteriocins kill sensitive cells are currently unknown. Previous work has identified several genes in *B. subtilis* and *S. aureus* that alter the sensitivity to sublancin. The *mscL* gene encodes the large mechanosensitive channel and its deletion confers sublancin resistance in both *S. aureus* and *B. subtilis.*[16] Addition of increased amounts of NaCl also results in increased resistance to sublancin, presumably due to the MscL channel being forced closed. This observation has led to speculation as to whether sublancin is able to enter the cell through this channel. Interestingly, since the connection between sublancin and MscL was reported, streptomycin has also been reported to use the MscL channel to enter the cell.[17] In *B. subtilis* the alternative sigma factor σ^W is known to play a role in the resistance to sublancin through its regulation of the *yqeZ-yqfA-yqfB* operon.[18] The role these genes play in resistance to sublancin is unknown, but it is likely to be at the cell surface due to their membrane localization.[19]

This chapter, presents studies showing that the phosphoenolpyruvate:sugar phosphotransferase system (PTS) of *B. subtilis* plays a major role in sensitivity to sublancin. In the case of other bacteriocins where the PTS was found to be involved, addition of the PTS-

requiring sugars resulted in increased sensitivity to the respective bacteriocin. However, for sublancin, the addition of PTS-requiring sugars leads to increased resistance, suggesting that sublancin has a distinct mechanism of action.

3.2 RESULTS AND DISCUSSION

3.2.1 Sublancin displays sub micromolar MIC against *Bacillus* strains

The antibacterial activity of sublancin against selected *Bacillus* strains was first determined by solid agar diffusion assays containing sublancin at a range of concentrations (0.097 mM – 50 mM). After confirmation that *B. subtilis* ATCC 6633 and *B. halodurans* C-125 were sensitive, the minimum inhibitory concentrations (MICs) were determined by the broth dilution method.[20,21] A series of dilutions of sublancin (0.097 μM – 50 μM) were made and incubated with a defined number of bacterial cells in LB medium. Plates were incubated for 18-24 h at 37 °C, and growth was assessed by measuring the optical density of each well at $O.D._{600nm}$. The MICs were determined by fitting the data to a dose-response curve. The MICs of sublancin against *B. halodurans* C-125 and *B. subtilis* ATCC 6633, in liquid cultures, were 0.312 μM and 0.625 μM, respectively (Figure 3.1).

3.2.2 Bactericidal activity of sublancin

One element for consideration, when trying to understand how an antimicrobial compound functions, is whether it is bactericidal or bacteriostatic. Furthermore, some bacteria lyse after being killed, others lyse immediately, and yet others undergo non-lytic death.[22,23] The ability of sublancin to kill or arrest the sensitive *Bacillus* strains was therefore evaluated. *B. subtilis* ATCC 6633 and *B. halodurans* C-125 cultures were grown to mid log phase, transferred

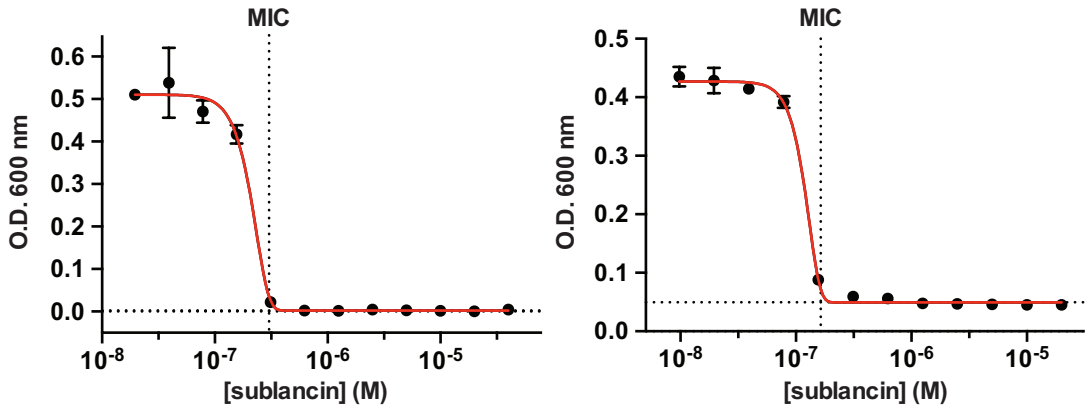

Figure 3.1 Determination of the specific activity of sublancin against Bacillus subtilis ATCC 6633 (left) and Bacillus halodurans C-125.

Determination of the specific activity of sublancin against *Bacillus subtilis* ATCC 6633 (left) and *Bacillus halodurans* C-125 (right) by the broth dilution method. Shown are the means of a single experiment conducted in triplicate as a representative of three independent experiments. For both graphs $R^2 > 0.99$. Error bars indicate standard deviations. When error bars are not visible, the error was smaller than the size of the symbol.

to a 48-well plate and exposed to sublancin (1x and 4x MIC). After the addition of sublancin, the $O.D._{600nm}$ was monitored periodically. After a 6-hour incubation period, the *B. halodurans* C-125 and *B. subtilis* ATCC 6633 cultures showed a decrease in optical density, suggesting sublancin has bactericidal activity (Figure 3.2). To verify whether sublancin's activity was bactericidal, colony forming units (CFUs) were determined by plating, which confirmed the bactericidal activity observed by O.D. readings. The decrease in optical density was not nearly as large as the decrease in CFUs, which implies that sublancin kills without immediate lysis.

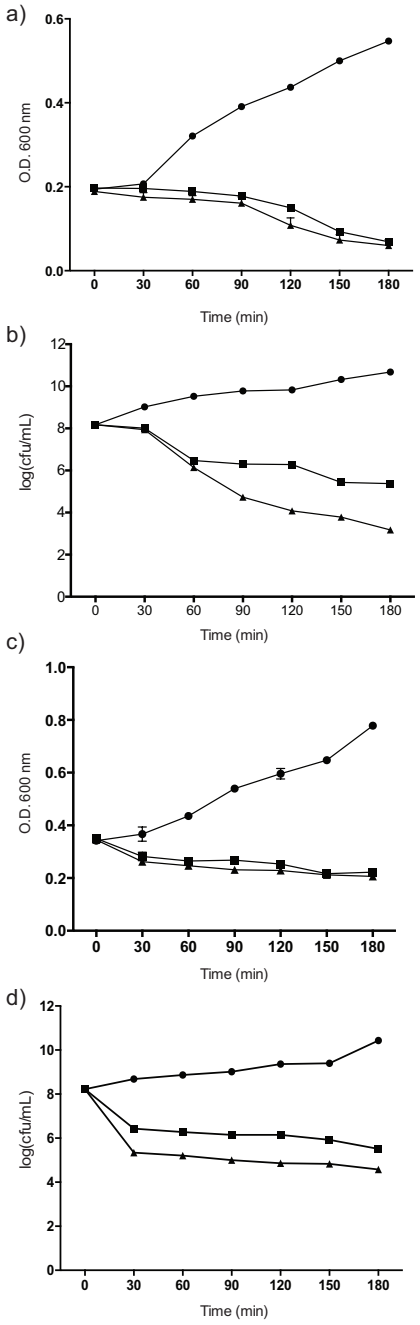

Figure 3.2 Growth inhibition of *B. subtilis* ATCC 6633 and *B. halodurans* C-125 by sublancin 168.

Time-dependent changes in $O.D._{600nm}$ of cultures of *B. subtilis* ATCC 6633 in the absence (circles) or presence of sublancin 168 at 1xMIC (squares) and 4xMIC (triangles). (b) Aliquots of the cultures in panel (a) were analyzed for colony forming units (CFUs). (c) Time-dependent changes in $O.D._{600nm}$ of cultures of *B. halodurans* C-125. The same symbols are used as in panel (a). (d) Aliquots of the cultures in panel (c) were analyzed for CFUs. The mean values of the data from one experiment conducted in triplicate are shown. The data are representative of three independent experiments. Error bars indicate standard deviations. When error bars are not visible, they were a smaller than the size of the symbol used.

3.2.3 Sublancin does not affect the integrity of the cell membrane

Some bacteriocins destabilize the membrane or form pores.[4,24] Nisin is the prototypical pore-forming bacteriocin, which binds to lipid II within the membrane.[2] To determine whether sublancin affects membrane integrity, we challenged cultures of *B. subtilis* ΔSPβ, *B. subtilis* ATCC 6633 and *B. halodurans* C-125 with several different concentrations of sublancin. We monitored the membrane integrity of *B. subtilis* ATCC 6633 and *B. halodurans* C-125 by flow cytometric analysis, using the cell impermeable propidium iodide (PI) dye, after a 30 min exposure to sublancin. Our nisin control showed an increase in fluorescence due to membrane permeabilization, but sublancin did not, even at concentrations as high as 32xMIC for *B. subtilis* ATCC 6633 and 64xMIC for *B. halodurans* C-125 (Figure 3.3). In addition, our collaborators in the van Dijl group monitored the membrane integrity of *B. subtilis* ΔSPβ with the LIVE/DEAD® *Bac*Light™ bacterial cell viability assay at 30 and 90 min after addition of sublancin (Figure 3.4). At both time points we found no change in membrane integrity. When the same strain was exposed to nisin as a positive control, a dramatic loss of membrane integrity was seen already after 30 min incubation. Collectively, these experiments show that sublancin does not affect membrane integrity and likely acts through an alternative mechanism.

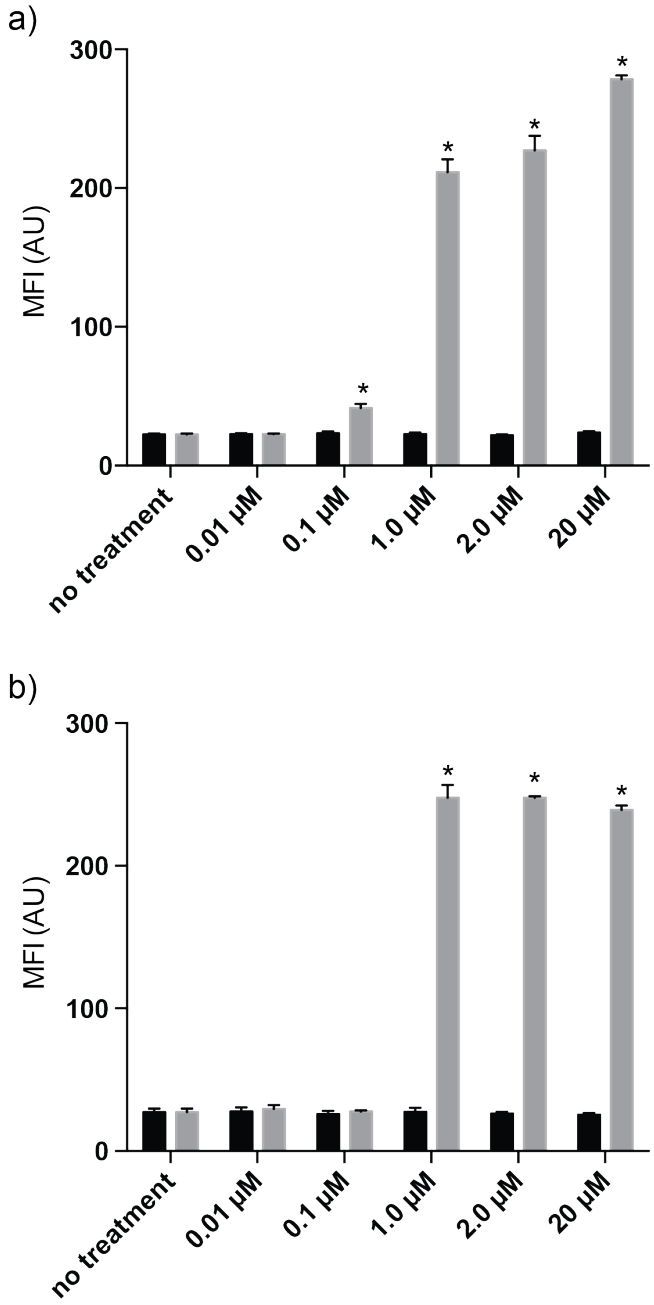

Figure 3.3 Membrane integrity assays by measuring propidium iodide (PI) uptake.

Addition of sublancin at the indicated concentrations (black bars) does not alter the membrane permeability of (a) *B. halodurans* C-125 and (b) *B. subtilis* ATCC 6633. Nisin was used as positive control (grey bars). * indicates a $P < 0.05$ between nisin (0.1 µM – 20 µM) treated cells relative to no treatment. In all experiments in which the cells were exposed to sublancin, the increase in MFI relative to control was not statistically significant ($P > 0.05$). The means of the data from a single experiment conducted in triplicate are shown. The data are representative of those from three independent experiments. Error bars indicate standard deviations.

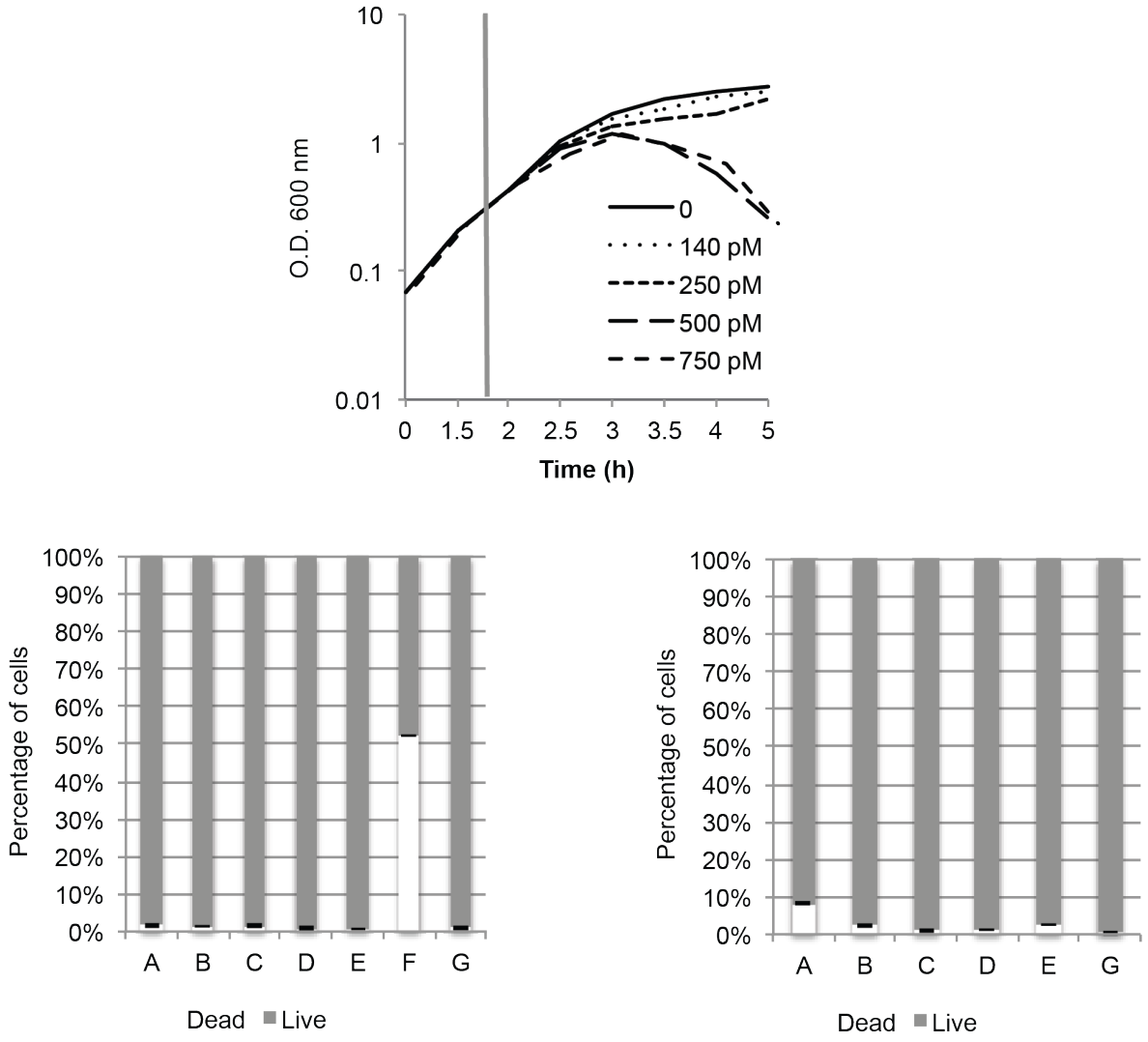

Figure 3.4 Sublancin does not affect the integrity of the bacterial membrane.

(Top) Growth curve of the *B. subtilis* Δ*SPβ* strain in the presence of different concentrations of sublancin. Sublancin was added at $O.D._{600nm}$ 0.5 (vertical grey line). Measurements were performed in the Synergy™ H4 Hybrid Multi-Mode Microplate BioTeK plate Reader every 10 minutes, in triplicate, and the means of the growth curve was plotted. (Bottom) LIVE/DEAD® *Bac*Light™ bacterial cell viability assay of the Δ*SPβ* strain 30 (left) and 90 (right) min after exposure to sublancin. Grey bars depict bacteria with an intact membrane and white bars depict bacteria with a compromised membrane, error bars depict standard deviation of the triplicate. A 100 nM sublancin, B 200 nM sublancin, C 300 nM sublancin, D 400 nM sublancin, E 500 nM sublancin, F Nisin (10 nM) was used as a positive control that does affect the integrity of the membrane, and G negative control, no addition of an antimicrobial agent. Figure courtesy of Dr. Emma Denham.

3.2.4 Resistance frequency

The manifestation of antibiotic resistance to clinically used antibiotics suggests that resistance is likely to develop against any antibacterial compound. It is useful however to analyze the frequency at which resistance to novel antibacterial compounds arises.[25] The spontaneous resistance frequency is defined as the number of resistant mutants per total number of viable cells that grow after an established period of time. The resistance frequency of sublancin was determined by plating aliquots of bacterial culture onto agar containing the antibacterial compound at 4xMIC. Aliquots were also plated onto agar plates with no antibiotic to determine the number of viable bacterial cells in the liquid culture. The resistance frequencies determined were relatively high, with resistance frequencies of 10^{-5} for *B. halodurans* C-125 and 10^{-6} for *B. subtilis* ATCC 6633. To verify that colonies observed were indeed resistant to the antibiotic, they were sub-cultured in sublancin-free LB media and plated on LB agar containing the antibacterial compound at a concentration of 4xMIC. For both strains, the plated resistant strains grew a full lawn.

3.2.5 Identification of *B. subtilis* chromosomal regions that affect sensitivity to sublancin

We aimed at finding genetic factors that affect sensitivity to sublancin. To do this, our collaborators in the van Dijl group first employed the set of deletion mutants described by Tanaka et al.[26] These mutants were created in a strain in which the prophages of *B. subtilis* had been deleted, including SPβ. Therefore, all mutant strains lack the gene encoding the immunity protein for sublancin, *sunI,*[27] making it an ideal collection of mutants for identifying interesting genomic regions with respect to sublancin sensitivity. During the screening, the van Dijl group used LB agar without NaCl, as it was previously shown that *B. subtilis* is more sensitive to

sublancin in low osmotic conditions.[16] The strains were plated in duplicate on LB agar plates and spotted with 2 μL of an overnight culture of the sublancin-producing strain *B. subtilis* 168. Strain JJS-DIn010, in which *rsiW* and *sigW* are deleted, was found to have increased sensitivity (i.e. a larger zone of clearing around the producing colony) (Figure 3.5). This finding is in concordance with previously reported observations,[18] suggesting that the assay was able to identify strains with altered sensitivity. Another strain was identified (JJS-DIn042), in which the genes *ykvS*, *ykvT*, *ykvU*, *stoA*, *zosA*, *ykvY*, *ykvZ*, *glcT*, *ptsG*, *ptsH* and *ptsI* were deleted. JJS-DIn042 was resistant to the effects of sublancin (Figure 3.5) under conditions where the ΔSPβ strain did not survive. Because of this interesting observation, the van Dijl group investigated this region further by constructing several different individual gene deletion mutants. This approach revealed that only the deletion of the *pts* operon (*ptsGHI*) resulted in resistance to sublancin (Figure 3.6 and Table 3.1). In contrast, a deletion of *glcT*, which plays a regulatory role in the *pts* operon,[28] did not result in sublancin resistance (Fig. 3.6).

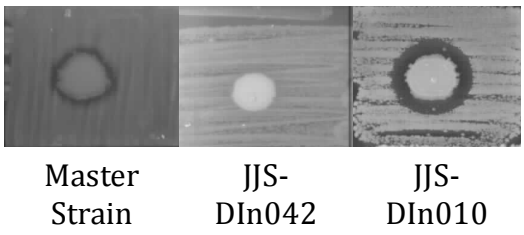

Figure 3.5 *B. subtilis* strain screen for reduced sublancin sensitivity.
The *B. subtilis* strains described by Tanaka et al [26] were screened for increased and reduced sensitivity to sublancin. The parental strain of the collection is labelled as 'master strain'. In JJS-DIn042 the region from *ykvS* to *ptsI* is deleted and in JJS-DIn010 *rsiW* and *sigW* are deleted. Figure courtesy of Dr. Emma Denham.

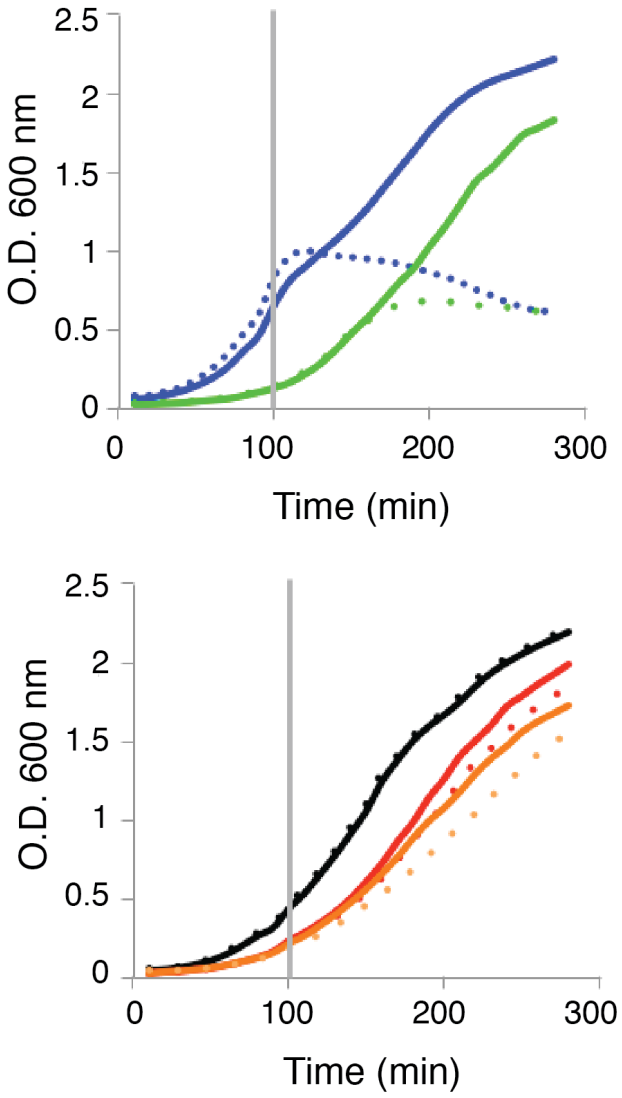

Figure 3.6 *B. subtilis* deletion mutant growth curves.

Growth curves of mutant strains with individual deletions of the genes that are responsible for the resistance in strain JJS-DIn042. Top panel - Blue line – *B. subtilis* ΔSPβ, green line - *B. subtilis* ΔSPβ-*glcT*. Bottom panel - black line - *B. subtilis* ΔSPβ-*ptsG*, red line - *B. subtilis* ΔSPβ-*ptsH*, orange line *B. subtilis* ΔSPβ-*ptsI*. Solid lines – no sublancin. Dotted lines – 200 nM sublancin added at 100 min as indicated by the vertical grey line. Deletion of any of the genes within the *ptsGHI* operon results in resistance to sublancin. Deletion of the gene encoding the transcriptional anti-terminator *glcT* had no effect on the sensitivity of *B. subtilis* to sublancin. The means of the data from a single experiment conducted in triplicate are shown. The data are representative of those from three independent experiments. Figure courtesy of Dr. Emma Denham.

Table 3.1 Phenotype of single gene deletion strains of *B. subtilis* ΔSPβ upon exposure to sublancin.

Mutation	Sublancin resistant or sensitive
ykvS	Sensitive
ykvT	Sensitive
ykvU	Sensitive
stoA	Sensitive
zosA	Inconclusive
ykvY	Sensitive
ykvZ	Sensitive
glcT	Sensitive
ptsG	Resistant
ptsH	Resistant
ptsI	Resistant

PtsG is the major glucose transporter of the phosphotransferase system,[29] and PtsH and PtsI are general components of the sugar transport system that phosphorylates the incoming sugar (Figure 3.7).[30] PtsH is more commonly known as HPr, and I will refer to it as such in this chapter; PtsI is also called EI. In *B. subtilis,* the PTS transfers a phosphate group from phosphorylated PtsI to HPr, which in turn transfers the phosphate to a variety of different PTS permeases. For utilization of glucose, HPr transfers the phosphate to the IIA domain of the sugar permease PtsG. The IIA domain then phosphorylates the IIB domain of PtsG, which in turn transfers the phosphate to the incoming sugar. Lastly, the phosphorylated sugar moves into glycolysis. It is intriguing that the PTS was identified in our screen for sublancin sensitivity, as the most common PTS substrate is glucose whereas sublancin is glycosylated. A functional homologue of HPr is present in *B. subtilis*, *i. e.* Crh. Our collaborators in the van Dijl group therefore tested a *crh* deletion mutant in the presence of sublancin, but no change in sensitivity

was observed compared to the wild-type (data not shown), suggesting the sensitivity to sublancin is specifically dependent on HPr.

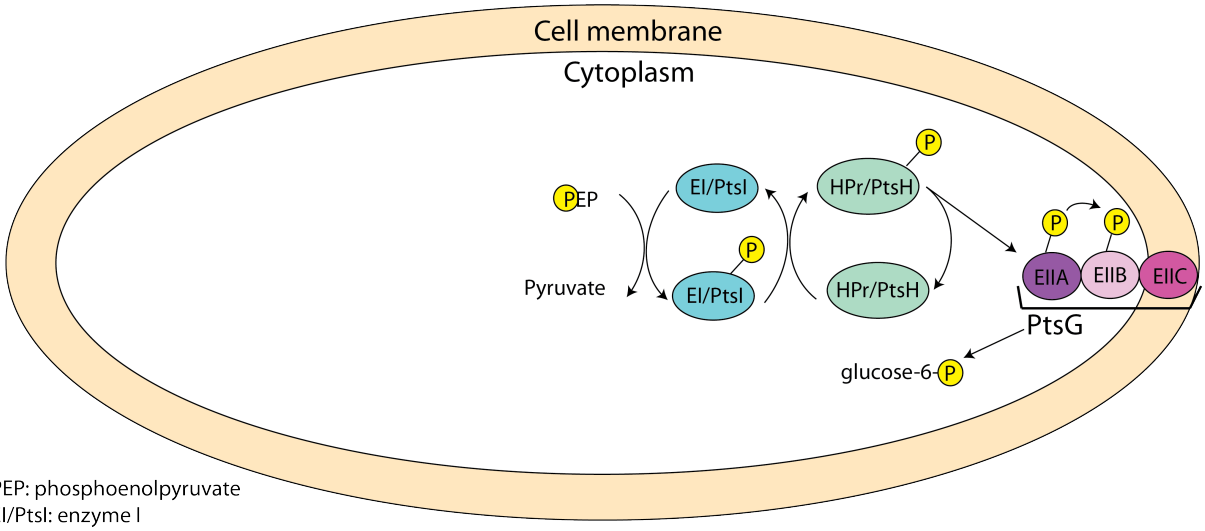

Figure 3.7 Representation of the glucose phosphotransferase system in *Bacilli.*

PtsG is the major glucose transporter of the phosphotransferase system,[29] and PtsH and PtsI are general components of the sugar transport system that phosphorylates the incoming sugar.[30] PtsH is more commonly known as HPr, and PtsI is also called EI. In *B. subtilis,* the PTS transfers a phosphate group from phosphorylated PtsI to HPr, which in turn transfers the phosphate to a variety of different PTS permeases. For utilization of glucose, HPr transfers the phosphate to the IIA domain of the sugar permease PtsG. The IIA domain then phosphorylates the IIB domain of PtsG, which in turn transfers the phosphate to the incoming sugar. Lastly, the phosphorylated sugar moves into glycolysis

3.2.6 Comparative genomics

Bacteria often acquire stable resistance to antibiotics due to gene mutations. A comparative genomics analysis was therefore performed to identify the mutations that conferred resistance to *B. halodurans* C-125 after exposure to sublancin. The gDNA of sensitive *B. halodurans* C-125 cells and of four of the spontaneous resistant mutants obtained as described above was extracted and sequenced using a HiSeq2000 Illumina sequencer. The wild-type *B. halodurans* strain was mapped to the published *B. halodurans* C-125 genome sequence

(accession no. NC_002570.2) to generate a consensus sequence that was used for SNP detection in sublancin-resistant mutants of *B. halodurans*. Comparison of gDNA of the wild-type sensitive strain with the four sublancin resistant mutants revealed several mutations (Table 3.2). One strain contained three mutations in the intergenic region between the transcriptional anti-terminator (Locus tag: BH0845) and *ptsG* (Locus tag: BH0844), another strain contained a missense mutation in the gene for mannitol-1-phosphate 5-dehydrogenase (Locus tag: BH3851), and most interestingly, the three strains that did not have a mutation in the intergenic region mentioned above all had non-sense mutations in the gene for the glucose-specific transporter subunit IIC that is part of the multidomain protein PtsG (Figure 3.7 and Table 3.3). The missense mutation prevents production of PtsG, and the three mutations in the intergenic region between the antiterminator and *ptsG* are predicted to considerably stabilize the structure of the terminator (Figure 3.8), thus potentially also preventing *ptsG* transcription. Once more, these findings point to the PTS being important for sensitivity to sublancin.

Table 3.2 SNPs in genes of sublancin-resistant *B. halodurans* C-125 mutants determined by Illumina sequencing.

Nucleotide position	Locus tag	Genetic component	Frequency	SNP mutation
919515	BH0844	PTS system glucose-specific transporter subunit IIC	3/4	G → T
920055 **920075** **920079**	Between BH0844 & BH0845	Intergenic region between transcriptional antiterminator and PTS system glucose-specific enzyme II, ABC components	1/4	G → A C → T A → G
3977494	BH3851	Mannitol-1-phosphate 5-dehydrogenase	1/4	T → C

SNPs in genes of sublancin-resistant *B. halodurans* C-125 mutants determined by Illumina sequencing. The mutation in BH0844 results in a stop codon instead of a Tyr codon at position 160. The predicted domain organization of PtsG of *B. halodurans* C-125 is: amino acids 1-424 domain IIC, 425-524 domain IIB, and 525-675 domain IIA (see schematic drawing of the predicted domain organization in table 3.3). Hence, the stop codon would delete most of PtsG and the respective truncated product would likely not be expressed as a stable protein. The mutation in BH3851 results in a His to Arg mutation. As shown in Figure 3.8, the mutations in the intergenic region result in a change in the predicted terminator structure that may affect transcription of *ptsG*.

Table 3.3 Predicted topology of PtsG from *B. halodurans* C-125.

Begin	End	Length	Localization
1	11	11	Inside
12	32	21	Membrane
33	43	11	Outside
44	60	17	Membrane
61	66	6	Inside
67	83	17	Membrane
84	88	5	Outside
89	109	21	Membrane
110	120	11	Inside
121	149	29	Membrane
150	168	19	Outside
169	189	21	Membrane
190	209	20	Inside
210	232	23	Membrane
233	276	44	Outside
277	295	19	Membrane
296	301	6	Inside
302	319	18	Membrane
320	324	5	Outside
325	349	25	Membrane
350	355	6	Inside
356	373	18	Membrane
374	378	5	Outside
379	401	23	Membrane
402	675	274	Inside

Predicted topology of PtsG from *B. halodurans* C-125 (BH0844). The multidomain PtsG is 675 amino acids in length. PtsG IIC (region 1-424) is a transmembrane domain. PtsG IIB (region 425-524) and PtsG IIA (region 525-675) are cytoplasmic domains. Prediction obtained from the CAMPS (Computational Analysis of the Membrane Protein Space) database (identifiers: Q9KEK8_BACHD, GI:15613407).

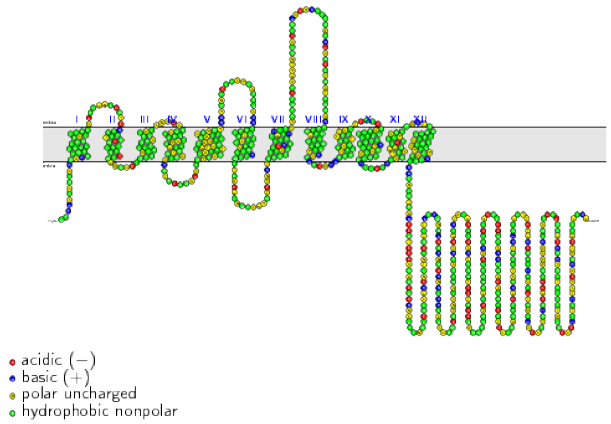

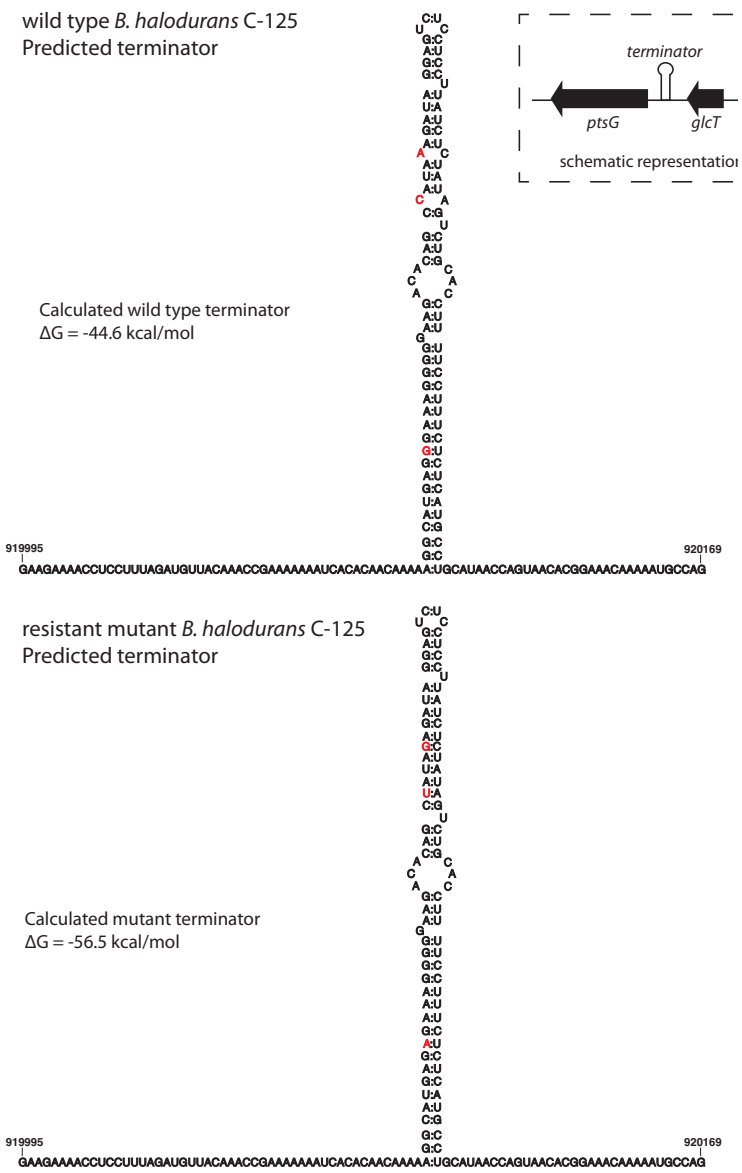

Figure 3.8 *B. halodurans* ptsG terminator.

Predicted secondary structures of the terminator of (top) wild-type *B. halodurans* C-125 (accession no. NC_002570.2) and (bottom) the sublancin resistant mutant *ptsG* leader mRNA. Inset shows a schematic representation of the genomic locus. Terminators are shown in the antisense strand since flanking genes translate in an antisense fashion. The terminator starts at position 920136 and ends at position 920046. The ptsG starts at position 919994. Single nucleotide polymorphisms (SNPs) are labelled in red. The RNAstructure Web Server (http://rna.urmc.rochester.edu/RNAstructure Web/index.html) at the University of Rochester Medical Center and the RNAfold Web Server (http://rna.tbi.univie.ac.at/) at the University of Vienna were used to predict the secondary structures using default parameters. All three mutations result in new Watson-Crick base-paired bases that increase the strength of the terminator. The predicted free energy values for the terminator loops were calculated using the RNAstructure Web Server.

3.2.7 Gene expression profile by microarray analysis of *B. halodurans* C-125

Antimicrobial resistance mutants provide valuable insights, but the information obtained from a resistance phenotype is not always representative of the identity of the target. We therefore also monitored changes in global gene expression upon exposure of *B. halodurans* C-125 to sublancin. The expression profiles revealed four genes that are part of sulfur metabolism that are highly up-regulated (changes from 9-14 fold, Table 3.4). The analysis also revealed up-regulated genes involved in transmembrane transporter activities, whereas genes involved in amino sugar and nucleotide sugar metabolism were up- and down-regulated. Interestingly, the genes for HPr and for PtsG that were also identified in the set of deletion mutants and in the comparative genomics analysis were down-regulated (Table 3.4) as was another PTS protein that is homologous to YpqE in *B. subtilis*, a putative phosphotransferase enzyme IIA component.[31] These data again suggest that, like in *B. subtilis,* the PTS is involved in the sensitivity of *B. halodurans* towards sublancin.

Table 3.4 Expression profile of *B. halodurans* C-125 in response to sublancin.

Category and Locus Tag	Entrez Gene ID	Gene	Name	Fold Change in transcript level
Sulfur metabolism				
BH1487	890521	*sat*	Sulfate adenyltransferase	16
BH1486	890994	*cysH*	3'-phosphoadenosine 5'-phosphosulfate reductase	14
BH0088	891637	*cysK*	cysteine synthase A	11
BH1489	890544	*NA*	adenylylsulfate kinase	9
Transmembrane transporter activity				
BH1488	890630	*NA*	sodium-dependent phosphate transporter	12
BH3129	890493	*cysW*	sulfate ABC transporter (permease)	7
BH3128	890497	*cysT*	sulfate ABC transporter (permease)	5
BH3127	894370	*NA*	sulfate ABC transporter (sulfate-binding protein)	5
BH3130	890510	*cysA*	sulfate ABC transporter (ATP-binding protein)	5
Amino sugar and nucleotide sugar metabolism				
BH0421	892066	*nagA*	N-acetylglucosamine-6-phosphate deacetylase	9
BH3130	894561	*nagB*	N-acetylglucosamine-6-phosphate isomerase	5
BH0675	893039	*NA*	beta-hexosamidase A precursor	5
BH1086	894063	*glgD*	required for glycogen biosynthesis	4
BH1087	892001	*glgC*	glucose-1-phosphate adenylyltransferase	4
BH0422	893420	*NA*	PTS system, N-acetylglucosamine-specific enzyme II, ABC component	3
BH1874	892569	*XSA*	alpha-L-arabinosidase	3

Continued on next page

Table 3.4 (cont.)

Category and Locus Tag	Entrez Gene ID	Gene	Name	Fold Change in transcript level
BH0673	893046	*NA*	PTS system, n-acetylglucosamine-specific enzyme II, ABC component (EIIABC-Nag)	2
BH3784	894582	*murZ*	UDP-N-acetylglucosamine 1-carboxyvinyltransferase	-2
BH0065	892269	*gcaD*	UDP-N-acetylglucosamine pyrophosphorylase	-2
BH2564	894513	*murB*	UDP-N-acetylenolpyruvoylglucosamine reductase	-2
BH0797	892380	*NA*	Glucose kinase	-2
BH0267	894435	*NA*	phosphoglucosamine mutase	-3
BH0844	892408	*ptsG*	PTS system, glucose-specific enzyme II, ABC component	-4
BH3715	894300	*NA*	UDP-glucose 4-epimerase	-6
BH3343	891275	*pgi*	glucose-6-phosphate isomerase	-8
BH3074	890548	*ptsH*	PTS system, histidine-containing phosphocarrier protein (HPr)	-8
BH1515	890569	*ypqE**	PTS system, glucose-specific enzyme II, A component	-9

** Closest homolog in B. subtilis is a IIA stand-alone domain YpqE with unknown specificity.*
NA: specific gene name not available for B. halodurans C-125.

Changes in transcript levels in *B. halodurans* C-125 in response to the addition of sublancin. Positive numbers indicate up-regulated transcripts, negative numbers indicate down-regulated transcripts.

3.2.8 Addition of PTS sugars to the growth media results in increased resistance to sublancin

Several bacteriocins have previously been shown to target PTS proteins as part of their mode of action. In these reported cases, addition of the relevant sugar resulted in an increased sensitivity to the bacteriocin.[6,7,11] This effect is due to elevated uptake of the respective bacteriocins via the PTS. We therefore investigated whether this was also true for sublancin. The PTS is able to use many sugars, employing a different transporter for each sugar together with the HPr and PtsI proteins (Figure 3.7). Once the sugar is phosphorylated, it moves into glycolysis at the relevant metabolic junction. To investigate the influence of added sugars, the van Dijl group diluted *B. subtilis* ΔSPβ cultures in LB media (without NaCl) containing different sugars and grew these in 96-well microtiter plates with shaking to an $O.D._{600nm}$ 0.5 before addition of sublancin at the MIC of 200 nM, as measured for this strain under these conditions. The presence of the PTS sugars glucose, sucrose and fructose, prevented the growth inhibition imposed by sublancin (Figure 3.9) since no significant reduction in O.D. was observed. In contrast, the non-PTS sugars citrate, galactose and succinate had no influence on sublancin's activity (Figure 3.9). The two exceptions were the non-PTS sugars glycerol and malate. In this respect it is noteworthy that the glycerol kinase GlpK requires phosphorylation by HPr for glycerol utilization.[29,32] Malate is a preferred carbon source for *B. subtilis* and is known to influence the carbon catabolite repression response.[33] In this context it is noteworthy that a decrease in antimicrobial activity was also reported for glycocin F upon supplementation of the media with GlcNAc, which is the sugar that is attached to glycocin F at two positions (further discussion in chapter 4).[34]

To further delineate the effects of sugars on sublancin sensitivity, our collaborators in the van Dijl group spotted purified sublancin onto lawns of *B. subtilis* ΔSPβ, which were grown on

agar plates containing the defined M9 minimal medium supplemented with glucose, malate or citrate. When glucose was present the cells were always resistant to sublancin. In contrast, with citrate a large zone of clearing was observed. In the presence of malate an intermediately sized zone of inhibition was observed. This observation underpins the view that the carbon source affects the sensitivity to sublancin (Figure 3.10).

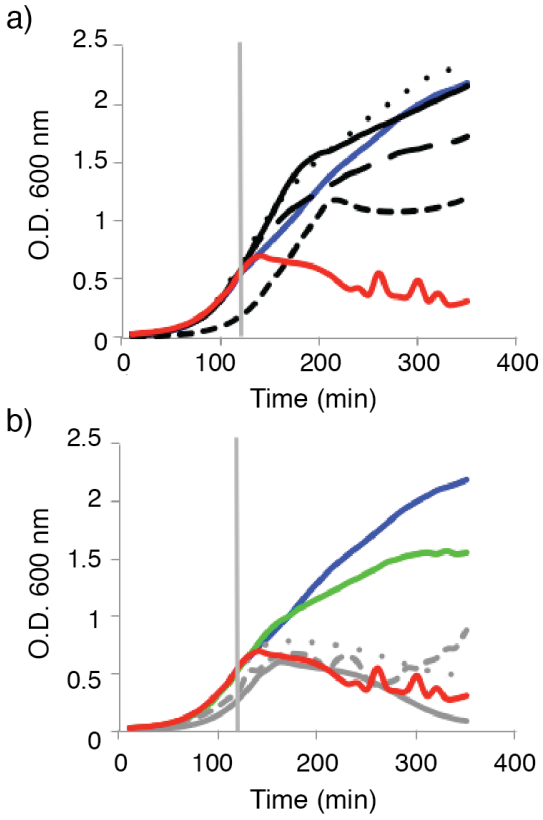

Figure 3.9 Effect of the addition of PTS sugars on growth of *B. subtilis* ΔSPβ treated with sublancin.
Addition of PTS sugars to LB blocks growth inhibition by sublancin (a) Growth curves of *B. subtilis* ΔSPβ in LB medium with salt with added PTS sugars. Blue line – no addition of sublancin, red line – addition of sublancin, black solid line – addition of 0.3% glucose, black dotted line – addition of 0.3% fructose, black long dashed line – addition of 0.3% sucrose, black short dashed line – addition of 0.3% glycerol. Sublancin was added at 120 min as indicated by the vertical grey line. (b) Growth curve of the ΔSPβ strain in LB medium with addition of non-PTS sugars. Blue line – no addition of sublancin, red line – addition of sublancin, green line – addition of 0.4% malate, grey short dashed line – addition of 0.4 % citrate, grey dotted line – addition of 0.4% galactose, grey solid line – addition of 0.4% succinate. The means of the data from a single experiment conducted in triplicate are shown. The data are representative of those from three independent experiments. Figure courtesy of Emma Denham.

Figure 3.10 *B. subtilis* ΔSPβ growth on M9 agar plates with a variety of carbon sources.
B. subtilis ΔSPβ was spread over M9 agar plates containing 0.3% glucose, 0.4% citrate or 0.4% malate. Sublancin (2 µL of 100 nM) was spotted on the plates. The presence of glucose in the media resulted in resistance to sublancin. Figure courtesy of Emma Denham.

Since glucose was found to prevent the effect of sublancin, we wondered whether it would be possible to rescue sublancin-treated cells by addition of glucose. Dr. Emma Denham therefore grew the bacteria on LB medium (with NaCl) and added sublancin at $O.D._{600nm}$ 0.5. The cells were then incubated for 30 min before addition of the same PTS and non-PTS sugars as in the previous experiment (Figure 3.11). Glucose almost instantaneously rescued the cells from the growth inhibition that sublancin imposed on the cells. Fructose also rescued the cells, but to a smaller extent than glucose. The non-PTS sugar glycerol rescued the cells in a similar manner to fructose. Malate was also able to rescue the cells, but this took approximately 100 min following the addition of the sugar, whereas the effect for glycerol and fructose was observed immediately after the addition of the respective sugar. In contrast, the addition of the other non-PTS sugars or sucrose had no effect on the survival of the bacteria.

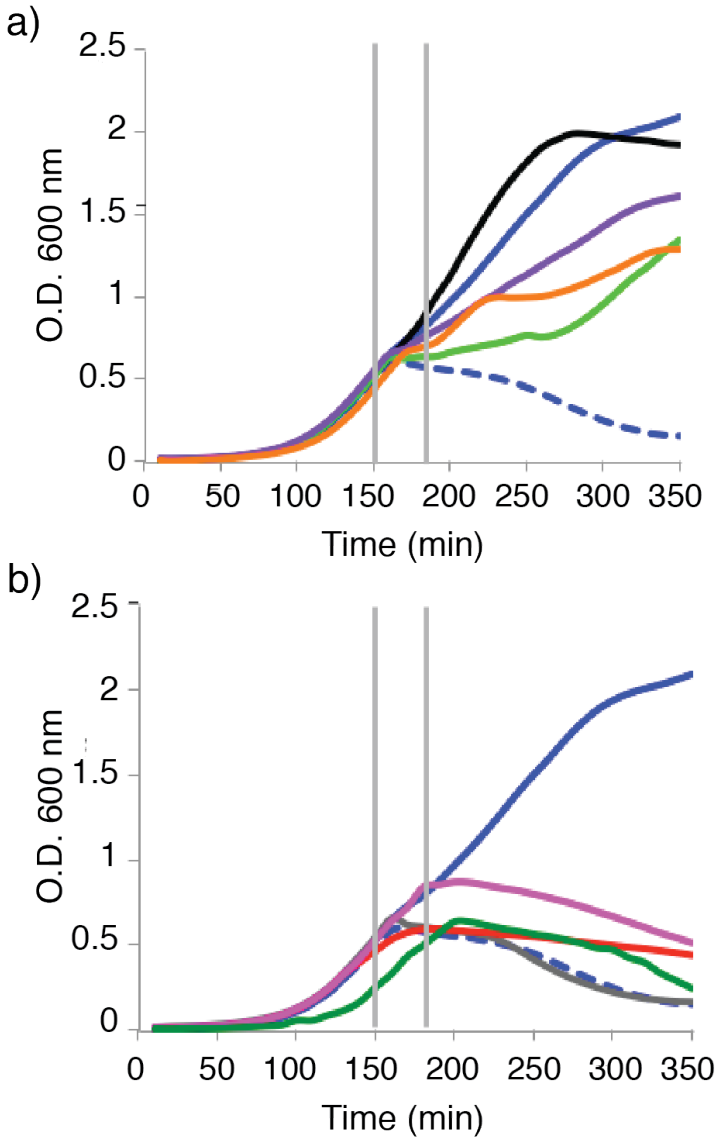

Figure 3.11 Effect of PTS sugars on growth of Bacteria after a 30 min after exposure to sublancin.

(Top) Growth curve of the ΔSPβ strain with sublancin added at 150 min followed by the addition of PTS and non-PTS sugars 30 min later as depicted by the two vertical lines, respectively. Blue line – no sublancin, blue dashed line – addition of sublancin, black line – 0.3% glucose, purple line – 0.3% fructose, orange line – 0.3% glycerol, green line - 0.4% malate, (final concentration of sugars shown). (Bottom) Growth curve of the ΔSPβ strain with sublancin added at 150 min followed by the addition of PTS and non-PTS sugars 30 min later as depicted by the two vertical lines, respectively. Blue line – no sublancin, blue dashed line – addition of sublancin, grey line – 0.4% citrate, red line – 0.3% sucrose, pink line – 0.4% galactose, green line – 0.4% succinate (final concentration of sugars shown). The means of the data from a single experiment conducted in triplicate are shown. The data are representative of those from three independent experiments. Figure courtesy of Emma Denham.

The observed rescue of growth by addition of the different PTS sugars and glycerol suggests that the PTS transporter is not being irreversibly inactivated by sublancin, but perhaps instead sublancin affects the pathway that leads to phosphorylation of the sugar. The addition of sublancin and the PTS sugar at the same time could result in competition for phosphorylation of the sugar or the glucose on sublancin (or its metabolite). With this in mind we looked at the phosphorylation sites on the HPr protein.

3.2.9 Phosphorylation of HPr is responsible for sensitivity to sublancin

The HPr protein is phosphorylated on two sites. The first, His15, is phosphorylated by PtsI. HPr then transfers the phosphate group to PtsG, and the phosphate is subsequently used to phosphorylate the incoming sugar. The second, Ser46, is phosphorylated by HPr kinase (HPrK) in conditions of large glycolytic flux. This phosphorylation subsequently allows HPr to form a complex with the catabolite control protein A (CcpA). This HPr-CcpA complex mediates carbon catabolite repression by binding to its cognate operator regions. To link sublancin sensitivity to one of these HPr-mediated processes, our collaborators in the van Dijl group tested two *B. subtilis* ΔSPβ strains with point mutations at one of the two HPr phosphorylation sites. As shown in Figure 3.12, *B. subtilis* ΔSPβ carrying the S46A point mutation in HPr was fully sensitive to sublancin. In contrast, the strain carrying the H15A point mutation in HPr displayed an increased level of resistance to sublancin. This observation suggests that *hprK* and *ccpA* deletion mutants would remain sensitive to sublancin, since the carbon catabolite-repressing function of HPr is not affected. This prediction was indeed confirmed, as the deletion of either of these two genes had no effect on sublancin sensitivity (Figure 3.12). Also, the addition of glucose to the Δ*ccpA* mutant conferred resistance to sublancin (not shown), providing further evidence that it is not the

carbon catabolite-repressing branch of HPr regulation that leads to sublancin sensitivity. Instead, it seems to be the PTS branch involving the His15 phosphorylation site that is responsible for the effects on sublancin sensitivity. However, how phosphorylation of His15 of HPr is exactly tied to sublancin sensitivity is presently unknown.

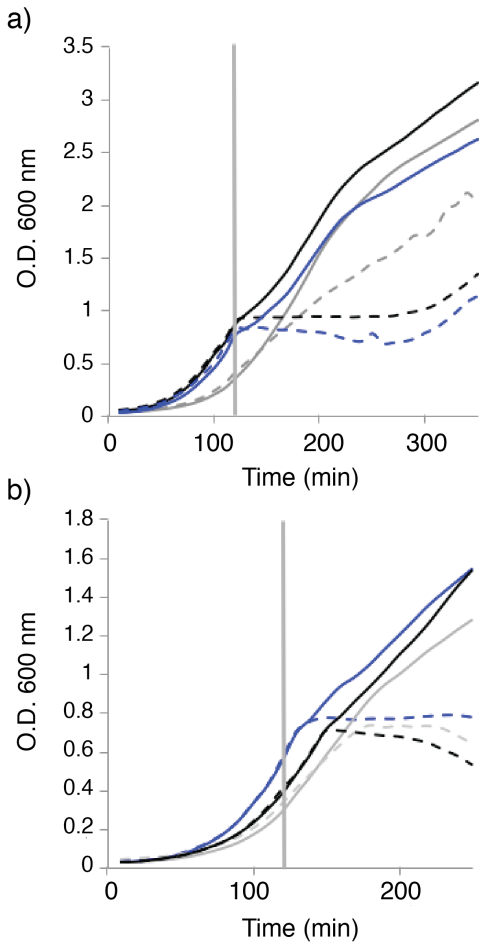

Figure 3.12 The H15A mutation in HPr results in increased resistance to sublancin.

(a) The two phosphorylation sites in the HPr protein were mutated individually to alanine residues. The growth curves of the resulting strains are shown, with 200 nM sublancin added at 120 min as depicted by the vertical line. Blue line - *B. subtilis* ΔSPβ**,** grey line - *B. subtilis* ΔSPβ-H15A**,** black line - *B. subtilis* ΔSPβ-S46A. Solid line – no sublancin. Dashed line – plus sublancin. (b) Blue line - *B. subtilis* ΔSPβ**,** grey line - *B. subtilis* ΔSPβ-*hprK***,** black line - *B. subtilis* ΔSPβ-*ccpA*. Solid line – no sublancin. Dashed line – plus sublancin. The Δ*ccpA* and Δ*hprK* mutations have no effect on the sensitivity of the cells to sublancin. 200 nM sublancin added at 120 min. The means of the data from a single experiment conducted in triplicate are shown. The data are representative of those from three independent experiments. Figure courtesy of Emma Denham.

3.3 SUMMARY

Sublancin is a bacteriocin that was recently found to be glycosylated as part of its maturation process and this glucosylation is required for activity.[14] We show in this chapter that sublancin is bactericidal and that it does not kill by pore formation or disruption of membrane integrity. Four different lines of evidence point towards the phosphoenolpyruvate:sugar phosphotransferase system as a factor affecting the activity of the bacteriocin. Experiments with deletion mutants of *B. subtilis* identified PtsG, HPr, and PtsI, but not GlcT and Crh, as important for sensitivity to sublancin. In addition, three of four *B. halodurans* sublancin-resistant mutants contained stop-codon mutations within the *ptsG* gene, with the fourth resistant strain having three mutations that potentially interfere with *ptsG* expression. The transcriptional profile also indicated a strong down-regulation of PTS genes upon exposure to sublancin and, lastly, addition of PTS sugars decreased the sensitivity to sublancin.

The PTS has been previously described as affecting sensitivity to other bacteriocins, including dysgalacticin and lactococcin A.[6,7,35] Dysgalactin appears to bind to the glucose and mannose transporters of the PTS.[7] Dysgalacticin was shown to block the uptake of glucose and the non-metabolisable analog 2-deoxyglucose, and also to perturb the membrane of the cell causing the dissipation of membrane potential.[7] This activity appears to be different from the mechanism used by sublancin as addition of glucose or any other PTS sugar blocked the killing activity of sublancin and membrane disruption was not observed. Lactococcin A also uses components of the mannose PTS in its mode of action. Lactococcin A binds to the membrane-located complex of the IIC and IID subunits of the mannose transporter,[6] resulting in dissipation of the membrane potential.[24] Like the observations with dysgalactin, decreased growth rates were

observed for cells grown with mannose or glucose as the sole carbon source in the presence of lactococcin A.[6] The studies in this chapter suggest that sublancin is also functioning in a different manner to lactococcin A, since the studies with gene deletion strains and spontaneous resistance mutants both point at the phosphorylation components of the PTS as being key to sublancin sensitivity rather than the membrane components. Furthermore, when we monitored sublancin susceptibility using M9 minimal medium supplemented with glucose as the single carbon source, cells were completely immune to the effects of sublancin. A third bacteriocin, the circular molecule garvicin ML requires the maltose-binding protein for activity. Growth in media where the sole carbon source is either maltose or galactose again resulted in increased sensitivity to this bacteriocin.[36]

Two regions of the *B. subtilis* chromosome have now been identified that result in resistance to sublancin. The first being *mscL*, encoding a mechanosensitive channel as described by Kouwen et al.,[16] and in this work the proteins encoded by the *ptsGHI* operon. Several scenarios may describe the mechanism by which sublancin is interacting with the PTS. Firstly, it is intriguing that it is the glucose transporter that was identified, given that sublancin is modified with an S-linked glucose moiety. The glucose moiety on sublancin could potentially be recognized by the transporter to facilitate entry into the cell or potentially to kill it through its interaction with this system. A competition between the sublancin and glucose could explain the observed decrease in sensitivity upon addition of glucose. We note that HPr and domains IIAB of PtsG are located in the cytoplasm (Figure 3.7), and hence for this mechanism to be correct, the glucose on sublancin would have to traverse the transporter or bypass the glucose transporter via the MscL channel. In this respect it is noteworthy that the other sugars that were able to protect the bacteria from sublancin are either gluconeogenic, or feed into glycolysis lower down the

pathway, therefore possibly bypassing the need for the glucose transporter. When we tested strains that express variants of the HPr protein with point mutations that remove the phosphorylation sites, the mutation that led to increased resistance to sublancin was H15A. Phosphorylation of His15 is responsible for transferring a phosphate group to the incoming PTS sugar. This points towards a critical role of phosphorylation in the growth inhibition by sublancin and seems to suggest that sublancin may need to be phosphorylated upon its entry into the cell in order to exert its bactericidal effect. Interestingly, bacterial growth was rescued when PTS sugars were added to the growth medium 30 min after the challenge with sublancin. This finding implies that either the specific growth-inhibiting mechanism employed by sublancin is reversible, or that the addition of the PTS sugars results in the cell using a different biological process that allows survival.

In conclusion, we show that sublancin exerts its bactericidal effects in a novel manner. At present it is not clear how exactly sublancin is interacting with the PTS and several questions remain for future research. Is there a physical interaction between sublancin and the PTS in the inhibited cells? Is there a link between the PTS and the MscL channel? How is sublancin actually inhibiting growth of the cell? How does the strong structural similarity of glycocin F and sublancin fit into the mechanism and what role does the three-dimensional structure of the peptide components of these glycocins (chapter 2) play?[37,38] In a time where bacteria are becoming resistant to the antimicrobial compounds that we currently use in clinical practice, research to understand how infections can be fought in alternative manners is essential. The apparently novel mechanism by which sublancin kills sensitive species of bacteria, such as the major pathogen *S. aureus*, may offer biological insights for the development of new antimicrobial strategies.

3.4 EXPERIMENTAL

3.4.1 Materials, cultures, and conditions

All chemicals and HPLC grade solvents were purchased from Sigma-Aldrich (St. Louis MO). Growth media were obtained from Difco Laboratories (Detroit MI). Tris, MOPS, and HEPES buffers were obtained from Fisher. Matrix-assisted laser desorption/ionization time-of-flight mass spectrometry (MALDI-TOF MS) was performed at the Mass Spectrometry Laboratory within the School of Chemical Sciences at UIUC using a Bruker Daltonics UltrafleXtreme MALDI TOFTOF instrument. Salt-containing MS samples were purified via Millipore Zip-Tip$_{C18}$ pipette tips (Billerica MA). Ninety-six and forty-eight well assay plates were from Corning Incorporated (Corning NY) and were read using a multi mode, single-channel Synergy H4 microplate reader from Biotek® instruments, Inc (Winooski, VT). Trays used for agar well diffusion assays were obtained from Nalge Nunc (Rochester NY).

3.4.2 Bacterial growth

For all strains used in this study, see Table 3.6. *B. subtilis* 168, *B. subtilis* ATCC 6633 and *B. halodurans* C-125 were grown in Lysogeny Broth (LB) at 37 °C with vigorous shaking (250 rpm) and on LB agar plates. *B. subtilis* was also grown on M9 agar plates (M9 as described,[39] but with the addition of 1.5 % final concentration agar) with and without the addition of sugars at final concentrations of 0.3 % glucose, 0.4 % malate or 0.4 % citrate as specified below. The LB agar used for sublancin inhibition plate assays did not include NaCl.

---

[c] I would like to thank Dr. Barbara Pilas for assistance with the flow cytometry,[d] Dr. Alvaro Hernandez for assistance with the comparative genomics and [e] Dr. Jenny Drnevich and Dr. Mike Band at the Roy J. Carver Biotechnology Center and W.M. Keck Center for Comparative and Functional Genomics for assistance with the microarray data.

Antibiotics were used for selection when necessary at the following concentrations: spectinomycin 100 μg/mL, kanamycin 20 μg/mL, phleomycin 4 μg/mL, chloramphenicol 5 μg/mL and erythromycin 2 μg/mL. Stock sublancin solutions were prepared using PBS.

3.4.3 Production and isolation of sublancin 168

Purification of sublancin from its natural producer, *Bacillus subtilis* 168, was performed as previously reported.[14] Briefly, a culture of *B. subtilis* 168 was grown in LB media at 37 °C for 12-15 h under vigorous agitation. The overnight culture was used to inoculate (at 1%) 500 mL volumes of Medium A in 2 L flasks. Medium A consists of 900 mL of Medium A nutrient broth combined with 100 mL of 10X Medium A salts. Medium A nutrient broth was prepared by dissolving 20.0 g sucrose, 11.7 g citric acid, 4.0 g Na_2SO_4, 4.2 g $(NH_4)_2HPO_4$, and 5.0 g yeast extract in 900 mL of millipore water. The pH was adjusted to 6.8-6.9 using NaOH and the medium was autoclaved. Medium A salts (10X) were prepared by dissolving 7.62 g KCl, 4.18 g $MgCl_2$-6 H_2O, 0.543 g $MnCl_2$-4 H_2O, 0.49 g $FeCl_3$-6 H_2O, and 0.208 g $ZnCl_2$ in 1 L of millipore water followed by sterilization via 0.22 μm filtration. The Medium A cultures were grown at 37 °C for 28-48 h with vigorous agitation. A color change to pinkish-brown was observed and the pH of cultures had lowered to 6-6.5. Cultures were acidified to pH 2.5 with concentrated phosphoric acid and centrifuged to remove cells and insoluble material. Sublancin was isolated by ammonium sulfate precipitation. Briefly, a 500 mL volume of sublancin-containing culture supernatant was combined with 245 g $(NH_4)_2SO_4$ in a 1 L glass bottle to provide a 75% ammonium sulfate saturation at 4 °C. The precipitation mixture was stirred at 4 °C for 24 h and precipitated sublancin was isolated from the solution by centrifugation. The pelleted peptide was re-solubilized in 50/50 ACN/water with 0.1% TFA and was analyzed by MALDI-TOF MS. A 1

μL aliquot of sample was combined with 1 μL of matrix consisting of saturated α-cyano-4-hydroxy-cinnamic acid matrix in 50% ACN/50% water with 0.1% TFA, and the total volume was spotted onto a MALDI target and dried under ambient conditions prior to analysis. The sublancin containing product were combined, lyophilized to dryness, and stored under N_2 at −80 °C until purification by preparative HPLC.

Preparative HPLC was performed using a Waters Delta 600 instrument equipped with a Phenomenex Jupiter Proteo C12 column (10 μm, 90 Å, 250 mm x 15 mm) equilibrated in 2% B (solvent A = 0.1% TFA in water, solvent B = 0.0866% TFA in 80% ACN/20% water). Lyophilized sublancin material was resuspended in 2% B, filtered with a 0.45 μm filter and applied to the column. Sublancin was eluted by maintaining the mobile phase at 2% B for 1 min, followed by an increase to 100% B over 45 min with a flow rate of 10.0 mL/min. Under these conditions, sublancin eluted at 22.7 min. All fractions were analyzed by MALDI-TOF MS as described above. Fractions containing purified sublancin were lyophilized to dryness and stored under N_2 at −80 °C until further use. Typical yields were 9 mg sublancin per liter of processed Medium A culture.

3.4.4 Strain construction

Chromosomal DNA was prepared from *B. subtilis* 168 using a standard procedure as previously described.[40] Deletion mutants in *B. subtilis* 168 were created as described by Tanaka et al.[26] and oligonucleotides used are shown in Table S1 in the supplemental material. *B. subtilis* 168 was transformed using PCR products or chromosomal DNA following a standard procedure as previously described.[41]

Table 3.5 Oligonucleotides used in generation of *B. subtilis* deletion mutants.

yvkS-ykvWP1	ttctacacgaggcattacatt
yvkS-ykvWP2	CGACCTGCAGGCATGCAAGCTccctttttctttctattgacga
yvkS-ykvWP3	CGAGCTCGAATTCACTGGCCGTCGaggctgctggctttttat
yvkS-ykvWP4	cacatgggtttcttcatttt
ykvY-glcTP1	ctttgataaaaccggaactg
ykvY-glcTP2	CGACCTGCAGGCATGCAAGCTtgttcctccctgccattt
ykvY-glcTP3	CGAGCTCGAATTCACTGGCCGTCGattcagtttatccttataacgtg
ykvY-glcTP4	gtgtttgatgttttcctggt
ptsG-ptsIP1	ctacaaagaggcattggaag
ptsG-ptsIP2	CGACCTGCAGGCATGCAAGCTaagaattgacctcctcttttt
ptsG-ptsIP3	CGAGCTCGAATTCACTGGCCGTCGtaacatggctaggagggata
ptsG-ptsIP4	aggaaaaacgaccctgtg

Oligonucleotides used to generate deletion mutants described in Table 3.1. Capital letters indicate overlapping regions with phleomycin resistance cassette, lower case letters indicate regions complementary to *B. subtilis* genome.

3.4.5 Minimum inhibitory concentration (MIC) determination

MICs were determined by the broth dilution method.[42] Serial dilutions of sublancin were prepared in sterile deionized water (SDW). Forty-eight well microtiter plates (Corning Costar) were utilized for both *B. subtilis* ATCC 6633 and *Bacillus halodurans* C-125. The total volume of culture in each well was 300 µL; the experimental wells contained 30 µL of 10x stock sublancin at defined concentrations and 270 µL of a 1-in-10 dilution (approximately 1 x 10^8 colony-forming units (CFU) mL^{-1}) of a culture of indicator strain diluted in fresh LB growth medium. In addition, each plate contained several blanks (270 µL fresh growth medium and 30 µL SDW) and control wells (270 µL of untreated 1-in-10 diluted culture and 30 µL SDW). The optical density at 600 nm ($O.D._{600nm}$) was recorded at hourly intervals from 0 to 6 h with an additional measurement at 18 h using a BioTek Synergy 4H plate reader. Plates were incubated under vigorous agitation at 37 °C. The readings of triplicate experiments were averaged. Growth curves were developed using control (culture and SDW only) readings to ensure sufficient O.D.

changes for accurate inhibition assessment. Curve fits for MIC determination were produced by fitting the data with Origin8.5 software using a dose-response curve with the equation: y = A1 + (A2 – A1) / (1 +$10^{(Logx0-x)p}$), with *p* = variable Hill slope.

Table 3.6 Strains.

Strain	**Genotype**	**Reference**
168	Wild-type *B. subtilis* strain	Laboratory Collection
ΔSPβ	Wild-type *B. subtilis* 168 strain lacking the entire SPβ prophage	[13]
C-125	Wild-type *B. halodurans*	[43]
ATCC 6633	Wild-type *B. subtilis*	[44]
168 Deletion collection	Collection of *B. subtilis* mutants lacking large genomic regions	[26]
ΔSPβ::cat	Chloramphenicol selectable ΔSPβ prophage mutant of *B. subtilis*	[13]
Δ*yvkS-yvkW*	*B. subtilis* Δ*yvkS-yvkW*::phleo	This study
Δ*ykvY-glcT*	*B. subtilis* Δ*ykvY-glcT*::phleo	This study
Δ*ptsG-ptsI*	*B. subtilis* Δ*ptsG-ptsI*::phleo	This study
ΔSPβ-QB5435	*B. subtilis* Δ*pstG*::*cat*; QB5435 → SPβ	[28]
ΔSPβ-MZ303	*B. subtilis* Δ*ptsH*::*cat;* MZ303 → SPβ	[45]
ΔSPβ-GP864	*B. subtilis* Δ*ptsI*::*ermC*; GP864 → SPβ	[46]
ΔSPβ-QB5407	*B. subtilis* Δ*ccpA*::*spec*; QB5407 → SPβ	[47]
ΔSPβ-GP202	*B. subtilis* Δ*hprK*::*spec*; GP202 → SPβ	[48]
ΔSPβ::cm-GP506	*B. subtilis ptsH* H15A; SPβcm → GP506	[49]
ΔSPβ::cm-GP507	*B. subtilis ptsH* S46A; SPβcm → GP576	[50]

3.4.6 Sublancin killing kinetics against sensitive *Bacillus* species

Sensitive cultures were grown to mid log phase in LB medium as described above, transferred to 48-well microtiter plates (Corning Costar) and exposed to sublancin at 1x and 4xMIC. Immediately after the addition of sublancin, the $O.D._{600nm}$ was determined using a BioTek Synergy H4 plate reader. The cultures were incubated for 6 h and the $O.D._{600nm}$ was recorded every 30 min. To verify that cells were killed, CFU counting was performed by serial dilution and plating.

3.4.7 Sublancin sensitivity screen of a gene deletion collection of *B. subtilis*

Sublancin-induced growth inhibition assays were performed using the procedure described by Dorenbos et al.,[13] but with modification to enable the screening of large numbers of strains. Overnight cultures of *B. subtilis* mutants and background control strain were grown in 96-well microtiter plates in a plate shaker at 37 °C with shaking at 800 rpm. Bioassay dishes were prepared with LB agar without adding salt. The plates were thoroughly dried before being divided into 48 squares for inoculation. Cotton swabs were dipped into individual wells of the overnight culture before being spread on the appropriate square. Plates were allowed to dry, before spotting 2 µL of an overnight culture of the *B. subtilis* 168 wild-type strain in the centre of each inoculated square. Plates were incubated overnight and visual analysis was used to determine zones of inhibition that were smaller or larger than that of the background strain. Strains with altered zones of inhibition were checked a further three times to ensure the phenotype was reproducible.

3.4.8 Sublancin sensitivity assay in liquid medium

Overnight cultures of *B. subtilis* grown in LB were diluted 1:100 in the same medium and grown to $O.D._{600nm}$ 0.5. The bacteria were then diluted 1:20 in a 96-well microtiter plate before

growth was monitored in a Synergy4 Biotek plate reader every 10 min (37 °C, with shaking). When the bacteria reached $O.D._{600nm}$ 0.185 (equivalent to 0.5 for a 1 cm path length), sublancin was added at the desired concentration, before resuming the monitoring of growth. Sugars were added at the following final concentrations: glucose 0.3%, malate 0.4%, sucrose 0.3 %, fructose 0.3%, glycerol 0.3%, citrate 0.4%, galactose 0.4% and succinate 0.4%.

3.4.9 Membrane integrity assay [c]

B. subtilis was grown to $O.D._{600nm}$ 0.5, before purified sublancin was added at different concentrations (100 – 500 nM). As a positive control, nisin was added at 10 nM final concentration and a negative control sample contained no bacteriocin. Samples were taken at 30 and 90 min and prepared for LIVE/DEAD® BacLight™ analysis (Molecular Probes, Life Technologies).[51] Samples were monitored by flow cytometry using an Accuri C6. The percentages of cells with intact or reduced membrane integrity were calculated. In addition membrane potential was also measured using the membrane potential-sensitive dye, 3-3' diethyloxacarbocyanine iodide ($DiOC_2$, Molecular Probes/Invitrogen). *B. subtilis* ATCC 6633 and *B. halodurans* C-125 cultures (in triplicate) were grown to a density of 4×10^6 cells mL^{-1} and aliquots were transferred to tubes containing $DiOC_2$ (final concentration of 300 nM). Cells were incubated with the dye for 20 min at 30 °C under aeration conditions prior to the addition of either sublancin or nisin at 1 and 4xMIC. Following addition of peptides, cultures were incubated at room temperature with aeration for an additional 15 min prior to analysis. The membrane potential was assessed by measuring the *B. subtilis*-associated $DiOC_2$ fluorescence by flow cytometry (BD Biosciences LSR II flow cytometer) with excitation at 488 nm with an argon laser and measurement of emission through a band-pass filter at 530/30 nm. A minimum of 10,000 events were detected for each sample and the data was analyzed using the FCS

Express 3.00.0311 V Lite Stand-alone software. The data were plotted as the geometric mean of the fluorescence intensity (MFI).

3.4.10 Propidium iodide uptake [c]

Membrane integrity was also evaluated by measuring the uptake of propidium iodide (PI). *B. subtilis* ATCC 6633 and *B. halodurans* C-125 cultures were grown to a density of 4 x 10^6 cells mL^{-1} and then diluted with fresh LB medium to an $O.D._{600nm}$ of 0.1. Cells were transferred to tubes containing PI (final concentration 25 μM; Molecular Probes Inc., Leiden, NL), HEPES (1 mM), and sublancin (0, 0.2, 2.0, 20 μM) or nisin (0, 0.2, 2.0, 20 μM), incubated for 30 min at RT, and analyzed. Data acquisition was performed with a BD Biosciences LSR II flow cytometer, using excitation at 488 nm with an argon laser and measurement of emission through a band-pass filter at 695/40 nm. A minimum of 50,000 events was detected for each sample, and experiments were performed in triplicate. Data analysis to calculate the geometric mean fluorescence intensity (MFI) of gated cell populations was performed using FCS Express 3.00.0311 V Lite Stand-alone software.

3.4.11 Generation of stable sublancin resistant mutants and resistant mutant frequency determination

Genetically stable, sublancin resistant mutants were generated by growing the sublancin susceptible strains *B. halodurans* C-125 and *B. subtilis* ATCC 6633 in LB as described above (no additional sugars added) until an $O.D._{600nm}$ of 1.0 (mid log phase, 1 cm light path). The cultures were plated on agar plates containing 1x or 4x their respective sublancin MICs. Distinct colonies were observed by 24 h. Resistant colonies were picked, grown in LB and plated on LB plates containing sublancin at 4xMIC to confirm resistance. This procedure generated genetically

stable sublancin mutants. The number of resistant mutants that emerged from each sublancin susceptible culture was obtained by generating a serial dilution of each culture. Each dilution was plated on sublancin-containing plates. The total number of cells was determined by plating an appropriate (10^{-5}, 10^{-6}, 10^{-7}, 10^{-8}, 10^{-9}) dilution of the cultures on non-selective LB agar medium. Colonies from sublancin-containing and non-selective plates were counted after 24 h of incubation. The resistance frequency was determined as the mean number of resistant cells divided by the total number of viable cells per culture.

3.4.12 Single Nucleotide Polymorphism (SNP) detected by whole genome sequencing [d]

Genomic DNA (gDNA) of the wild-type *B. halodurans* C-125 and four different sublancin resistant isolates was extracted using an UltraClean® Microbial DNA isolation kit (MO BIO). The gDNAs thus obtained were sequenced using a HiSeq2000 Illumina sequencer, which generated close to 180 million single-reads per lane, for an overall coverage of 360x for the 5 MB genomes. All libraries were individually barcoded and constructed with the TruSeq Sample Prep kits (Illumina). The SNPs and the corresponding genes for resistant *B. halodurans* C-125 were identified. In addition, the wild-type *B. halodurans* C-125 strain was mapped to the published *B. halodurans* C-125 sequence (accession no. NC_002570.2) with CLC Genomics Workbench (CLC bio), using default parameters. A consensus sequence of the wild-type and reference genome was obtained and used for SNP detection in sublancin resistant mutants of *B. halodurans*.

3.4.13 PCR amplification and validation of *B. halodurans* resistant mutants single nucleotide polymorphisms

PCR validation can serve as an iterative and informative process to modify and optimize the SNP filtering criteria to improve SNP calling.[52] Primers flanking SNP-containing genes were synthesized and used for PCR amplification of the respective genes. The mutations reported herein were all confirmed by PCR (Table S2 in the supplemental material).

3.4.14 *B. halodurans* C-125 gene expression profile [e]

A culture of *B. halodurans* C-125 was grown in LB at 37 °C with vigorous shaking until mid log phase, at which point the culture was split into two 150 mL cultures with one subjected to a sub-inhibitory concentration of sublancin (0.5xMIC). RNA isolation was performed using the RNeasy mini kit (Qiagen) and subsequently treated with RNase-Free DNase (Qiagen). The RNA was dissolved in RNase-free water and quantified using a NanoDrop 2000c spectrophotometer (Thermo Scientific). For each sample (i.e. with and without sublancin), 20 μg of total RNA was isolated from three biological replicates. cDNA synthesis was performed using the SuperScript® Double-Stranded cDNA Synthesis Kit (Invitrogen) as per the manufacturer's instructions (NimbleGen Arrays User's Guide, Version 5.1) and quantified with NanoDrop. Total cDNA was labeled overnight with the One-Color DNA labeling kit (NimbleGen) as per the manufacturer's instructions. Arrays were scanned using an Axon 4000B array scanner.

A *B. halodurans* C-125 Nimblegen custom array, containing a probe set of 22 unique 45mer-60mer oligonucleotide probes for each of the 4066 genes of this bacterium, was used. NimbleScan software (v 2.6.0.0, Roche NimbleGen) was used to generate one normalized value per probe set using the RMA algorithm (background correction, normalization and summarization; data not logged). The data were then imported into R[53] using the limma

package[54] and log2-transformed. Statistical analysis for differential expression between the mutant and wild-type groups was performed, taking into account the correlation due to processing batch.[55,56] Raw p-values were corrected for multiple hypotheses testing using the False Discovery Rate method.[57] Annotation for the probe sets was primarily provided by Nimblegen and included BH ids (e.g., BH0001), gene names, descriptions, genomic locations and URL links to NCBI. Entrez Gene IDs and official gene symbols were downloaded from the *B. halodurans* genome record in NCBI (NC_002570). For analysis, we filtered to identify those genes that were altered by at least a 1.5-fold change in transcription (up-regulation and down-regulation). For data mining, we used DAVID bioinformatics resources that consist of an integrated biological knowledge base and analytic tools that use the results from the statistical analysis to explore and interpret gene regulation data.[58]

3.5 REFERENCES

(1) Arnison, P. G.; Bibb, M. J.; Bierbaum, G.; Bowers, A. A.; Bugni, T. S.; Bulaj, G.; Camarero, J. A.; Campopiano, D. J.; Challis, G. L.; Clardy, J.; Cotter, P. D.; Craik, D. J.; Dawson, M.; Dittmann, E.; Donadio, S.; Dorrestein, P. C.; Entian, K.-D.; Fischbach, M. A.; Garavelli, J. S.; Göransson, U.; Gruber, C. W.; Haft, D. H.; Hemscheidt, T. K.; Hertweck, C.; Hill, C.; Horswill, A. R.; Jaspars, M.; Kelly, W. L.; Klinman, J. P.; Kuipers, O. P.; Link, A. J.; Liu, W.; Marahiel, M. A.; Mitchell, D. A.; Moll, G. N.; Moore, B. S.; Müller, R.; Nair, S. K.; Nes, I. F.; Norris, G. E.; Olivera, B. M.; Onaka, H.; Patchett, M. L.; Piel, J.; Reaney, M. J. T.; Rebuffat, S.; Ross, R. P.; Sahl, H.-G.; Schmidt, E. W.; Selsted, M. E.; Severinov, K.; Shen, B.; Sivonen, K.; Smith, L.; Stein, T.; Süssmuth, R. E.; Tagg, J. R.; Tang, G. L.; Truman, A. W.; Vederas, J. C.; Walsh, C. T.; Walton, J. D.; Wenzel, S. C.; Willey, J. M.; van der Donk, W. A. *Nat Prod Rep* **2013**, *30*, 108. "Ribosomally Synthesized and Post-translationally Modified Peptide Natural Products: Overview and Recommendations for a Universal Nomenclature".

(2) Breukink, E.; Wiedemann, I.; van Kraaij, C.; Kuipers, O. P.; Sahl, H. G.; de Kruijff, B. *Science* **1999**, *286*, 2361. "Use of the cell wall precursor lipid II by a pore-forming peptide antibiotic".

(3) Schneider, T.; Sahl, H. G. *Curr Opin Investig Drugs* **2010**, *11*, 157. "Lipid II and other bactoprenol-bound cell wall precursors as drug targets".

(4) Breukink, E.; de Kruijff, B. *Nat Rev Drug Discov* **2006**, *5*, 321. "Lipid II as a target for antibiotics".

(5) Islam, M. R.; Nagao, J.; Zendo, T.; Sonomoto, K. *Biochem Soc Trans* **2012**, *40*, 1528. "Antimicrobial mechanism of lantibiotics".

(6) Diep, D. B.; Skaugen, M.; Salehian, Z.; Holo, H.; Nes, I. F. *Proc Natl Acad Sci U S A* **2007**, *104*, 2384. "Common mechanisms of target cell recognition and immunity for class II bacteriocins".

(7) Swe, P. M.; Cook, G. M.; Tagg, J. R.; Jack, R. W. *J Antimicrob Chemother* **2009**, *63*, 679. "Mode of action of dysgalacticin: a large heat-labile bacteriocin".

(8) Metlitskaya, A.; Kazakov, T.; Kommer, A.; Pavlova, O.; Praetorius-Ibba, M.; Ibba, M.; Krasheninnikov, I.; Kolb, V.; Khmel, I.; Severinov, K. *J Biol Chem* **2006**, *281*, 18033. "Aspartyl-tRNA synthetase is the target of peptide nucleotide antibiotic Microcin C".

(9) Nolan, E. M.; Walsh, C. T. *Biochemistry* **2008**, *47*, 9289. "Investigations of the MceIJ-catalyzed posttranslational modification of the microcin E492 C-terminus: linkage of ribosomal and nonribosomal peptides to form "trojan horse" antibiotics".

(10) Grinter, R.; Milner, J.; Walker, D. *PLoS One* **2012**, *7*, e33033. "Ferredoxin containing bacteriocins suggest a novel mechanism of iron uptake in Pectobacterium spp".

(11) Garneau, S.; Martin, N. I.; Vederas, J. C. *Biochimie* **2002**, *84*, 577. "Two-peptide bacteriocins produced by lactic acid bacteria".

(12) Wang, Q.; Zeng, X.; Wang, S.; Hou, C.; Yang, F.; Ma, X.; Thacker, P.; Qiao, S. *Anat Rec (Hoboken)* **2014**, *297*, 1454. "The bacteriocin sublancin attenuates intestinal injury in young mice infected with Staphylococcus aureus".

(13) Dorenbos, R.; Stein, T.; Kabel, J.; Bruand, C.; Bolhuis, A.; Bron, S.; Quax, W. J.; Van Dijl, J. M. *J Biol Chem* **2002**, *277*, 16682. "Thiol-disulfide oxidoreductases are essential for the production of the lantibiotic sublancin 168".

(14) Oman, T. J.; Boettcher, J. M.; Wang, H.; Okalibe, X. N.; van der Donk, W. A. *Nat Chem Biol* **2011**, *7*, 78. "Sublancin is not a lantibiotic but an S-linked glycopeptide".

(15) Dubois, J. Y.; Kouwen, T. R.; Schurich, A. K.; Reis, C. R.; Ensing, H. T.; Trip, E. N.; Zweers, J. C.; van Dijl, J. M. *Antimicrob Agents Chemother* **2009**, *53*, 651. "Immunity to the bacteriocin sublancin 168 Is determined by the SunI (YolF) protein of Bacillus subtilis".

(16) Kouwen, T. R.; Trip, E. N.; Denham, E. L.; Sibbald, M. J.; Dubois, J. Y.; van Dijl, J. M. *Antimicrob Agents Chemother* **2009**, *53*, 4702. "The large mechanosensitive channel MscL determines bacterial susceptibility to the bacteriocin sublancin 168".

(17) Iscla, I.; Wray, R.; Wei, S.; Posner, B.; Blount, P. *Nat Commun* **2014**, *5*, 4891. "Streptomycin potency is dependent on MscL channel expression".

(18) Butcher, B. G.; Helmann, J. D. *Mol Microbiol* **2006**, *60*, 765. "Identification of Bacillus subtilis sigma-dependent genes that provide intrinsic resistance to antimicrobial compounds produced by Bacilli".

(19) Dempwolff, F.; Möller, H. M.; Graumann, P. L. *J Bacteriol* **2012**, *194*, 4652. "Synthetic motility and cell shape defects associated with deletions of flotillin/reggie paralogs in Bacillus subtilis and interplay of these proteins with NfeD proteins".

(20) Andrews, J. M. *J Antimicrob Chemother* **2001**, *48 Suppl 1*, 5. "Determination of minimum inhibitory concentrations".

(21) Clinical and Laboratory Standards Institute/NCCLS; 7th ed. 2006; Vol. 26.

(22) Cotroneo, N.; Harris, R.; Perlmutter, N.; Beveridge, T.; Silverman, J. A. *Antimicrob Agents Chemother* **2008**, *52*, 2223. "Daptomycin exerts bactericidal activity without lysis of Staphylococcus aureus".

(23) McDowell, T. D.; Lemanski, C. L. *J Bacteriol* **1988**, *170*, 1783. "Absence of autolytic activity (peptidoglycan nicking) in penicillin-induced nonlytic death in a group A streptococcus".

(24) van Belkum, M. J.; Kok, J.; Venema, G.; Holo, H.; Nes, I. F.; Konings, W. N.; Abee, T. *J Bacteriol* **1991**, *173*, 7934. "The bacteriocin lactococcin A specifically increases permeability of lactococcal cytoplasmic membranes in a voltage-independent, protein-mediated manner".

(25) Davies, J.; Davies, D. *Microbiol Mol Biol Rev* **2010**, *74*, 417. "Origins and evolution of antibiotic resistance".

(26) Tanaka, K.; Henry, C. S.; Zinner, J. F.; Jolivet, E.; Cohoon, M. P.; Xia, F.; Bidnenko, V.; Ehrlich, S. D.; Stevens, R. L.; Noirot, P. *Nucleic Acids Res* **2013**, *41*, 687. "Building the repertoire of dispensable chromosome regions in Bacillus subtilis entails major refinement of cognate large-scale metabolic model".

(27) Westers, H.; Dorenbos, R.; van Dijl, J. M.; Kabel, J.; Flanagan, T.; Devine, K. M.; Jude, F.; Seror, S. J.; Beekman, A. C.; Darmon, E.; Eschevins, C.; de Jong, A.; Bron, S.; Kuipers, O. P.; Albertini, A. M.; Antelmann, H.; Hecker, M.; Zamboni, N.; Sauer, U.; Bruand, C.; Ehrlich, D. S.; Alonso, J. C.; Salas, M.; Quax, W. J. *Mol Biol Evol* **2003**, *20*, 2076. "Genome engineering reveals large dispensable regions in Bacillus subtilis".

(28) Stülke, J.; Martin-Verstraete, I.; Zagorec, M.; Rose, M.; Klier, A.; Rapoport, G. *Mol Microbiol* **1997**, *25*, 65. "Induction of the Bacillus subtilis ptsGHI operon by glucose is controlled by a novel antiterminator, GlcT".

(29) Gonzy-Treboul, G.; de Waard, J. H.; Zagorec, M.; Postma, P. W. *Mol Microbiol* **1991**, *5*, 1241. "The glucose permease of the phosphotransferase system of Bacillus subtilis: evidence for IIGlc and IIIGlc domains".

(30) Deutscher, J.; Francke, C.; Postma, P. W. *Microbiol Mol Biol Rev* **2006**, *70*, 939. "How phosphotransferase system-related protein phosphorylation regulates carbohydrate metabolism in bacteria".

(31) Reizer, J.; Bachem, S.; Reizer, A.; Arnaud, M.; Saier, M. H., Jr.; Stülke, J. *Microbiology* **1999**, *145 (Pt 12)*, 3419. "Novel phosphotransferase system genes revealed by genome analysis - the complete complement of PTS proteins encoded within the genome of Bacillus subtilis".

(32) Darbon, E.; Galinier, A.; Le Coq, D.; Deutscher, J. *J Mol Microbiol Biotechnol* **2001**, *3*, 439. "Phosphotransfer functions mutated Bacillus subtilis HPr-like protein Crh carrying a histidine in the active site".

(33) Meyer, F. M.; Jules, M.; Mehne, F. M.; Le Coq, D.; Landmann, J. J.; Görke, B.; Aymerich, S.; Stülke, J. *J Bacteriol* **2011**, *193*, 6939. "Malate-mediated carbon catabolite repression in Bacillus subtilis involves the HPrK/CcpA pathway".

(34) Stepper, J.; Shastri, S.; Loo, T. S.; Preston, J. C.; Novak, P.; Man, P.; Moore, C. H.; Havlicek, V.; Patchett, M. L.; Norris, G. E. *FEBS Lett* **2011**, *585*, 645. "Cysteine S-glycosylation, a new post-translational modification found in glycopeptide bacteriocins".

(35) Kjos, M.; Nes, I. F.; Diep, D. B. *Appl Environ Microbiol* **2011**, *77*, 3335. "Mechanisms of resistance to bacteriocins targeting the mannose phosphotransferase system".

(36) Gabrielsen, C.; Brede, D. A.; Hernandez, P. E.; Nes, I. F.; Diep, D. B. *Antimicrob Agents Chemother* **2012**, *56*, 2908. "The maltose ABC transporter in Lactococcus lactis facilitates high-level sensitivity to the circular bacteriocin garvicin ML".

(37) Garcia De Gonzalo, C. V.; Zhu, L.; Oman, T. J.; van der Donk, W. A. *ACS Chem Biol* **2014**, *9*, 796. "NMR structure of the S-linked glycopeptide sublancin 168".

(38) Venugopal, H.; Edwards, P. J.; Schwalbe, M.; Claridge, J. K.; Libich, D. S.; Stepper, J.; Loo, T.; Patchett, M. L.; Norris, G. E.; Pascal, S. M. *Biochemistry* **2011**, *50*, 2748. "Structural, dynamic, and chemical characterization of a novel S-glycosylated bacteriocin".

(39) Buescher, J. M.; Liebermeister, W.; Jules, M.; Uhr, M.; Muntel, J.; Botella, E.; Hessling, B.; Kleijn, R. J.; Le Chat, L.; Lecointe, F.; Mäder, U.; Nicolas, P.; Piersma, S.;

Rugheimer, F.; Becher, D.; Bessières, P.; Bidnenko, E.; Denham, E. L.; Dervyn, E.; Devine, K. M.; Doherty, G.; Drulhe, S.; Felicori, L.; Fogg, M. J.; Goelzer, A.; Hansen, A.; Harwood, C. R.; Hecker, M.; Hübner, S.; Hultschig, C.; Jarmer, H.; Klipp, E.; Leduc, A.; Lewis, P.; Molina, F.; Noirot, P.; Peres, S.; Pigeonneau, N.; Pohl, S.; Rasmussen, S.; Rinn, B.; Schaffer, M.; Schnidder, J.; Schwikowski, B.; Van Dijl, J. M.; Veiga, P.; Walsh, S.; Wilkinson, A. J.; Stelling, J.; Aymerich, S.; Sauer, U. *Science* **2012**, *335*, 1099. "Global network reorganization during dynamic adaptations of Bacillus subtilis metabolism".

(40) Bron, S.; Venema, G. *Mutation research* **1972**, *15*, 1. "Ultraviolet inactivation and excision-repair in Bacillus subtilis. I. Construction and characterization of a transformable eightfold auxotrophic strain and two ultraviolet-sensitive derivatives".

(41) Anagnostopoulos, C.; Spizizen, J. *J. Bacteriol.* **1961**, *81*, 741. " Requirements for transformation in *Bacillus subtilis*".

(42) Wiegand, I.; Hilpert, K.; Hancock, R. E. *Nat Protoc* **2008**, *3*, 163. "Agar and broth dilution methods to determine the minimal inhibitory concentration (MIC) of antimicrobial substances".

(43) Takami, H.; Nakasone, K.; Takaki, Y.; Maeno, G.; Sasaki, R.; Masui, N.; Fuji, F.; Hirama, C.; Nakamura, Y.; Ogasawara, N.; Kuhara, S.; Horikoshi, K. *Nucleic Acids Res* **2000**, *28*, 4317. "Complete genome sequence of the alkaliphilic bacterium Bacillus halodurans and genomic sequence comparison with Bacillus subtilis".

(44) Nishio, C.; Komura, S.; Kurahashi, K. *Biochem Biophys Res Commun* **1983**, *116*, 751. "Peptide antibiotic subtilin is synthesized via precursor proteins".

(45) Arnaud, M.; Vary, P.; Zagorec, M.; Klier, A.; Débarbouillé, M.; Postma, P.; Rapoport, G. *J Bacteriol* **1992**, *174*, 3161. "Regulation of the sacPA operon of Bacillus subtilis: identification of phosphotransferase system components involved in SacT activity".

(46) Singh, K. D.; Schmalisch, M. H.; Stülke, J.; Görke, B. *J Bacteriol* **2008**, *190*, 7275. "Carbon catabolite repression in Bacillus subtilis: quantitative analysis of repression exerted by different carbon sources".

(47) Faires, N.; Tobisch, S.; Bachem, S.; Martin-Verstraete, I.; Hecker, M.; Stülke, J. *J Mol Microbiol Biotechnol* **1999**, *1*, 141. "The catabolite control protein CcpA controls ammonium assimilation in Bacillus subtilis".

(48) Hanson, K. G.; Steinhauer, K.; Reizer, J.; Hillen, W.; Stülke, J. *Microbiology* **2002**, *148*, 1805. "HPr kinase/phosphatase of Bacillus subtilis: expression of the gene and effects of mutations on enzyme activity, growth and carbon catabolite repression".

(49) Reizer, J.; Bergstedt, U.; Galinier, A.; Küster, E.; Saier, M. H., Jr.; Hillen, W.; Steinmetz, M.; Deutscher, J. *J Bacteriol* **1996**, *178*, 5480. "Catabolite repression resistance of gnt

operon expression in Bacillus subtilis conferred by mutation of His-15, the site of phosphoenolpyruvate-dependent phosphorylation of the phosphocarrier protein HPr".

(50) Deutscher, J.; Reizer, J.; Fischer, C.; Galinier, A.; Saier, M. H., Jr.; Steinmetz, M. *J Bacteriol* **1994**, *176*, 3336. "Loss of protein kinase-catalyzed phosphorylation of HPr, a phosphocarrier protein of the phosphotransferase system, by mutation of the ptsH gene confers catabolite repression resistance to several catabolic genes of Bacillus subtilis".

(51) Goosens, V. J.; Mars, R. A.; Akeroyd, M.; Vente, A.; Dreisbach, A.; Denham, E. L.; Kouwen, T. R.; van Rij, T.; Olsthoorn, M.; van Dijl, J. M. *Antioxid Redox Signal* **2013**, *18*, 1159. "Is proteomics a reliable tool to probe the oxidative folding of bacterial membrane proteins?".

(52) Minoche, A. E.; Dohm, J. C.; Himmelbauer, H. *Genome Biol* **2011**, *12*, R112. "Evaluation of genomic high-throughput sequencing data generated on Illumina HiSeq and genome analyzer systems".

(53) R Development Core Team; R Foundation for Statistical Computing: 2010.

(54) Smyth, G. K. In *Bioinformatics and Computational Biology Solutions using R and Bioconductor*; Gentleman, R., Carey, V. J., Huber, W., Irizarry, R. A., Dudoit, S., Eds.; Springer New York, 2005, p 397.

(55) Smyth, G. K. *Statistical Applications in Genetics and Molecular Biology* **2004**, *3*, 1. "Linear Models and Empirical Bayes Methods for Assessing Differential Expression in Microarray Experiments".

(56) Smyth, G. K.; Michaud, J.; Scott, H. S. *Bioinformatics* **2005**, *21*, 2067. "Use of within-array replicate spots for assessing differential expression in microarray experiments".

(57) Yoav, B.; Yosef, H. *J R Stat Soc Series B* **1995**, *57*, 289. "Controlling the False Discovery Rate: A Practical and Powerful Approach to Multiple Testing".

(58) Huang da, W.; Sherman, B. T.; Lempicki, R. A. *Nat Protoc* **2009**, *4*, 44. "Systematic and integrative analysis of large gene lists using DAVID bioinformatics resources".

CHAPTER 4. DELINEATING THE ROLE OF GLYCOSYLATION ON SUBLANCIN'S BIOLOGICAL ACTIVITY

4.1 INTRODUCTION

Some of the unique properties of sublancin as an antimicrobial have been defined in chapter 3. Sublancin is bactericidal, it does not compromise the integrity of the cell membrane, and multiple lines of evidence have determined that the phosphotransferase system is involved in the sensitivity to sublancin. This chapter describes the importance of the sugar moiety for antimicrobial activity in addition to other studies designed to provide further insights into sublancin's mode of action.

4.2 RESULTS AND DISCUSSION

4.2.1 Cross-resistance determination

In an effort to understand sublancin's mode of action, chapter 3 described the generation of sublancin-resistant *B. halodurans* C-125 mutant strains. Susceptibility assessments of sublancin-resistant *B. halodurans* C-125 strains with commercially available antimicrobials allowed for the comparison of sublancin's antibacterial activity in order to determine whether patterns of cross-resistance occurred. Even though cross-resistance is undesirable in a clinical setting it can help in the identification of sublancin's target since compounds with similar binding sites are expected to exhibit similar resistance profiles.[1,2] The antibacterial activity of sublancin and commercially available antimicrobial agents against *B. halodurans* C-125 and sublancin-resistant *B. halodurans* C-125 strains was determined by the MIC broth dilution method.[3,4] A series of dilutions of sublancin (0.097 μM – 100 μM) were made and incubated with a defined number of bacterial cells in LB medium. Plates were incubated for 18-24 h at 37

°C, and growth was assessed by measuring the optical density of each well at $O.D._{600nm}$. The MICs were determined by fitting the data to a dose-response curve. The MICs of sublancin and commercially available antimicrobials against *B. halodurans* C-125 and sublancin-resistant *B. halodurans* C-125 are shown in Table 4.1. There was no cross-resistance observed given that the MIC values of common antibiotics for sensitive *B. halodurans* C-125 strains were comparable to those for the sublancin-resistant *B. halodurans* C-125 mutant strains. The lack of cross resistance indicates that sublancin is not likely to exert its antimicrobial action by inhibiting protein synthesis, DNA replication or cell wall biosynthesis in a manner similar to the compounds tested.

Table 4.1 Cross-resistance susceptibility of sublancin-resistant B. halodurans C-125 strains.

Mode of Action Target		?	Protein synthesis				DNA replication		Cell wall biosynthesis			
		Sublancin	Tetracycline	Fusidic Acid	Kanamycin	Linezolid	Ciprofloxacin	Ofloxacin	Nisin	Daptomycin	Vancomycin	Ampicillin
Bacterial Strain	*B. halodurans* C-125	0.312	0.391	0.391	25	3.12	0.781	6.25	0.098	1.56	0.391	0.781
	Sublancin-resistant B. halodurans C-125 001	> 100	0.190	1.56	25	1.56	0.391	6.25	0.098	0.312	0.391	0.781
	Sublancin-resistant B. halodurans C-125 002	> 100	0.391	0.391	25	3.12	0.391	6.25	0.098	1.56	0.391	0.781
	Sublancin-resistant B. halodurans C-125 003	> 100	0.024	0.024	50	1.56	0.190	12.5	0.049	1.56	0.391	0.781
	Sublancin-resistant B. halodurans C-125 004	> 100	0.024	0.024	25	1.56	0.190	12.5	0.049	1.56	0.391	0.781

The MIC of sublancin and commercially available antimicrobial agents was determined using the MIC broth dilution method against *B. halodurans* C-125 and sublancin-resistant *B. halodurans* C125. Shown are the MICs in μM. There was no cross-resistance observed given that the MIC values determined for sensitive *B. halodurans* C-125 strains were comparable to those for the sublancin-resistant *B. halodurans* C-125 mutant strains.

4.2.2 Sublancin post-antimicrobial effect (PAE)

An important parameter is the post-antimicrobial effect (PAE) that describes the persistent suppression of cells regrowth following exposure and later removal of the antimicrobial compound. Growth inhibition activity can occur reversibly or irreversibly. Irreversible growth inhibition can occur if the antimicrobial strongly binds to its target or alters it in a way that makes it detrimental for cell growth (i.e. it is toxic). On the other hand, reversible activity happens when the antimicrobial binds weakly and can be washed off allowing the cells to recover from its effects. We wondered whether sublancin's growth inhibition was reversible. To answer this question, an overnight culture of *B. subtilis* ATCC 6633 was grown to exponential phase and divided into three sets of three samples (Figure 4.1): untreated, treated with 1 time the sublancin MIC (1xMIC), and 4 times the sublancin MIC (4xMIC). Cultures were incubated for 2 h, optical density was measured, and cells were then pelleted. Cell pellets were resuspended in the same media (set 1) or in fresh media with (set 2) or without (set 3) sublancin. Growth was assessed at 6 h and 18 h. At 6 h, sublancin continued to show growth inhibitory activity, but at 18 h cells were growing. There are a number of explanations for the observed increase in bacterial growth. Sublancin may be degraded following target binding and cell death, and cells that survive initial sublancin exposure continue to grow. Alternatively, resistant mutants may be present, or an enzyme could be secreted that deactivates sublancin (e.g. a protease or glycosidase). We further tested whether the growth observed at 18 h was due to resistance. Cells at the 18 h time point were washed and re-exposed to fresh sublancin (i.e., untreated, 1xMIC, and 4xMIC). Optical density measurements were taken at 2, 6, and 18 h from the time fresh sublancin was added. It was observed that the cells in all three samples continued to grow, thus suggesting that the cells may have acquired resistance.

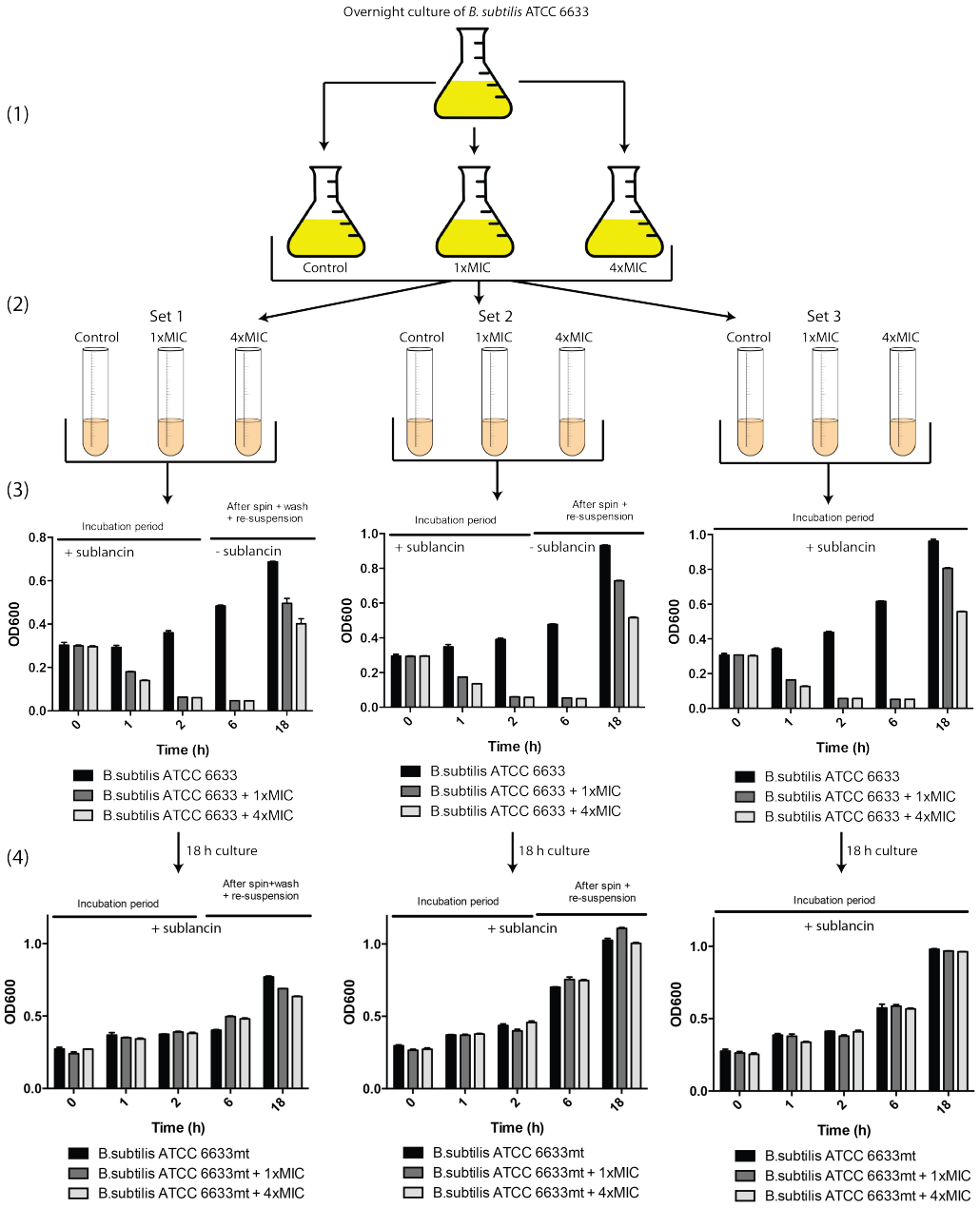

Figure 4.1 Sublancin post-antimicrobial effect.

(1) An overnight culture of *B. subtilis* ATCC 6633 was grown to exponential phase and divided into three sets of three samples (Figure 4.1): untreated, 1 time the sublancin MIC (1xMIC), and 4 times the sublancin MIC (4xMIC). (2) Cultures were incubated for 2 h, optical density was measured, and cells were then pelleted. (3) Cell pellets were resuspended in the same media (set 1) or in fresh media with (set 2) or without (set 3) sublancin. Growth was assessed at 6 h and 18 h. At 6 h, sublancin continued to show growth inhibitory activity, but at 18 h, cells were growing. (4) Cells at the 18 h time point were washed and re-exposed to fresh sublancin (i.e., untreated, 1xMIC, and 4xMIC). Optical density measurements were taken at 2, 6, and 18 h from the time fresh sublancin was added. It was observed that the cells continued to grow, thus suggesting that the cells may have acquired resistance.

4.2.3 Sublancin-resistant *Bacillus* mutants present after an 18 h incubation

To establish whether *B. subtilis* growth at the 18 h time point was due to resistance, an overnight culture of *B. subtilis* ATCC 6633 was grown to exponential phase and split into three aliquots (Figure 4.2): (1) untreated *B. subtilis* ATCC 6633 cells, (2) cells grown at 1xMIC of sublancin, and (3) cells grown at 4xMIC of sublancin. After the 18 h incubation period, an aliquot of each sample was plated on 4xMIC sublancin plates or LB plates without sublancin. Greater than 90% resistance was observed in plates from aliquots obtained from samples incubated with sublancin and close to 0.001% resistance was observed in the control plates (i.e. cells that were not previously treated with sublancin). Consequently, the growth observed at 18 h in the experiments described above could be attributed to the relatively rapid emergence of resistance.

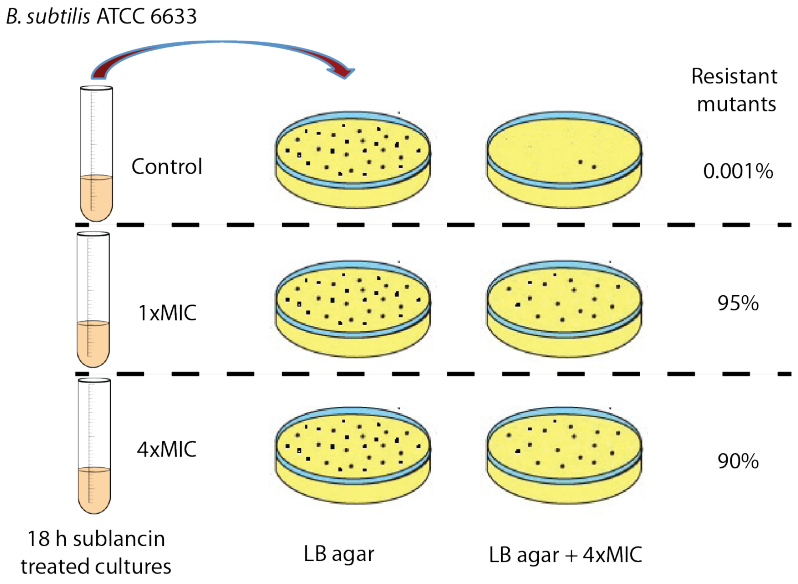

Figure 4.2 Percentage of sublancin-resistant *Bacillus* mutants after an 18 h incubation.
An overnight culture of *B. subtilis* ATCC 6633 was grown to exponential phase and split into three aliquots (Figure 4.2): (1) untreated *B. subtilis* ATCC 6633 cells, (2) cells grown at 1xMIC of sublancin, and (3) cells grown at 4xMIC of sublancin. After the 18 h incubation period, an aliquot of each sample was plated on 4xMIC sublancin plates or LB plates without sublancin.

4.2.4 Solid agar diffusion bioactivity assay of *Bacillus* cells incubated with sublancin for 18 h

We suspected that sublancin degradation could be an additional plausible explanation for the increase in viable cells observed at 18 h. Degradation could be caused by the presence of a secreted peptidase or glycosidase. We first addressed the question of degradation by analytical HPLC. We investigated whether sublancin could be observed in the supernatant of sublancin-exposed cells (both sensitive or resistant) after incubating for 18 h. Unfortunately the complex media mixture produced after 18 h hindered the clean observation of sublancin or its degradation products.

Due to the inability to detect whether sublancin was present at the 18 h incubation period, we decided to address the issue of degradation via a solid agar diffusion assay. *B. subtilis* ATCC 6633 sensitive cells and sublancin-resistant *B. subtilis* ATCC 6633 cells were treated with sublancin for 18 h. The cells were centrifuged and the supernatant spotted on a bioassay plate containing sensitive *B. subtilis* ATCC 6633. We observed that supernatant from sublancin-sensitive and sublancin-resistant *B. subtilis* ATCC 6633 cultures did not inhibit growth. The previously pelleted cells were then re-suspended in fresh media with fresh sublancin for an additional hour, the cells were centrifuged and the supernatant from the re-exposed (sublancin-sensitive and sublancin-resistant *B. subtilis* ATCC 6633) cultures was plated. Even though fresh sublancin was added, these samples produced partial zones of inhibition, suggestive of sublancin being degraded. It is important to note that the concentration of sublancin used was 4xMIC rather than 1xMIC which may explain the partial inhibition zones after the additional hour of exposure to sublancin (i.e. at 4xMIC it is more difficult for the cells to degrade all sublancin when

compared to incubation at 1xMIC). The data suggest that sublancin may be degraded by the resistant strains thus offering a potential explanation to the growth observed at 18 h of incubation with sublancin. However, since spent medium of sensitive *B. subtilis* ATCC 6633 also resulted in a decrease in the zone of growth inhibition, it appears that sublancin is inherently unstable under these conditions.

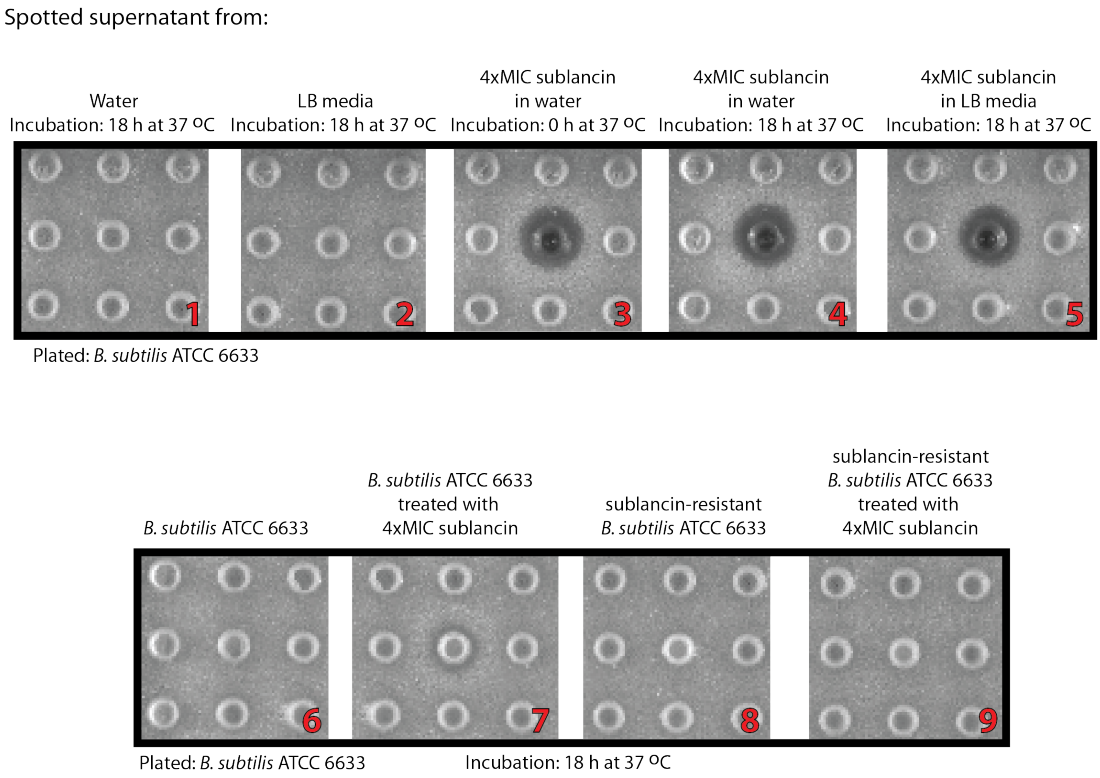

Figure 4.3 Solid agar diffusion bioactivity assay of 18 h sublancin incubated *Bacillus* cells.

B. subtilis ATCC 6633 sensitive cells and *B. subtilis* ATCC 6633 resistant cells were grown in LB media and treated with sublancin for 18 h at 37 °C. The cells were centrifuged and 10 µL of supernatant was spotted on a bioassay plate containing sensitive *B. subtilis* ATCC 6633. For each numbered panel the following samples were spotted: (1) Water (2) LB media (3) 4xMIC sublancin in water (4) 4xMIC sublancin incubated in water for 18 h. (5) Supernatant from 4xMIC sublancin incubated in LB media for 18 h. (6) Supernatant from *B. subtilis* ATCC 6633, no sublancin added. (7) Supernatant from *B. subtilis* ATCC 6633 treated with 4xMIC sublancin. (8) Supernatant from sublancin-resistant *B. subtilis* ATCC 6633, no sublancin added. (9) Supernatant from sublancin-resistant *B. subtilis* ATCC 6633 treated with 4xMIC sublancin. We observed that supernatant from sublancin-sensitive and sublancin-resistant *B. subtilis* ATCC 6633 cultures treated with 4xMIC sublancin did not significantly inhibit growth. The previously pelleted cells were then re-suspended in fresh media with fresh sublancin for an additional hour, the cells were centrifuged and the supernatant plated on the bioassay plate.

4.2.5 Importance of glycosylation in the activity of sublancin

The generation of structural analogs of antibiotics allows for a deeper understanding of potential regions that may be important for an antibiotic's activity. Oman et al. reported that the acid hydrolysis of the glucose moiety from sublancin abolished sublancin's activity.[5] It was hypothesized that without glycosylation, the correct disulfide bridges are not formed given that the free thiol would cause the rearrangement of the disulfide bonds by thiol-disulfide exchange. However, from the NMR structure of sublancin shown in chapter 2 it appears very unlikely that there would be thiol-disulfide exchange due to the compact and well defined structure of sublancin.[6] Further investigation by Dr. Huan Wang, a former postdoctoral student in the van der Donk lab, suggested that the S-glycosylation of sublancin by its S-glycosyltransferase (SunS) might be important for the self-resistance *of B. subtilis* 168 against sublancin 168. Dr. Wang reconstituted unglycosylated sublancin-C22S *in vitro* and showed that the sublancin-C22S analog was active against *B. subtilis* ATCC 6633 and sublancin's producer, *B. subtilis* 168. In contrast, Stepper et al. showed that in the case of glycocin F, de-O-GlcNac-glycocin F was inactive showing that the O-linked GlcNac moiety is essential for glycocin F activity.[7] Intrigued by the conflicting findings of whether or not the sugar installed on sublancin was in fact required for activity, we decided to make additional unglycosylated sublancin analogs, and if active, test whether the mechanism of action of these analogs was similar to that of wild type sublancin.

4.2.5.1 Heterologous expression of sublancin-C22S, C22N and C22T in *E. coli*

We generated sublancin-C22S, C22N, and C22T by heterologous expression of the corresponding SunA-C22X mutant in *E. coli* followed by *in vitro* modifications. The SunA-C22X precursor was cloned with a factor Xa cleavage site between the leader and core peptide sequence and as an N-terminal fusion protein with a hexa-histidine tag (His_6-SunAXa-C22X).

Upon purification by immobilized metal affinity chromatography and desalting by solid phase extraction (SPE), His_6-SunAXa-C22X was folded in the presence of oxidized glutathione and reduced glutathione. The leader peptide of folded His_6-SunAXa-C22X was then cleaved with factor Xa to afford the desired analogs.[5] The extent of the modifications and oxidative folding was verified by MALDI-TOF MS (Figures 4.4, 4.5 and 4.6).

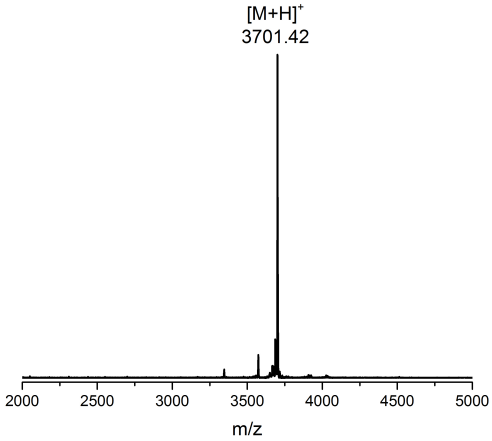

Figure 4.4 MALDI-TOF MS analysis of sublancin-C22S.

Sublancin-C22S was obtained by heterologous expression of His_6-SunAXa-C22S in *E. coli* followed by *in vitro* oxidative folding and leader peptide removal. The reaction was analyzed by MALDI-TOF MS. Expected $[M+H]^+$: 3701.19, observed: 3701.42.

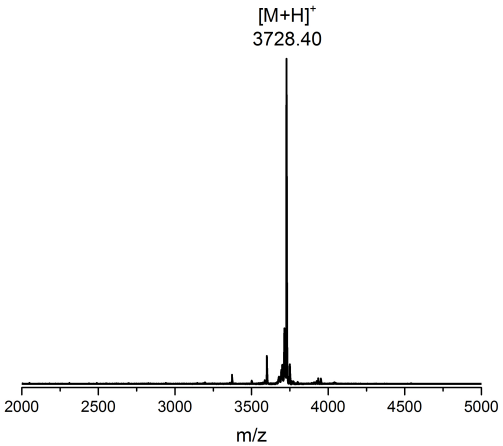

Figure 4.5 MALDI-TOF MS analysis of sublancin-C22N.

Sublancin-C22N was obtained by heterologous expression of His_6-SunAXa-C22N in *E. coli* followed by *in vitro* oxidative folding and leader peptide removal. The reaction was analyzed by MALDI-TOF MS. Expected $[M+H]^+$: 3728.21, observed: 3728.40.

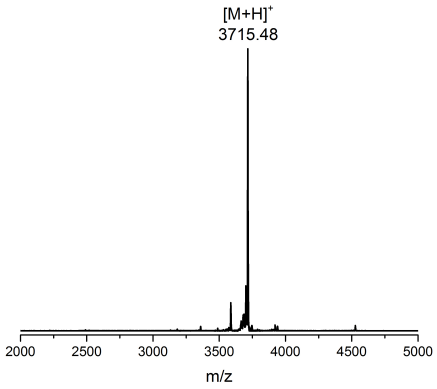

Figure 4.6 MALDI-TOF MS analysis of sublancin-C22T.

Sublancin-C22T was obtained by heterologous expression of His_6-SunAXa-C22T in *E. coli* followed by *in vitro* oxidative folding and leader peptide removal. The reaction was analyzed by MALDI-TOF MS. Expected $[M+H]^+$: 3715.21, observed: 3715.48.

4.2.5.2 Synthesis of sublancin C22S

Sublancin C22S, C22N, and C22T were originally obtained by heterologous expression of the corresponding SunA mutants in *E.coli*. Due to the low yield observed by overexpression, a synthetic route was identified as a more feasible method of obtaining larger amounts of such analogues. Wild type sublancin has been previously synthesized by native chemical ligation (NCL).[8] Sublancin C22S was synthesized following the previously published methodology with a few modifications (Figure 4.7). Sublancin C22S was first synthesized in two fragments by microwave assisted solid phase peptide synthesis (SPPS). The N-terminal fragment contained amino acids 1-13 (Figure 4.8) and the C-terminal fragment contained amino acids 14-37 (Figure 4.9).[8] After preparation of the fragments by microwave assisted SPPS the thioesterification (treatment with ethyl-3-mercaptopriopionate, N,N'-diisopropylcarbodiimide (DIC), 1-hydroxybenzotriazole (HOBt), and N,N-diisopropylethylamine (DIPEA) as base) was performed manually to the N-terminal fragment. Both fragments were cleaved from resin and purified by HPLC. The identity of the purified fragments was confirmed by MALDI-TOF MS. Linear sublancin C22S was obtained by native chemical ligation (Figure 4.10). The thioester N-terminal

fragment was reacted with the C-terminal fragment in the presence of mercaptophenylacetic acid (MPAA) and tris(2-carboxyethylphosphine (TCEP) in 6 M guanidine hydrochloride/ 0.2 M Na_2HPO_4 buffer at pH 7.2 followed by HPLC purification. The disulfide bridges were formed by oxidative folding by addition of oxidized glutathione, and reduced glutathione.[5] The extent of oxidative folding was verified by MALDI-TOF MS.

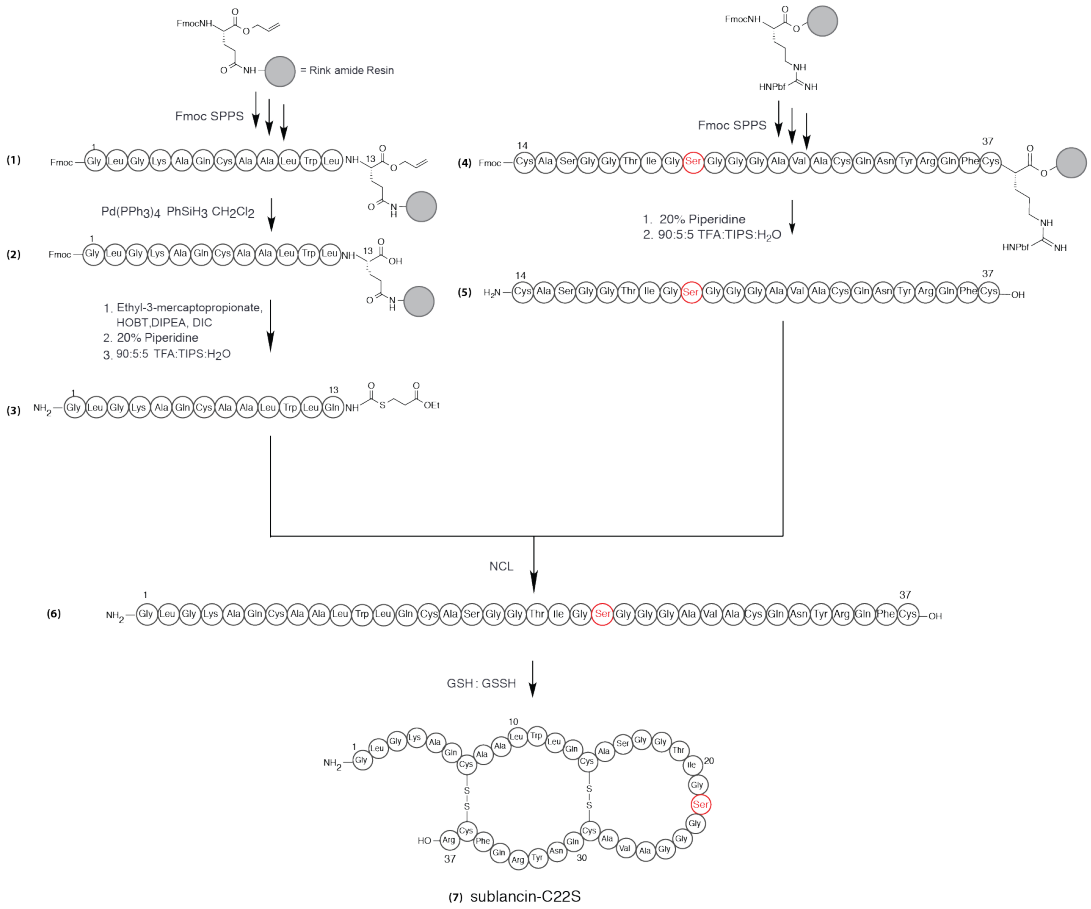

Figure 4.7 Synthesis of sublancin C22S.

An N-terminal fragment encompassing amino acids 1 to 13 and a C-terminal fragment including amino acids 14 to 37 were generated by microwave-assisted SPPS. The N-terminal fragment was derivatized by attachment of a thioester moiety. Native chemical ligation united the two fragments followed by oxidative folding. The N-terminal thioester fragment was reacted with the C-terminal fragment in the presence of mercaptophenylacetic acid (MPAA) and tris 2-carboxyethylphosphine (TCEP) in guanidine hydrochloride/Na_2HPO_4 buffer followed by HPLC purification. The glucose moiety was not attached and the disulfide bridges were formed by oxidative folding by addition of oxidized glutathione, and reduced glutathione.[5] The extent of oxidative folding was verified by MALDI-TOF MS.

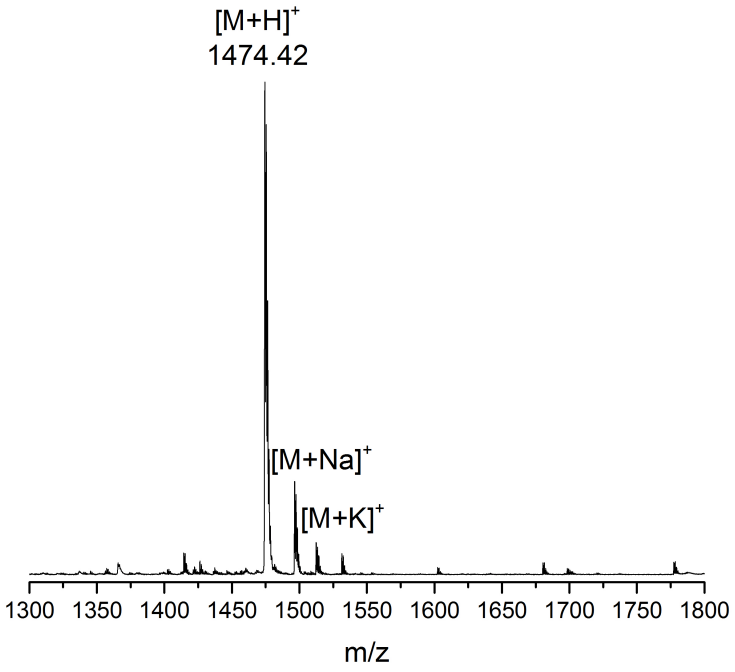

Figure 4.8 MALDI-TOF MS analysis of sublancin1-13 thioester fragment.

The N-terminal fragment containing residues 1 to 13 was prepared by microwave assisted SPPS followed by manual thioesterification. The product was analyzed by MALDI-TOF MS. Expected $[M+H]^+$: 1474.75, observed: 1474.42.

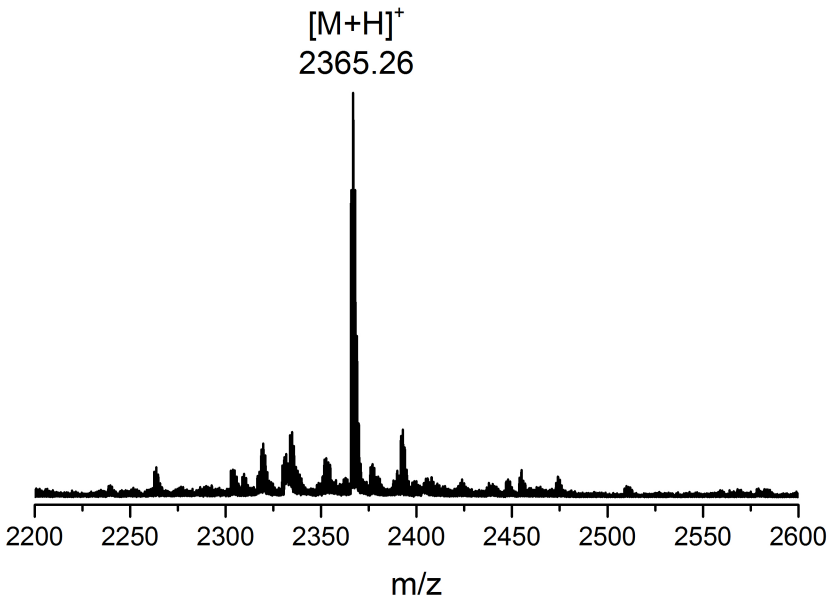

Figure 4.9 MALDI-TOF MS analysis of sublancin-C22S-14-37 fragment.

The C-terminal fragment containing residues 14 to 37 of sublancin-C22S was prepared by microwave assisted SPPS. The product was analyzed by MALDI-TOF MS. Expected $[M+H]^+$: 2364.63, observed: 2365.26.

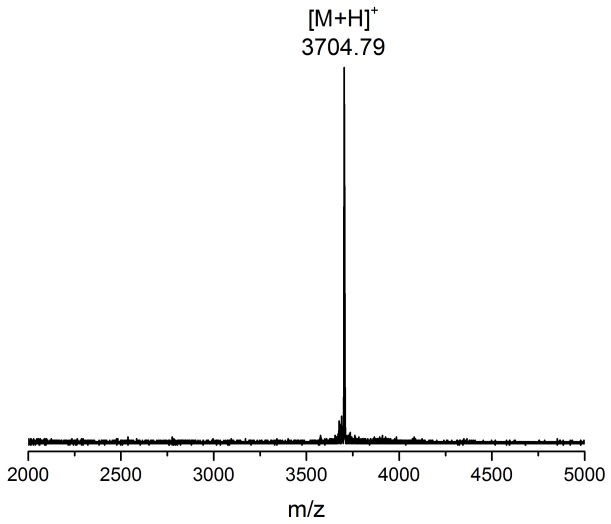

Figure 4.10 MALDI-TOF MS analysis of the NCL of sublancin1-13 thioester fragment and sublancin-C22S-14-37 fragment.
Sublancin-C22S was obtained by NCL of sublancin1-13 thioester fragment and sublancin-C22S-14-37 fragment. The reaction was analyzed by MALDI-TOF MS. Expected $[M+H]^+$: 3705.21, observed: 3704.79.

4.2.5.3 Sublancin C22S, C22N, and C22T analogues are inactive against Bacillus species

Bioassays of sublancin-C22S, C22N, and C22T against sublancin producer *B. subtilis* 168 and sublancin sensitive *B. subtilis* ATCC 6633 demonstrated that the peptide analogs were not bioactive (Figure 4.11) even at concentrations 300X MIC of wild type sublancin (Figure 4.12). The peptides were folded with different ratios of reduced and oxidized glutathione in order to push sublancin into the folded state (Figures 4.13 and 4.14). These findings contradict the observations made by Dr. Huan Wang and show that the sugar is required for activity as originally described by Dr. Oman.[5] The reaction buffer used by Dr. Huan Wang for oxidative folding and leader peptide removal contained TCEP. To test whether TCEP affected bacterial growth, a control bioassay plate of increasing concentrations of TCEP against sublancin sensitive *B. halodurans* C-125 was performed. We observed that at concentrations higher than 6.25 mM TCEP was able to inhibit bacterial growth (Figure 4.13). We believe that the discrepancy of sublancin-C22S activity is due to the addition of TCEP to the buffer.

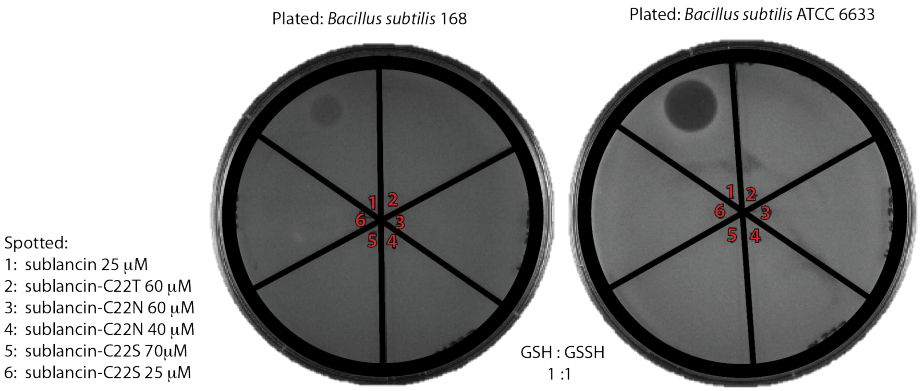

Figure 4.11 Bioassay of heterologously expressed and *in vitro* modified sublancin-C22S, C22N, and C22T against *Bacillus* strains.

Bioassays of sublancin-C22S, C22N, and C22T against sensitive *Bacillus subtilis* ATCC 6633 (right) demonstrated that all sublancin-C22X analogs are inactive when compared to wild type sublancin. A faint inhibition zone was observed for wild type sublancin against *Bacillus subtilis* 168 due to the high concentrations of sublancin spotted on the plates (left). Each peptide was folded using a 1:1 ratio of reduced and oxidized glutathione, 10 μL of each peptide was spotted.

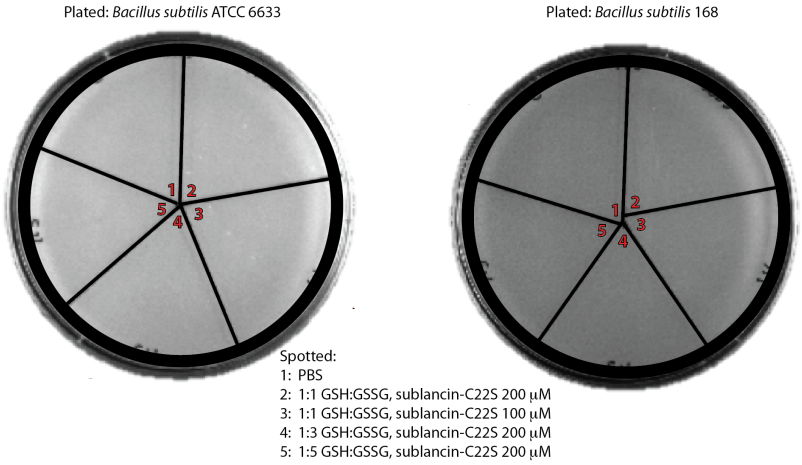

Figure 4.12 Bioassay of sublancin-C22S against *Bacillus* strains.

Bioassays of sublancin-C22S against sensitive *Bacillus subtilis* ATCC 6633 (left) and sublancin-producer *B. subtilis* 168 (right). Peptide was oxidatively folded with different ratios of reduced and oxidized glutathione. The bioassays demonstrated that sublancin-C22S was inactive even at concentrations 300X MIC when compared to wild type sublancin. Each peptide was folded using a 1:1, 1:3, or 1:5 ratio of reduced and oxidized glutathione, 10 μL of each peptide was spotted.

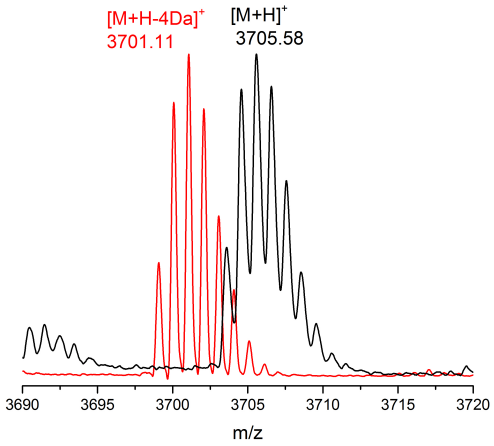

Figure 4.13 MALDI-TOF MS folded sublancin-C22S.

Sublancin-C22N was obtained by *in vitro* oxidative folding of the product from the NCL reaction. The reaction was analyzed by MALDI-TOF MS. Expected $[M+H]^+$: 3705.21, observed $[M+H]^+$: 3705.58, expected $[M+H-4Da]^+$: 3701.19, observed $[M+H-4Da]^+$: 3701.11.

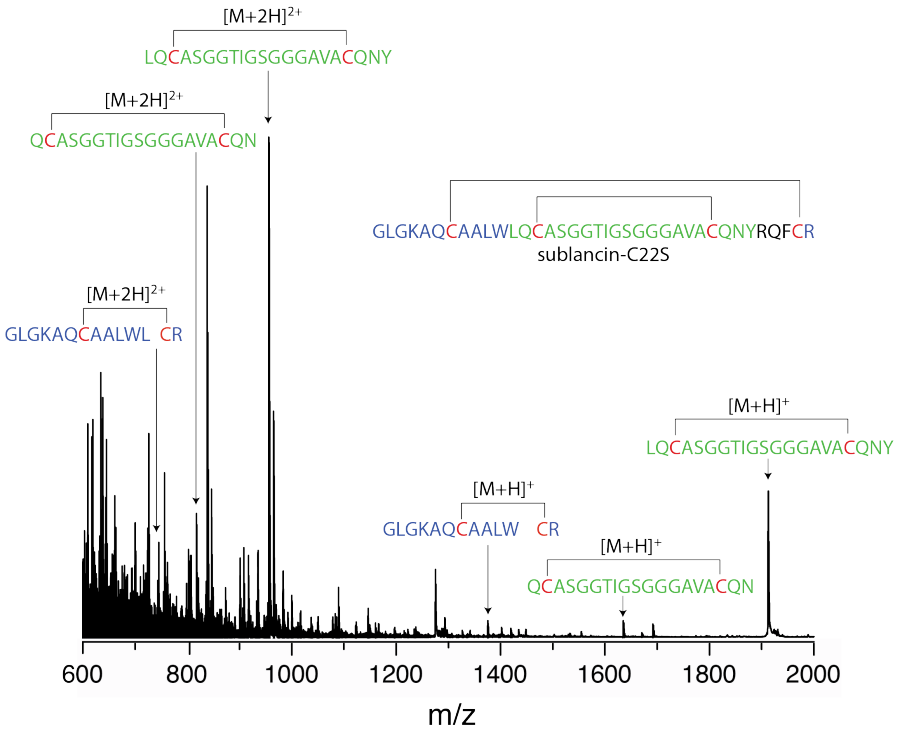

Figure 4.14 MALDI-TOF MS analysis of sublancin digested with chymotrypsin.

Sublancin-C22S was digested with chymotrypsin under reducing conditions and analyzed by MALDI-TOF MS. The resulting mass spectrum is shown. Chymotrypsin cleavage sites include F, W, Y, L and N residues. The masses of the observed ions and their corresponding digest fragments are assigned. The results are consistent with sublancin-C22S being oxidatively folded to generate the native disulfide topology.

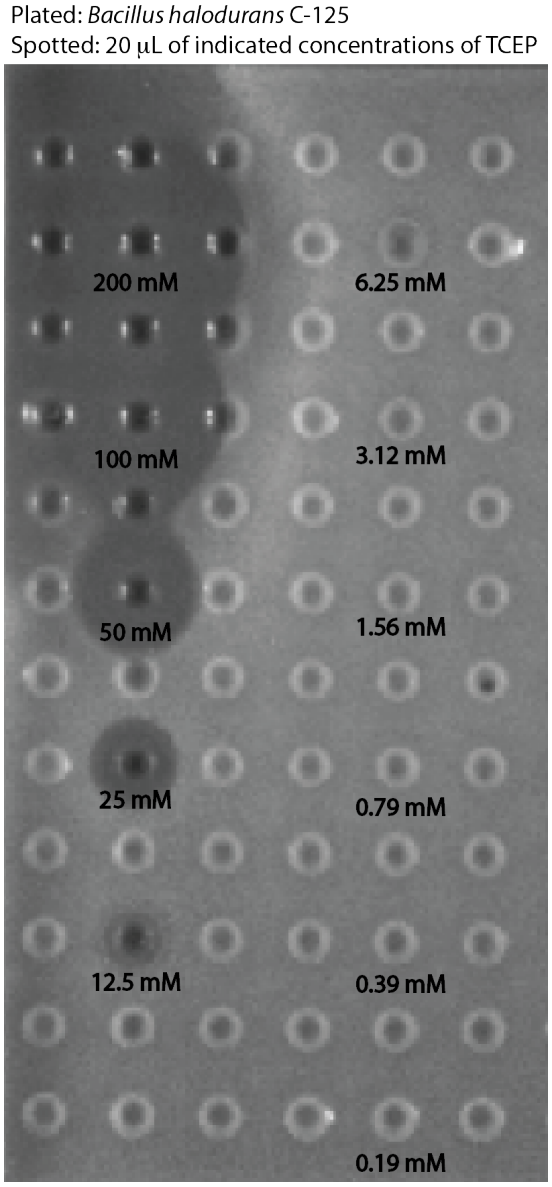

Figure 4.15 Bioassay of TCEP against *Bacillus* strains.

Bioassays of TCEP against sensitive *Bacillus halodurans* C-125. TCEP dilutions were prepared and 20 μL of indicated stocks were spotted. The bioassays demonstrated that at concentrations higher than 6.25 mM TCEP was able to inhibit bacterial growth

4.2.5.4 Phenotype of sublancin-sugar analogs when PTS sugars are added to the growth media of Bacillus cells

In 2011, Dr. Oman probed the NDP-sugar specificity of SunS and observed that when SunS was incubated with His_6-SunA and Mg^{2+} in the presence of UDP-Glc, UDP-GlcNAc, UDP-Gal, GDP-Man or UDP-Xyl, SunA was glycosylated at Cys22.[5] In addition, all sugar-modified peptides were amenable to oxidative folding producing various sublancin analogues with the correct disulfide connectivities as determined by proteolytic digests and ESI-MS^n analysis.[9] In order to probe the phenotypes of the reconstituted sublancin-sugar analogs we followed the same procedure implemented by Dr. Oman. We prepared sublancin-Glc, sublancin-GlcNAc, sublancin-Gal, and sublancin-Man. The biological activity of sublancin-sugar analogs was tested against sensitive *B. halodurans* C-125 and sublancin-resistant *B. halodurans* C-125 mutant strains grown in LB agar media and M9 minimal media supplemented with various carbon sources. When 20 μL of 10 μM reconstituted sublancin-sugar analogs were spotted on LB agar plates containing *B. halodurans* C-125, the peptide retained its antimicrobial activity against the sensitive strain regardless of what sugar was installed on sublancin (Figure 4.16). Given that PTS sugars were able to rescue *Bacillus* sensitive cells (as described in Chapter 3) from the effect of sublancin,[10] the phenotypes of sensitive and sublancin-resistant *B. halodurans* C-125 cells were probed against all sublancin-sugar analogs produced *in vitro*. The bacterial cells tested were grown in M9 minimal media plates supplemented with various carbon sources. When 20 μL of 10 μM reconstituted sublancin-sugar analogs were spotted on M9 minimal media agar plates containing *B. halodurans* C-125 and supplemented with a single carbon source (either glucose, N-acetylglucosamine, mannose, galactose or fructose), regardless of what sugar was installed on sublancin, or what carbon source the bacteria grew in, the peptide retained its

antimicrobial activity against sensitive strains and was inactive against sublancin-resistant strains (Figure 4.17 and Table 4.2). These findings are intriguing since Stepper et al. showed that out of twelve sugars added to MRS agar medium (sorbitol, rhamnose, ManNAc, mannose, glucose, glucosamine, GalNAc, galactose, fructose, xylose, MurNAc and GlcNAc) only GlcNAc was fully protective of ATCC 8014 cells when exposed to glycocin F and ManNAc was only partially protective.[7] One possible explanation could be that only 2.5 μL of 0.5 M carbon source was added to the MRS agar medium whereas in our experiment we added 3% (final concentration) of carbon source to the M9 minimal media agar plates.

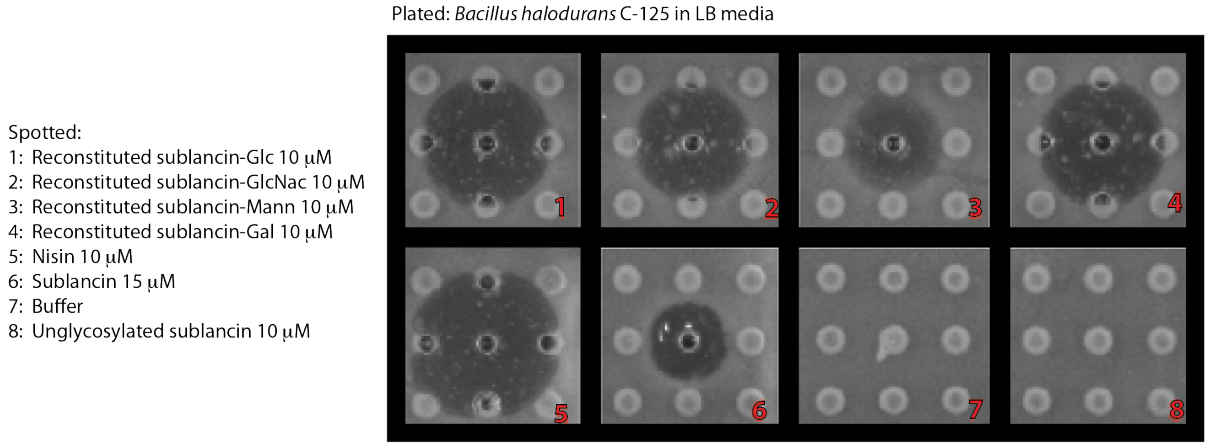

Figure 4.16 Bioassay of reconstituted sublancin-sugar analogs against *B. halodurans* C-125.
Sublancin-Glc, sublancin-GlcNAc, sublancin-Gal, and sublancin-Mann were reconstituted in vitro as previously described by Dr. Oman.[9] A bioassay of sublancin-sugar analogs against sensitive *Bacillus halodurans* C-125 demonstrated that regardless of what sugar was installed on sublancin the peptide retains its antimicrobial activity. Each peptide was folded using a 1:1 ratio of reduced and oxidized glutathione, 20 μL of each peptide was spotted.

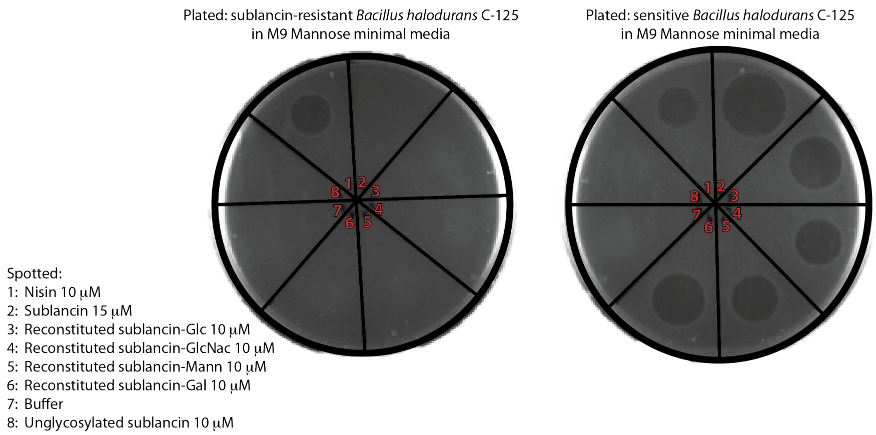

Figure 4.17 Bioassay of reconstituted sublancin-sugar analogs against *B. halodurans* C-125.
Sublancin-Glc, sublancin-GlcNAc, sublancin-Gal, and sublancin-Man were reconstituted in vitro as previously described by Dr. Oman.[9] Shown is a representative example for bacteria grown in M9 minimal media supplemented with mannose. A bioassay of sublancin-sugar analogs against sensitive *Bacillus halodurans* C-125 demonstrated that regardless of what sugar was installed on sublancin the peptide retained its antimicrobial activity. Each peptide was folded using a 1:1 ratio of reduced and oxidized glutathione, 20 µL of each peptide was spotted. Similar inhibition phenotypes were observed for bacteria grown in M9 minimal media supplemented with glucose, N-acetylglucosamine or galactose.

Table 4.2 Results from bioassay of reconstituted sublancin-NDP-sugar analogs against *B. halodurans* C-125 and sublancin-resistant *B. halodurans* C-125.

	Agar media					
Bacterial Strain	Glucose M9 minimal media	N-Acetylglucosamine M9 minimal media	Mannose M9 minimal media	Fructose M9 minimal media	Galactose M9 minimal media	LB media
B. halodurans C-125	1: Nisin	1: Nisin 2: Sublancin 3: Recons. sublancin-Glc 4: Recons. sublancin-GlcNAc 5: Recons. sublancin-Man 6: Recons.sublancin-Gal	1: Nisin 2: Sublancin 3: Recons. sublancin-Glc 4: Recons. sublancin-GlcNAc 5: Recons. sublancin-Man 6: Recons.sublancin-Gal	1: Nisin 2: Sublancin 3: Recons. sublancin-Glc 4: Recons. sublancin-GlcNAc 5: Recons. sublancin-Man 6: Recons.sublancin-Gal	1: Nisin 2: Sublancin 3: Recons. sublancin-Glc 4: Recons. sublancin-GlcNAc 5: Recons. sublancin-Man 6: Recons.sublancin-Gal	1: Nisin 2: Sublancin 3: Recons. sublancin-Glc 4: Recons. sublancin-GlcNAc 5: Recons. sublancin-Man 6: Recons.sublancin-Gal
Sublancin-resistant B. halodurans C-125 001	no growth	1: Nisin	1: Nisin	1: Nisin	1: Nisin	1: Nisin
Sublancin-resistant B. halodurans C-125 002	no growth	1: Nisin	1: Nisin	1: Nisin	1: Nisin	1: Nisin
Sublancin-resistant B. halodurans C-125 003	no growth	1: Nisin	1: Nisin	1: Nisin	1: Nisin	1: Nisin
Sublancin-resistant B. halodurans C-125 004	no growth	1: Nisin	1: Nisin	1: Nisin	1: Nisin	1: Nisin

Sublancin-Glc, sublancin-GlcNAc, sublancin-Gal, and sublancin-Man were prepared *in vitro* as previously described by Dr. Oman.[9] *B. halodurans* C-125 and sublancin-resistant *B. halodurans* C-125 were grown in M9 minimal media with either glucose, N-acetylglucosamine, mannose, fructose or galactose as the carbon source. Indicated with numbers are the antimicrobial peptides that displayed activity against each particular strain. The right-most column displays the results from the bacterial strains grown in LB media as shown previously in Figure 4.16. The plates for growth with mannose are show in in Figure 4.17. The lack of growth of resistant *B. halodurans* C-125 on M9 medium with glucose is consistent with a disabled PTS system for glucose and consistent with the genome sequencing data in chapter 3.

4.3 SUMMARY

Sublancin's antimicrobial properties were further studied. We were unable to demonstrate cross-resistance of other antibiotics with sublancin-resistant *B. halodurans* C-125, which suggests that sublancin is not likely exerting its antimicrobial action in a manner similar to the commercially available compounds examined. In addition, sublancin demonstrated a PAE of 18 h when *B. subtilis* ATCC 6633 sensitive cells were exposed to up to 4xMIC of sublancin for 120 min followed by removal of the peptide. Furthermore, it was demonstrated that sublancin shows bactericidal kinetics. The growth observed after 18 h of exposure of sensitive cells to sublancin was due to sublancin degradation and/or generation of resistant mutants. My studies also addressed the question of whether or not the sugar moiety of sublancin is important for its activity. Bioactivity assays of sublancin-C22S, C22N, and C22T demonstrated that the sugar moiety of sublancin is required for activity. What sugar is installed on the peptide is not as critical since all sublancin-sugar analogs were active against *Bacillus*-sensitive cells. In chapter 5 attempts to identify sublancin's localization in the target cell will be discussed.

4.4 EXPERIMENTAL

4.4.1 Materials, cultures, and conditions

All chemicals and HPLC grade solvents were purchased from Sigma-Aldrich (St. Louis MO) and growth media were obtained from Difco Laboratories (Detroit MI). Tris, MOPS, and HEPES buffers were obtained from Fisher and α-cyano-4-hydroxy-cinnamic acid was obtained from Fluka. Matrix-assisted laser desorption/ionization time-of-flight mass spectrometry (MALDI-TOF MS) was performed at the Mass Spectrometry Laboratory of the School of Chemical Sciences at UIUC using a Bruker Daltonics UltrafleXtreme MALDI TOFTOF instrument. Salt-

containing MS samples were purified via Millipore Zip-Tip$_{C18}$ pipette tips (Billerica MA). Forty-eight well assay plates were purchased from Corning Incorporated (Corning NY) and were read using a multi mode, single-channel Synergy H4 microplate reader from Biotek® instruments, Inc (Winooski, VT). Trays used for agar well diffusion assays were obtained from Nalge Nunc (Rochester NY).

4.4.2 Minimum inhibitory concentration (MIC) determination for cross-resistance analysis

MICs were determined by the broth dilution method.[11] Serial dilutions of sublancin were prepared in sterile deionized water (SDW). Forty-eight well microtiter plates (Corning Costar) were utilized for both *B. subtilis* ATCC 6633 and *Bacillus halodurans* C-125. The total volume of culture in each well was 300 µL; the experimental wells contained 30 µL of 10x stock sublancin at defined concentrations (0.097 mM – 100 mM) and 270 µL of a 1-in-10 dilution (approximately 1 x 10^8 colony-forming units (CFU) mL^{-1}) of a culture of indicator strain diluted in fresh LB growth medium. In addition, each plate contained several blanks (270 µL fresh growth medium and 30 µL SDW) and control wells (270 µL of untreated 1-in-10 diluted culture and 30 µL SDW). The optical density at 600 nm ($O.D._{.600nm}$) was recorded at hourly intervals from 0 to 6 h with an additional measurement at 18 h using a BioTek Synergy 4H plate reader. Plates were incubated under vigorous agitation at 37 °C. The readings of triplicate experiments were averaged. Growth curves were developed using control (culture and SDW only) readings to ensure sufficient O.D. changes for accurate inhibition assessment. Curve fits for MIC determination were produced by fitting the data with Origin8.5 software using a dose-response curve with the equation: $y = A1 + (A2 - A1) / (1 + 10^{(Logx0 - x)p})$, with p = variable Hill slope.

4.4.3 Construction of His_6-SunA_Xa-C22X mutant plasmid

Site-directed mutagenesis of SunA /SunAXa was performed by multistep PCR. First, the amplification of SunAXa was carried out by thirty cycles of denaturing (94 °C for 20s), annealing (58 °C for 30 s), and extending (72 °C for 20s) using the SunAXA-FP (Table 4.3) and an appropriate mutant reverse primer to yield the 5' fragment of the mutant SunAXA gene (FP reaction). The PCR mixtures included 1×FailSafe PreMix G (PICENTRE Biotechnologies), DMSO (4%), Phusion DNA polymerase (Finnzymes) (0.04 U/μL), dNTP (2 mM) and primers (1 μM each). In parallel, a PCR reaction using an appropriate mutant forward primer and the SunAXA-RP primer was also conducted to produce 3' fragments of the mutated SunA gene using the same PCR conditions as the FP reaction (RP reaction). The overlapping products from the FP and RP reaction were combined in equal amounts and extended by seven cycles of denaturing, annealing and extending using the same PCR conditions. Following the extension, the SunA-FP and SunA-RP primers were added (final concentration, 2 μM) and the mixture was incubated for another 25 cycles of denaturing, annealing and extending. The product was amplified by PCR and then purified by 2% agarose gel electrophoresis. The resulting DNA fragments and the pET15 vector were digested with NdeI and XhoI at 37 °C for 2 h. The digested products were purified by agarose gel electrophoresis. The resulting DNA insert was ligated with the digested pET15 vector at 24 °C for 5 h using T4 DNA ligase. *E. coli* DH5α cells were transformed with the ligation mixtures by heat shock. Cells were plated on LB-ampicillin agar plates and grown for 15 h at 37 °C. Several colonies were picked and used to inoculate separate 5 mL cultures of LB-ampicillin medium. The cultures were grown at 37 °C for 15 h, and plasmids were isolated using a QIAprep Spin Miniprep Kit (QIAGEN). The sequences of the resulting plasmid products were confirmed by DNA sequencing.

Table 4.3 Primer sequences used for the construction of SunAXa-C22X analogs.

Primers	Sequence (5' to 3')
SunAXa_FP	*CTAGG* ***CATATG*** ATG GAA AAG CTA TTT AAA GAA GTT AAA CTA GAG GAA CTC GAA AAC
SunAXa_RP	*CTGGA* ***CTCGAG*** TTA TCT GCA GAA TTG ACG ATA GTT TTG ACA AGC AAC AGC TCC GCC
SunAXa-C22S_FP	GCT AGT GGC GGT ACA ATT GGT AGC GGT GGC GG
SunAXa-C22S_RP	ACA AGC AAC AGC TCC GCC ACC GCT ACC AAT TGT ACC
SunAXa-C22N_FP	GCT AGT GGC GGT ACA ATT GGT AAC GGT GGC GG
SunAXa-C22N_RP	ACA AGC AAC AGC TCC GCC ACC GTT ACC AAT TGT ACC
SunAXa-C22T_FP	GCT AGT GGC GGT ACA ATT GGT ACC GGT GGC GG
SunAXa-C22T_RP	ACA AGC AAC AGC TCC GCC ACC GGT ACC AAT TGT ACC

The restriction sites for NdeI and XhoI are shown in bold and mutated bases are underlined.

4.4.4 Overexpression and purification of His6-SunA_Xa-C22X mutant precursor peptides

E. coli BL21(DE3) cells were transformed via electroporation with either a pET15b SunA_Xa-C22S, SunA_Xa-C22N or SunA_Xa-C22T mutant construct. A single colony transformant was used to inoculate a 100 mL culture of LB media supplemented with 100 μg/mL ampicillin. The culture was grown at 37 °C for 12 h and was used to inoculate 2 L of TB containing 100 μg/mL ampicillin and cells were grown at 37 °C to OD600 ≈ 0.8-1.0. IPTG was added to a final concentration of 0.2 mM and the culture was incubated at 18 °C for additional 12 h. Cells overexpressing His_6- SunA_Xa-C22X were harvested by centrifugation at 12,000 xg for 20 min at 4 °C, and the pellet was resuspended in 30 mL of start buffer (20 mM NaH_2PO_4, pH 7.5, 500 mM NaCl, 0.5 mM imidazole, 20% glycerol) and sonicated (cycles of 4 s bursts, 9.9 s rest) on ice for 20 min to lyse the cells. Cell debris was removed by centrifugation at 23,700 xg for 30 min at 4 °C. The supernatant was discarded and the pellet containing the insoluble peptide was resuspended once more in 30 mL of start buffer. The sonication and centrifugation steps

were repeated. The pellet was then resuspended in 30 mL of buffer 1 (6 M guanidine HCl, 20 mM NaH_2PO_4, pH 7.5, 500 mM NaCl, 0.5 mM imidazole). Insoluble material was removed by centrifugation at 14000 ×g for 30 min at 4 °C, followed by filtration of the supernatant through a 0.45 μm filter. The filtered sample was applied to a 5 mL HisTrap HP (GE Healthcare Life Sciences) immobilized metal affinity chromatography (IMAC) column previously charged with $NiSO_4$ and equilibrated in buffer 1. The column was washed with two column volumes of buffer 1, followed by two column volumes of buffer 2 (4 M guanidine HCl, 20 mM NaH_2PO_4 , pH 7.5, 500 mM NaCl, 30 mM imidazole). The peptide was eluted with 2 column volumes of elution buffer (4 M guanidine HCl, 20 mM NaH_2PO_4 (pH 7.5), 500 mM NaCl, 1 M imidazole). The fractions were desalted using a ZipTipC18 and analyzed by MALDI-TOF MS. The Ni-NTA-purified peptides were desalted by two different methods depending on scale. The first method involved preparative reversed-phase HPLC (Waters Delta 600) employing a Waters C4 PrepPak cartridge. The purification was performed at room temperature by applying a linear gradient of 2% solvent A (80% acetonitrile and 0.1% TFA in water) to 100% solvent A over 45 min with the second solvent 0.1% TFA in water (solvent B). The flow rate was set to 8 mL/min and the absorbance at 220 nm was monitored. Fractions containing the desired peptide were pooled and lyophilized (Labconco). The product was analyzed by MALDI-ToF MS and stored at −20 °C. This desalting method was performed with cultures over 4 L. Peptides obtained from small cultures were desalted by using C4 solid phase extraction columns (Grace Vydac) as directed by the product manual. All fractions were analyzed by MALDI-TOF-MS and fractions containing the desired product were combined and lyophilized. The product was kept at −20 °C for short-term storage and −80 °C for long-term storage. Typical yields from 2 L of culture were 0.05 mg

for His_6_SunA-C22S mutant, 0.1 mg for His_6_SunA-C22N mutant and 0.1 mg for His_6_SunA-C22T mutant.

4.4.5 Overexpression and purification of His_6-SunS

E. coli BL21 (DE3) cells were transformed via electroporation with the pET28b SunS construct obtained from Dr. Trent Oman.[5] A single colony transformant was used to inoculate a 30 mL culture of LB supplemented with 50 μg/mL kanamycin. The culture was grown at 37 °C for 12 h and was used to inoculate 3 L of LB containing 50 μg/mL kanamycin, and cells were grown at 37 °C to OD600 ≈ 0.6. The culture was incubated at 4 °C on ice for 20 min, then IPTG was added to a final concentration of 0.5 mM and the culture was incubated at 18 °C for an additional 16-20 h. Cells were harvested by centrifugation at 12,000 ×g for 15 min at 4 °C, and the pellet was resuspended in 30 mL of start buffer (20 mM Tris (pH 8.0), 500 mM NaCl, 1 mM TCEP, 10% glycerol) and stored at −80 °C. All protein purification steps were performed at 4 °C. The cell paste was suspended in start buffer and the cells were lysed using a high pressure homogenizer (Avestin, Inc.). Cell debris was pelleted via centrifugation at 23,700 ×g for 20 min at 4 °C. The supernatant was injected via a superloop onto a fast protein liquid chromatography (FPLC) system (ÄKTA, GE Heathcare Life Sciences) equipped with a 5 mL HisTrap HP IMAC column previously charged with $Ni2^+$ and equilibrated in start buffer. The column was washed with 50 mL of buffer A (30 mM imidazole, 20 mM Tris, pH 7.5, 300 mM NaCl) and the protein was eluted using a linear gradient of 0-100% B (buffer B = 200 mM imidazole, 20 mM Tris, pH 7.5, 300 mM NaCl) over 40 min at a 2 mL/min flow rate. UV absorbance (280 nm) was monitored and fractions were collected and analyzed by SDS-PAGE (4-20% Tris-glycine READY gel, BioRAD). The fractions containing SunS were combined and concentrated using an Amicon Ultra-15 Centrifugal Filter Unit (10 kDa MWCO, Millipore). Gel filtration purification

was used to further purify SunS. The concentrated protein sample was injected onto an FPLC system (ÄKTA) equipped with an XK16 16/60 (GE Healthcare Life Sciences) column packed with SuperDex 75 resin previously equilibrated in 20 mM HEPES (pH 7.5), 200 mM KCl. The protein was eluted with a flow rate of 0.9 mL/min. Both UV (280 nm) and conductance were monitored and fractions were collected. Misfolded/aggregated protein was efficiently separated from soluble, correctly folded protein and the desired fractions were combined and concentrated using an Amicon Ultra-15 Centrifugal Filter Unit. The resulting protein sample was stored at −80 °C. Protein concentration was determined using a Bradford Assay Kit (Pierce) and typically yields were 8 mg of His_6-SunS from 3 L of cell culture.

4.4.6 Glycosylation of SunAXa by SunS

Sugar modified His_6-SunAXa was prepared in 1000 µL of 50 mM Tris (pH 7.5), 1 mM $MgCl_2$, 1 mM TCEP, 50 mM NDP-sugar, 200 µM His_6-SunA and 10 µM His_6-SunS. The reaction was incubated at 25 °C for 12 h. The extent of sugar modification was verified by removing a 5 µL aliquot of the reaction, quenching with 5% TFA to pH 1-2, desalting using a $ZipTip_{C18}$, and analysis by MALDI-TOF and ESI Q/TOF MS.

4.4.7 In vitro oxidative folding of sublancin analogues

Peptides were dissolved in 50 mM Tris buffer (500 µL, pH 7.5) containing oxidized glutathione (GSH) (2 mM final conc.), and reduced GSH (2 mM final conc.). The mixture was incubated at 25 ^{o}C and the reaction monitored by MALDI-TOF and ESI Q/TOF MS. A loss of 4 Da indicated the formation of two disulfide bonds. Folded analogues were purified by preparative HPLC using a linear gradient of 2% solvent A (80% acetonitrile and 0.1% TFA in water) to 40% solvent A over 40 min with the second solvent 0.1% TFA in water (solvent B).

4.4.8 Synthesis of sublancin-C22S_1-13 fragment, de-allylation and C-terminal thioesterification

The N-terminal fluorescently labeled sublancin analog was synthesized using the procedure applied by Hsieh and coworkers[8] to prepare wild type sublancin with a few modifications. Ser was used at position 22 rather than glycosylated Cys when elongating the fragment containing amino acids 14 to 37 by microwave assisted solid phase synthesis. Briefly, standard cycles for SPPS were performed using a fritted glass reaction vessel equipped with a N_2 inlet for resin/reagent agitation and a suction outlet for draining. Fmoc deprotection was achieved by agitating resin with 20% piperidine in dimethylformamide (DMF) for 20 min. After draining the reaction vessel, the resin was washed with DMF (3 x 30 s) and CH_2Cl_2 (2 x 30 s). The appropriately side-chain protected Fmoc-amino acid (5 equiv.) in DMF (5-10 mL) was pre-activated with (N,N'-diisopropylcarbodiimide) (DIC) and HOBt (5 equiv. each) for 5 min, then added to the resin and agitated for 45-60 min. After draining the reaction vessel, the resin was washed with DMF (3 x 30 s) and CH_2Cl_2 (2 x 30 s). The completion of all couplings was assessed by a Kaiser test; double couplings were performed as needed but were generally unnecessary. Test cleavages were performed after all coupling steps by removing a small portion of resin from the reaction vessel and treating with 90:5:5 TFA:H_2O:triisopropylsilane for 1 h under N2. After removing the cleaved resin by filtration, the filtrate was concentrated under a stream of N_2. The peptide was precipitated with cold Et_2O, isolated by centrifugation and dissolved in 1:1 H_2O/MeCN. An aliquot of this solution was analyzed by MALDI-TOF MS.

Allyl deprotection: The fully assembled resin (25 μmol) was swollen in dry CH_2Cl_2 (3 mL) for 30 min under nitrogen, followed by addition of a solution of $Pd(PPh_3)_4$ (25 mg, 22 μmol) and $PhSiH_3$ (123 μL, 108 mg, 1 mmol, 40 equiv.) in 1:1 CH_2Cl_2:DMF (5 mL). The resin

was shaken for 2 h and subsequently washed with DCM (5 x 5 mL), DMF containing 0.5 % diethyldithiocarbamate (DEDTC) as a palladium scavenger (3 x 2 mL), DMF (5 x 5 mL) and DCM (5 x 5 mL). An aliquot of this solution was analyzed by MALDI-TOF MS.

N-terminal Fmoc deprotection: A solution of 1:4 piperidine:DMF (2 x 5 mL) was added to the resin and the flask was agitated for 5 min. The resin was subsequently drained and washed with DMF (5 x 3 mL), CH_2Cl_2 (5 x 3 mL) and DMF (5 x 3 mL).

C-terminal thioesterification: A solution of ethyl-3-mercaptopropionate (77 µl, 600 umol, 24 equiv.), HCTU (310 mg, 750 µmol 30 equiv.), and DIPEA (161 µl, 121 mg, 938 µmol, 37.5 equiv.) in 4:1 CH_2Cl_2DCM:DMF (1.5 mL) was added to the resin-bound peptide and the reaction vessel was shaken for 1 h at 25 ºC. The procedure was repeated once and the resin was washed with CH_2Cl_2 (5 x 5 mL), DMF (5 x 5 mL) and CH_2Cl_2 (10 x 5 mL).

Cleavage from resin: A mixture of TFA, triisopropylsilane and water (90:5:5) was added to the resin. After 2 h, the resin was washed with TFA (4 x 4 mL). After removing the cleaved resin by filtration, the filtrate was concentrated under a stream of N_2. The peptide was precipitated with cold Et_2O, isolated by centrifugation and dissolved in 1:1 H_2O/MeCN. An aliquot of this solution was spotted onto a MALDI-TOF MS target for analysis. If the test cleavage was successful and MALDI-TOF MS spectra looked good, all peptide was cleaved from resin by treating with 90:5:5 TFA:TIPS:H_2O. After removing the cleaved resin by filtration, the filtrate was concentrated under a stream of N_2. The peptide was precipitated with cold Et_2O, isolated by centrifugation and dissolved in 1:1 H_2O/MeCN. The peptide was then lyophilized to dryness, taken up in 0.1% TFA/H_2O and analyzed by analytical RP-HPLC affording the desired N-terminal fragment.

4.4.9 Synthesis of sublancin-C22S_14-37 fragment, de-allylation and C-terminal thioesterification

Fmoc-Arg-Wang resin (0.8 g) was used with a loading capacity of 0.5 mmol/g. The resin was first swollen in 5 mL of dimethylformamide (DMF) by sparging with N_2 in a coarse fritted filter. After draining the reaction vessel, the resin was washed with DMF (3 x 30 s). Fmoc deprotection was achieved by agitating the resin with 20% piperidine in DMF for 20 min. The resin was then drained and washed with DMF (3 x 30 s), CH_2Cl_2 (2 x 30 s) and DMF (3 x 30 s). A Kaiser test to probe the efficiency of the deprotection was completed as necessary. Three solutions were used: 5 g of ninhydrin in 100 mL of ethanol, 80 g of phenol in 20 mL of ethanol, and 2 mL of 1 mM aq. KCN in 98 mL of pyridine. A small amount of beads was removed from the reaction vessel and placed in a 6x50 mm test tube. Three drops of each of the three solutions were then added to the test tube. Three drops of each solution were also added to a second test tube containing no beads, which serves as the negative control. The test tube was shaken in front of a heat gun or put in a hot water bath for 1 min. A deep blue-purple color observed after 30 s to 1 min indicates a positive test (i.e. the presence of a free amine).

Coupling steps were completed using 4 equivalents of amino acids relative to the resin loading. The appropriate side-chain protected Fmoc-amino acid in DMF (5-10 mL) was pre-activated with DIC (N,N'-diisopropylcarbodiimide) and HOBt (4 equiv. each, 1.6 mmol) for 5 min, then added to resin and agitated for 45-60 min. After draining the reaction vessel, the resin was washed with DMF (3 x 30 s), CH_2Cl_2 (2 x 30 s) and DMF (3 x 30 s). The completion of all couplings was assessed by a Kaiser test; Test cleavages were performed after all coupling steps by removing a small portion of dry resin from the reaction vessel and treating with 90:5:5 TFA/H_2O/triisopropylsilane for 1 h under N_2. After removing the cleaved resin by filtration, the

filtrate was concentrated under a stream of N_2. The peptide was precipitated with cold Et_2O, isolated by centrifugation and dissolved in 1:1 H_2O/MeCN. An aliquot of this solution was spotted onto a MALDI-TOF MS target for analysis. Any remaining free resin sites were capped by agitation in 90:8:2 DMF:acetic anhydride:DIPEA for 15 min. If the test cleavage was successful and MALDI spectra looked good, all peptide was cleaved from the resin by treating with 90:5:5 TFA:TIPS:H_2O. After removing the resin by filtration, the filtrate was concentrated under a stream of N_2. The peptide was precipitated with cold Et_2O, isolated by centrifugation and dissolved in 1:1 H_2O/MeCN. The peptide was then lyophilized to dryness, taken up in 0.1% TFA/H_2O and analyzed by analytical RP-HPLC.

4.4.10 Native chemical ligation

Ligation buffer was prepared by dissolving 4-mercaptophenylacetic acid (MPAA, final conc. = 200 mM) and TCEP (final conc. = 20 mM) in 6 M guanidine hydrochloride/0.2 M Na_2HPO_4 buffer. The pH was adjusted to 7.2 by the addition of 5.0 M HCl and the mixture was degassed with argon. A solution of the sublancin1-13 thioester (1 mM) and sublancin14-37-C22X (0.5 mM) was prepared in the above ligation buffer and the pH was carefully adjusted to 7.0-7.2 by addition of 2.0 M NaOH. The reaction was flushed with argon and allowed to incubate at 25 $^{\circ}$C for 24 or 42 h with reaction monitoring by LC-MS. The reaction was quenched by the addition of 0.1% formic acid in water at 24 h and 42 h. TCEP (20 mg/mL) was added to the ligation mixture prior to purification by reversed phase (C18) analytical HPLC.

4.4.11 Chymotrypsin digests of sublancin and sublancin analogs under non-reducing conditions

Sublancin and sublancin analogs were digested in 100 mM Tris (pH 7.5), and 0.1 mg/mL

chymotrypsin (Worthington). All reactions were incubated at 25 °C for 5 h and then quenched with 5% TFA to pH 1-2. Quenched samples were desalted with a $ZipTip_{C18}$ prior to analysis by MALDI-TOF MS or analyzed by LC-ESI-Q/TOF MS.

4.4.12 Phenotype of sublancin-sugar analogs when PTS sugars are added to the growth media of *Bacillus* cells

Sublancin and sublancin analogs were first prepared by *in vitro* modification of His_6-SunAXa peptide by SunS to install the sugars. Oxidative folding afforded the disulfide linkages and the leader peptide was removed by proteolytic cleavage by Factor Xa. Sugar modified His_6-SunA Xa was prepared in 100 μL of 50 mM Tris (pH 7.5), 1 mM $MgCl_2$, 1 mM TCEP, 5 mM NDP-sugar, 200 μM His_6-SunA Xa, and 2 μM His_6-SunS. The reaction was incubated at 25 °C for 12 h. The extent of sugar modification was verified by removing a 5 μL aliquot of the reaction, quenching with 5% TFA to pH 1-2, desalting using a $ZipTip_{C18}$, and analysis by MALDI-TOF and ESI Q/TOF MS. Following analysis, the disulfides of the modified sublancin and sublancin analog core peptide were formed by addition of Tris (pH 7.5), oxidized glutathione (GSSG), and reduced glutathione (GSH), to final concentrations of 50 mM, 2 mM, and 2 mM, respectively. The total volume of the oxidative folding reaction was 100 μL and the reaction was incubated at 25 °C for an additional 12 h. The extent of disulfide formation was monitored by removing a 5 μL aliquot of the reaction, quenching with 5% TFA to pH 1-2, desalting using a $ZipTip_{C18}$, and analyzing by MALDI-TOF MS. Following analysis, the leader peptide was proteolytically cleaved by the addition of NaCl and $CaCl_2$ to 100 mM and 2 mM, respectively, and the addition of Factor Xa to 0.075 mg/mL (final concentrations). The reaction was incubated at 25 °C for 1 h and the extent of cleavage was monitored by MALDI-TOF MS as stated above.

Disulfide formation was observed as a peak with a −4 Da mass difference compared with material that was not subjected to oxidative folding.

For each prepared sublancin analog 15 μL of the 100 μL reactions described above were spotted on either an overnight culture of sensitive *B. halodurans C-125* or sublancin resistant *B. halodurans C-125*. *B. halodurans C-125* strains were grown in LB or M9 minimal media, supplemented with various carbon sources, under aerobic conditions at 37 °C for 16 h. Ninety-six well agar plates were prepared by combining 20 mL of molten LB or M9 minimal medium agar (cooled to 42 °C) with 100 μL of dense overnight culture (approx 10^8-10^9 CFU/mL). The seeded agar was poured into a sterile OmniTray (Nunc) and allowed to solidify at 25 °C for 30 min. An additional 30 mL of molten LB medium was cooled to 42 °C, combined with 150 μL of culture, and poured over the lower solidified agar layer. A sterile 96-well PCR plate was placed in the molten agar upper layer and was allowed to solidify at 25 °C for 45 min. After sufficient solidification, the 96-well PCR plate was removed. The total 20 μL volume of each concentrated *in vitro* reaction was dispensed into separate newly formed wells. Authentic sublancin standards were spotted in 15 μL volumes at the concentrations indicated. Plates were left at 25 °C for 24 h and antibacterial activity was qualitatively determined by the presence or absence of growth inhibition.

4.5 REFERENCES

(1) Fischbach, M. A.; Walsh, C. T. *Science* **2009**, *325*, 1089. "Antibiotics For Emerging Pathogens".

(2) O'Neill, A. J.; Chopra, I. *Expert Opin Investig Drugs* **2004**, *13*, 1045. "Preclinical evaluation of novel antibacterial agents by microbiological and molecular techniques".

(3) Andrews, J. M. *J Antimicrob Chemother* **2001**, *48 Suppl 1*, 5. "Determination of minimum inhibitory concentrations".

(4) Clinical and Laboratory Standards Institute/NCCLS; 7th ed. 2006; Vol. 26.

(5) Oman, T. J.; Boettcher, J. M.; Wang, H.; Okalibe, X. N.; van der Donk, W. A. *Nat Chem Biol* **2011**, *7*, 78. "Sublancin is not a lantibiotic but an S-linked glycopeptide".

(6) Garcia De Gonzalo, C. V.; Zhu, L.; Oman, T. J.; van der Donk, W. A. *ACS Chem Biol* **2014**, *9*, 796. "NMR structure of the S-linked glycopeptide sublancin 168".

(7) Stepper, J.; Shastri, S.; Loo, T. S.; Preston, J. C.; Novak, P.; Man, P.; Moore, C. H.; Havlicek, V.; Patchett, M. L.; Norris, G. E. *FEBS Lett* **2011**, *585*, 645. "Cysteine S-glycosylation, a new post-translational modification found in glycopeptide bacteriocins".

(8) Hsieh, Y. S.; Wilkinson, B. L.; O'Connell, M. R.; Mackay, J. P.; Matthews, J. M.; Payne, R. J. *Org Lett* **2012**, *14*, 1910. "Synthesis of the bacteriocin glycopeptide sublancin 168 and S-glycosylated variants".

(9) Oman, T. J. PhD Thesis, University of Illinois at Urbana-Champaign, 2011.

(10) Garcia De Gonzalo, C. V.; Denham, E. L.; Mars, R. A. T.; Stülke, J.; van der Donk, W. A.; van Dijl, J. M. *Antimicrob. Agents Chemother.* **2015**, *59*, 10.1128/AAC.01519. "The Phosphoenolpyruvate:Sugar Phosphotransferase system is involved in sensitivity to the glucosylated bacteriocin sublancin".

(11) Wiegand, I.; Hilpert, K.; Hancock, R. E. *Nat Protoc* **2008**, *3*, 163. "Agar and broth dilution methods to determine the minimal inhibitory concentration (MIC) of antimicrobial substances".

CHAPTER 5. SUBLANCIN IN VIVO LOCALIZATION STUDIES [a]

5.1 INTRODUCTION

Bacteriocins are ribosomally synthesized peptides produced by a wide range of bacterial species. Given the known pore forming activity of several families of antimicrobial peptides,[1-4] chapter 3 described whether sublancin dissipated the membrane potential of *Bacilli* at levels comparable to nisin.[5] Extensive dissipation of membrane potential was observed within a few minutes of incubation with nisin. However, sublancin did not appear to damage the cell membrane as no significant decrease in the membrane potential was observed (Figures 3.3 and 3.4). Furthermore, Oman et al. demonstrated that sublancin does not bind to lipid II, a common mode of action of many natural product antibiotics.[5,6] Collectively these experiments suggest that sublancin does not compromise the cell membrane integrity but do not rule out recruitment of key components from the membrane as playing a role in the mechanism of action.

As discussed in chapter 3, the phosphotransferase system is important for sublancin sensitivity. Different components of the PTS have different localization. Govindarajan et al. have shown that EI and HPr are located near the poles in *Escherichia coli* and *Bacillus subtilis* cells.[7,8] Enzyme II (EII) permeases, which transport the sugar into the cell, are multidomain structures that can either exist as a single polypeptide, IIABC or as two peptides, IIBC and IIA.[9] The IIABC and IIBC sugar permeases have been shown to be located in the cell membrane. The individual IIA components are spread evenly throughout the cytoplasm of the bacterial cells.[8] To characterize the antibacterial action of sublancin it is important to determine where this rare

---

[a] All STORM and SR-SIM images were obtained in collaboration with Seonjin Park from Taekjip Ha research group.

ribosomally synthesized and post-translationally modified S-glycopeptide localizes within the cell of a sensitive bacterium.

To this end, as described in this chapter, we have used confocal and super-resolution fluorescence microscopy together with tagged sublancin analogs to visualize sublancin in the cell. For this purpose, fluorescent groups were incorporated into sublancin using two strategies: 1) reaction at the N-terminus with N-hydroxysuccinimide (NHS) esters and 2) coupling of amines with the unique carboxylic acid at the C-terminus of sublancin. Here we describe the application of these fluorescent tags to investigate whether sublancin localizes to the cell membrane, and, if so, whether it is uniformly localized or is present at septa and/or poles of the bacteria.

5.2 RESULTS AND DISCUSSION

5.2.1 N-terminal fluorescent sublancin analogs are inactive against *Bacillus* sensitive cells

Fluorescent labeling of antibiotics is a strategy used to understand how these compounds localize in their target cells.[10] For the purpose of gaining insight into the mechanism by which sublancin exhibits bactericidal activity, sublancin analogs were produced. Hsieh et al. had previously synthesized sublancin by solid phase peptide synthesis (SPPS) and native chemical ligation (NCL).[11] We implemented a similar methodology to synthesize fluorescently labeled SunA analogs (Figure 5.1). We similarly employed the use of commercially available Fmoc-Glu-OAllyl, which was immobilized onto Rink amide resin for the synthesis of the N-terminal fragment, and NovaPEG Wang resin carrying immobilized Fmoc-Arg(Pbf)-OH for the C-terminal fragment. Instead of using thioglycosyltamino acids to put on the sugar moiety we synthesized the full-length peptide first followed by *in vitro* glycosylation by SunS.

Sublancin, a 37 amino acid peptide, was first synthesized in two fragments designed based on the requirement of an available cysteine for NCL. The peptide bond between Gln13 and Cys14 was a suitable junction for native chemical ligation, therefore an N-terminal fragment containing amino acids 1-13 and a C-terminal fragment containing amino acids 14-37 bearing an N-terminal cysteine were synthesized.[11] After preparation of the fragments by microwave assisted Fmoc SPPS, the fluorescent labeling and thioesterification were performed manually on the N-terminal fragment. Both fragments were then cleaved from the resin while simultaneously deprotecting the side chains, purified by HPLC, and characterized by MALDI-TOF MS (Figures 5.2, 5.3, and 5.4). Unglycosylated fluorescent linear sublancin was obtained by NCL of the two fragments (Figure 5.5). The thioester N-terminal fragment was reacted with the C-terminal fragment in the presence of mercaptophenylacetic acid (MPAA) and tris 2-carboxyethylphosphine (TCEP) in guanidine hydrochloride/Na_2HPO_4 buffer followed by HPLC purification. The glucose moiety was subsequently attached to Cys22 by an *in vitro* enzymatic modification performed by the glycosyltransferase SunS followed by HPLC purification (Figure 5.6). Ultimate incorporation of disulfides by oxidation in the presence of oxidized glutathione and reduced glutathione afforded the desired analogs.[12] The extent of the sugar modification and oxidative folding was verified by MALDI-TOF MS.

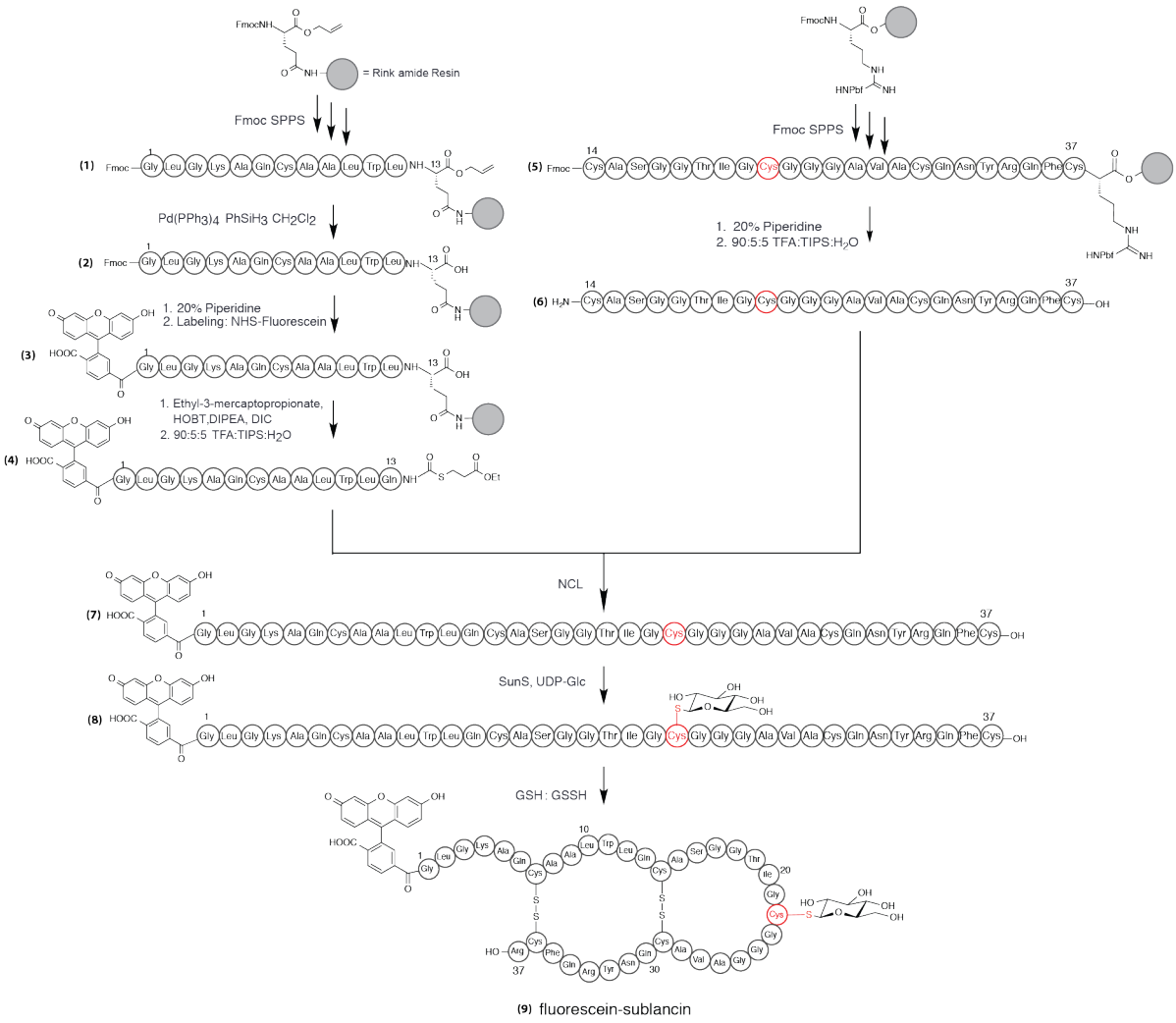

Figure 5.1 Synthesis of fluorescently labeled sublancin.

An N-terminal fragment encompassing amino acids 1 to 13 and a C-terminal fragment including amino acids 14 to 37 were generated by microwave-assisted SPPS. The N-terminal fragment was derivatized by attachment of both fluorescein and thioester moieties. Native chemical ligation united the two fragments followed by glycosylation and oxidative folding. The N-terminal thioester fragment was reacted with the C-terminal fragment in the presence of mercaptophenylacetic acid (MPAA) and tris 2-carboxyethylphosphine (TCEP) in guanidine hydrochloride/Na_2HPO_4 buffer followed by HPLC purification. The glucose moiety was later attached to Cys22 by an *in vitro* enzymatic modification performed by the glycosyltransferase SunS followed by purification via HPLC.

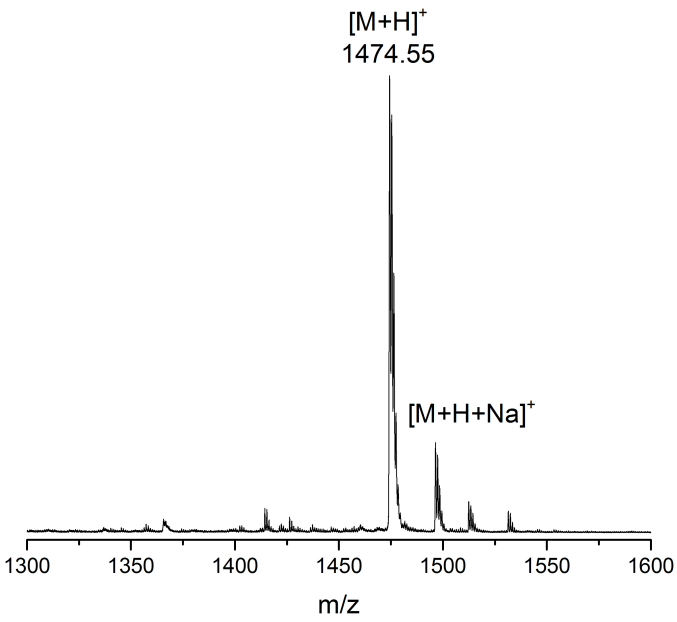

Figure 5.2 MALDI-TOF MS analysis of sublancin1-13 thioester fragment.

A control N-terminal fragment, without the fluorescein, was synthesized. The N-terminal fragment containing residues 1 to 13 was extended by microwave assisted SPPS followed by manual thioesterification. The product was analyzed by MALDI-TOF MS. Expected $[M+H]^+$: 1474.75, observed: 1474.55.

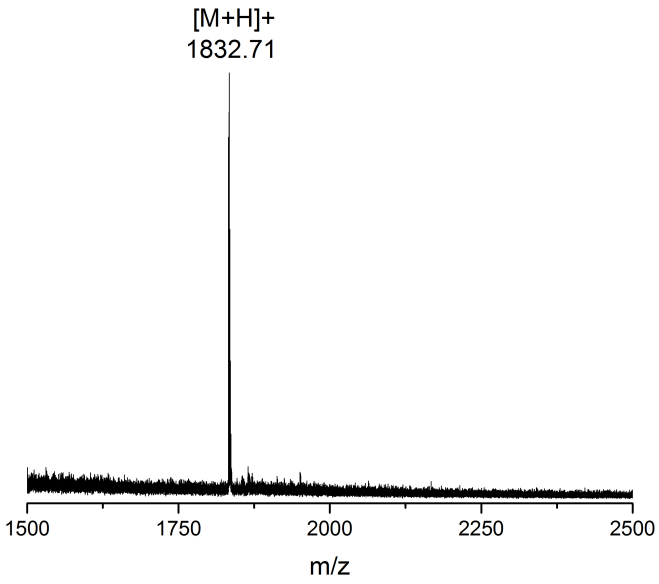

Figure 5.3 MALDI-TOF MS analysis of fluorescein-sublancin1-13 thioester fragment.

The fluorescein N-terminal fragment containing residues 1 to 13 was extended by microwave assisted SPPS followed by manual fluorescent labeling and thioesterification. The product was analyzed by MALDI-TOF MS. Expected [M+H]: 1832.80, observed: 1832.71.

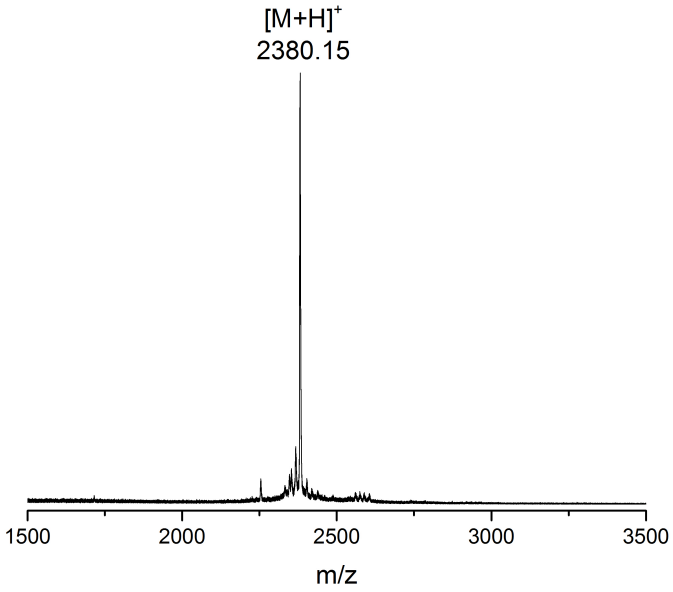

Figure 5.4 MALDI-TOF MS analysis of sublancin14-37 fragment.

The C-terminal fragment containing residues 14 to 37 was extended by microwave assisted SPPS. The product was analyzed by MALDI-TOF MS. Expected [M+H]: 2380.69, observed: 2380.15.

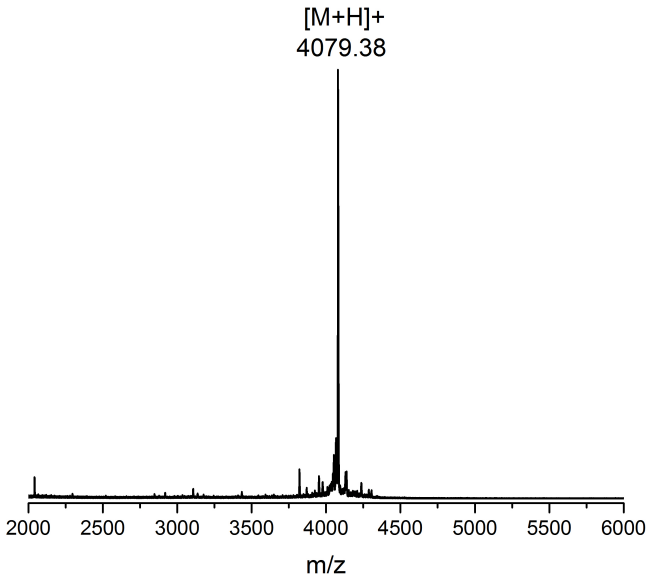

Figure 5.5 MALDI-TOF MS analysis of fluorescein labeled linear SunA core peptide (no glucose).

Unglycosylated fluorescent labeled linear SunA core peptide was obtained by NCL of the two fragments. The product was analyzed by MALDI-TOF MS. Expected [M+H]: 4079.59, observed: 4079.38.

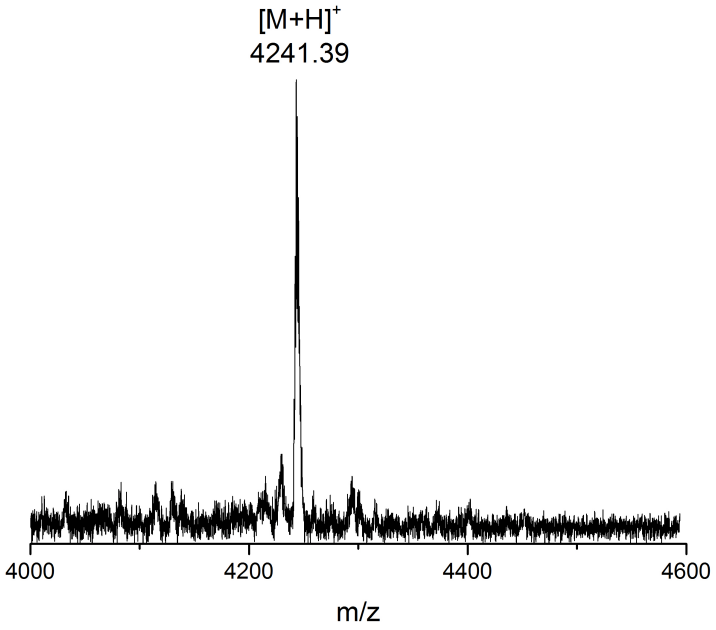

Figure 5.6 MALDI-TOF MS analysis of fluorescein-sublancin.

Linear fluorescein-sublancin was obtained by native chemical ligation of the two fragments, followed by *in vitro* glycosylation and oxidative folding. The reaction was analyzed by MALDI-TOF MS. Expected [M+H]: 4241.73, observed: 4241.39.

Bioassays of N-terminal fluorescein-labeled sublancin against sublancin-sensitive strains *B. halodurans* C-125 and *B. subtilis* ATCC 6633 demonstrated that the peptide was not bioactive (Figure 5.7). A possible explanation for the loss of activity is the inability of sublancin to fold correctly. As seen in Chapter 2, the N-terminus of sublancin folds inwards and helps keep the loop region in place. We suspect that the fluorescein moiety sterically blocks interactions between the N-terminal portion and the loop region, thus preventing the correct folding of the fluorescent peptide.

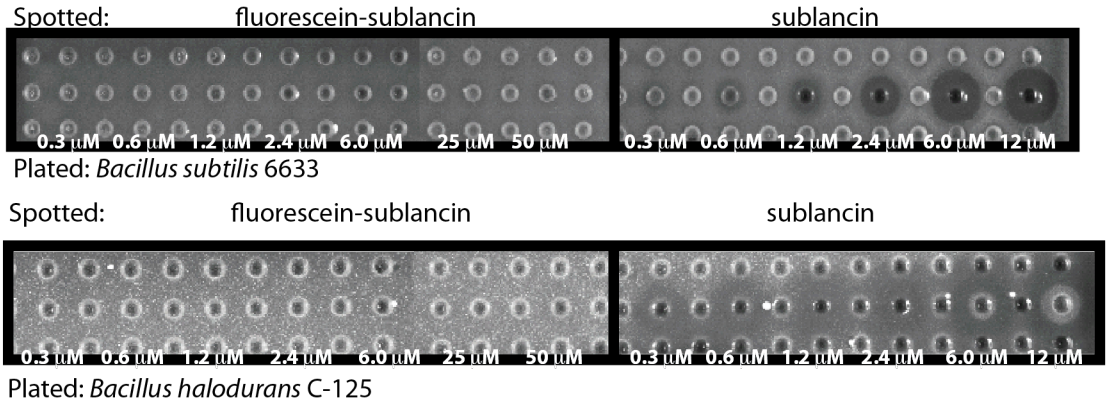

Figure 5.7 Bioassay of N-terminal fluorescein labeled sublancin against *Bacillus* strains.
Antimicrobial activity assays of synthetic N-terminally labeled fluorescein-sublancin and sublancin (control) against *B. subtilis* ATCC 6633 (top) and *B. halodurans* C-125 (bottom). The concentration of peptide used is indicated. Authentic sublancin standards produced by and purified from *B. subtilis* 168 were used as positive controls.

5.2.2 C-terminal fluorescent sublancin analogs are active against sensitive *Bacillus* cells

Given that N-terminal labeling of sublancin resulted in the loss of activity, we shifted our focus to other potential modifications. Previous studies on peptides that target lipid II have taken advantage of unique carboxylic acids in the peptide structure of interest.[13] Fortunately, sublancin also contains a unique carboxylic acid at the C-terminus due to the lack of glutamates and aspartate residues throughout its core sequence. In addition, the solution NMR structure of sublancin (Figures 2.5, 2.7, and 2.8) shows that the C-terminal tail does not interact with the bulk of the structure and therefore it is not expected to affect the folding of sublancin; thus, we hoped that C-terminally labeled sublancin would be bioactive.

The unique carboxylic acid of naturally produced sublancin was labeled with fluoresceinyl glycine amide (a.k.a. 5-(aminoacetamido)fluorescein (AAA-flu), Figure 5.8) via a HOAt/EDC coupling reaction in dimethylformamide (DMF) followed by HPLC purification and MALDI-TOF MS analysis (Figure 5.9). Bioassays of C-terminal fluoresceinyl glycine amide labeled sublancin against *B. subtilis* ATCC 6633 demonstrated roughly four-fold decrease in

activity as compared to wild type sublancin based on the size of the zone of growth inhibition (Figure 5.10). We also tested the activity of this fluorescent analog against the producer strain, *Bacillus subtilis* 168, as a control. The producer strain contains the immunity protein SunI and was thus expected to be resistant to the labeled analogs. The faint inhibition zones observed against the producer strain are due to the very high concentrations of sublancin and sublancin analogs used.

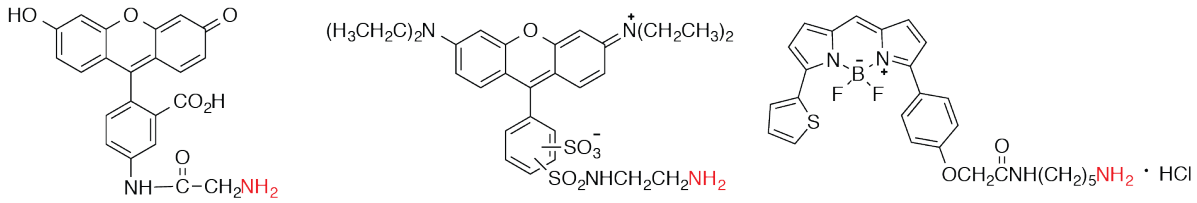

Fluoresceinyl Glycine Amide
[5-(Aminoacetamido)Fluorescein]
Molecular formula: $C_{22}H_{16}N_2O_6$
Molecular weight: 404.38
Excitation λex 492 nm
Emission λem: 514 nm

Lissamine™rhodamine B ethylenediamine
Molecular formula: $C_{29}H_{36}N_4O_6S_2$
Molecular weight: 600.74
Excitation λex 570 nm
Emission λemx: 590 nm

BODIPY® TR Cadaverine
Molecular formula: $C_{26}H_{28}BClF_2N_4O_2S$
Molecular weight: 544.85
Excitation λex: 588 nm
Emission λem: 620 nm

Figure 5.8 Amine-containing fluorophores used for labeling of sublancin at the C-terminus.
Fluoresceinyl glycine amide (left), LissamineTMRhodamine B ethylenediamine (center) and BODIPY®TR Cadaverine (right) dyes were used to label wild type sublancin at the C-terminus via HOAt/EDC coupling in DMF.

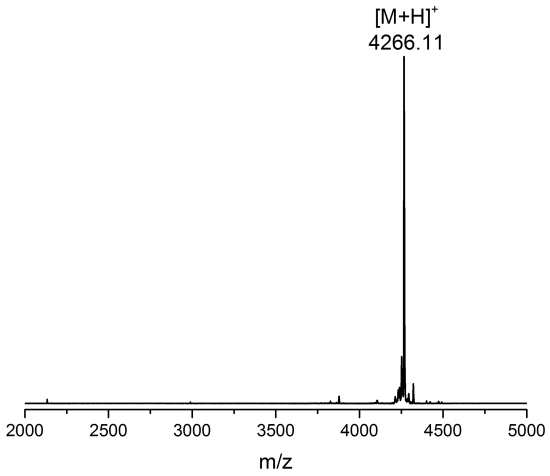

Figure 5.9 MALDI-TOF MS analysis of sublancin-fluorescein.
The unique carboxylic acid of naturally produced sublancin was labeled with fluoresceinyl glycine amide via a HOAt/EDC coupling in DMF followed by HPLC purification and MALDI-TOF MS analysis. Expected [M+H]: 4265.76, observed: 4266.11.

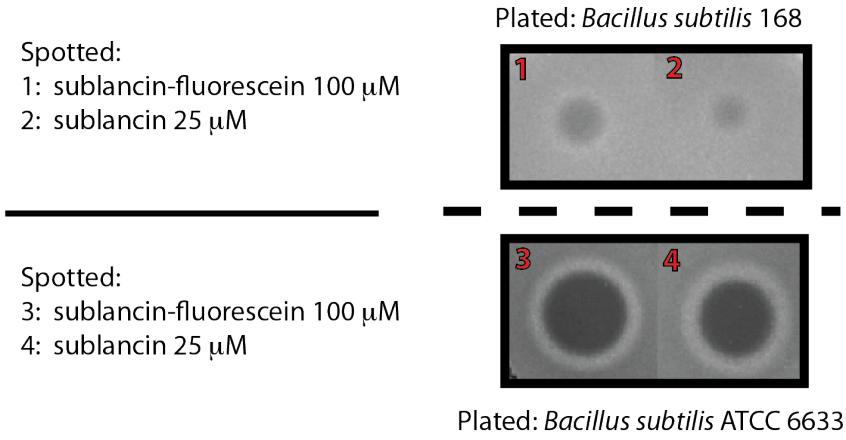

Figure 5.10 Sublancin-fluorescein bioactivity assay against producer and sensitive *Bacillus* strains.
Bioactivity assay of sublancin-fluorescein against its producer strain *Bacillus subtilis* 168 (panels 1 & 2) and the sensitive strain *Bacillus subtilis* ATCC 6633 (panels 3 & 4). In panels 1 and 3, 10 μL of 100 μM sublancin-fluorescein were spotted. In panels 2 and 4, 10 μL of 25 μM of sublancin were spotted. Faint inhibition zones were observed due to the high concentrations of sublancin and sublancin analogs spotted on the plates.

5.2.3 Confocal fluorescent microscopy studies

Wide-field fluorescence microscopy images are produced by flooding the entire sample evenly with light from the source. In contrast, confocal microscopy uses a pinhole in front of the detector to eliminate any out-of-focus signal.[14] Confocal microscopy produces higher resolution images as compared to wide-field fluorescence microscopy, but unfortunately any fluorophores within 200 nm of each other will appear as one fuzzy spot.[15]

Bacillus halodurans C-125 sensitive cells were incubated with sublancin-fluorescein, washed with buffer and immobilized with 2% low-gelling agarose before being imaged by confocal microscopy. Confocal microscopy imaging revealed the localization of the peptide to specific regions throughout the *Bacillus* cells, with higher fluorescence observed concentrated at the poles and septa. It was difficult to obtain clear images using fluorescein due to the rapid photobleaching under extensive laser exposure.[16] Furthermore, extensive laser exposure caused

the 2% low-gelling agarose to start melting, allowing the cells to move. To solve the issue of photobleaching, more photo stable fluorescent sublancin analogs were synthesized. Due to the higher stability of rhodamine and BODIPY dyes, I labeled sublancin with both Lissamine^{TM} rhodamine B ethylenediamine and BODIPY®TR cadaverine (Figure 5.8) at the C-terminus following the procedure used for fluoresceinyl glycine amide (Figures 5.11 and 5.12). Bioassays of sublancin C-terminally labeled with Lissamine^{TM} rhodamine B ethylenediamine or BODIPY®TR cadaverine against sensitive *Bacillus subtilis* ATCC 6633 demonstrated a decrease in activity compared to wild type sublancin (Figure 5.13).

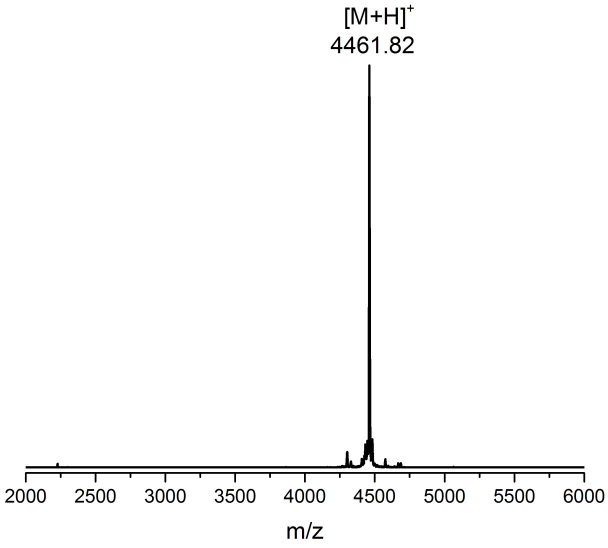

Figure 5.11 MALDI-TOF MS analysis of sublancin-LissamineRhodamine.

Sublancin was labeled with Lissamine^{TM} rhodamine B ethylenediamine via a HOAt/EDC coupling in DMF followed by purification by reversed phase (C18) HPLC and analyzed by MALDI-TOF MS. Expected [M+H]: 4462.13, observed: 4461.82.

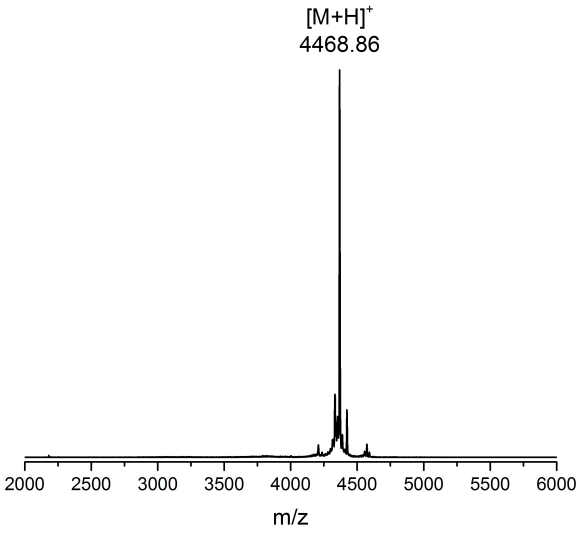

Figure 5.12 MALDI-TOF MS analysis of sublancin-BODIPY.

Sublancin was labeled with BODIPY®TR cadaverine via HOAt/EDC coupling in DMF followed by purification by reversed phase (C18) HPLC and analyzed by MALDI-TOF MS. Expected [M+H]: 4469.68, observed: 4468.86.

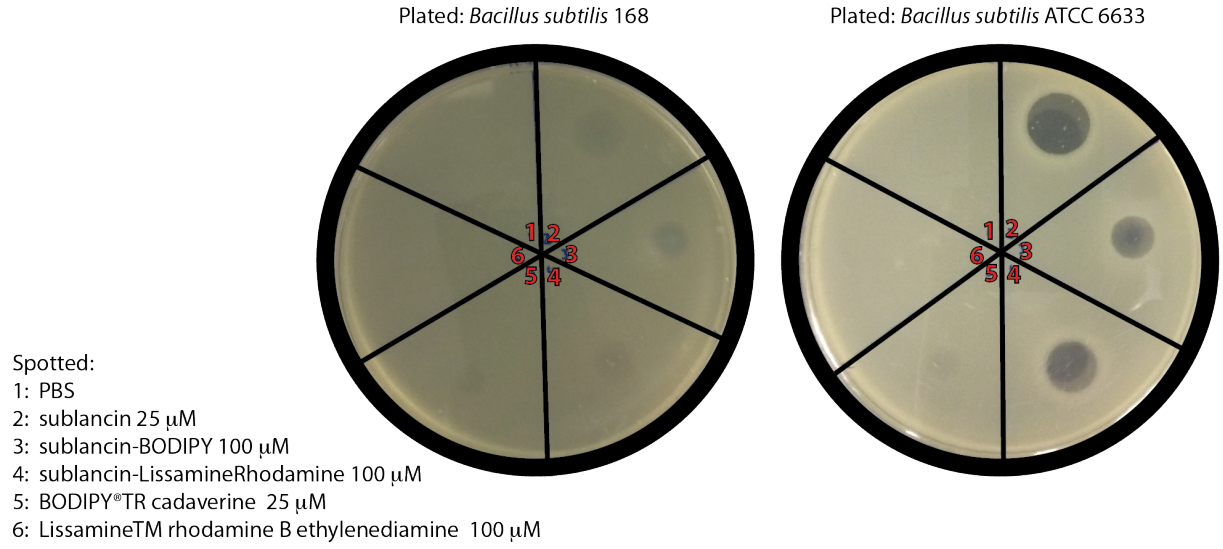

Figure 5.13 Sublancin-BODIPY and sublancin-LissamineRhodamine bioassays against sublancin producer and sensitive *Bacillus* strains.

Bioassays of C-terminal BODIPY®TR cadaverine and Lissamine™ rhodamine B ethylenediamine labeled sublancin against sensitive *Bacillus subtilis* ATCC 6633 (right) demonstrated a decrease in activity compared to wild type sublancin. Faint inhibition zones were observed due to the high concentrations of sublancin and sublancin analogs spotted on the plates (left).

Confocal microscopy with sublancin-BODIPY and sublancin-LissamineRhodamine resulted in a more intense and stable fluorescent signal under extensive laser exposure. As with fluorescein, untreated cells and sublancin treated *Bacilli* did not display autofluorescence. Figure 5.14 shows data demonstrating localization of sublancin to specific regions of the bacterial cells. Obtaining Z-stacks of the samples resulted in the melting of the agarose used to immobilize the cells. Unfortunately we were unable to determine with precision whether sublancin localizes to the cell membrane or inside the cell.

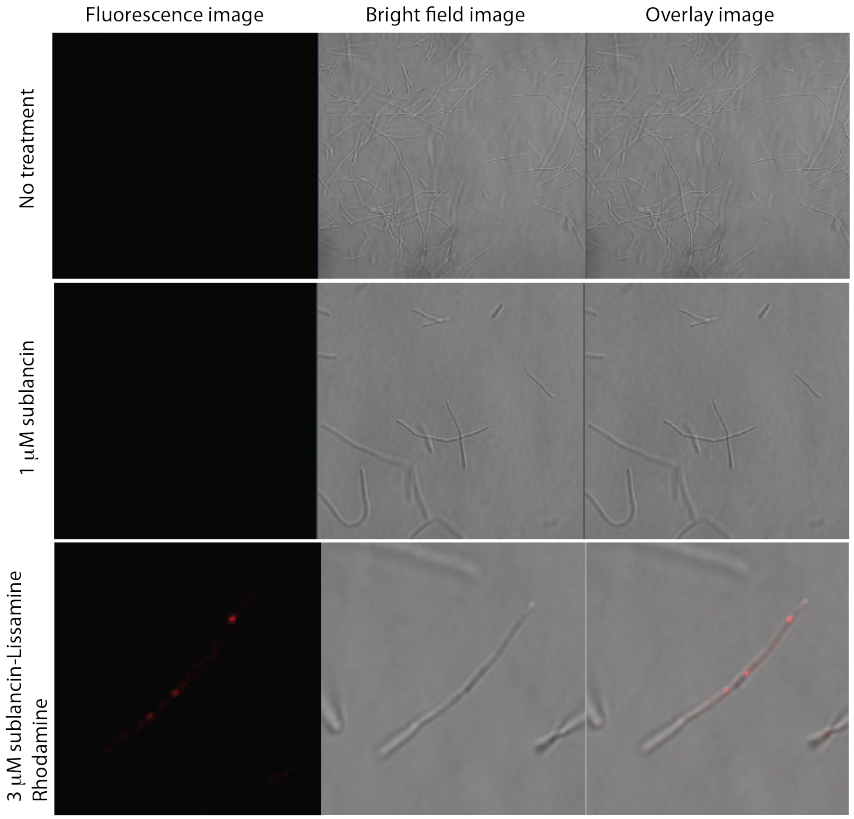

Figure 5.14 Confocal fluorescence microscope images of *Bacillus halodurans* C-125 cells treated with sublancin-LissamineRhodamine.

Bacillus halodurans C-125 cells were treated with sublancin-LissamineRhodamine at 37 ºC for 30 min. Images were collected under 560 nm excitation. Dark left most panels show the fluorescence images, middle panels show the differential interference contrast (DIC) or bright field images and the right panels show the overlay image for not treated (top), 1 μM sublancin treated (middle) and 3 μM sublancin-LissamineRhodamine treated *Bacillus* cells (bottom).

5.2.4 Localization studies using super resolution microscopy

Every fluorescent molecule is able to give out a finite number of photons before it is bleached; in other words, every photon is precious. Stochastic optical reconstruction microscopy (STORM) is a technique that utilizes the successive activation and time-resolved localization of photoswitchable fluorescent molecules to create high-resolution images.[17,18] STORM offers an alternative method to confocal microscopy for determining with higher precision whether the fluorescent sublancin analogs localize to the cell membrane. The fluorescent dyes used so far (fluorescein, BODIPY, Lissamine Rhodamine) are not photoswitchable. We proceeded to label sublancin with Cyanine 5-amine a bright, far-red-fluorescent dye with excitation ideally suited for 647 nm lasers (Figures 5.15 and 5.16). As demonstrated for other sublancin C-terminal fluorescent analogs, sublancin-Cy5 was active against *Bacillus* strains (Figure 5.17). The minimum inhibitory concentration (MIC) of sublancin-Cy5 against *Bacillus halodurans* C-125 was determined to be 1.82 μM, about 5.5 times higher than that for wild type sublancin (Figure 5.17).

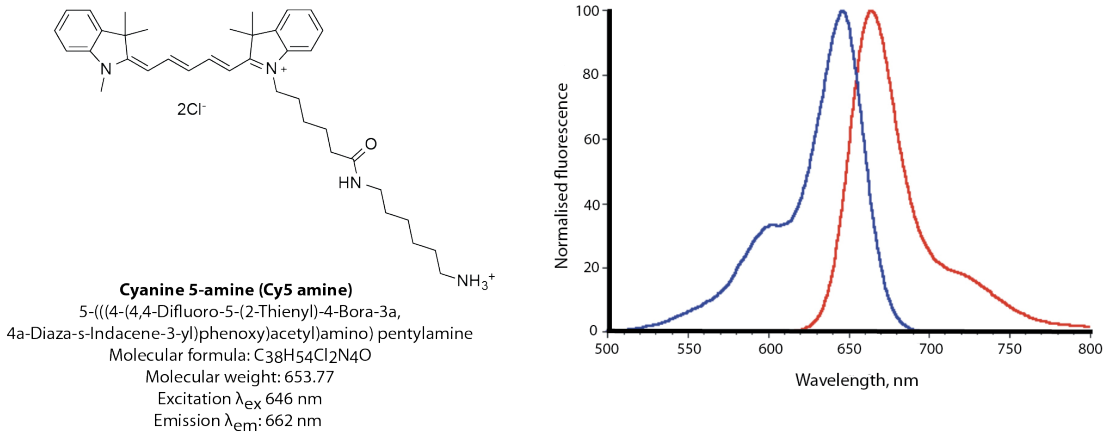

Figure 5.15 Cyanine 5-amine dye structure and absorption and emission spectra.
Adsorption spectra (blue) and emission spectra (red) are shown (http://www.lumiprobe.com/p/cy5-amine)

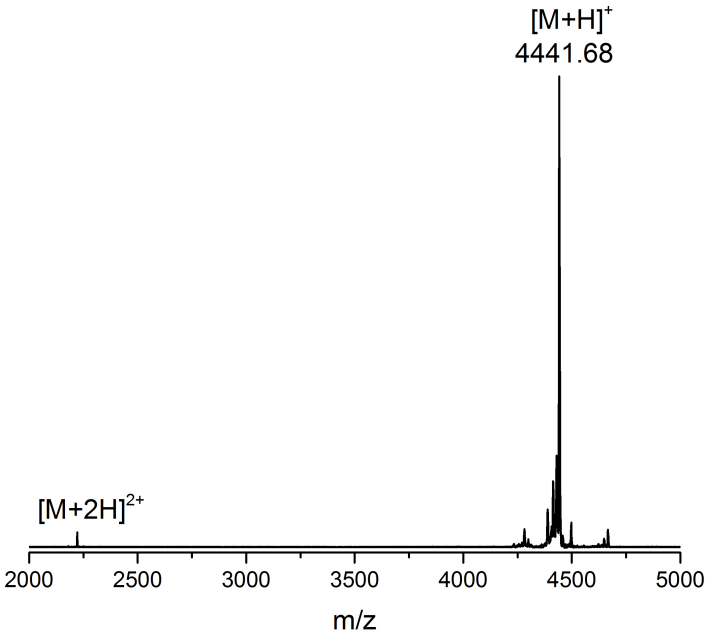

Figure 5.16 MALDI-TOF MS analysis of sublancin-Cy5.

Sublancin was labeled with Cyanine 5-amine via a HOAt/EDC coupling in DMF followed by purification by reversed phase (C18) HPLC and analyzed by MALDI-TOF MS. Expected [M+H]: 4442.17, observed: 4441.68.

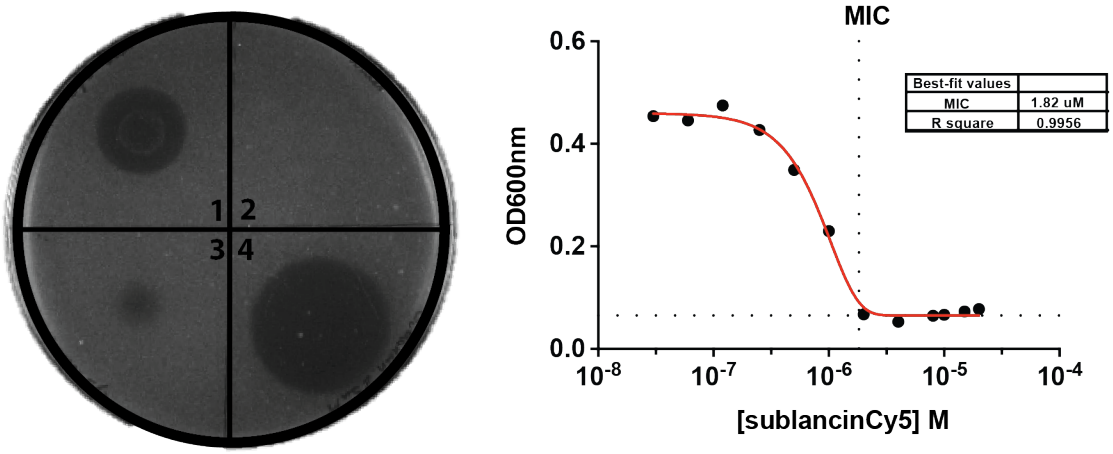

Figure 5.17 Bioactivity assay and MIC of sublancin-Cy5 against *B. halodurans* C-125.

Bioactivity assay of sublancin-Cy5 (left). The following were spotted in the bioassay: (1) 60 μM sublancin-Cy5, (2) Phosphate-buffered saline (PBS), (3) 100 μM Cyanine 5-amine (observed spot is the blue dye) and (4) 25 μM sublancin. MIC determination of sublancin-Cy5 against *B. halodurans* C-125 (right). The MIC was determined to be 1.82 μM, about 5.5 times greater than that of *B. subtilis* 168 produced sublancin.

STORM images from *Bacillus halodurans* C-125 treated with 3 μM or 1 μM sublancin-Cy5 and then washed five times with buffer had too much background (Figure 5.18a,b). Treating the bacteria with 1 μM sublancin-Cy5 and washing 10 times resulted in reduced background intensity (Figure 5.18c,d,e). *B. halodurans* C-125 cells grow in chains, making it difficult to distinguish one cell from the next. To do so, we examined a smaller area in more detail (Figure 5.18c,d), combining the 20,000 frames taken to create the STORM images to generate a 3D representation of the area surrounding three intense fluorescent signals (Figure 5.18d). A screen shot of the 3D representation clearly shows the outline of a cell with increased fluorescence at the poles (Figure 5.18e).

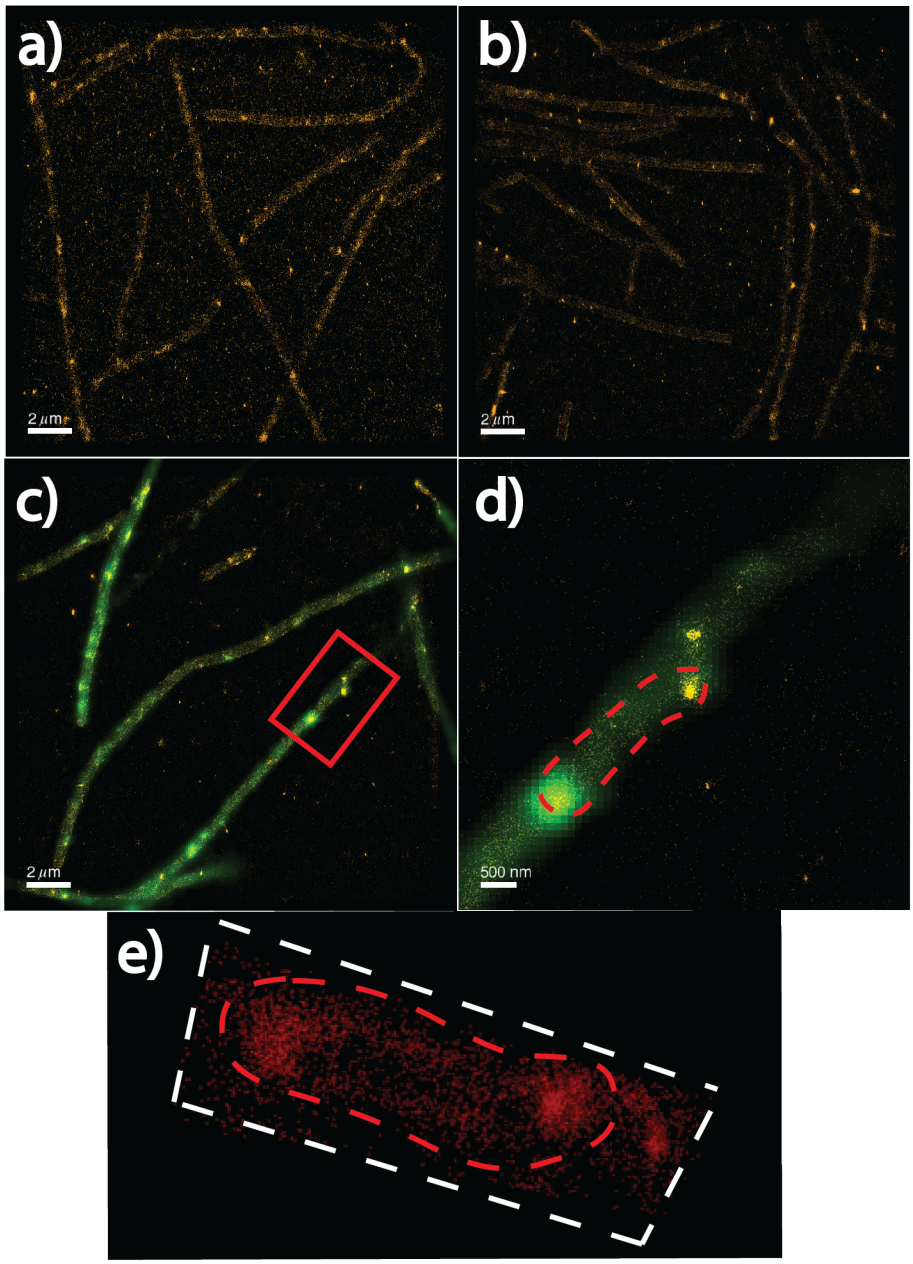

Figure 5.18 STORM image of sublancin-Cy5 incubated with *Bacillus halodurans* C-125.

STORM images from *Bacillus halodurans* C-125 treated with (a) 3 μM or (b) 1 μM sublancin-Cy5 and then washed five times with buffer had too much background. (c,d,e) *Bacillus halodurans* C-125 treated with 1 μM sublancin-Cy5 and washed 10 times. (d) Zoomed in image of the red boxed area from (c), image (d) was used to create a 3D representation of the area surrounding the three intense fluorescent signals. (e) A 2D screen shot of the 3D representation of (d) showing the outline of a cell with increased fluorescence at the poles. The orange line represents the outline of the cell based on the bright field image.

Unable to determine convincingly whether sublancin acts by entering the cells because of the background fluorescent noise, Seonjin Park from the Taekjip Ha lab and I proceeded to take images using super resolution structured illumination microscopy (SR-SIM). Unlike STORM, which takes advantage of photoactive molecules, SR-SIM is a wide field technique that uses a grating pattern to illuminate the sample. The pattern aids in the computational removal of out-of-focus blur.[19] SIM images also have enhanced lateral resolution achieved by acquiring multiple raw images of the biological sample while rotating the grid pattern at a specified angle (usually 60 degrees) and using a specialized algorithm to reconstruct a final image.[19] A Zeiss Elyra S1 instrument was used to take Z-stack images of *B. halodurans* C-125 treated with 1 μM sublancin-Cy5. The SIM images showed that sublancin localizes to the membrane of the cell and is not spread inside the cell (Figures 5.19, and 5.20). Consistent with data from confocal microscopy and STORM, areas of intense fluorescence include the septa and the poles.

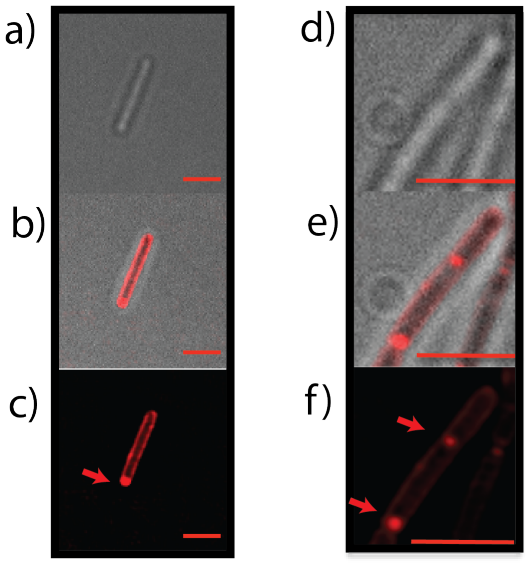

Figure 5.19 SR-SIM image of sublancin-Cy5 incubated with *Bacillus halodurans* C-125.
(a, d) Wide field images, (b, e) overlays of fluorescent and wide field images (c, f) fluorescent images taken using a 642 nm laser showing sublancin-Cy5 localizing to the membrane and poles of the bacteria. The red lines denote a 2 μm length. Red arrows point to the septa and poles of the cells.

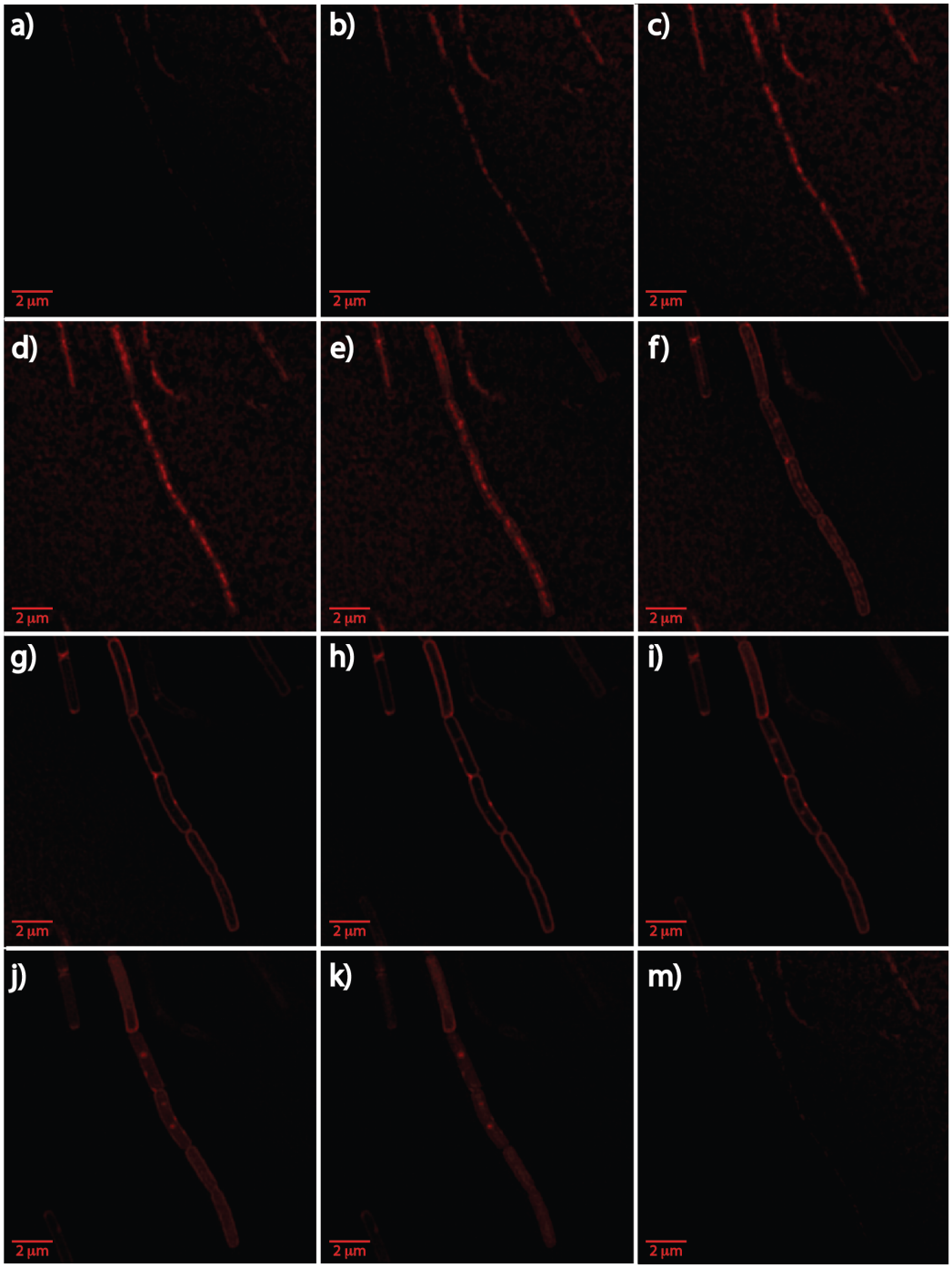

Figure 5.20 SR-SIM Z-stack slides of sublancin-Cy5 incubated with *Bacillus halodurans* C-125.

Consecutive SR-SIM Z-stack images (a) bottom of stack and (m) top of stack of *Bacillus halodurans* C-125 cells treated with 1 µM sublancin-Cy5. The slides are each 0.100 µm of a 1.60 µm total thickness. The red lines denote a 2 µm length.

5.2.5 Unlabelled wild type sublancin decreases the binding of sublancin-Cy5 as observed by SR-SIM

SR-SIM imaging showed that sublancin-Cy5 localizes to the cell membrane and poles. To determine whether sublancin-Cy5 and naturally produced sublancin both bind to the same target we carried out competition experiments between the two peptides. *Bacillus halodurans* C-125 cells were grown to exponential phase and treated with 1 μM sublancin-Cy5 only, 1 μM sublancin-Cy5 and 0.2 μM sublancin, or 1 μM sublancin-Cy5 and 1 μM sublancin. The samples were then incubated for 30 min at 37 ºC, followed by 10 washes with buffer before analysis by SR-SIM. As the concentration of sublancin was increased we observed a decrease in the normalized mean fluorescence intensity per bacterial cells suggesting that these two antibiotics may compete for the same target (Figure 5.21). The normalized mean fluorescence was calculated by the addition of fluorescence from all Z-stacks taken from a single imaging event and dividing by the number of bacteria imaged.

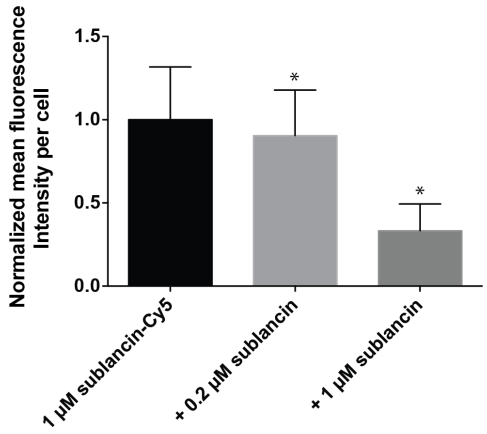

Figure 5.21 Competition of sublancin and sublancin-Cy5.

Bacillus halodurans C-125 cells were grown to exponential phase and treated with 1 μM sublancin-Cy5, 1 μM sublancin-Cy5 and 0.2 μM sublancin, or 1 μM sublancin-Cy5 and 1 μM sublancin. As the concentration of wild type sublancin was increased the fluorescence intensity decreased, suggesting that the two peptides compete for the same target. * indicates a $P < 0.05$ between addition of sublancin relative to sublancin-Cy5 treated cells. The means of the data from a single experiment conducted in triplicate are shown. The data are representative of those from three independent experiments. Error bars indicate standard deviations.

5.2.6 Glucose and NaCl decrease the binding of sublancin-Cy5 to sensitive bacterial cells

Glucose and sodium chloride have both been found to affect the sensitivity to sublancin. When sensitive strains are exposed to sublancin and grown in media containing glucose, the activity of sublancin is lost (Chapter 3). When sublancin sensitive strains are grown in media lacking sodium chloride a clear inhibition zone is observed after the addition of sublancin. As the salt content of the media is increased from 0 to 5%, the sensitive cells become resistant to the effect of sublancin.[20] We investigated whether the addition of glucose, sodium chloride or a combination of both at either 5% or 10% concentration had an effect on the binding of sublancin-Cy5. In order to obtain more evidence that sublancin-Cy5 and sublancin share the same target, *Bacillus halodurans* C-125 cells were treated for 30 min with sublancin-Cy5 and glucose and/or sodium chloride. By SR-SIM we observed that as the percentage of glucose or sodium chloride was increased, the fluorescence decreased. The greatest effect was observed when glucose and sodium chloride were added in combination (Figure 5.22). The glucose-induced decrease in fluorescence is in agreement with the observation described in chapter 3 that the growth of sensitive strains with PTS sugars (e.g. glucose) results in sublancin resistance. If sublancin-Cy5 competes with glucose it is expected that increased availability of glucose would inhibit the interaction of sublancin and the PTS system. The decrease in fluorescence resulting from addition of sodium chloride agrees with MscL channel involvement in sublancin sensitivity.[20] As described in chapter 1, the MscL channel controls the efflux of osmoprotectants and osmolytes upon osmotic shock. When cells experience an abrupt decrease or increase in the osmolarity of their extracellular environment they allow ions and osmolytes to rapidly exit or enter the cell in order to maintain adequate turgor pressure. It is hypothesized that sublancin susceptibility relates

an open state of the MscL channel by acting in an opportunistic fashion. When the channel opens sublancin is able to enter the cell.

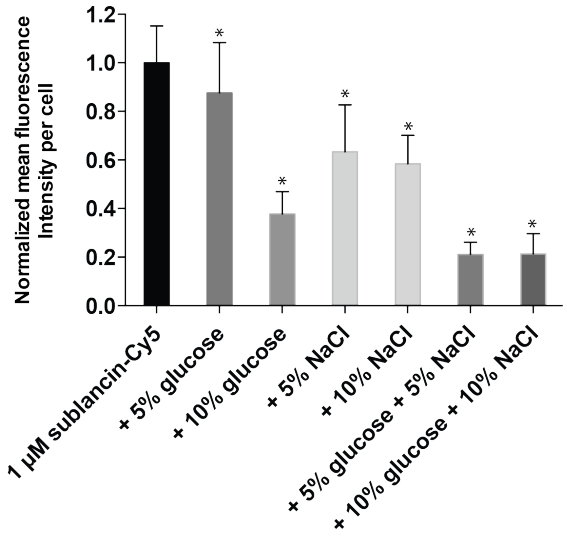

Figure 5.22 Effect of glucose and NaCl on the activity of sublancin-Cy5.

Bacillus halodurans C-125 cells were treated for 30 min with sublancin-Cy5 and glucose and/or sodium chloride. As the percentage of glucose or sodium chloride was increased the fluorescence decreased. The greatest effect was observed when glucose and sodium chloride were added in combination. * indicates a $P < 0.05$ between addition of glucose, sodium chloride or a combination of both relative to sublancin-Cy5 treated cells. The means of the data from a single experiment conducted in triplicate are shown. The data are representative of those from three independent experiments. Error bars indicate standard deviations.

5.3 SUMMARY AND OUTLOOK

In an effort to identify sublancin's localization in bacterial cells, a series of fluorescent analogues were synthesized and studied by fluorescent microscopy. The work presented in this chapter involved the use of manual and microwave assisted solid phase peptide synthesis to obtain an N-terminally labelled sublancin analog and the use of regular peptide coupling with the native producer to obtain C-terminally labelled sublancin analogs. The evidence shown represents the first in vivo localization studies of the glycocin class of RiPP natural products. The

competition experiments with wild type sublancin, glucose and sodium chloride show that the fluorescent analogs have the same target as wild type, as revealed by a decrease in fluorescence. Furthermore, although sublancin does not disrupt the membrane potential of the cell (chapter 3), we observed that it localizes to the cell membrane, poles and septa of sensitive *Bacillus* cells. In chapter 3 I discussed the involvement of the PTS in sublancin sensitivity. It has been shown that in *E.coli,* EII is localized to the cell membrane, and that EI and HPr are at the poles until HPr is phosphorylated and later released from the poles to then localize throughout the cell.[8] In the future, it would be very interesting to monitor the localization of GFP-HPr *B. subtilis*[8] when incubated with glucose, sublancin-Cy5, and both.

5.4 EXPERIMENTAL

5.4.1 Materials, cultures, and conditions

All chemicals and HPLC grade solvents were purchased from Sigma-Aldrich (St. Louis MO). Growth media were obtained from Difco Laboratories (Detroit MI) and Luria Bertoni (LB) was also purchased from BD Biosciences. Tris, MOPS, and HEPES buffers were obtained from Fisher and α-cyano-4-hydroxy-cinnamic acid was obtained from Fluka. Matrix-assisted laser desorption/ionization time-of-flight mass spectrometry (MALDI-TOF MS) was performed at the Mass Spectrometry Laboratory within the School of Chemical Sciences at UIUC using a Bruker Daltonics UltrafleXtreme MALDI TOFTOF instrument. Salt-containing MS samples were purified via Millipore Zip-Tip_{C18} pipette tips (Billerica MA). Forty-eight well assay plates were purchased from Corning Incorporated (Corning NY) and were read using a multi mode, single-channel Synergy H4 microplate reader from Biotek® instruments, Inc (Winooski, VT). Trays used for agar well diffusion assays were obtained from Nalge Nunc (Rochester NY).

5.4.2 Synthesis of N-terminal fluorescently labeled sublancin analog

The N-terminal fluorescently labeled sublancin analog was synthesized using the procedure applied by Hsieh and coworkers[11] to prepare wild type sublancin with the exception of the attachment of a NHS-fluorescein tag to Gly1 of the N-terminal fragment (containing amino acids 1-13) following de-O-allylation of the fragment. Unless otherwise noted, standard cycles for SPPS were performed using a fritted glass reaction vessel equipped with a N_2 inlet for resin/reagent agitation and a suction outlet for draining. Fmoc deprotection was achieved by agitating resin with 20% piperidine in dimethylformamide (DMF) for 20 min. After draining the reaction vessel, the resin was washed with DMF (3 x 30 s) and CH_2Cl_2 (2 x 30 s). The appropriately side-chain protected Fmoc-amino acid (5 equiv.) in DMF (5-10 mL) was pre-activated with (N,N'-diisopropylcarbodiimide) (DIC) and HOBt (5 equiv. each) for 5 min, then added to the resin and agitated for 45-60 min. After draining the reaction vessel, the resin was washed with DMF (3 x 30 s) and CH_2Cl_2 (2 x 30 s). The completion of all couplings was assessed by a Kaiser test; double couplings were performed as needed but were generally unnecessary. Test cleavages were performed after all coupling steps by removing a small portion of dry resin from the reaction vessel and treating with 90:5:5 TFA:H_2O:triisopropylsilane for 1 h under N_2. After removing the cleaved resin by filtration, the filtrate was concentrated under a stream of N_2. The peptide was precipitated with cold Et_2O, isolated by centrifugation and dissolved in 1:1 H_2O/MeCN. An aliquot of this solution was analyzed by MALDI-TOF MS.

5.4.3 De-allylation of sublancin 1-13 fragment and C-terminal thioesterification

Allyl deprotection: The fully assembled resin (25 μmol) was swollen in dry CH_2Cl_2 (3 mL) for 30 min under nitrogen, followed by addition of a solution of $Pd(PPh_3)_4$ (25 mg, 22 μmol) and $PhSiH_3$ (123 μl, 108 mg, 1 mmol, 40 equiv.) in 1:1 CH_2Cl_2:DMF (5 mL). The resin

was shaken for 2 h and subsequently washed with DCM (5 x 5 mL), DMF containing 0.5 % diethyldithiocarbamate (DEDTC) as a palladium scavenger (3 x 2 mL), DMF (5 x 5 mL) and DCM (5 x 5 mL). An aliquot of this solution was analyzed by MALDI-TOF MS.

N-terminal Fmoc deprotection: A solution of 1:4 piperidine:DMF (2 x 5 mL) was added to the resin and the flask was agitated for 5 min. The resin was subsequently drained and washed with DMF (5 x 3 mL), CH_2Cl_2 (5 x 3 mL) and DMF (5 x 3 mL). The resulting resin-bound amine was reacted immediately with fluorescein NHS.

N-terminal Fluorescein NHS coupling: Fluorescein NHS (2 equiv.), the N-terminal amine, and DIPEA (43.5 µl, 32.3 mg, 10 equiv.) were combined in DMF (5 mL). The completion of the couplings was assessed by a Kaiser test. The reaction was shaken for 8 h followed by washing with DCM (5 x 5 mL), DMF (5 x 5 mL) and DCM (10 x 5 mL). An aliquot of this solution was analyzed by MALDI-TOF MS.

C-terminal thioesterification: A solution of ethyl-3-mercaptopropionate (77 µl, 600 umol, 24 equiv.), HCTU (310 mg, 750 µmol 30 equiv.), and DIPEA (161 µl, 121 mg, 938 µmol, 37.5 equiv.) in 4:1 CH_2Cl_2DCM:DMF (1.5 mL) was added to the resin-bound fluorescein-labeled peptide and the reaction vessel was shaken for 1 h at 25 ºC. The procedure was repeated once and the resin was washed with CH_2Cl_2 (5 x 5 mL), DMF (5 x 5 mL) and CH_2Cl_2 (10 x 5 mL).

Cleavage from resin: A mixture of TFA, triisopropylsilane and water (90:5:5) was added to the resin. After 2 h, the resin was washed with TFA (4 x 4 mL). After removing the cleaved resin by filtration, the filtrate was concentrated under a stream of N_2. The peptide was precipitated with cold Et_2O, isolated by centrifugation and dissolved in 1:1 H_2O/MeCN. An aliquot of this solution was spotted onto a MALDI-TOF MS target for analysis. If the test cleavage was successful and MALDI-TOF MS spectra looked good, all peptide was cleaved from

resin by treating with 90:5:5 TFA:TIPS:H_2O. After removing the cleaved resin by filtration, the filtrate was concentrated under a stream of N_2. The peptide was precipitated with cold Et_2O, isolated by centrifugation and dissolved in 1:1 H_2O/MeCN. The peptide was then lyophilized to dryness, taken up in 0.1% TFA/H_2O and analyzed by analytical RP-HPLC affording the desired N-terminal fragment.

5.4.4 Synthesis of Sublancin 14-37 fragment

Fmoc-Arg-Wang resin (0.8 g) was used with a loading capacity of 0.5 mmol/g. The resin was first swollen in 5 mL of dimethylformamide (DMF) by sparging with N_2 in a coarse fritted filter. After draining the reaction vessel, the resin was washed with DMF (3 x 30 s). Fmoc deprotection was achieved by agitating the resin with 20% piperidine in DMF for 20 min. The resin was then drained and washed with DMF (3 x 30 s), CH_2Cl_2 (2 x 30 s) and DMF (3 x 30 s). A Kaiser test to probe the efficiency of the deprotection was completed as necessary. Three solutions were used: 5 g of ninhydrin in 100 mL of ethanol, 80 g of phenol in 20 mL of ethanol, and 2 mL of 1 mM aq. KCN in 98 mL of pyridine. A small amount of beads was removed from the reaction vessel and placed in a 6x50 mm test tube. Three drops of each of the three solutions were then added to the test tube. Three drops of each solution were also added to a second test tube containing no beads, which serves as the negative control. The test tube was shaken in front of a heat gun or put in a hot water bath for 1 min. A deep blue-purple color observed after 30 s to 1 min indicates a positive test (i.e. the presence of a free amine).

Coupling steps were completed using 4 equivalents of amino acids relative to the resin loading. The appropriate side-chain protected Fmoc-amino acid in DMF (5-10 mL) was pre-activated with DIC (N,N'-diisopropylcarbodiimide) and HOBt (4 equiv. each, 1.6 mmol) for 5 min, then added to resin and agitated for 45-60 min. After draining the reaction vessel, the resin was

washed with DMF (3 x 30 s), CH_2Cl_2 (2 x 30 s) and DMF (3 x 30 s). The completion of all couplings was assessed by a Kaiser test; Test cleavages were performed after all coupling steps by removing a small portion of dry resin from the reaction vessel and treating with 90:5:5 TFA/H_2O/triisopropylsilane for 1 h under N_2. After removing the cleaved resin by filtration, the filtrate was concentrated under a stream of N_2. The peptide was precipitated with cold Et_2O, isolated by centrifugation and dissolved in 1:1 H_2O/MeCN. An aliquot of this solution was spotted onto a MALDI-TOF MS target for analysis. Any remaining free resin sites were capped by agitation in 90:8:2 DMF:acetic anhydride:DIPEA for 15 min. If the test cleavage was successful and MALDI spectra looked good, all peptide was cleaved from the resin by treating with 90:5:5 TFA:TIPS:H_2O. After removing the resin by filtration, the filtrate was concentrated under a stream of N_2. The peptide was precipitated with cold Et_2O, isolated by centrifugation and dissolved in 1:1 H_2O/MeCN. The peptide was then lyophilized to dryness, taken up in 0.1% TFA/H_2O and analyzed by analytical RP-HPLC.

5.4.5 Native chemical ligation of sublancin fragments

Ligation buffer was prepared by dissolving 4-mercaptophenylacetic acid (MPAA, final conc. = 200 mM) and TCEP (final conc. = 20 mM) in 6 M guanidine hydrochloride/0.2 M Na_2HPO_4 buffer. The pH was adjusted to 7.2 by the addition of 5.0 M HCL and the mixture was degassed with argon. A solution of the NHS-Fluorescein-sublancin1-13 thioester (1 mM) and sublancin14-37 (0.5 mM) was prepared in the above ligation buffer and the pH was carefully adjusted to 7.0-7.2 by addition of 2.0 M NaOH. The reaction was flushed with argon and allowed to incubate at 25 $^{\circ}$C for 24 or 42 h with reaction monitoring by LC-MS. The reaction was quenched by the addition of 0.1% formic acid in water at 24 h and 42 h. TCEP (20 mg/mL) was added to the ligation mixture prior to purification by reversed phase (C18) analytical HPLC.

5.4.6 Synthesis of C-terminal fluorescently labeled sublancin

Fluoresceinyl glycine amide (5-(aminoacetamido)fluorescein, AAA-flu), LissamineTM rhodamine B ethylenediamine, BODIPY® TR cadaverine or Cy5-amine, were coupled to the unique carboxylic acid of sublancin by incubation overnight at room temperature in 100 µl DMF containing 50 nmol peptide, 50 nmol fluorophore-amine and 60 nmol of both EDC and HOAt. After evaporation of the DMF, the labeled sublancin was purified from the reaction mixture using reversed phase (C18) HPLC.

5.4.7 Preparation of culture samples for microscopy

Overnight cultures of *B. halodurans* C-125 and *B. subtilis* ATCC 6633 were prepared in LB and grown at 37 ºC under vigorous agitation. A 150 µL aliquot from each overnight culture was used to inoculate 5 mL of LB. The cultures were grown to an OD of 0.5 then transferred to 2.0 mL Eppendorf tubes and centrifuged at 1,500 × g for 3 min. Into the tubes with cells were added cold solutions of fluorescently labeled sublancin at the desired concentration in 1X Dulbecco's Phosphate-Buffered Saline (D-PBS) (1 mL, Fisher Scientific). The reactions were incubated at 37 ºC for 30 min then centrifuged at 1,500 × g for 1 min at 25 °C. The supernatant was carefully removed and the cells were carefully suspended in 1 mL of 1X D-PBS. The solution was again centrifuged at 1,500 × g for 1 min at 25 °C, the supernatant was removed, and cells were carefully suspended in 1 mL of 1X D-PBS. Finally, the suspension was centrifuged and D-PBS was removed to give a final volume of 250 µL.

5.4.8 Confocal microscopy slide preparation

Aliquots of the suspension (10 µL) and liquified low-gelling agarose (10 µL, 1.5%) were added to a microscopy plate and the localization of the lantibiotic was analyzed by confocal fluorescence microscopy. The microscopy images were taken by focusing the cells first in the

bright field channel and recording an image. The channel was later switched to the fluorescence settings with appropriate excitation. An excitation wavelength of 488 nm was used for fluorescein and 560 nm for Lissamine Rhodamine and Bodipy. The laser power was adjusted and the confocal plane was changed stepwise to a obtain a clear image.

5.4.9 Stochastic super resolution (STORM) and SR-SIM microscopy slide preparation

Microscopy slides were coated with poly-L-lysine (Sigma, sold as 0.10% (w/v) solution in water), a positively charged amino acid polymer, by incubation with the coating solution 30 min at room temperature followed by washing with water or buffer. The surface was then dried with nitrogen. The bacterial cells treated with fluorescently labeled sublancin were resuspended in 500 µL (final volume) of Tris buffer (10 mM NaCl, 50 mM Tris pH 8.5, 10% glucose). For every 500 µL of Tris buffer, 5 µL of 1 M MEA (2-mercaptoethylamine hydrochloride, 10 µM final concentration), 3 µL of 70 mg/mL pyranose oxidase and 1 µL of 16 mg/ml of catalase were added. Pyranose oxidase and catalase function as oxygen scavengers to suppress photobleaching by oxygen. MEA serves as oxygen scavenger and as a triplet quencher, thereby recovering molecules from the dark state to let them blink over and over. A 405 nm laser was used for STORM. The microscopy images were taken by focusing the cells first in the bright field channel and recording an image. The channel was later switched to the fluorescence settings with appropriate excitation for cyanine 5-amine. An excitation wavelength of 642 nm was used. The laser power was adjusted and the confocal plane was changed stepwise to a obtain a clear image.

5.4.10 Competition experiment between sublancin-Cy5 and sublancin, glucose or sodium chloride.

Overnight cultures of *B. halodurans* C-125 were prepared in LB and grown as described under the culture sample microscopy preparation, with the exception that into the 2.0 mL Eppendorf tubes cold solutions of fluorescently labeled sublancin and either glucose, sodium chloride or sublancin were added, at the desired concentration in 1X Dulbecco's Phosphate-Buffered Saline (D-PBS) (1 mL, Fisher Scientific). The reactions were incubated at 37 °C for 30 min. At this time the reactions were centrifuged at 4 °C (1 min, 1,500 × g). The supernatant was carefully removed and the cells were carefully suspended in 1 mL of 1X D-PBS (wash step). The solution was again centrifuged, the supernatant was removed, and cells were carefully suspended in 1 mL of 1X D-PBS a total of 10 times. Finally, the suspension was centrifuged and D-PBS was removed to give a suspension of around 250 μL. The microscopy slides were prepared as described above. The microscopy images were taken by focusing the cells first in the bright field channel and recording an image. The channel is later switched to the fluorescence settings with appropriate excitation for cyanine 5-amine. An excitation wavelength of 642 nm was used. The laser power was adjusted and the confocal plane was changed stepwise to a obtain a clear image.

5.5 REFERENCES

(1) Novo, D. J.; Perlmutter, N. G.; Hunt, R. H.; Shapiro, H. M. *Antimicrob Agents Chemother* **2000**, *44*, 827. "Multiparameter flow cytometric analysis of antibiotic effects on membrane potential, membrane permeability, and bacterial counts of Staphylococcus aureus and Micrococcus luteus".

(2) Brogden, K. A. *Nat Rev Microbiol* **2005**, *3*, 238. "Antimicrobial peptides: pore formers or metabolic inhibitors in bacteria?".

(3) Jenssen, H.; Hamill, P.; Hancock, R. E. *Clin Microbiol Rev* **2006**, *19*, 491. "Peptide antimicrobial agents".

(4) Mihajlovic, M.; Lazaridis, T. *Biochim Biophys Acta* **2010**, *1798*, 1494. "Antimicrobial peptides bind more strongly to membrane pores".

(5) Breukink, E.; de Kruijff, B. *Nat Rev Drug Discov* **2006**, *5*, 321. "Lipid II as a target for antibiotics".

(6) Oman, T. J.; Lupoli, T. J.; Wang, T.-S. A.; Kahne, D.; Walker, S.; van der Donk, W. A. *J Am Chem Soc* **2011**, *133*, 17544. "Haloduracin α Binds the Peptidoglycan Precursor Lipid II with 2:1 Stoichiometry".

(7) Govindarajan, S.; Elisha, Y.; Nevo-Dinur, K.; Amster-Choder, O. *MBio* **2013**, *4*, e00443. "The general phosphotransferase system proteins localize to sites of strong negative curvature in bacterial cells".

(8) Lopian, L.; Elisha, Y.; Nussbaum-Shochat, A.; Amster-Choder, O. *EMBO J* **2010**, *29*, 3630. "Spatial and temporal organization of the E. coli PTS components".

(9) Saier, M. H., Jr.; Reizer, J. *J Bacteriol* **1992**, *174*, 1433. "Proposed uniform nomenclature for the proteins and protein domains of the bacterial phosphoenolpyruvate: sugar phosphotransferase system".

(10) Mochon, A. B.; Liu, H. *PLoS Pathog.* **2008**, *4*, e1000190. "The antimicrobial peptide histatin-5 causes a spatially restricted disruption on the Candida albicans surface, allowing rapid entry of the peptide into the cytoplasm".

(11) Hsieh, Y. S.; Wilkinson, B. L.; O'Connell, M. R.; Mackay, J. P.; Matthews, J. M.; Payne, R. J. *Org Lett* **2012**, *14*, 1910. "Synthesis of the bacteriocin glycopeptide sublancin 168 and S-glycosylated variants".

(12) Oman, T. J.; Boettcher, J. M.; Wang, H.; Okalibe, X. N.; van der Donk, W. A. *Nat Chem Biol* **2011**, *7*, 78. "Sublancin is not a lantibiotic but an S-linked glycopeptide".

(13) Hasper, H. E.; Kramer, N. E.; Smith, J. L.; Hillman, J. D.; Zachariah, C.; Kuipers, O. P.; de Kruijff, B.; Breukink, E. *Science* **2006**, *313*, 1636. "An alternative bactericidal mechanism of action for lantibiotic peptides that target lipid II".

(14) Pawley, J. *Handbook of Biological Confocal Microscopy*; Springer US, 2006.

(15) Sauer, M.; Hofkens, J.; Enderlein, J. *Handbook of Fluorescence Spectroscopy and Imaging*; WILEY-VCH Verlag GmbH & Co. KGaA, 2010.

(16) Price, R.; Jerome, W. *Basic Confocal Microscopy*; Springer Science & Business Media, 2011.

(17) Fernandez-Suarez, M.; Ting, A. Y. *Nat Rev Mol Cell Biol* **2008**, *9*, 929. "Fluorescent probes for super-resolution imaging in living cells".

(18) Rust, M. J.; Bates, M.; Zhuang, X. *Nat Methods* **2006**, *3*, 793. "Sub-diffraction-limit imaging by stochastic optical reconstruction microscopy (STORM)".

(19) Shao, L.; Kner, P.; Rego, E. H.; Gustafsson, M. G. L. *Nat Methods* **2011**, *8*, 1044. "Super-resolution 3D microscopy of live whole cells using structured illumination".

(20) Kouwen, T. R.; Trip, E. N.; Denham, E. L.; Sibbald, M. J.; Dubois, J. Y.; van Dijl, J. M. *Antimicrob Agents Chemother* **2009**, *53*, 4702. "The large mechanosensitive channel MscL determines bacterial susceptibility to the bacteriocin sublancin 168".

CHAPTER 6. MECHANISTIC UNDERSTANDING OF SUBLANCIN'S S-GLYCOSYLTRANSFERASE SUNS[a]

6.1 INTRODUCTION

Five glycocins have been characterized in recent years, sublancin 168,[1] glycocin F,[2] thurandacin A and B,[3] and ASM1.[4,5] These five compounds share the highly unusual structural feature of a sugar moiety that is β-linked to the thiol of a Cys. Sublancin, the shortest known glycocin, and contains a glucose moiety linked to Cys22 (Figure 1.3)[1,6] that is installed by the *S*-glycosyltransferase SunS, which selectively transfers sugar moieties from activated nucleotide sugars to the thiol group of Cys22.[1,7] On the basis of its sequence as well as structural characterization of sublancin (chapter 2), SunS is an inverting glycosyltransferase and belongs to the GT-A glycosyltransferases of the GT-2 family.[8] SunS demonstrates high chemo- and site-selectivity for the thiol group of Cys22 of the substrate peptide SunA but exhibits tolerance towards various nucleotide sugar donors.[1] The work described in this chapter presents the first X-ray structure of an S-glycosyltransferase and the kinetic characterization of mutants of various residues in its active site that provide insights into the enzymatic mechanism.

---

[a] In this chapter I performed the SunS substrate binding studies and obtained the kinetic parameters for the glycosyltransferase SunS, as well as the kinetic parameters for two SunS mutants. All other experiments were performed by former lab members Dr. Huan Wang and Dr. Ran Zhang.

6.2 RESULTS AND DISCUSSION

6.2.1 Determination of SunS kinetic parameters

To determine the kinetic parameters of catalysis by SunS, Dr. Ran Zhang and Dr. Huan Wang, previous postdocs in the van der Donk group, first used a continuous coupled assay that measures the rate of UDP formation. Because UDP formation reports on both transglycosylation of the sugar moiety from UDP-glucose to the SunA peptide and on hydrolysis of UDP-glucose, they also determined the rate of hydrolysis in the absence of SunA. In addition, I developed a non-continuous LC-MS assay to report specifically on transglycosylation. As shown in Table 6.1, for wild type SunS, k_{cat} for transglycosylation was 53 ± 5 min^{-1} with K_m values for UDP-glucose and SunA below the detection limits of the coupled assay (<10 μM). The LC-MS assay did allow determination of the K_m values for UDP-glucose (4 ± 1 μM) and SunA (1.5 ± 0.3 μM). The k_{cat} for hydrolysis of UDP-glucose in the absence of SunA was about an order of magnitude slower than transglycosylation (Table 6.1), indicating that the peptide is a better glycosyl acceptor than water; the K_m value of UDP-Glc for hydrolysis measured by the coupled assay remained below 10 μM.

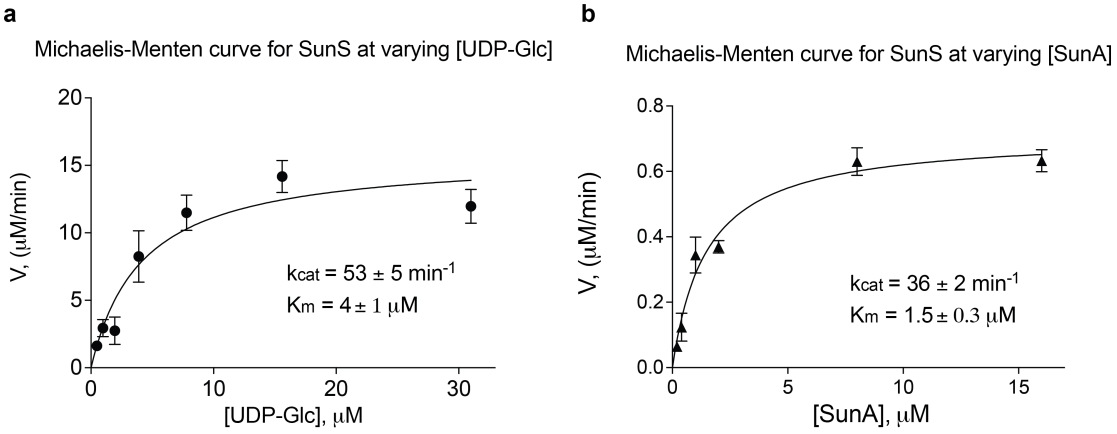

Figure 6.1 Kinetics of SunS with UDP-Glc and SunA peptide as determined by the LC-MS assay.
The LC-MS assay determination of the K_m values for (a) UDP-glucose (4 ± 1 μM) and (b) SunA (1.5 ± 0.3 μM).

Table 6.1 Kinetic parameters of catalysis by SunS determined by the coupled assay.

	K_m	k_{cat}
Enzymatic hydrolysis (SunS + UDP-Glc)	<10 μM	4.7 ± 0.2 min^{-1}
Glycosylation (saturated UDP-Glc + varied [SunA])	<10 μM	56 ± 1 min^{-1}
Glycosylation (saturated [SunA] + varied UDP-Glc])	<10 μM	55 ± 1 min^{-1}

6.2.2 Substrates binding order

The order of substrate binding was investigated by examining the patterns of product inhibition. We performed inhibition assays in which SunS was inhibited by UDP at non-saturating UDP-Glc concentrations (1.0 μM) and varying peptide concentrations (0.2 to 16 μM). For an ordered mechanism where UDP-Glc is the first substrate to bind and UDP leaves last, UDP would be expected to be a non-competitive inhibitor with respect to SunA under these conditions. Analysis of the data is consistent with non-competitive inhibition. The K_m was not affected. At UDP concentrations of 0, 15, and 30 μM the K_m values were 1.6, 1.6, and 1.8 μM respectively, but the effective Vmax decreased, 0.74, 0.38, and 0.18 μM/min respectively. K_m and Vmax values were obtained from non-linear regression of the data using the Michaelis-Menten equation (Figure 6.2). We then performed inhibition assays to evaluate SunS inhibition by UDP at saturating peptide concentrations (40 μM) and varying UDP-Glc concentrations (0.49 μM to 31 μM). For an ordered mechanism where UDP-Glc is the first substrate to bind and UDP the last product to leave, UDP is expected to be a competitive inhibitor with respect to UDP-Glc under these conditions. Analysis of the data was consistent with competitive inhibition by UDP with respect to UDP-Glc at saturating SunA concentrations (Figure 6.3). Vmax was not affected, but the effective K_m increased. Vmax values of 15.9, 13.3 and 15.3 μM/min and K_m values of 5,

12, and 39 μM were obtained for 0, 50, and 100 μM UDP respectively by non-linear regression of the data using the Michaelis-Menten equation (Figure 6.3). Alternative modes of inhibition were statistically less well supported as indicated by the α-values (Figure 6.2 and 6.3). Graphpad Prism5[9] was used for the statistical analysis. The mixed model is a general equation, that includes competitive, uncompetitive and noncompetitive inhibition as special cases. The mixed model contains the alpha (α) parameter, and this parameter indicates the mechanism of inhibition.[9] When α =1, the inhibitor does not alter binding of substrate to the enzyme, and the mixed-model describes noncompetitive inhibition. When α is much larger than 1, binding of inhibitor prevents binding of the substrate and the mixed-model becomes identical to competitive inhibition. The observations (α = 1.02 for UDP inhibition of UDP-Glc and α = 17.02 for UDP-inhibition of SunA) are consistent with an ordered bi bi kinetic mechanism in which UDP-glucose binds first and UDP is released from the enzyme last (Figure 6.4).

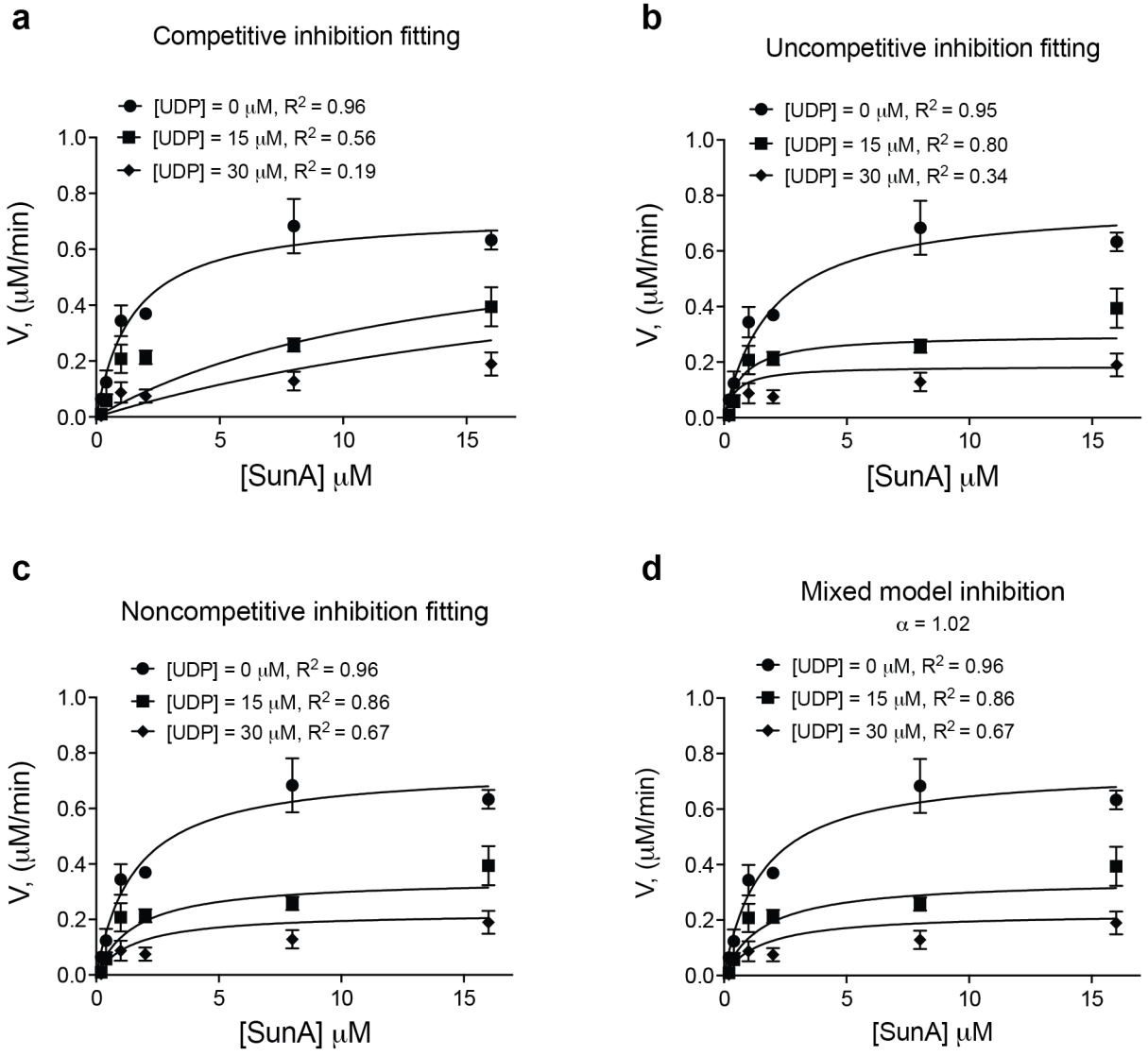

Figure 6.2 UDP a noncompetitive inhibitor of SunS with respect to SunA.

Michaelis-Menten curves for the inhibition of SunS by UDP at non-saturating UDP-Glc concentrations (1.0 μM) and varying peptide concentrations (0.2 to 16 μM). Shown are curves fitted to all possible modes of inhibition (a) competitive, (b) uncompetitive, (c) noncompetitive. Graphpad Prism5 was used for the statistical analysis. The mixed model is a general equation, that includes competitive, uncompetitive and noncompetitive inhibition as special cases. The mixed model contains the alpha (α) parameter, and this parameter indicates the mechanism of inhibition. When α =1, the inhibitor does not alter binding of substrate to the enzyme, and the mixed-model describes noncompetitive inhibition. The data is consistent with noncompetitive inhibition by UDP with respect to sunA.

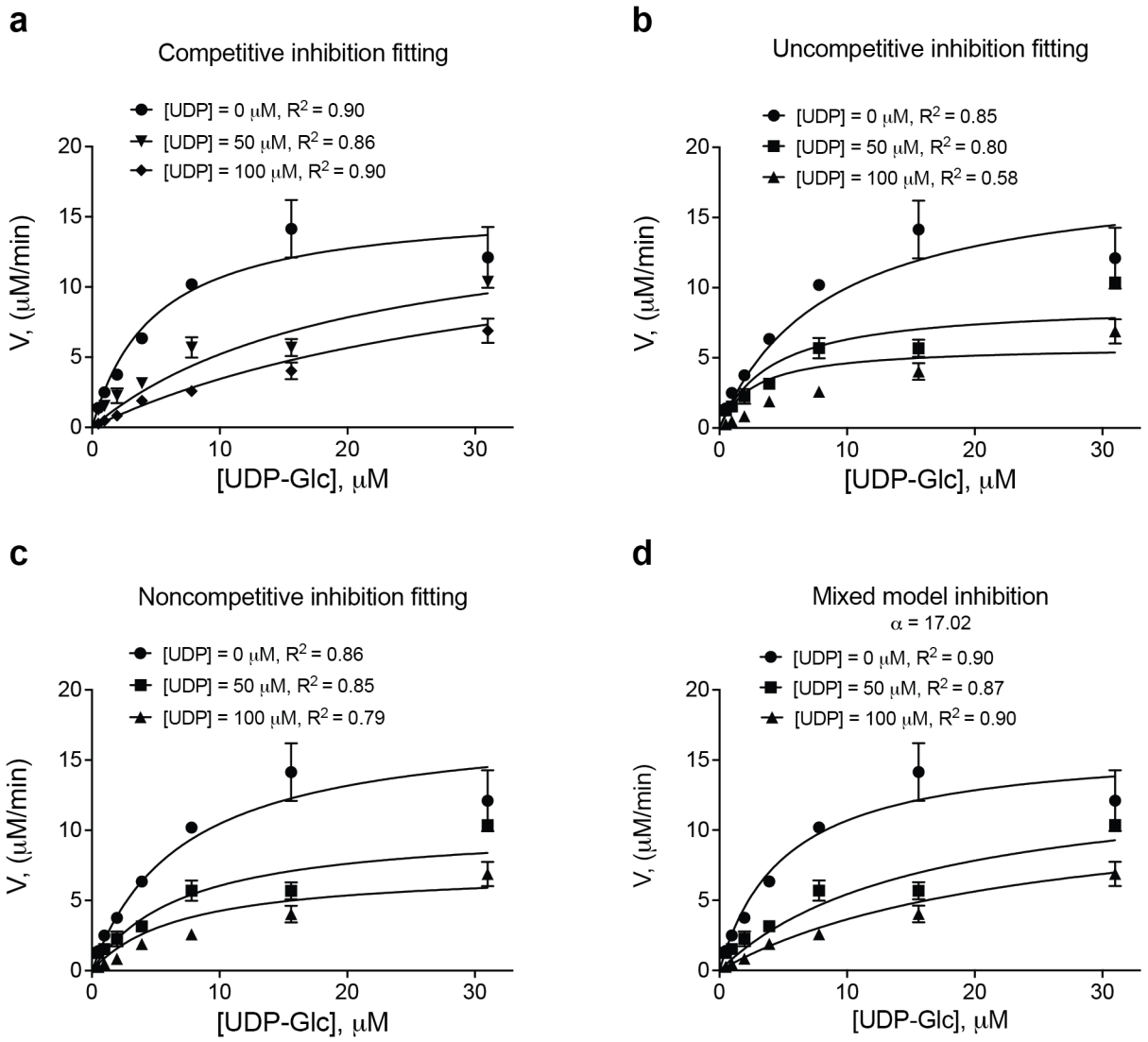

Figure 6.3 UDP a competitive inhibitor of SunS with respect to UDP-Glc.

Michaelis-Menten curves for the inhibition of SunS by UDP at saturating peptide concentrations (40 μM) and varying UDP-Glc concentrations (0.49 μM to 31 μM). Shown are curves fitted to all possible modes of inhibition (a) competitive, (b) uncompetitive, (c) noncompetitive. Graphpad Prism5 was used for the statistical analysis. The mixed model is a general equation, that includes competitive, uncompetitive and noncompetitive inhibition as special cases. The mixed model contains the alpha (α) parameter, and this parameter tells you about the mechanism of inhibition. When α is much larger than 1, binding of inhibitor prevents binding of the substrate and the mixed-model becomes identical to competitive inhibition. The data is consistent with competitive inhibition by UDP with respect to UDP-Glc.

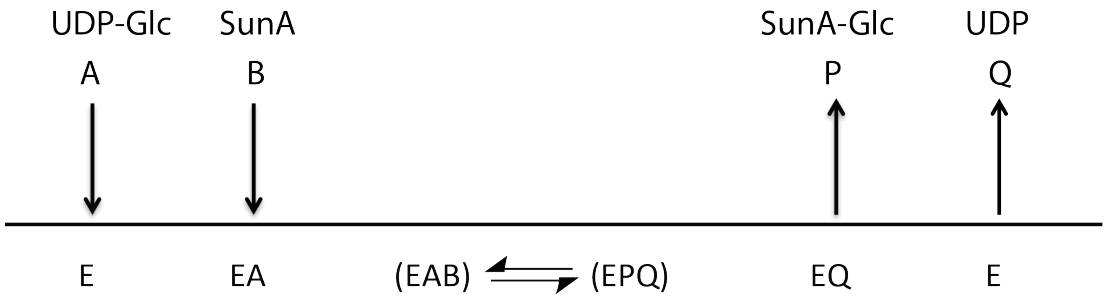

Figure 6.4 Proposed substrate binding order of SunS.

Depiction of SunS ordered bi-bi mechanism of substrate binding. The ordered mechanism is based on the co-crystal structure complex and supporting kinetic experiments. A: UDP-Glc, B: SunA, P: SunA-Glc, Q: UDP, E: SunS, EA: SunS•UDP-Glc complex, EAB: SunS•UDP-Glc•SunA complex, EPQ•SunS•SunA-Glc•UDP complex, and EQ: SunS•UDP complex.

6.2.3 Crystal structure of the S-glycosyltransferase SunS

Our collaborators in the Nair laboratory at the University of Illinois solved the crystal structure of the 422 amino acid SunS protein and a co-crystal structure of truncated SunS-1-335 with bound UDP-Glc (Figure 6.5). SunS is comprised of three distinct regions, an N-terminal catalytic domain with a Rossmann-like architecture,[10] followed by a tetratricopeptide repeat (TPR) unit[11,12] domain and a C-terminal dimerization domain. Sequence alignment of SunS with O-glycosyltransferases (OGTs) that have high sequence similarity, identified by BLAST analysis, show that it contains the conserved short DxD motif in the enzyme's active site (Figure 6.6). On the basis of its sequence as well as structural characterization of sublancin, SunS is an inverting glycosyltransferase and belongs to the GT-A glycosyltransferases of the GT-2 family (Figure 6.7).

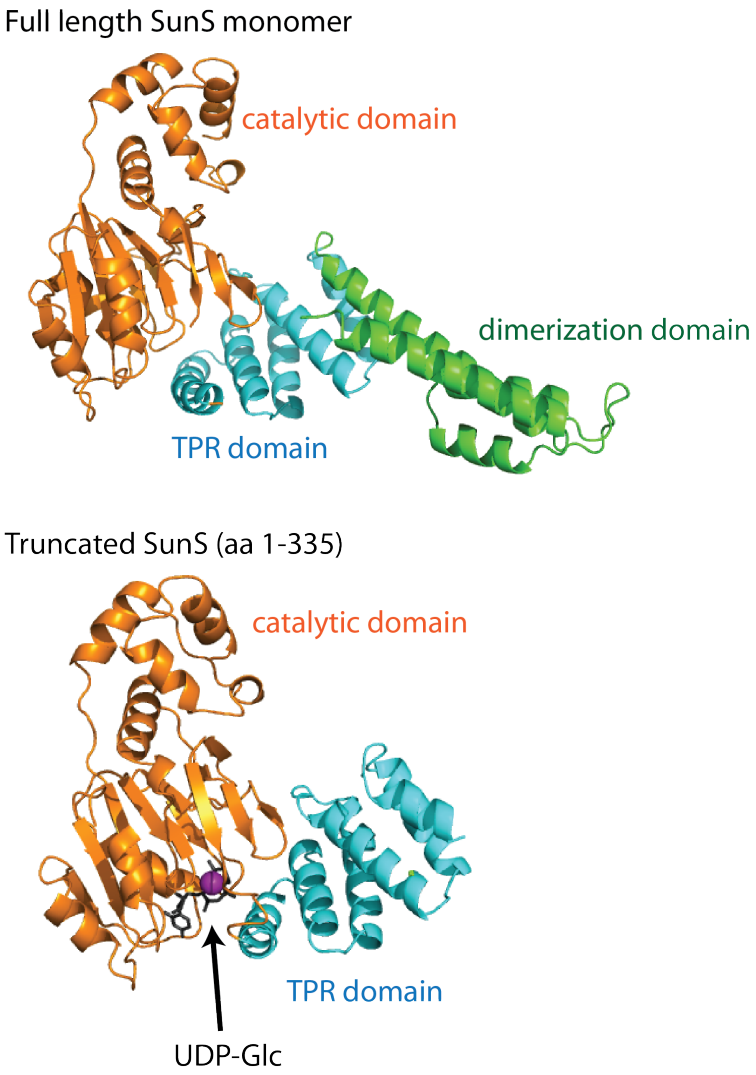

Figure 6.5 Overall structure of SunS and SunS-1-335 complex with UDP-Glc.

(a) Overall fold of SunS and (b) SunS-1-335:UDP-Glc complex in a ribbon representation. The N-terminal catalytic domain is shown in orange, the TRP domain in cyan, the C-dimerization domain in green, the UDP-Glc substrate is shown in black and the divalent Mg^{2+} metal in purple.

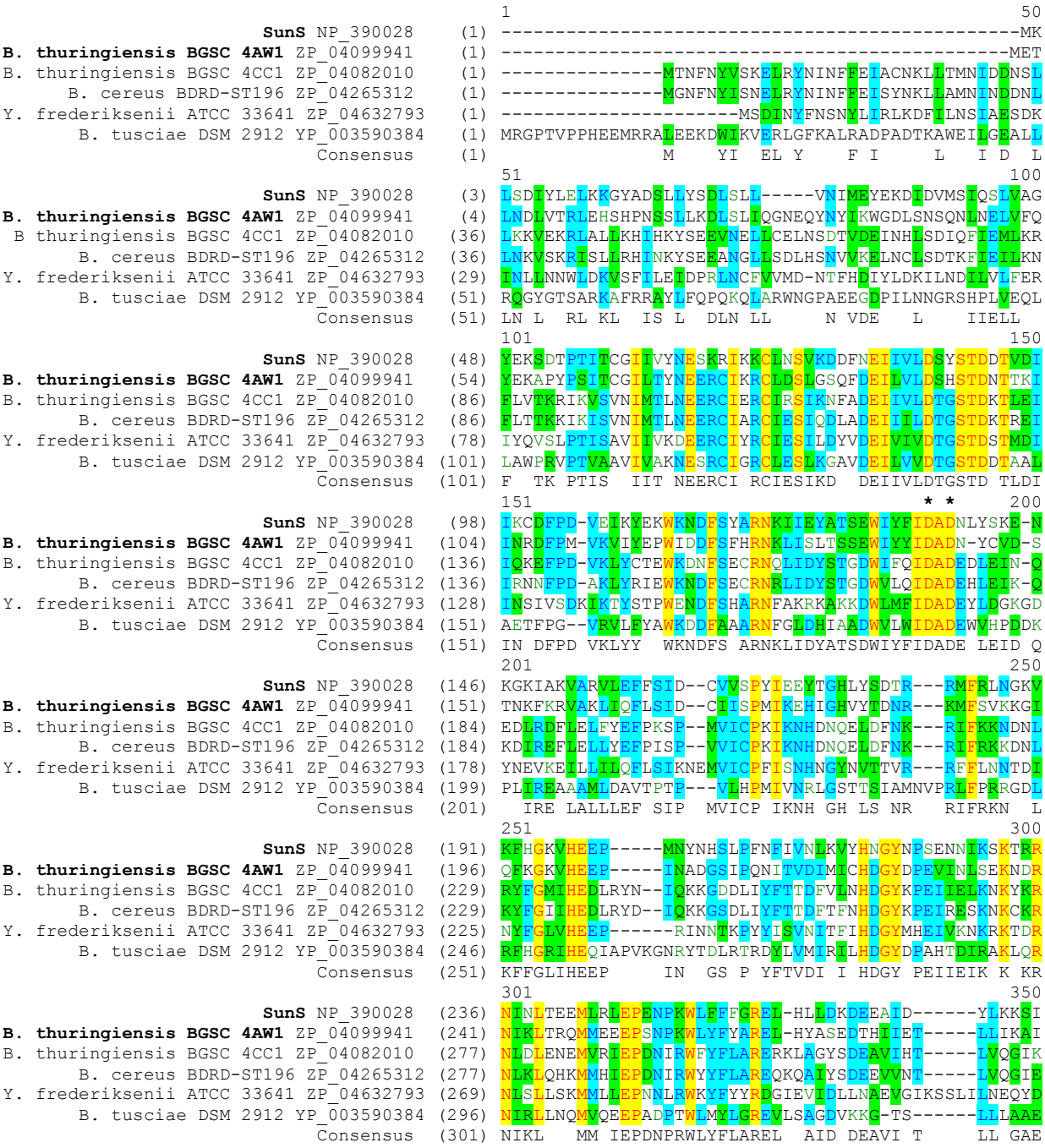

Figure 6.6 (continued on next page)

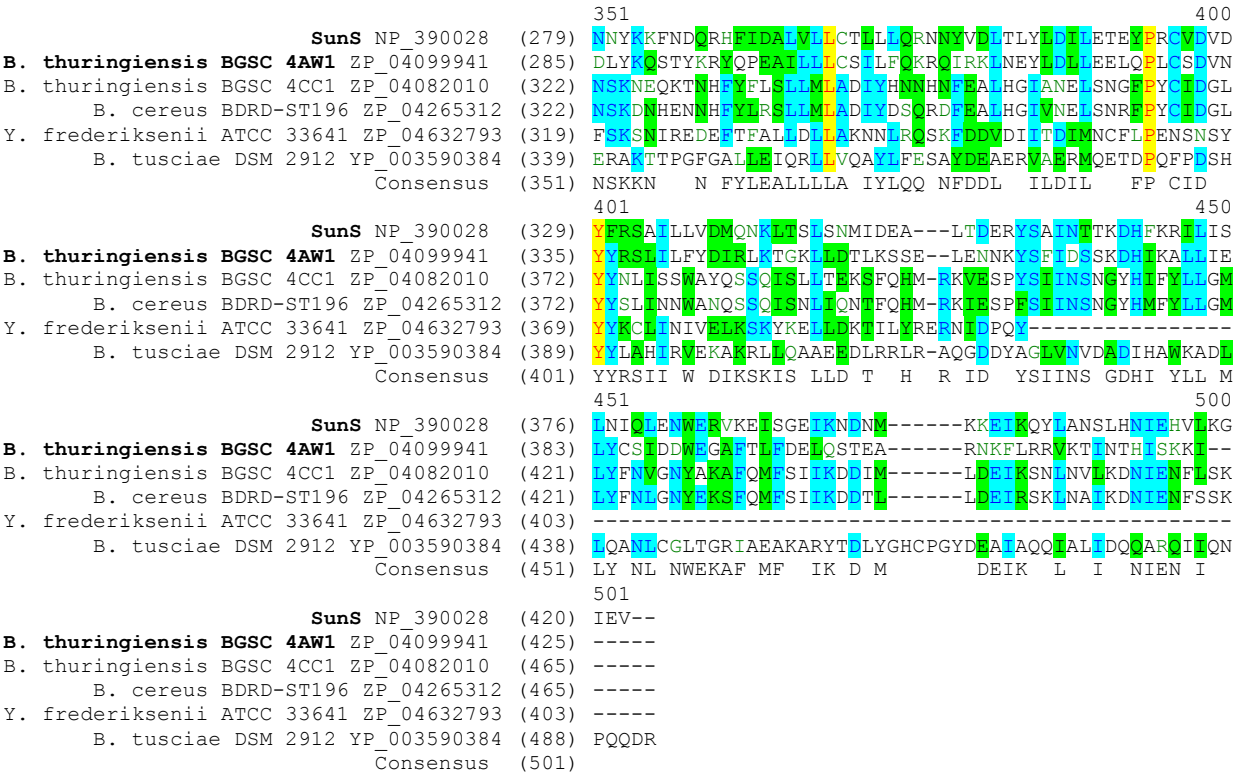

Figure 6.6 BLAST sequence alignment of SunS with glycosyltransferases.

Sequence alignment of SunS with glycosyltransferases that have high sequence homology identified by BLAST analysis. All proteins (hypothetical and experimentally characterized in bold font) are located in a cluster with a putative peptide substrate. Shown is the sequence alignment of SunS and the top hits from the BLAST search. The conserved DxD motif involved in coordinating a divalent metal cation (usually Mg^{2+} or Mn^{2+}) is marked by two asterisks.

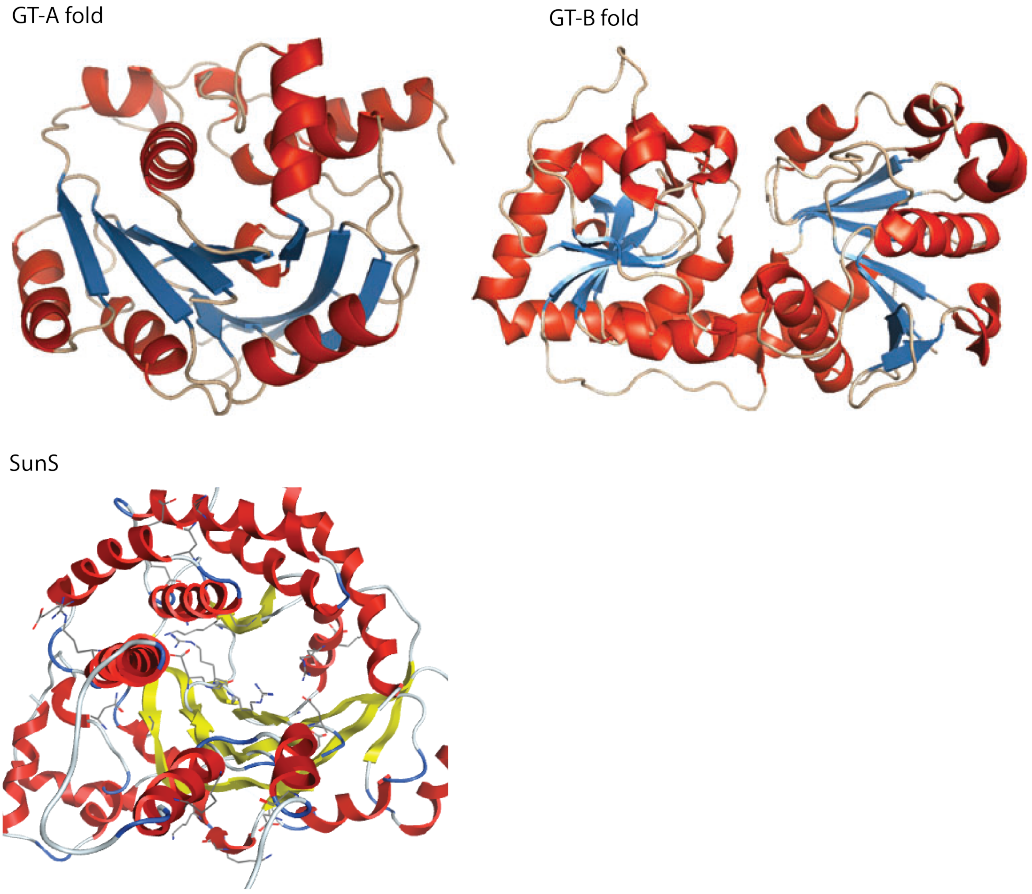

Figure 6.7 SunS fold compared to previously reported glycosyltransferase folds.
Overall folds observed for glycosyltransferase enzymes. (Top left) The GT-A fold of the inverting glycosyltransferase SpsA from *Bacillus subtilis*, Protein Data Bank (pdb, 1qgq), (Top right) the GT-B fold of the bacteriophage T4 B-glucosyltransferase (pdb, 1jg7), and (Bottom) the SunS fold. SunS resembles the GT-A fold. The figures representing the GT-A and GT-B fold are reproduced with permission from "Glycosyltransferases: Structures, Functions, and Mechanisms" 2008. *Annu. Rev. Biochem.* 77, 521-555.[8]

The truncated SunS-1-335 was unable to perform the transglycosylation reaction, even though the C-terminal 87 amino acids do not obviously interact with the active site in the wild type structure. The abolished activity of SunS-1-335 may explain why intact UDP-Glc was present in the structure of the truncated protein. Analytical gel filtration analysis demonstrated that SunS exists as a dimer *in vitro* whereas the C-terminally truncated SunS-1-335 is a monomer, indicating the importance of the C-terminal domain for dimerization *in vitro* and

suggesting that dimerization is important for enzyme activity. The GT-A fold of SunS harbors the binding site for UDP-Glucose in a pocket in the catalytic domain adjacent to the interface with the TPR domain (Figures 6.5 and 6.8). TPR domains are proposed to mediate protein-protein interactions and to help in the assembly of multiple protein complexes.[13] The catalytic and TPR domains line a narrow cleft, which likely accommodates the peptide substrate for binding (Figure 6.9). The shape of the cleft requires the peptide substrate to be in an extended conformation to bind. Indeed, we found that for SunS activity to be observed, the peptide substrate SunA needed to be in the reduced form in which it can adopt such an extended conformation; SunS did not modify peptides containing the disulfide cross-links that are present in mature sublancin.

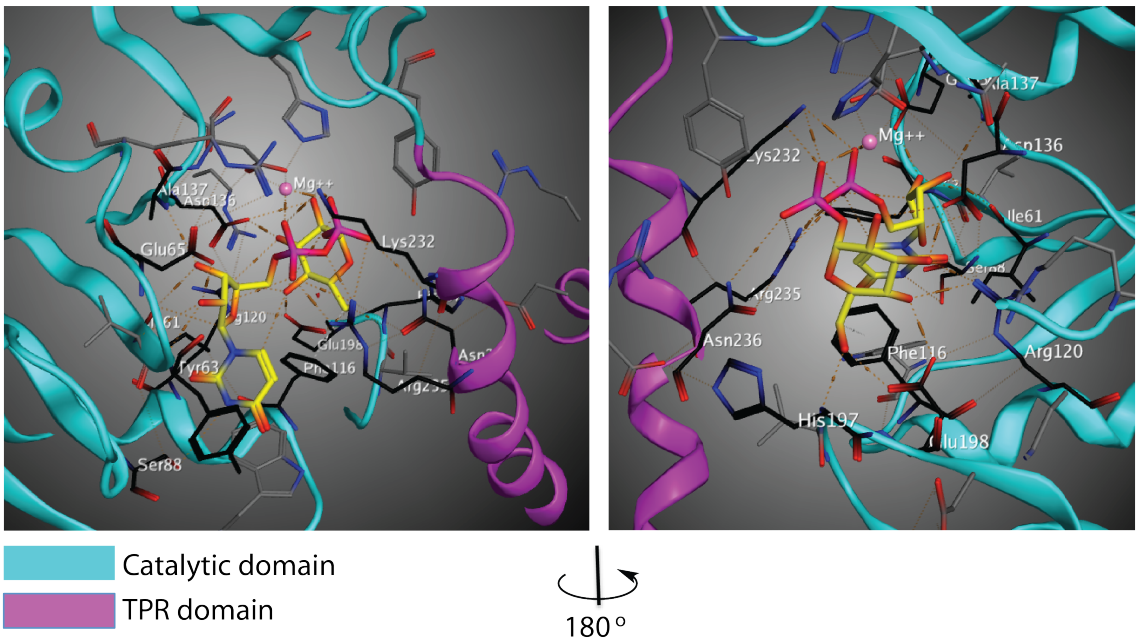

Figure 6.8 UDP-Glc binding pocket.

The binding site for UDP-Glucose in a pocket in the catalytic domain adjacent to the interface with the TPR domain. Catalytic domain depicted in cyan, TPR domain depicted in magenta, UDP-Glc substrate is shown in yellow and important substrate binding residues are labeled in white.

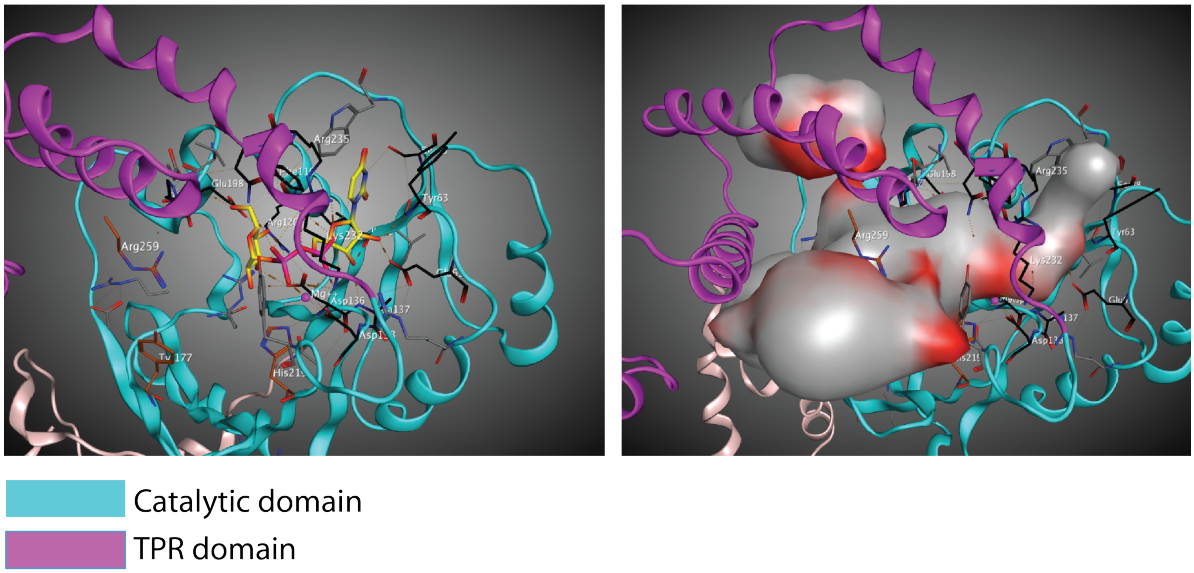

Figure 6.9 SunA peptide putative binding cleft.

The catalytic and TPR domains line a narrow cleft, which likely accommodates the peptide substrate for binding The shape of the cleft requires the peptide substrate to be in an extended conformation to bind. Catalytic domain depicted in cyan, TPR domain depicted in magenta, UDP-Glc substrate is shown in yellow and the putative SunA binding cleft is shown in grey as a space filling projection.

6.2.4 Site directed mutagenesis studies

The structure of the SunS-1-335-UDP-Glc complex identified potentially important substrate binding residues (Figure 6.10). The side chain carboxyl oxygen atoms of Asp136 form hydrogen bonds with the O2 and O3 hydroxyl groups of glucose, and the side chain carboxylate oxygens of Glu198 interact with the O4 and O6 hydroxyl groups of glucose. Moreover, the η-nitrogen of Arg120 forms hydrogen bonds with the O4 hydroxyl group and the carboxylate oxygen of Asp136. To investigate the importance of these residues, Dr. Huan Wang individually mutated these potentially important substrate-binding residues to Ala. The mutations did not greatly affect the UDP-Glc hydrolysis activity but abolished glycosyltransferase activity, as determined by the coupled enzymatic assay and LC-MS analysis, respectively (Figure 6.10, Table 6.2). Given the observed well-defined glucose binding network, it was surprising that

SunS was able to conjugate several other sugars to the SunA peptide in previous studies.[1] However, 69% to 95% conversion was observed when those studies were conducted at high concentrations of nucleotide sugars (5 mM). Determination of the kinetic parameters for glycosyl transfer in this work clearly demonstrates the strong preference of SunS for UDP-Glc as the k_{cat} values for transglycosylation with UDP-GlcNAc and GDP-Man were strongly attenuated and the K_m values were also considerably higher (Table 6.3). UDP-Gal was a better substrate with respect to k_{cat} but its K_m was greatly increased to 2.1 ± 0.4 mM. Surprisingly, the rates and K_m values for hydrolysis of these substrate analogs were not substantially changed compared to those for UDP-Glc (Table 6.4). These observations suggest that binding of the SunA substrate imposes more stringent restrictions on the sugar-nucleotide binding pocket, probably because of a conformational change upon peptide binding. Although we were unable to obtain a structure of a ternary complex, a conformational change upon substrate binding was observed for the O-glycosyltransferase OGT that conjugates GlcNAc to Ser and Thr residues.[14]

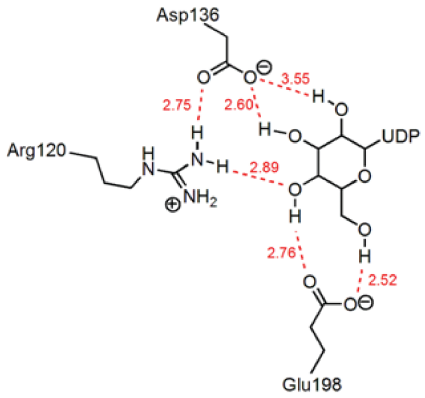

Figure 6.10 Glucose binding residues.

The side chain carboxyl oxygen atoms of Asp136 form hydrogen bonds with the O2 and O3 hydroxyl groups of glucose, and the side chain carboxylate oxygens of Glu198 interact with the O4 and O6 hydroxyl groups of glucose. The protons attached to the η-nitrogen of Arg120 forms hydrogen bonds with the O4 hydroxyl group and the carboxylate oxygen of Asp136. Distances in angstroms are depicted in red.

Table 6.2 Summary of the hydrolytic activity and glycosyltransferase activity of SunS and SunS mutants obtained by the coupled enzymatic assay.

SunS mutants	$k_{cat\text{-}hydrolysis}$ / min^{-1} [a]	$k_{cat\text{-}glycosylation}$ / min^{-1} [a]	Relative activity determined by LC-MS / %
wt-SunS	4.7 ± 0.2 [d]	55± 5[c], 55 ± 4 [d]	100 ± 5 [e]
SunS-1-335	0.29 ± 0.03 [d]	-[b]	<5 [e]
E65A	2.9 ± 0.4 [d]	210 ± 20[c], 127 ± 14 [d]	90 ± 2 [e]
W112F	1.9 ± 0.2 [d]	170 ± 20[c], 122 ± 17 [d]	82 ± 5 [e]
R120A	2.9 ± 0.6 [d]	-[b]	<5 [e]
D136A	4.2 ± 0.1 [d]	-[b]	<5 [e]
D138A	4.7 ± 0.8 [d]	-[b]	<5 [e]
D138A/D136A	2.2 ± 0.3 [d]	-[b]	<5 [e]
H197F	6.5 ± 0.5 [d]	-[b]	<5 [e]
H197N	2.1 ± 0.3 [d]	-[b]	<5 [e]
E198A	7.2 ± 0.5 [d]	-[b]	<5 [e]
H219A	1.3 ± 0.2 [d]	-[b]	<5 [e]
K232A	5.7 ± 0.5 [d]	11 ± 1 [d]	15 ± 2 [e]
R235A	4.8 ± 0.6 [d]	15 ± 1 [d]	34 ± 4 [e]
R259A	4.3 ± 0.2 [d]	-[b]	<5 [e]
R259H	4.8 ± 0.6 [d]	-[b]	<5 [e]

[a] The k_{cat} values of hydrolytic and glycosyltransferase activity were measured by the coupled enzymatic assay. In all cases, K_m for UDP-glucose was <10 μM. [b] The enzymatic coupled assay detects the generation of UDP. When $k_{cat\text{-}glycosylation}$ is close to $k_{cat\text{-}hydrolysis}$, the enzymatic coupled assay cannot accurately measure the rate of glycosylation reactions. In all cases labeled [b], we did not detect transglycosylation activity by LC-MS under the conditions of the coupled assay. For the other mutants (E65A, W112F, K232A, K235A), the LC assay demonstrated that transglycosylation occurred ($k_{cat\text{-}glycosylation}$: wt-SunS 58 ± 21 min^{-1}, E65A 47 ± 6 min^{-1}, W112F 57 ± 17 min^{-1}). [c] Values obtained in my work using the LC-MS assay. [d] values obtained by Dr. Huan Wang using the coupled assay. [e] Values obtained by DR. Huan Wang using the LC-MS assay.

Table 6.3 Michaelis-Menten kinetic parameters for transglycosylation of different nucleotide-sugars at saturating concentration of SunA with wt-SunS as measured by the coupled enzymatic assay.

Nucleotide Sugar	K_m / μM	$k_{cat\text{-}glycosylation}$ / min^{-1}
UDP-Glc	1.5 ± 0.3	55 ± 4
UDP-Gal	(2.1 ± 0.4) × 10^3	32 ± 2
GDP-Man	16 ± 2	1.9 ± 0.1
UDP-GlcNAc	12 ± 2	1.3 ± 0.1

Table 6.4 Michaelis-Menten kinetic parameters of SunS catalyzed hydrolysis of different nucleotide sugars as measured by the coupled enzymatic assay.

Nucleotide Sugar	K_m / μM	$k_{cat\text{-}hydrolysis}$ / min^{-1}
UDP-Glc	<10	2.7 ± 0.4
UDP-Gal	<10	2.3± 0.2
GDP-Man	<10	2.6± 0.2
UDP-GlcNAc	<10	2.5± 0.1

In most known inverting GT-A glycosyltransferases, a divalent metal cation such as Mg^{2+} or Mn^{2+} is important to facilitate the departure of the nucleoside diphosphate leaving group.[8] In the Sun-1-335-UDP-Glc complex, a Mg^{2+} is coordinated by three pyrophosphate oxygens of UDP-Glc, two carboxyl oxygens of Asp138, and the ε^2N of the imidazole side chain of His219 (Figure 6.11). Replacement of Asp138 and His219 with Ala by site-directed mutagenesis showed that both residues are strictly required for transglycosylation activity. Three pyrophosphate oxygen atoms of UDP-Glc also form hydrogen bonds to the side chains of Lys232, Arg235, and Asn236 (Figure 6.11). The positively charged Lys232 and Arg235 may facilitate catalysis by stabilizing the developing negative charge on the pyrophosphate during the glycosyl transfer reaction. Unlike the mutants in the glucose binding pocket and the metal binding ligands, SunS-K232A and R235A still retained partial transglycosylation activity (Figure 6.12, Table 6.2). However, mutation of Asn236, which interacts with both the β-phosphate of UDP-Glc and the guanidine group of Arg235, to Ala abrogated the transglycosylation activity of SunS.

SunS interacts with the hydroxyl groups of the ribose moiety of UDP-Glc through the carboxyl oxygen of Glu65, the backbone amide nitrogens of Ala137 and Tyr63, and the backbone amide oxygen of Ile61. The indole of Trp112 is nearly coplanar with the uracil moiety of UDP-Glc and might also contribute to substrate binding. Indeed, the SunS mutants E65A and W112F both displayed increased K_m values for UDP-Glc compared to wt-SunS without impairing the glycosyltransferase activity (Table 6.2), consistent with roles as non-catalytic

substrate binding residues. Surprisingly, the k_{cat} values measured by the coupled enzyme assay in the presence of SunA for SunS-E65A and SunS-W112F are larger than the k_{cat} of wt-SunS. To verify that these numbers indeed reflect transglycosylation, LC-MS was also used to monitor the kinetics. The k_{cat} values thus obtained showed that two mutants had very similar activities than wt-SunS. Thus the presence of SunA likely promotes UDP-Glc hydrolysis to account for the higher k_{cat} values in the coupled assay.

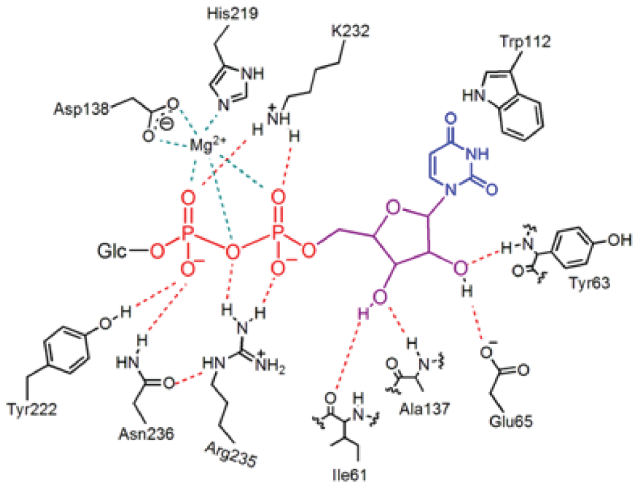

Figure 6.11 UDP binding residues.

A Mg^{2+} is coordinated by three pyrophosphate oxygens of UDP-Glc, two carboxyl oxygens of Asp138, and the ε^2N of the imidazole side chain of His219. Three pyrophosphate oxygen atoms of UDP-Glc form hydrogen bonds to the side chains of Lys232, Arg235, and Asn236 which interacts with both the β-phosphate of UDP-Glc. SunS interacts with the hydroxyl groups of the ribose moiety of UDP-Glc through the carboxyl oxygen of Glu65, the backbone amide nitrogens of Ala137 and Tyr63, and the backbone amide oxygen of Ile61. The indole of Trp112 is nearly coplanar with the uracil moiety of UDP-Glc and might also contribute to substrate binding. Pyrophosphate moiety is shown in red, the ribose moiety in purple and the uracil moiety in blue.

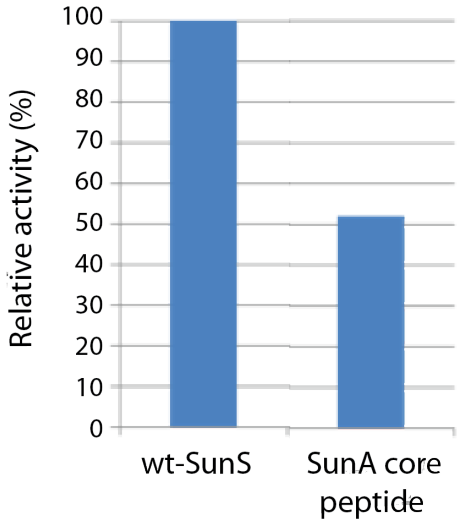

Figure 6.12 Relative activities of SunS on SunA core peptide relative to SunA.

Histogram showing the relative activity of wild-type SunS (wt-SunS) protein (k_{cat}) on SunA core peptide relative to SunA as substrate. The relative activities were determined by the coupled enzymatic assay.

The identity of the catalytic residue that accepts the proton from the peptide-based nucleophile is of particular interest in protein glycosyltransferases. Because we have been unable to obtain a ternary structure with a nucleotide and SunA or a synthetic peptide, an active site base cannot be identified with certainty, although even with ternary structures, identification of the active site base is not straightforward for glycosyl transferases.[15,16] His197 and Arg259 are both highly conserved in characterized and putative S-glycosyltransferases (Figure 6.6) and are positioned in the binary complex in the area above the β-face of the glucose where a catalytic base would be expected. Mutation of His197 to Asn or Phe abolished the transglycosylation activity of SunS. Similarly, SunS-R259A exhibited no glycosyltransferase activity. To further investigate the potential identity of the catalytic base, the pH-activity profile of SunS was determined by Dr. Ran Zhang. A fit of the profile suggests that a residue with a pK_a of 6.5 needs to be deprotonated, which is close to the pK_a of protonated histidine (Figure 6.13). Considering

the high pK_a of the guanidinium group of arginine (pK_a ~12), Arg259 is not likely to be the catalytic base.

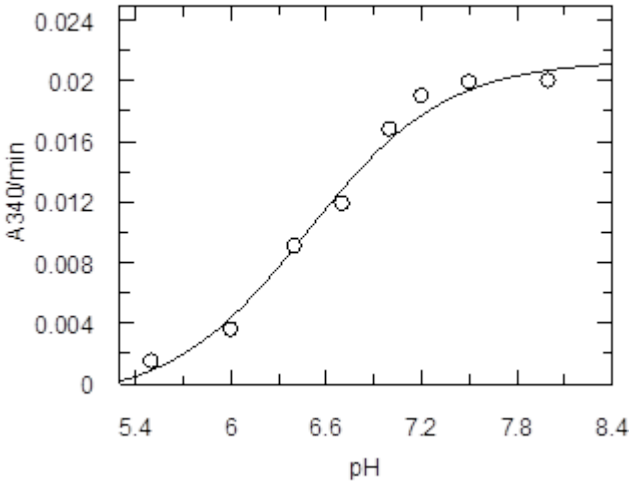

Figure 6.13 pH profile of the glycosyltransferase activity of SunS.

The $k_{cat\text{-}apparent}$-pH profile of the glycosyltransferase activity of SunS. At each pH value, Dr. Ran Zhang verified that substrate concentrations were saturating. Because of the very low K_m values that could not be determined with our assays, only the dependence of k_{cat} on pH could be investigated.

Recent studies on human OGT suggested that the α-phosphate of the nucleotide-sugar might serve as the catalytic base.[16] However, in the crystal structure of SunS-1-335 in complex with UDP-Glc, the α-phosphate is positioned on the α-face of glucose and at a relatively long distance from C1 of glucose, and none of the other pyrophosphate oxygens appears to be in an appropriate position to act as a catalytic base. Therefore, we tentatively propose a mechanism with His197 as the catalytic base (Figure 6.14), although a general base may not be needed if the mechanism of glycosyl transfer to Cys resembles that of other inverting glycosyl transfer processes, which are thought to occur via an oxocarbenium ion–like transition state.[8,15,17] Even in the neutral form (i.e. not deprotonated), Cys would still be a relatively good nucleophile to trap the electrophilic oxocarbenium structure, and this may explain the selectivity of SunS for Cys over Ser.

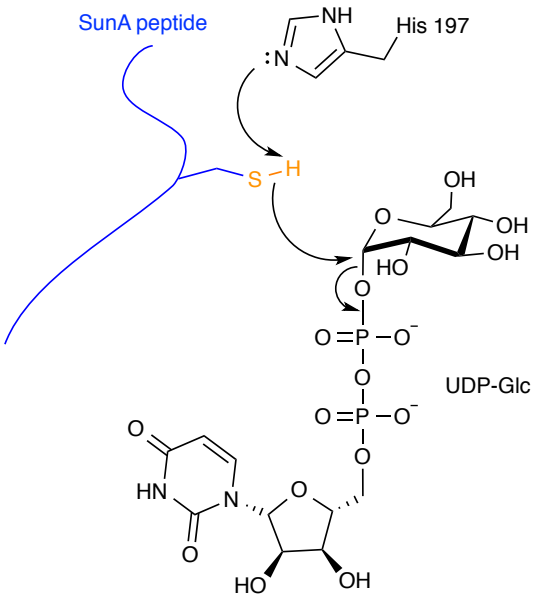

Figure 6.14 Proposed mechanism of SunS.

The mechanism shown is based on the structure and the co-crystal complex of truncated SunS-1-334 with UDP-Glc and supporting kinetic experiments. The SunA peptide is shown in blue with only the reactive cysteine thiol shown. His197 is the proposed catalytic base, although a general base may not be needed if the mechanism of glycosyl transfer to Cys resembles that of other inverting glycosyl transfer processes, which are thought to occur via an oxocarbenium ion–like transition state.

6.2.5 Substrate selectivity with respect to SunA

SunA is initially synthesized with an N-terminal leader peptide, which is thought to be removed in the last step of maturation, and a C-terminal core peptide that is converted into sublancin. Previous studies have shown that SunS can be used to glycosylate SunA mutants, but the efficiency of this process has not been investigated.[1,7] We first investigated the importance of the leader peptide. Comparison of the kinetics of modification of full length SunA and just the core peptide, showed that the k_{cat} is two-fold larger for the full-length peptide; the K_m for both substrates remained below 10 μM. These results indicate that the leader peptide of SunA contributes to substrate processing by SunS but is not essential. We next turned to mutants in which the two Gly residues flanking Cys22 were replaced with either Ala, Phe, Glu or Lys

(Table 6.5). These mutations did not significantly alter the low K_m values for the peptide substrate. Ala mutations of the flanking residues of Cys22 also had minimal effects on k_{cat}, but mutation to Phe and Glu reduced the k_{cat} values by about 5-fold. Interestingly, the G21K and G23K mutants of SunA could not be modified by SunS under the conditions of the coupled enzymatic assay, indicating that the positive charge of the Lys side chain has a significant detrimental impact. The observed kinetic parameters for these substrate mutants are consistent with a previous model that a helical segment of the substrate spanning residues 6-16 is important for substrate recognition and that Cys22 located on a flexible loop then accesses the glycosylation active site, which is quite tolerant of changes in the sequence in the loop.

Table 6.5 Michaelis-Menten kinetic parameters of SunA mutants at saturating concentration of UDP-Glc.

peptide	K_m (μM)	k_{cat} (min^{-1})
SunA	<10	55 ± 2
SunA G21A	<10	21 ± 1
SunA G23A	<10	57 ± 1
SunA G21E	<10	11 ± 1
SunA G23E	<10	12 ± 1
SunA G21F	<10	15 ± 1
SunA G23F	<10	11 ± 1
SunA G21K	-	-
SunA G23K	-	-

Michaelis-Menten kinetic parameters of SunA mutants at saturating concentration of UDP-Glc with wt-SunS during glycosyl transfer reactions measured by the coupled enzymatic assay. Values of k_{cat} may include a contribution of hydrolysis, which is around 1-2 min^{-1}.

6.3 SUMMARY

Five glycocins have been characterized in recent years and all five peptides share the highly unusual structural feature of a sugar moiety that is β-linked to the thiol of a Cys. The structures reported here represent the first X-ray structures of an S-glycosyltransferase and revealed an unusual domain architecture. BLAST sequence alignment analysis as well as structural characterization of SunS classified the enzyme as an inverting glycosyltransferase that belongs to the GT-A glycosyltransferases of the GT-2 family. The order of substrate binding was investigated by examining the patterns of product inhibition. The observations from the assays were consistent with an ordered bi bi kinetic mechanism in which UDP-glucose binds first and UDP is released from the enzyme last. Site directed mutagenesis identified catalytically important amino acids and the kinetic characteristics of mutants of various residues in the SunS active site provided insights into the enzymatic mechanism. Understanding the mechanism of S-glycosyltransferases may assist in the development of enzymes capable of installing S-linked sugars onto natural products and peptides, thus potentially increasing the therapeutic value of such compounds given that glycosylated natural products are readily found in nature and S-linkages are more stable than O-linkages.

6.4 EXPERIMENTAL

6.4.1 Materials, cultures, and conditions

All oligonucleotides were purchased from Integrated DNA Technologies. Restriction endonucleases, DNA polymerases and T4 DNA ligase were purchased from New England Biolabs or Invitrogen. Media components for bacterial cultures were purchased from Difco laboratories. Chemicals were purchased from Fisher Scientific or from Sigma-Aldrich unless noted otherwise. *E. coli* DH5α was used as host for cloning and plasmid propagation, and *E. coli*

BL21 (DE3) was used as a host for expression of proteins and peptides. Pyruvate kinase/lactate dehydrogenase enzymes from rabbit muscle were purchased from Sigma-Aldrich.

All polymerase chain reactions (PCR) were carried out on a C1000™ thermal cycler (Bio-Rad). DNA sequencing was performed by the Biotechnology Center at the University of Illinois at Urbana-Champaign, using appropriate primers. Matrix-assisted laser desorption/ionization time-of-flight mass spectrometry (MALDI-ToF MS) was carried out on Voyager-DE-STR (Applied Biosystems) and Bruker Daltonics UltrafleXtreme MALDI TOFTOF instruments. Salt-containing MS samples were purified via Millipore Zip-Tip$_{C18}$ pipette tips (Billerica MA). All kinetic assays were carried out in a Cary 4000 UV-Vis spectrometer equipped with a circulating water bath and Agilent 1100 LC/MSD Trap XCT Plus (LC/MS). The SunA and SunS mutants were prepared by site-directed mutagenesis.

6.4.2 Construction of His$_6$-SunS, His$_6$-SunS mutant genes and His$_6$-SunA mutant genes

Site-directed mutagenesis of SunA and SunS was performed by multistep PCR. First, the amplification of *sunA was* carried out by thirty cycles of denaturing (94 °C for 20 s), annealing (58 °C for 30 s), and extending (72 °C for 20 s) using the forward primer (SunA-FP) and an appropriate mutant reverse primer (SunA-RP) to yield the 5' fragment of the mutant SunA gene (FP reaction). The amplification of *sunS was* carried out by thirty cycles of denaturing (94 °C for 20 s), annealing (58 °C for 30 s/kb), and extending (72 °C for 20 s) using the forward primer (SunS-FP) and an appropriate mutant reverse primer (SunS-RP) to yield the 5' fragment of the mutant SunS gene (FP reaction). The PCR mixtures included 1×FailSafe PreMix G (PICENTRE Biotechnologies), DMSO (4%), Phusion DNA polymerase (Finnzymes; 0.04 U/μL), dNTPs (2 mM) and primers (1 μM each). In parallel, a PCR reaction using an appropriate mutant forward primer and the SunA-RP or SunS-RP primer was also conducted to produce 3' fragments of the

mutated *sunA and sunS* genes using the same PCR conditions as the FP reaction (RP reaction). The overlapping products from the FP and RP reaction were combined in equal amounts and extended by seven cycles of denaturing, annealing and extending using the same PCR conditions. Following the extension, the SunA-FP and SunA-RP primers were added (final concentration, 2 μM) and the mixture was incubated for another 25 cycles of denaturing, annealing and extending. Amplification of the final PCR product was confirmed and purified by 2% agarose gel electrophoresis. The resulting DNA fragments and the pET15 (for *sunA*) or pET28 (*sunS*) vectors were digested at 37 °C for 2 h. The digested products were purified by agarose gel electrophoresis. The resulting DNA insert was ligated with the digested vector at 16 °C for 10 h using T4 DNA ligase. *E. coli* DH5α cells were transformed with 2.5 μL of the ligation product by heat shock, and cells were plated on LB-ampicillin agar plates (pET15) or LB-kanamycin agar plates (pET28) and grown for 15 h at 37 °C. Several colonies were picked and used to inoculate separate 5 mL cultures of LB-ampicillin medium. The cultures were grown at 37 °C for 15 h, and plasmids were isolated using a QIAprep Spin Miniprep Kit (QIAGEN). The desired sequences of the resulting plasmid products were confirmed by DNA sequencing.

Table 6.6 Primer sequences used for the construction of SunAXa-C22X analogs.

SunA Primers	Sequence (5' to 3')
SunA_G21K FP	AGT GGC GGT ACA ATT AAA TGT GGT GGC GGA GCT
SunA_G21K RP	AGC TCC GCC ACC ACA TTT AAT TGT ACC GCC ACT
SunA_G21F FP	AGT GGC GGT ACA ATT TTC TGT GGT GGC GGA GCT
SunA_G21F RP	AGC TCC GCC ACC ACA GAA AAT TGT ACC GCC ACT
SunA_G23F FP	GGT ACA ATT GGT TGT TTC GGC GGA GCT GTT GCT
SunA_G23F RP	AGC AAC AGC TCC GCC GAA ACA ACC AAT TGT ACC
SunA_G21E FP	AGT GGC GGT ACA ATT GAA TGT GGT GGC GGA GCT
SunA_G21E RP	AGC TCC GCC ACC ACA TTC AAT TGT ACC GCC ACT
SunA_G21A FP	AGT GGC GGT ACA ATT GCG TGT GGT GGC GGA GCT
SunA_G21A RP	AGC TCC GCC ACC ACA CGC AAT TGT ACC GCC ACT
SunA_G23K FP	GGT ACA ATT GGT TGT AAA GGC GGA GCT GTT GCT
SunA_G23K RP	AGC AAC AGC TCC GCC TTT ACA ACC AAT TGT ACC
SunA_G23E FP	GGT ACA ATT GGT TGT GAA GGC GGA GCT GTT GCT
SunA_G23E RP	AGC AAC AGC TCC GCC TTC ACA ACC AAT TGT ACC
SunA_G23A FP	GGT ACA ATT GGT TGT GCG GGC GGA GCT GTT GCT

Table 6.6 (cont.)	
SunA_G23A RP	AGC AAC AGC TCC GCC CGC ACA ACC AAT TGT ACC
SunA_FP	CGG CAG CCA TAT GGA AAA GCT ATT TAA AGA
SunA_RP	GAT CCT CGA GTT ATC TGC AGA ATT GAC GAT AG

Table 6.7 Primer sequences used for the construction of SunS mutants.

SunS Primers	Sequence (5' to 3')
SunS-FP	GGC CAC ATA TGA AAC TGA GTG ATA TTT ATT TGG AAT TAA AGA AAG GCT ATG CCG ATT C
SunS-RP	ATG GCC TCG AGT CAT ACT TCA ATT CCT TTC AGG ACG TGT TCA ATA TTG TGG AGT GAG TTG
SunS-H197N FP	GGT AAA GTT AAA TTT CAT GGG AAA GTG AAC GAA GAA CCT ATG AAT TAT AAT CAT AGT C
SunS-H197N RP	GAC TAT GAT TAT AAT TCA TAG GTT CTT CGT TCA CTT TCC CAT GAA ATT TAA CTT TAC C
SunS-H197F FP	GGT AAA GTT AAA TTT CAT GGG AAA GTG TTT GAA GAA CCT ATG AAT TAT AAT CAT AGT C
SunS-H197F RP	GAC TAT GAT TAT AAT TCA TAG GTT CTT CAA ACA CTT TCC CAT GAA ATT TAA CTT TAC C
SunS R259A-FP	GG TTA TTC TTT TTC GGC GCC GAACTA CAT TTA CTT GAT AAA GAT G
SunS R259A-RP	CAT CTT TAT CAA GTA AAT GTA GTT CGG CGC CGA AAA AGA ATA ACC
SunS-R259H FP	CCA AAA TGG TTA TTC TTT TTC GGC CAT GAA CTA CAT TTA CTT GAT AAA GAT GAA
SunS-R259H RP	TTC ATC TTT ATC AAG TAA ATG TAG TTC ATG GCC GAA AAA GAA TAA CCA TTT TGG
SunS D138A-FP	GG ATT TAT TTT ATT GAT GCA GCC AAT TTA TAC TCT AAA GAA AAC AAA GGG
SunS D138A-RP	CCC TTT GTT TTC TTT AGA GTA TAA ATT GGC TGC ATC AAT AAA ATA AAT CC
SunS D136A-FP	CT TCC GAA TGG ATT TAT TTT ATT GAT GCA GAT AAT TTA TAC TCT AAA GAA AAC AAA GGG
SunS D136A-RP	CCC TTT GTT TTC TTT AGA GTA TAA ATT ATC TGC ATC AAT AAA ATA AAT CCA TTC GGA AG
SunS-D136AD138A FP	CCG AAT GGA TTT ATT TTA TTG CGG CAG CGA ATT TAT ACT CTA AAG AAA ACA AAG GG
SunS-D136AD138A RP	CCC TTT GTT TTC TTT AGA GTA TAA ATT CGC TGC CGC AAT AAA ATA AAT CCA TTC GG
SunS-H219A FP	GTG AAC CTT AAG GTT TAC GCG AAT GGA TAT AAT CCT TCA GAG
SunS-H219A RP	CTC TGA AGG ATT ATA TCC ATT CGC GTA AAC CTT AAG GTT CAC
SunS W112F-FP	CCT GAT GTT GAA ATT AAA TAT GAA AAG TTT AAG AAT GAT TTT TCC TAT GCT AG
SunS W112F-RP	CTA GCA TAG GAA AAA TCA TTC TTA AAC TTT TCA TAT TTA ATT TCA ACA TCA GG
SunS-W112A FP	CCT GAT GTT GAA ATT AAA TAT GAA AAG GCG AAG AAT GAT TTT TCC TAT GCT AG
SunS-W112A RP	CTA GCA TAG GAA AAA TCA TTC TTC GCC TTT TCA TAT TTA ATT TCA ACA TCA GG
SunS-E65A FP	ACA TGC GGT ATT ATA GTT TAT AAC GCG AGC AAG AGA ATT AAA AAG TGT TTA

Table 6.7 (cont.)	
SunS-E65A RP	TAA ACA CTT TTT AAT TCT CTT GCT CGC GTT ATA AAC TAT AAT ACC GCA TGT
SunS-E198A-FP	CGA AGA ATG TTT CGG CTC AAT GGT AAA GTT AAA TTT CAT GGG AAA GTG CAT
SunS-E198A-RP	ATG CAC TTT CCC ATG AAA TTT AAC TTT ACC ATT GAG CCG AAA CAT TCT TCG
SunS R120A-FP	TCC TAT GCT GCG AAT AAA ATT ATA GAG TAT GCT ACT TCC GAA TGG ATT TAT TTT
SunS R120A-RP	TTT ATT CGC AGC ATA GGA AAA ATC ATT CTT CCA CTT TTC ATA TTT AAT TTC AAC ATC
SunS-K232A-FP	TGA TTT TAT ATT ATT CTC TGA AGG ATT ATA TCC ATT ATG GTA AAC CTT AAG G
SunS-K232A-RP	TGA TTT TAT ATT ATT CTC TGA AGG ATT ATA TCC ATT ATG GTA AAC CTT AAG G
SunS-R235A RP	TTC TTC TGT GAG ATT TAT ATT CGC TCG TGT TTT TGA TTT TAT ATT
SunS-R235A FP	AAT ATA AAA TCA AAA ACA CGA GCG AAT ATA AAT CTC ACA GAA GAA
SunS-Y222A-FP	ATA ATG GAG CGA ATC CTT CAG AGA ATA ATA TAA AAT CAA AAA CAC GAA GGA ATA TAA AT
SunS-Y222A-RP	AGG ATT CGC TCC ATT ATA TTA TGG TAA ACC TTA AGG TTC ACA ATG AAA TTA AAA GG
SunS-N236A FP	GAG AAT AAT ATA AAA TCA AAA ACA CGA AGG GCG ATA AAT CTC ACA GAA GAA ATG
SunS-N236A RP	CAT TTC TTC TGT GAG ATT TAT CGC CCT TCG TGT TTT TGA TTT TAT ATT ATT CTC

6.4.3 Overexpression and purification of His_6-SunA precursor peptides

E. coli BL21 (DE3) cells were transformed via electroporation with a pET15b SunA or SunA mutant construct. A single colony transformant was used to inoculate 30 mL of LB supplemented with 100 μg/mL ampicillin. The culture was grown at 37 °C for 12 h and was used to inoculate 3 L of LB containing 100 μg/mL ampicillin and cells were grown at 37 °C to OD_{600} ≈ 0.6-0.8. IPTG was added to a final concentration of 0.75 mM and the culture was incubated at 37 °C for 3 h. Under such conditions, His_6-SunA peptides were expressed as insoluble peptides. Cells were harvested by centrifugation at 12,000 ×*g* for 25 min at 4 °C, and the pellet was resuspended in 30 mL of start buffer (20 mM NaH_2PO_4, pH 7.5, 500 mM NaCl, 0.5 mM imidazole, 20% glycerol) and stored at −80 °C. The cell paste was suspended in start buffer and the suspension was sonicated on ice for 20 min to lyse the cells. Cell debris was removed by

centrifugation at 23,700 ×*g* for 30 min at 4 °C. The supernatant was discarded and the pellet containing the insoluble peptide was resuspended in 30 mL of start buffer. The sonication and centrifugation steps were repeated. Again the supernatant was discarded and the pellet was resuspended in 30 mL of buffer 1 (6 M guanidine HCl, 20 mM NaH_2PO_4, pH 7.5, 500 mM NaCl, 0.5 mM imidazole). The sample was sonicated and insoluble material was removed by centrifugation at 23,700 ×*g* for 30 min at 4 °C, followed by filtration of the supernatant through a 0.45 μm filter. The filtered sample was applied to a 5 mL HisTrap HP (GE Healthcare Life Sciences) immobilized metal affinity chromatography (IMAC) column previously charged with $NiSO_4$ and equilibrated in buffer 1. The column was washed with two column volumes of buffer 1, followed by two column volumes of buffer 2 (4 M guanidine HCl, 20 mM NaH_2PO_4, pH 7.5, 500 mM NaCl, 30 mM imidazole). The peptide was eluted with 1-2 column volumes of elution buffer (4 M guanidine HCl, 20 mM NaH_2PO_4, pH 7.5, 500 mM NaCl, 1 M imidazole). The fractions were desalted using a ZipTipC18 and analyzed by MALDI-TOF MS. The fractions containing the desired peptide were pooled and desalted using C4 solid phase extraction columns (Grace Vydac) as directed by the product manual. The desalted peptide was lyophilized and purified by analytical reversed-phase high-performance liquid chromatography (RP-HPLC) using a Beckman Coulter System Gold HPLC equipped with a Grace-Vydac Protein C18 column (5 μm, 300 Å, 250 mm x 4.6 mm). Solvents for the RP-HPLC were solvent A (0.1% TFA in water) and solvent B (0.086% TFA in 80% acetonitrile / 20% water). A gradient of 2-100% of solvent B was executed for over 45 min at a flow rate of 1 mL/min, and peptides were detected by absorbance at 220 nm. The fractions were analyzed by MALDI-TOF-MS. All the fractions containing the desired product were combined and the organic solvents were removed by rotary evaporation, followed by lyophilization. The product was kept at −20 °C for short-term storage

and −80 °C for long-term storage. Typical yields from 1 L culture were 50 μg of His_6-SunA and His_6-SunA mutants.

6.4.4 Overexpression and purification of His_6-SunS and SunS mutants

E. coli BL21 (DE3) cells were transformed via electroporation with the pET28b SunS construct obtained from Dr. Trent Oman.[1] A single colony transformant was used to inoculate a 30 mL culture of LB supplemented with 50 μg/mL kanamycin. The culture was grown at 37 °C for 12 h and was used to inoculate 3 L of LB containing 50 μg/mL kanamycin, and cells were grown at 37 °C to OD600 ≈ 0.6. The culture was incubated at 4 °C on ice for 20 min, then IPTG was added to a final concentration of 0.5 mM and the culture was incubated at 18 °C for an additional 16-20 h. Cells were harvested by centrifugation at 12,000 ×g for 15 min at 4 °C, and the pellet was resuspended in 30 mL of start buffer (20 mM Tris (pH 8.0), 500 mM NaCl, 1 mM TCEP, 10% glycerol) and stored at −80 °C. All protein purification steps were performed at 4 °C. The cell paste was suspended in start buffer and the cells were lysed using a high pressure homogenizer (Avestin, Inc.). Cell debris was pelleted via centrifugation at 23,700 ×g for 20 min at 4 °C. The supernatant was injected via a superloop onto a fast protein liquid chromatography (FPLC) system (ÄKTA, GE Heathcare Life Sciences) equipped with a 5 mL HisTrap HP IMAC column previously charged with $Ni2^+$ and equilibrated in start buffer. The column was washed with 50 mL of buffer A (30 mM imidazole, 20 mM Tris, pH 7.5, 300 mM NaCl) and the protein was eluted using a linear gradient of 0-100% B (buffer B = 200 mM imidazole, 20 mM Tris, pH 7.5, 300 mM NaCl) over 40 min at a 2 mL/min flow rate. UV absorbance (280 nm) was monitored and fractions were collected and analyzed by SDS-PAGE (4-20% Tris-glycine READY gel, BioRAD). The fractions containing SunS were combined and concentrated using an Amicon Ultra-15 Centrifugal Filter Unit (10 kDa MWCO, Millipore). Gel filtration purification

was used to further purify SunS. The concentrated protein sample was injected onto an FPLC system (ÄKTA) equipped with an XK16 16/60 (GE Healthcare Life Sciences) column packed with SuperDex 75 resin previously equilibrated in 20 mM Tris (pH 7.5), 100 mM KCl, 1 mM TCEP, and 10% glycerol. The protein was eluted with a flow rate of 0.9 mL/min. Both UV absorbance (280 nm) and conductance were monitored and fractions were collected. Misfolded/aggregated protein was efficiently separated from soluble, correctly folded protein and the desired fractions were combined and concentrated using an Amicon Ultra-15 Centrifugal Filter Unit. The resulting protein sample was stored at −80 °C. Protein concentration was determined using a Bradford Assay Kit (Pierce) and typically yields were 8 mg of His_6-SunS or SunS mutants from 3 L of cell culture.

6.4.5 Kinetic assays of the glycosyltransferase activities of SunS and SunS mutants with SunA peptides using a coupled spectrophotometric assay

Typically, SunA or SunA mutant peptide (10-40 μM) was pre-incubated in 50 mM HEPES buffer (pH 7.5), 1 mM $MgCl_2$, 1 mM TCEP, 100 μM~5 mM nucleotide sugars, 0.7 mM phosphoenolpyruvate (PEP), 300 μM NADH, 20 units of pyruvate kinase and 28 units of lactate dehydrogenase at 37 °C for 10 min. Reactions were monitored at 340 nm for spontaneous hydrolysis of nucleotide sugars. When the spontaneous hydrolysis of nucleotide sugars reached a stable rate, enzymatic glycosylation was initiated by the addition of SunS or SunS mutants (0.02-2 μM). The initial rates of enzymatic hydrolysis and transglycosylation (<10% conversion) were determined by subtracting the spontaneous hydrolysis rate from the reaction rate after enzyme addition. All kinetic assays were carried out in a Cary 4000 UV-Vis spectrometer equipped with a circulating water bath. The assay volume was 100 μL. All the data were fitted using Origin 9.0 software or Graphpad prism 5.

6.4.6 Kinetic assay of the glycosyltransferase activities of SunS and SunS mutants towards SunA peptides by LC-MS analysis.

Typically, 40 µM SunA peptide was incubated with 1 mM TCEP, 1 mM $MgCl_2$, 1 mM UDP-Glc and 0.02 - 0.3 µM SunS or SunS mutant in 50 mM HEPES buffer (final concentrations), pH 7.5 at room temperature for 1 to 5 min. The reaction was quenched by addition of formic acid to a final concentration of 5% and subjected to LC-MS analysis without further manipulation. A 5 µL volume of quenched SunS reaction was applied to a Phenomenex Jupiter 5µ C18 300 Å (150 x 1.0 mm) column. Sugar-modified and unmodified His_6-SunA mutant peptide material were eluted by maintaining the mobile phase at 2% B for 1 min, followed by an increase to 80% B over 20 min with a flow rate of 1.0 mL/min. All fractions were analyzed by MALDI-TOF MS as described above. The relative amounts of sugar-modified and unmodified His_6-SunA peptide was determined by quantifying the peak area (A220 nm) corresponding to the M+8H ion of the substrate and product peptide by integration. Percent conversion was calculated by dividing the peak area of sugar-modified peptide by the sum of the sugar-modified and unmodified peak areas (Figures 6.15 and 6.16).

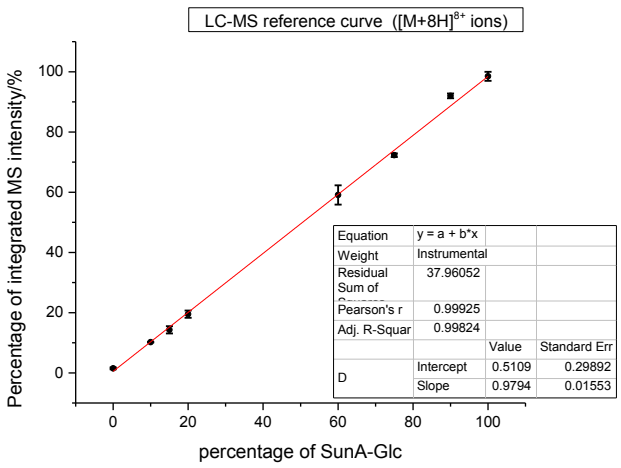

Figure 6.15 Standard curve for quantifying the conversion of SunA into the corresponding glycopeptide during in vitro kinetic assays.

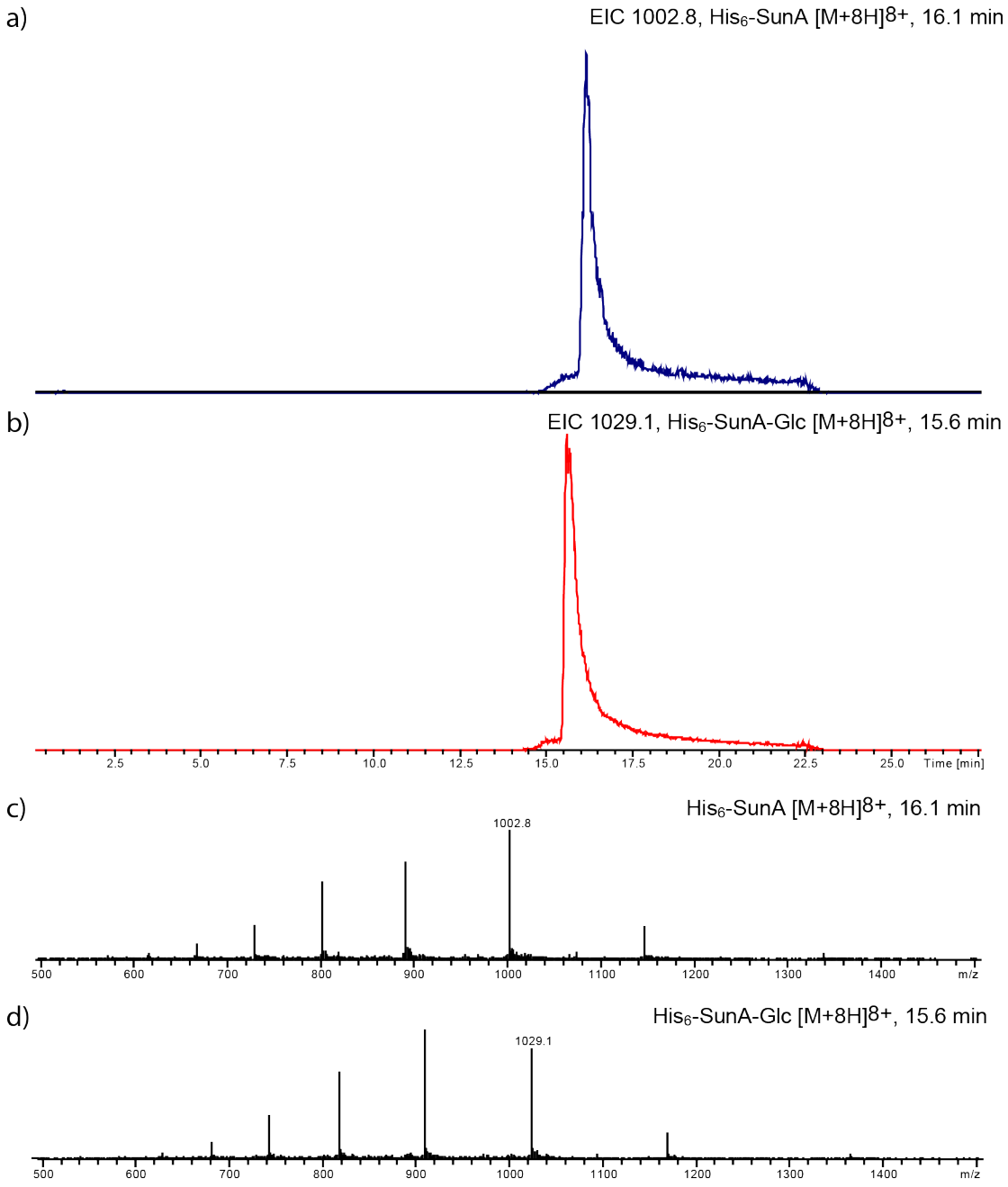

Figure 6.16 Extracted ion chromatograms of SunA and SunA-Glc.
The relative amounts of sugar-modified and unmodified His_6-SunA peptide was determined by quantifying the peak area (A220 nm) corresponding to the M+8H ion of the (a) substrate and (b) product peptide by integration. Percent conversion was calculated by dividing the peak area of sugar-modified peptide by the sum of the sugar-modified and unmodified peak areas. (c and d) isotopic distribution of substrate (SunA) and product (SunA-Glc) peptides. Expected SunA $[M+ 8H]^{8+}$: 1002.87 and Expected SunA-Glc $[M+ 8H]^{8+}$: 1030.0.

6.5 REFERENCES

(1) Oman, T. J.; Boettcher, J. M.; Wang, H.; Okalibe, X. N.; van der Donk, W. A. *Nat Chem Biol* **2011**, *7*, 78. "Sublancin is not a lantibiotic but an S-linked glycopeptide".

(2) Stepper, J.; Shastri, S.; Loo, T. S.; Preston, J. C.; Novak, P.; Man, P.; Moore, C. H.; Havlicek, V.; Patchett, M. L.; Norris, G. E. *FEBS Lett* **2011**, *585*, 645. "Cysteine S-glycosylation, a new post-translational modification found in glycopeptide bacteriocins".

(3) Wang, H.; Oman, T. J.; Zhang, R.; Garcia De Gonzalo, C. V.; Zhang, Q.; van der Donk, W. A. *J Am Chem Soc* **2014**, *136*, 84. "The glycosyltransferase involved in thurandacin biosynthesis catalyzes both O- and S-glycosylation".

(4) Norris, G. E.; Patchett, M. L. In *Natural Products Analysis*; John Wiley & Sons, Inc: 2014, p 507.

(5) Hata, T.; Tanaka, R.; Ohmomo, S. *Int J Food Microbiol* **2010**, *137*, 94. "Isolation and characterization of plantaricin ASM1: a new bacteriocin produced by Lactobacillus plantarum A-1".

(6) Garcia De Gonzalo, C. V.; Zhu, L.; Oman, T. J.; van der Donk, W. A. *ACS Chem Biol* **2014**, *9*, 796. "NMR structure of the S-linked glycopeptide sublancin 168".

(7) Wang, H.; van der Donk, W. A. *J Am Chem Soc* **2011**, *133*, 16394. "Substrate selectivity of the sublancin S-glycosyltransferase".

(8) Lairson, L. L.; Henrissat, B.; Davies, G. J.; Withers, S. G. *Annu Rev Biochem* **2008**, *77*, 521. "Glycosyltransferases: structures, functions, and mechanisms".

(9) GraphPad; 5 ed.; GraphPad Software Inc: 2015.

(10) Rao, S. T.; Rossmann, M. G. *J. Mol. Biol.* **1973**, *76*, 241. "Comparison of super-secondary structures in proteins".

(11) Goebl, M.; Yanagida, M. *Trends Biochem. Sci.* **1991**, *16*, 173. "The TPR snap helix: a novel protein repeat motif from mitosis to transcription".

(12) D'Andrea, L. D.; Regan, L. *Trends Biochem. Sci.* **2003**, *28*, 655. "TPR proteins: the versatile helix".

(13) Allan, R. K.; Ratajczak, T. *Cell Stress Chaperon* **2011**, *16*, 353. "Versatile TPR domains accommodate different modes of target protein recognition and function".

(14) Lazarus, M. B.; Nam, Y.; Jiang, J.; Sliz, P.; Walker, S. *Nature* **2011**, *469*, 564. "Structure of human O-GlcNAc transferase and its complex with a peptide substrate".

(15) Lazarus, M. B.; Jiang, J.; Gloster, T. M.; Zandberg, W. F.; Whitworth, G. E.; Vocadlo, D. J.; Walker, S. *Nat Chem Biol* **2012**, *8*, 966. "Structural snapshots of the reaction coordinate for O-GlcNAc transferase".

(16) Schimpl, M.; Zheng, X.; Borodkin, V. S.; Blair, D. E.; Ferenbach, A. T.; Schuttelkopf, A. W.; Navratilova, I.; Aristotelous, T.; Albarbarawi, O.; Robinson, D. A.; Macnaughtan, M. A.; van Aalten, D. M. *Nat Chem Biol* **2012**, *8*, 969. "O-GlcNAc transferase invokes nucleotide sugar pyrophosphate participation in catalysis".

(17) Breton, C.; Fournel-Gigleux, S.; Palcic, M. M. *Curr Opin Struct Biol* **2012**, *22*, 540. "Recent structures, evolution and mechanisms of glycosyltransferases".